CRCLEME

Cooperative Research Centre for
Landscape Environments
and Mineral Exploration

CSIRO
EXPLORATION
AND MINING

OPEN FILE
REPORT
SERIES

NICKEL HYDROGEOCHEMISTRY OF THE NE YILGARN CRATON, WESTERN AUSTRALIA

David J. Gray and Ryan R. P. Noble

CRC LEME OPEN FILE REPORT 212

February 2007

CRCLEME

(CRC LEME Report 243R, E&M Report P2006/524, 2006
2nd Impression 2007)

NICKEL HYDROGEOCHEMISTRY OF THE NE YILGARN CRATON, WESTERN AUSTRALIA

David J. Gray and Ryan R. P. Noble

CRC LEME OPEN FILE REPORT 212

February 2007

(CRC LEME Report 243R, E&M Report P2006/524, 2006
2nd Impression 2007)

CRC LEME is an unincorporated joint venture between CSIRO-Exploration & Mining, and Land & Water, The Australian National University, Curtin University of Technology, University of Adelaide, Geoscience Australia, Primary Industries and Resources SA, NSW Department of Primary Industries and Minerals Council of Australia.

Headquarters: CRC LEME c/o CSIRO Exploration and Mining, PO Box 1130, Bentley WA 6102, Australia

This Open File Report 212 is a second impression (second printing) of CRC LEME Restricted Report 243R. Confidentiality expired in February 2007.

Electronic copies of the publication in PDF format can be downloaded from the CRC LEME website: http://crcleme.org.au?Pubs?OFRindex.html. Information on this or other CRC LEME publications can be obtained from: http://crcleme.org.au

Hard copies will be retained in the Australian National Library, The State Library of Western Australia and the CSIRO Library at the Australian Resources Research Centre, Kensington Western Australia.

Reference:

Gray, DJ and Noble, RP, 2006. Nickel Hydrogeochemistry of the NE Yilgarn Craton, Western Australia. CRC LEME Restricted Report 243R. pp128. (Reissued as Open File Report 212, CRC LEME, Perth 2007).

1. Nickel Hydrogeochemistry – NE Yilgarn Craton.

ISSN 1329-4768
ISBN 1921 039 566

Addresses and affiliations of authors:

David J. Gray
Cooperative Research Centre for Landscape Environments and Mineral Exploration
c/- CSIRO Exploration and Mining
PO Box 1130
Bentley WA 6102

Ryan R.P. Noble
Cooperative Research Centre for Landscape Environments and Mineral Exploration
c/- CSIRO Exploration and Mining
PO Box 1130
Bentley WA 6102

The northeastern Yilgarn hydrogeochemistry project is providing a new knowledge base and developing methodologies for improved Ni mineral exploration in areas of regolith cover in the northeast Yilgarn Craton, WA. This report is specifically on groundwater investigations in the Agnew Wiluna greenstone belt in the northeast Yilgarn area and is produced for the four industry sponsors of this research: Anglo American, BHP Billiton, Inco and LionOre.

ABSTRACT

The hydrogeochemistry of the NE Yilgarn Craton of Western Australia has been examined to assess the utility of groundwater for regional exploration for Ni sulphide (NiS) mineralisation. The principal objective of this study is to develop reliable regional and smaller-scale hydrogeochemical vectors to NiS mineralisation in the NE Yilgarn Craton. To achieve this it is critical to understand groundwater expressions of NiS mineralisation, evaluate larger scale variation in element concentrations, test different collection, sample treatment and analytical protocols, and understand groundwater-induced dispersion processes in this environment.

Approximately 300 samples were collected from exploration drill holes, wells, farm bores and groundwater monitoring bores using a bailer system. An additional 210 samples were added to the assessment from previous work at the Harmony site and from regional background samples. Field measurements included pH, Eh, EC and temperature. Separate, field preserved sub-samples were collected for cation, anion, alkalinity and (using carbon sorption) Au/ PGE analysis. Additional methodology experimentation conducted on selected samples involved a comparison of 0.1µm and 0.45µm filtration and the use of anion and cation exchange resins to adsorb low concentrations of metals.

The hydrogeochemistry of the region is dominantly fresh and neutral, with increases in groundwater salinity in the base of palaeochannels and close to salt lakes. In contrast to other regions of the Yilgarn Craton, the waters in the NE are fairly homogeneous. They also have relatively low dissolved concentrations of metals compared with groundwaters from the central and southern Yilgarn. The results reported for this study indicate that hydrogeochemical sampling searching for NiS in the NE Yilgarn has significant potential for medium (100's m spacing) scale exploration. These findings may also be beneficial for smaller scale investigation to assess "near-miss" drilling in brownfields regions, as well as investigations in hydrogeochemically-similar greenfields regions. The geochemical halo around Ni deposits is sporadic, giving several false negatives; however, there are few false positives. Most high concentrations of metals associated with the Ni hydrogeochemical signature are indicative of sulphides and mineralisation. Chromium is the best indicator element for ultramafic rocks (particularly when S-poor), whereas Ni, Co, Pt and W are the best individual pathfinders for NiS mineralisation.

Hydrogeochemical differentiation and targeting for NiS is improved by using the Box-Cox transformation and deriving critical indices from the multielement data. The indices, consistent with the model for groundwater evolution around weathering sulphides, delineate the sulphide signature independent of the type of water *i.e.*, whether the major parameters of Eh and pH are different. The better performing indices for mineralisation targeting are Miner-S and Miner-FeS that use the mineralised signature (Ni+Co+W+Pt) and take away the groundwater signatures of weathering acid producing sulphides (Mo+Ba+Li+Al) and Fe-rich sulphides (pH-Eh+Fe+Mn). Massive NiS certainly gave stronger groundwater signatures than disseminated mineralisation, which commonly were only clearly delineated using these combined indices.

Mineral saturation indices were not generally beneficial to exploration, as nearly all samples were under saturated with respect to most ore minerals. A few exceptions included those minerals associated with U mineralisation. Although U exploration is not part of this study, preliminary results would indicate that hydrogeochemistry would be an effective tool for U exploration in the NE Yilgarn.

Method developments implemented in this study indicate the use of either 0.1 µm or 0.45 µm filter size may well be acceptable for groundwater exploration in the NE Yilgarn, but further study of Fe and Al is required. At this stage the concentrations of "dissolved" Fe and Al should be interpreted carefully in such neutral/fresh groundwaters, but seem to have little influence on the dilution or concentration of metals of interest in solution. Carbon sachets have been routinely used for Au

analysis, and can be used to achieve lower detection for Ag, Pd, Pt, U, W and other metals. This is important because PGE concentrations in NE Yilgarn groundwaters are too low (< 10 ppt) for direct solution analysis. The use of carbon extracted W, Pt and Pd has been a useful vector to Ni mineralisation. Results show that concentrations of Pt and, to a lesser degree, Pd are increased close to mineralisation. Improving the detection of PGEs in groundwater may enhance exploration success using hydrogeochemistry, particularly in the NE Yilgarn. Two exchange resins, in addition to the activated carbon, were tested in the Honeymoon Well region, but generally did not enhance analysis, with the exception of W on the Dowex MAC-3 anion resin. A major advantage of the carbon compared to the other exchange resins is the sorption of both negative and positive charged ions. The carbon technique uses unfiltered waters, is easy to use, and may be more practical to the mining and exploration industry hydrogeochemical sampling.

TABLE OF CONTENTS

LIST OF FIGURES

LIST OF TABLES

1. INTRODUCTION

A primary justification for the use of hydrogeochemistry in mineral exploration is that groundwater anomalies may be broader and more regular than the mineralisation and secondary dispersion halo in the regolith, thus enhancing the geochemical footprint. Hydrogeochemical studies also provide information on how various rocks are weathering. Understanding of active dispersion processes is enhanced, assisting in the development of weathering and geochemical models, considered essential for effective exploration in regolith-dominated terrains. The scope of this investigation includes the effect of underlying lithology on the observed water chemistry, thermodynamic modelling, mapping of the data, constructing a model of groundwater evolution around weathering Ni sulphides (NiS) and development of geochemical indices to act as vectors towards mineralisation. So as to have consistent groundwater characteristics, the study was limited to the Northern zone of the Leonora-Wiluna greenstone belt (Figure 1), hereafter designated as the NE Yilgarn. We have also tested new methodologies for groundwater exploration. This research was supported by CSIRO Exploration and Mining, CRC LEME and four industry sponsors: Anglo American Plc, BHP Billiton Ltd, Inco Ltd and LionOre Australia Pty Ltd.

Sampling for this project has been integrated with previous investigations at the Harmony Ni deposit and other studies demonstrating systematic regional variation in groundwater chemistry. The sampling forms the basis for a systematic study of the mine-scale and regional variation in groundwater chemistry related to NiS mineralisation. Other sites used in this study include the Jaguar deposit, Lawlers area and regional samples north of Wiluna. These data have been used to enhance the results of this project and are not considered part of the confidentiality agreement.

Regional well sampling has been used to test large-scale variation and potential for vectoring to mineralisation. Sampling and analytical methodologies were compared for time-effectiveness and accuracy, including on site filtering requirements and potential analytical short-cuts such as sorption of unfiltered water samples onto chelating resins. It is expected that the sampling methodology results will be valid in similar environments.

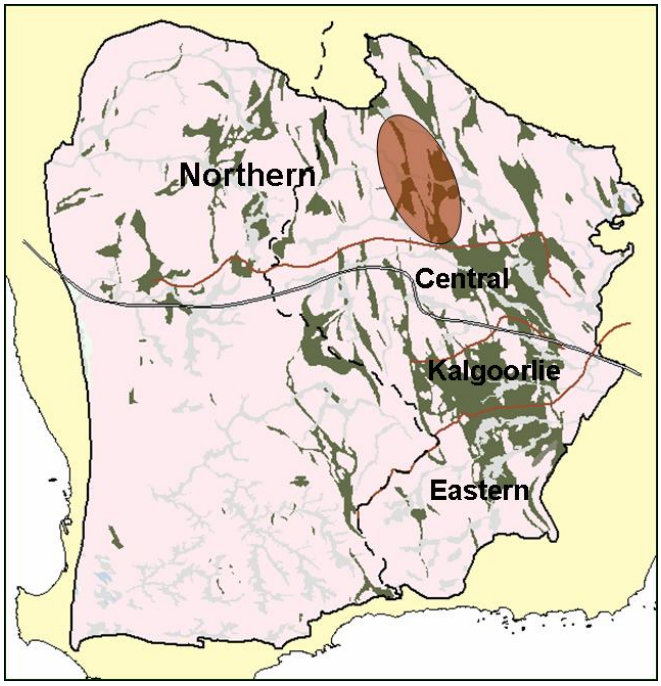

Figure 1: The general location of the study area (brown) and the defined major groundwater regions separated by the brown lines. Pink represents granite lithologies, green the greenstone belts.

2. SAMPLING AND ANALYSIS

2.1 Sampling

The project involved sampling groundwater from ore bodies in the following areas: Honeymoon Well, Yakabindie, Wildara/Waterloo and Camelot (Figure 2). Additional information was provided from previous work near the Harmony deposit and the background sites in the Lawlers area and north of Wiluna. Additional groundwater data from the Jaguar deposit is also used for comparison.

Approximately 300 water samples were collected. Fifty-one samples (NH001-051) were collected from the Wildara/Waterloo region in February 2005, with follow up sampling of another 24 samples (NH053-076) from Waterloo in August 2005. Sixty-four samples (NH101-165) were collected from the Camelot area over three occasions in 2005; 51 samples were taken from Yakabindie (NH201-251) in September 2005; and 78 samples (NH301-378) collected from the Honeymoon Well area in April 2006. If groundwater was present and the holes not contaminated with diesel or other petroleum products such as grease, the depth to water was recorded and water samples collected by bailer. Where farmers bores were used, water was collected from a flowing pipe, or if unavailable, from within 10 cm of the top of the water tank. Samples were analysed for pH and oxidation potential (Eh) on-site, with an aliquot collected for HCO_3 analysis by alkalinity titration. About 400 mL of water was filtered through a 0.1 µm membrane filter; about 250 mL of this was acidified (250 µL 15 M HNO_3), and analysed by ICP-MS and ICP-OES at Ultratrace Laboratories for the following elements (detection limits in parentheses):

Na (1 mg/L), K (0.1 mg/L), Mg (0.2 mg/L), Ca (0.1 mg/L), Ag (0.5 µg/L), Al (0.01 mg/L), As (0.001 mg/L), Au (0.01 µg/L), B (0.01 mg/L), Ba (0.01 mg/L), Be (0.5 µg/L), Bi (1 µg/L), Cd (0.0005 µg/L), Ce (0.5 µg/L), Co (0.0002 mg/L), Cr (0.005 mg/L), Cs (1 µg/L), Cu (0.002 mg/L), Dy (0.5 µg/L), Er (0.5 µg/L), Eu (1 µg/L), Fe (0.01 mg/L), Ga (0.5 µg/L), Gd (0.5 µg/L), Ge (0.002 mg/L), Hg (0.2 µg/L), Ho (0.5 µg/L), In (0.2 µg/L), La (0.5 µg/L), Li (0.01 mg/L), Lu (0.5 µg/L), Mn (0.002 mg/L), Mo (2 µg/L), Nd (0.5 µg/L), Ni (0.01 mg/L), P (0.1 mg/L), Pb (0.01 mg/L), Pd (0.5 µg/L), Pr (0.5 µg/L), Pt (0.1 µg/L), Rb (0.01 mg/L), S (0.1 mg/L), Sb (0.2 µg/L), Sc (0.001 mg/L), Si (0.1 mg/L), Sm (0.5 µg/L), Sn (1 µg/L), Sr (0.02 mg/L), Tb (0.5 µg/L), Te (0.5 µg/L), Th (0.1 µg/L), Ti (0.005 mg/L), Tl (0.2 µg/L), Tm (0.5 µg/L), U (2 µg/L), V (0.005 mg/L), W (1 µg/L), Y (1 µg/L), Yb (1 µg/L), Zn (0.005 mg/L). Detection limits occasionally varied depending on salinity levels, with the most saline samples having higher detection limits due to increased dilution requirements.

A filtered/unacidified aliquot was analysed at CSIRO ARRC Laboratories by Ion Chromatography (IC) for: Cl (25 mg/L), SO_4 (4 mg/L), Br (0.15 mg/L), F (0.15 mg/L), I (0.15 mg/L), NO_3 (0.15 mg/L) and PO_4 (0.15 mg/L). The IC equipment used was a Metrohm modular IC using an acid re-generated suppressor, MetroSep A Supp5 column, a carbonate/bicarbonate eluent (32 mM Na_2CO_3 and 10 mM $NaHCO_3$) and a conductivity detector.

Approximately half of the groundwater samples used for carbon extraction of the following metals: Ag (1 ng/L), Au (0.1 ng/L), Bi (0.2 ng/L), Cu (1 µg/L), Mo (0.05 µg/L), Ni (1 µg/L), Pd (1 ng/L), Pt (1 ng/L) and W (0.01 µg/L). One litre of unfiltered water was collected and rolled with the carbon sachet for 10 days. The carbon was then dried, ashed, digested in aqua regia and analysed by ICP-MS. The method has been previously tested for Au and PGE by shaking standards of varying concentrations, and in varying salinities, with activated carbon (Gray, unpublished data). Field and analytical blanks, as well as duplicates were used in all analyses to ensure accuracy.

At Honeymoon Well additional samples were collected using a 0.45µm filter for filtration comparison, and separately, for exchange resin extraction (Figure 3). Anion exchange resins (Dowex MAC-3) were analysed for Ag (1 µg/L), As (0.01 mg/L), Au (0.05 µg/L), Bi (1 µg/L), Mo (2 µg/L), Pd (0.5 µg/L), Pt (0.1 µg/L), Sb (2 µg/L), U (2 µg/L) and W (1 µg/L). Cation exchange resins

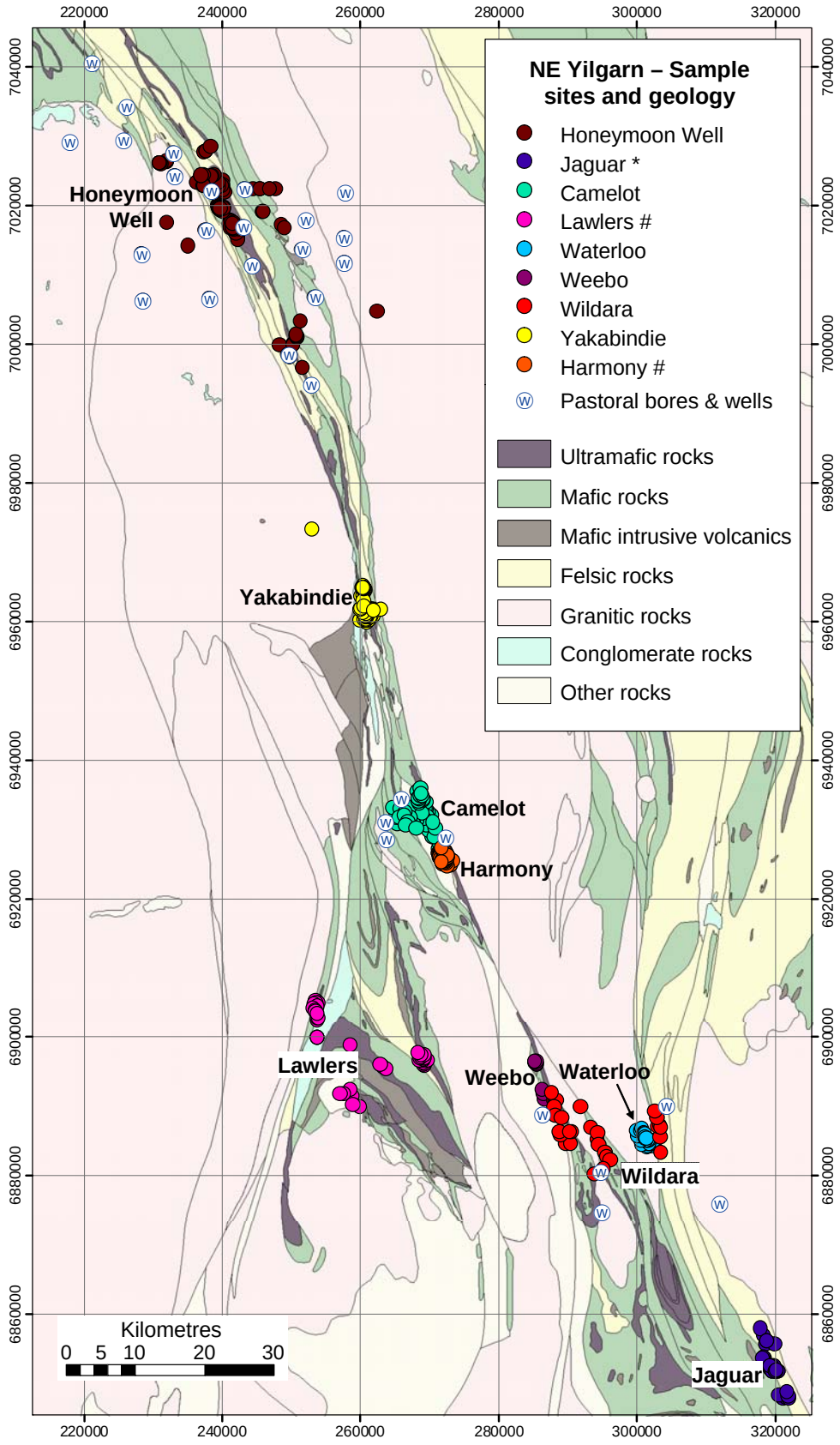

Figure 2: Geology of the NE Yilgarn Craton with locations of groundwater sampling sites.

Previous Investigations

* Not sampled as part of this project, but used for interpretation.

Other background sites incorporated into the interpretation are not shown.

(Aquasonic toxic metal sponge) were analysed for Ag (1 µg/L), Au (0.05 µg/L), Bi (1 µg/L), Co (0.002 mg/L), Cr (0.005 mg/L), Fe (0.005 mg/L), Ni (0.01 mg/L), Pb (0.01 mg/L), Pd (0.5 µg/L), Pt (0.1 µg/L) and U (2 µg/L). The exchange sachets used a 200 µm nylon mesh, which was filled with approximately 1 cm^3 of resin beads. The sachets were rolled with one litre of unfiltered water for 10 days, then removed and dried, shaken with 12 mL of 5% HCl for 2 hours, and the solution analysed. The full exchange resin regeneration method is in Appendix 6.

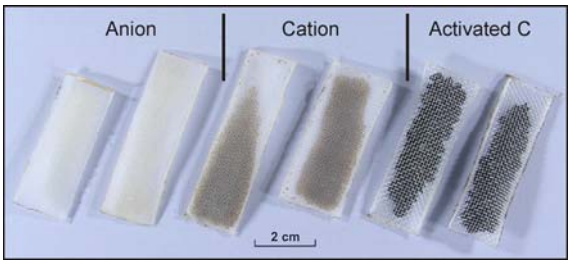

Figure 3: Exchange sachets used for hydrogeochemical sampling

2.2 Solution Modelling

Equilibrium activity diagrams were derived using The Geochemist's Workbench® and the Thermo.dat database. The solution species and degree of mineral saturation were computed from the solution compositions using the program PHREEQE (Parkhurst *et al*., 1980), which determines the chemical speciation of many of the major and trace elements. Saturation indices (SI) for each water sample were calculated for various minerals. If the SI for a mineral equals zero (empirically from -0.2 to 0.2 for the major element minerals, and -1 to 1 for the minor element minerals), the water is in equilibrium with that mineral, under the conditions specified. Where the SI is less than zero, the solution is under-saturated with respect to that mineral, so that, if present, the phase may dissolve. If the SI is greater than zero the solution is over-saturated with respect to this mineral, which can potentially precipitate from solution.

Note that SI determinations only specify possible reactions, as kinetic constraints may rule out reactions that are thermodynamically allowed. Thus, for example, waters are commonly in equilibrium with calcite, but may become dolomite over-saturated, due to the slow rate of precipitation of this mineral (Drever, 1982). However, this method provides some understanding of solution processes at a site and adds value in determining whether the spatial distribution of an element is correlated with geological phenomena such as lithology or mineralisation, or whether they are related to weathering or environmental effects. For example, if Ca distribution is controlled by equilibrium with gypsum in all samples, then the spatial distribution of dissolved Ca will reflect SO_4 concentration alone and have no direct exploration significance.

2.3 Solution Indices

Geochemical indices were developed for pH, Eh, Co, Ni, Al, As, Ba, Cr, Fe, Li and W. For each parameter, data was transformed to a close as possible to a "normal" distribution using a Box-Cox Generalized Power Transform [$y = (x^{\lambda}-1)/\lambda$, $y=\log_e(x)$ for $\lambda=0$] (Box and Cox, 1964). Following this, the transformed data were normalized so as to lie between 0 and 1. This does not change the relative position of each value, but affects the data grouping (*i.e*., the skew and kurtosis approach zero). Data from all NiS and background sites are used, so the indices scale samples or areas relative to all sites.

Derived indices allow different elements to be used together without unintentional weighting or bias. Thus, adding the Ni, Co and W indices gives a stronger, better defined anomaly than using a single element. Even subtracting indices considered to have a negative effect (*e.g*., Eh) is feasible.

3. AQUEOUS CHEMISTRY OF Ni IN NE YILGARN GROUNDWATERS

3.1 Regional factors

The NE Yilgarn waters are dominantly fresh (< 7000 mg/L; Figure 4) and neutral (mean pH of 7.3) and are clearly distinctive from other groundwater types of the Yilgarn (Figure 5).

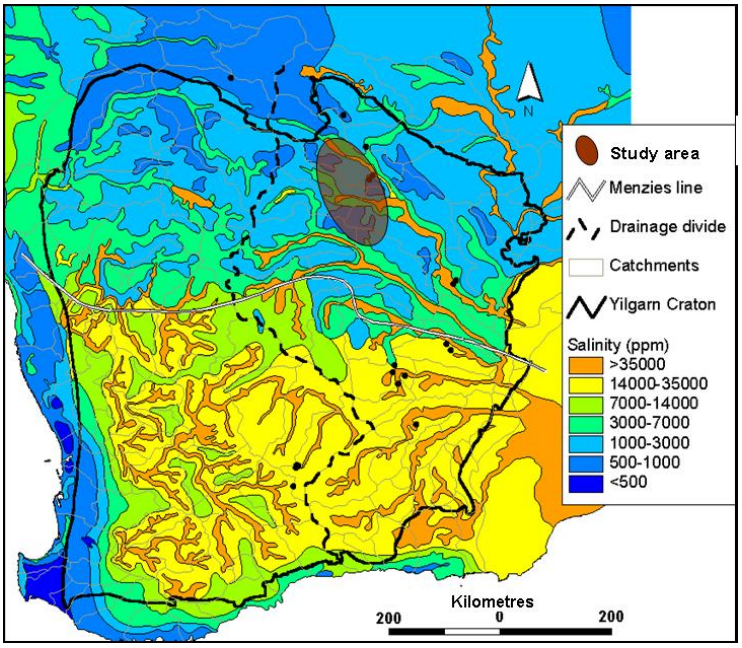

Figure 4: Modelled groundwater salinities in the Yilgarn Craton (Commander, 1989)

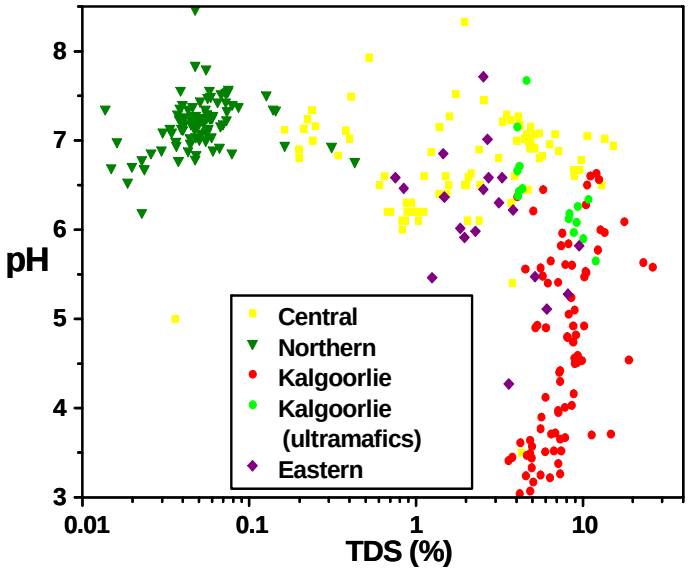

Figure 5: Groundwater total dissolved solids plotted against pH, defined by the major locales (Gray, 2001).

3.2 Nickel chemistry

The groundwaters in the NE Yilgarn commonly have Eh and pH conditions that can sustain significant dissolved Ni (and other base metals and pathfinder elements). Even Ni concentrations greater than 5 mg/L (which is highly anomalous) would be stable in solutions up to pH 8 (Figure 6). If the effect of Fe is considered (Figure 7), then NE Yilgarn groundwaters (Figure 8) could still commonly dissolve 0.05 mg/L Ni, which is still anomalous. *I.e.*, groundwater conditions in the region are conducive to relatively high Ni solubility.

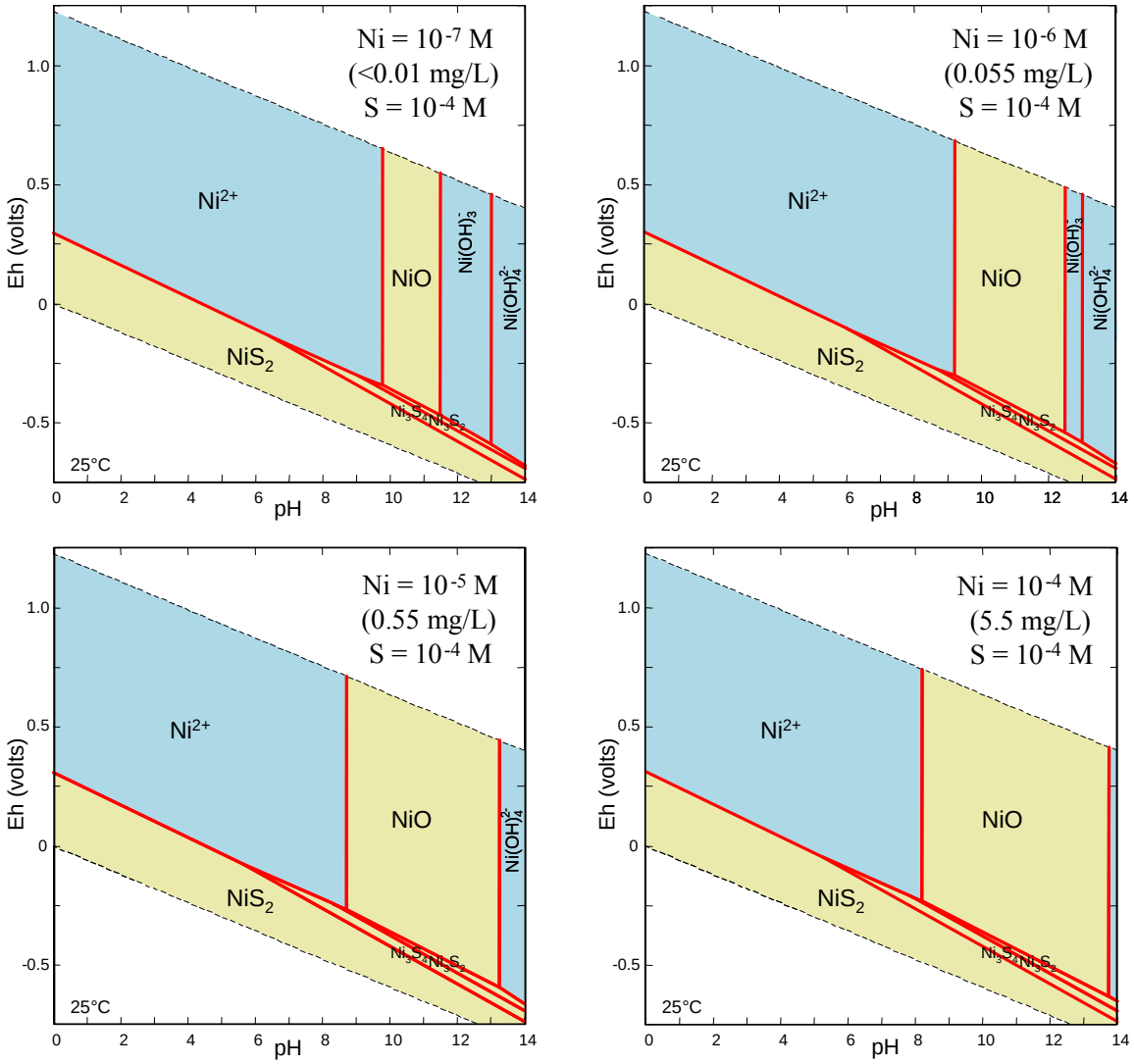

Figure 6 Soluble Ni fraction (blue) for varying pH and Eh, for differing Ni concentration, using S concentration indicative of NE Yilgarn groundwaters.

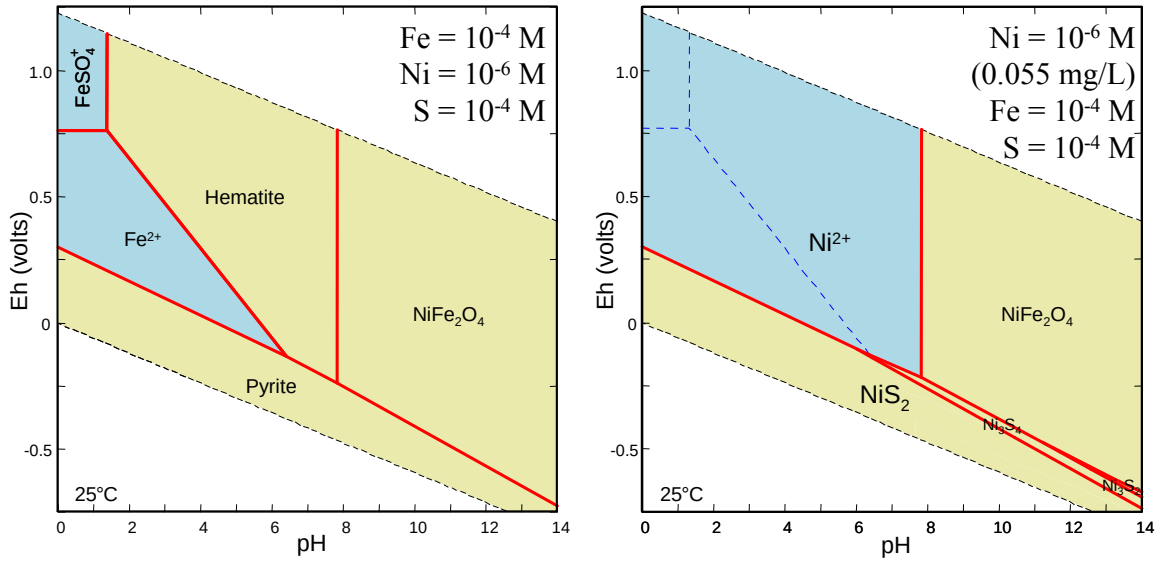

Figure 7 Solubility of Fe and influence on the available phase of Ni in the NE Yilgarn groundwaters.

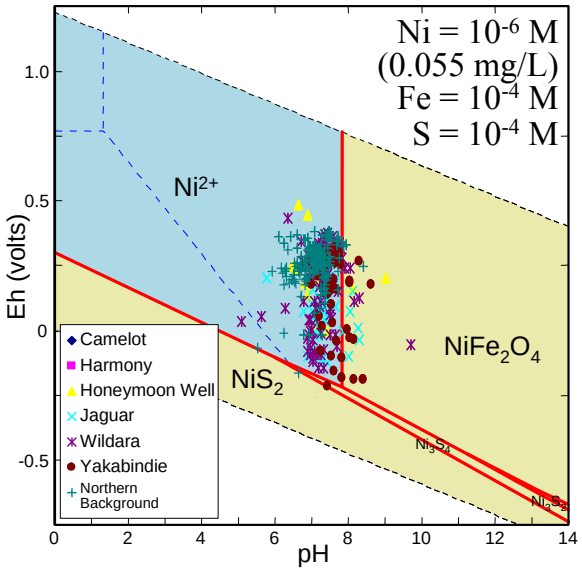

Figure 8 Selected NE Yilgarn groundwater samples plotted a Ni speciation diagram. Most samples occur in a range pH/Eh conditions where Ni^{2+} is soluble

Previous studies at the Harmony deposit (Gray *et al.*, 1999) showed very high dissolved Ni for groundwaters in contact with the weathered expression of NiS mineralisation (Figure 9). Contrast with background was particularly marked when only Northern groundwaters were used for comparison (Figure 10). Indeed even groundwaters up to 200 m from the NiS mineralisation have higher dissolved Ni than regional background

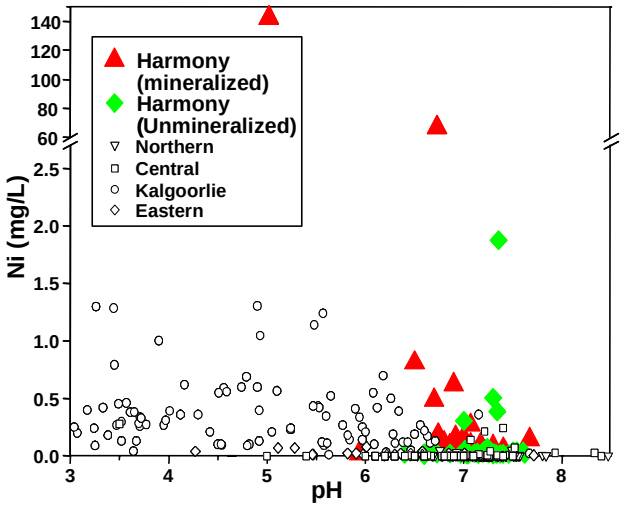

Figure 9: Groundwater Ni concentrations from the Harmony area compared to other background groundwater samples from the Yilgarn Craton.

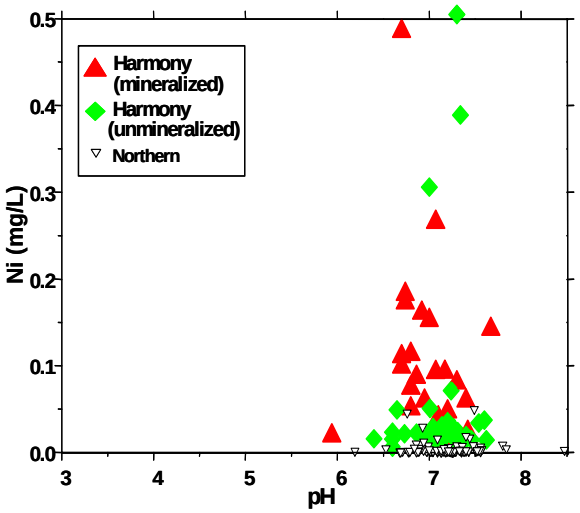

Figure 10: Groundwater Ni concentrations from the Harmony area compared to northern background groundwater samples.

3.3 Sulphide Indicators and groundwater evolution model

Groundwaters in contact with sulphides, whether mineralised or barren, have highly variable characteristics, but can be distinguished from background waters. They generally have one or more of the following properties:

1. Low Eh, and/or low O_2 saturation
2. Moderate to extremely high dissolved Fe content
3. Low pH

4. High concentrations of elements normally characteristic of acid lithologies (Ba, Li, Mn, Mo, V, W)
5. More rarely, detectable Al and REE (La, Ce etc), even in groundwaters above pH 6, despite these elements normally only being soluble below pH 5.5

These results are explained by reference to processes of evolution of groundwaters in contact with weathering sulphides (Figure 11). Most groundwaters in the NE Yilgarn are neutral with moderate Eh (> 300 mV; Gray, 2000). But, deeper groundwaters contacting weathering sulphides will be controlled by release of reduced phases such as SH^-, leading to Eh values below 150 mV[1]. Such reduced waters are observed for all sulphide regions investigated in this study (Figure 8).

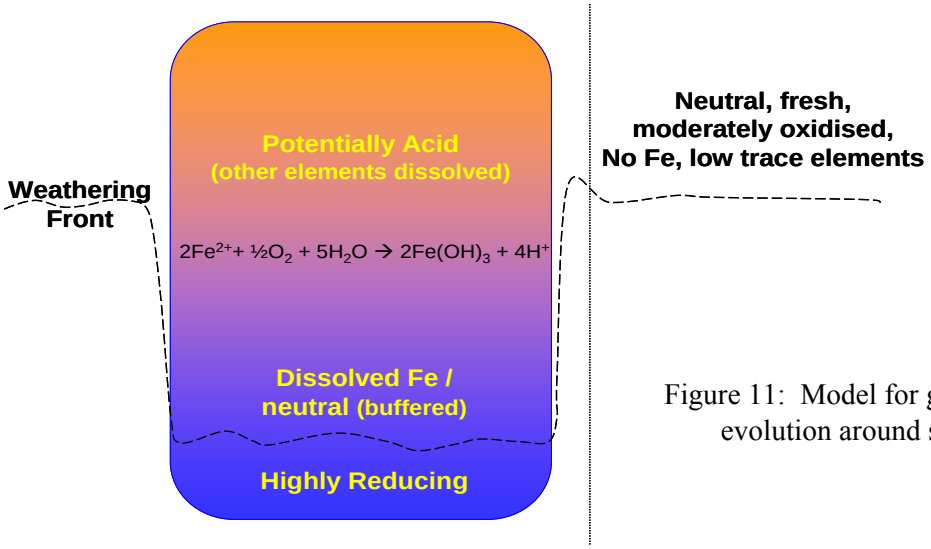

Figure 11: Model for groundwater evolution around sulphides.

A few groundwaters had pH values below 6 (Figure 8), consistent with acid-forming reactions. In general terms, oxidation of sulphide minerals occurs in different stages:

1. *Initial sulphide oxidation* and dissolution basically converts sulphide to sulphate, which can generate acidity for minerals with high S:metal ratios, such as pyrite (FeS_2) and vaesite (NiS_2):

Pyrite $2FeS_2 + 7O_2 + 2H_2O \rightarrow 2Fe^{2+} + 4SO_4^{2-} + 4H^+$
Vaesite $2NiS_2 + 7O_2 + 2H_2O \rightarrow 2Ni^{2+} + 4SO_4^{2-} + 4H^+$

Minerals with lower S:metal ratios produce less acidity during initial oxidation. An important NiS is violarite, which is a reactive intermediate formed via electrochemically mediated replacement of pentlandite and pyrrhotite in the upper part of the sulphide body (Butt *et al.*, 2006):

Violarite $FeNi_2S_4 + 7½O_2 + H_2O \rightarrow 2Ni^{2+} + Fe^{2+} + 4SO_4^{2-} + 2H^+$

There is no acid generation during initial oxidation of pyrrhotite (~FeS) or millerite (NiS):

Millerite $NiS + 2O_2 \rightarrow Fe^{2+} + SO_4^{2-}$

Indeed, for minerals with S:metal ratios less than one, such as pentlandite $(Ni,Fe)_9S_8$, and in particular low S minerals such as (relatively rare) heazlewoodite, initial sulphide oxidation will actually consume acidity:

[1] relative to the standard hydrogen potential; equivalent to less than -50 mV on a normal Eh meter (Ag/AgCl cell)

Pentlandite $\frac{1}{2}Ni_5Fe_4S_8 + 8.25O_2 + H^+ \rightarrow 2.5Ni^{2+} + 2Fe^{2+} + 4SO_4^{2-} + 0.5H_2O$

Heazlewoodite $2Ni_3S_2 + 9O_2 + 4H^+ \rightarrow 6Ni^{2+} + 4SO_4^{2-} + 2H_2O$

As the more common Ni sulphides in transitional environments are generally violarite and millerite, this indicates that economic NiS mineralisation is less likely to generate acid during initial weathering than barren Fe-rich sulphides.

2. Higher in the profile, more oxidising conditions will cause *oxidation of ferrous to ferric ion*, which then hydrolyses and precipitates as iron oxyhydroxides, potentially causing major pH reductions (Mann, 1983):

$$2Fe^{2+} + \frac{1}{2}O_2 + 5H_2O \rightarrow 2Fe(OH)_3 + 4H^+$$

This reaction requires significantly less O_2 and due to its location in the upper regolith, is much more weakly buffered than the initial weathering reactions, thus resulting in much stronger pH reduction. Note that these secondary Fe oxides will also reduce the dissolved Ni concentration due to adsorption and co-precipitation, though Ni concentrations are still expected to be above background. Although Ni^{2+} can also precipitate hydroxides and carbonates in the regolith:

$Ni^{2+} + 2OH^- \rightarrow Ni(OH)_2$ (theophrasite)

$Ni^{2+} + CO_3^{2-} \rightarrow NiCO_3$ (gaspeite)

These generate less acidity and can only occur in neutral to alkaline environments, and cannot directly lower pH to below 6.5.

Thus, there are complex mineralogical (*e*.g., presence and chemistry of sulphides, presence of carbonates) controls on groundwaters around NiS deposits; however, it is likely that groundwaters contacting NiS mineralisation will tend to be highly reduced at depth, contain dissolved Fe and Ni at intermediate depths, and in some cases be acidic (< pH 6) closer to the surface. But, Ni-rich and pyrite-poor sulphides may have less acid production, whereas more Fe-rich mineralogies are expected to cause greater acidity. As well as pH effects, there may be higher concentrations of many metals, such as Al, base metals and rare earth elements (REE), due to acid attack on wall rocks. Any acid effect will be small in disseminated sulphides, and accessory minerals such as serpentine, and particularly magnesite, will very effectively neutralize any acid production. Under present day conditions in much of the Yilgarn Craton these reactions occur slowly due to low dissolved oxygen at depth, and any acidity generated is commonly buffered by other minerals such as carbonates. Reductions in pH are subtle (though present), though some rare groundwaters have pH values down to 5, possibly due to weathering of more Fe-rich pods.

4. COMPILATION OF RESULTS FOR ALL SITES

Median ion concentrations for groundwaters from NE Yilgarn NiS deposits are presented in Table 1. Background NE Yilgarn waters are combined from previously collected samples. Elements of interest to exploration are plotted individually in the following Sections.

Table 1. Median compositions and standard deviations of NE Yilgarn groundwaters.

	Wildara	Camelot	Yakabindie	Honeymoon	Harmony	Background	Overall
WT (m)	44 ± 12	19 ± 11	21 ± 9	6 ± 4			23 ± 17
pH	7.3 ± 0.55	7.25 ± 0.47	7.63 ± 0.38	7.33 ± 0.55	7.05 ± 0.4	6.66 ± 0.41	7.26 ± 0.52
Eh (mV)	145 ± 147	264 ± 175	158 ± 162	209 ± 124	397 ± 51	206 ± 94	219 ± 160
TDS	1786 ± 2112	1771 ± 3631	2630 ± 2466	26314 ±39159	837 ± 475	1809 ± 4422	5115 ± 17117
HCO_3	240 ± 128	123 ± 71	238 ± 103	278 ± 373	89 ± 50	125 ± 83	184 ± 192
Na	467 ± 449	464 ± 1041	747 ± 615	7552 ± 11225	165 ± 84	456 ± 1342	1440 ± 4951
K	44 ± 132	20 ± 19	25 ± 22	614 ± 902	16 ± 7	28 ± 62	109 ± 399
Mg	111 ± 233	70 ± 76	161 ± 194	880 ± 1242	52 ± 36	84 ± 189	199 ± 561
Ca	68 ± 91	119 ± 245	69 ± 69	288 ± 245	66 ± 40	82 ± 78	109 ± 156
Cl	698 ± 982	827 ± 2208	1021 ± 1053	13753 ±20918	307 ± 175	780 ± 2203	2527 ± 9145
SO4	249 ± 445	173 ± 170	484 ± 596	3011 ± 4837	221 ± 182	288 ± 639	651 ± 2088
Br	3.1 ± 4.53	2.3 ± 3.81	4.63 ± 4.53	10.09 ± 12.55	1.95 ± 0.95	6.34 ± 11.34	4.79 ± 8.47
F	0.45 ± 0.34	0.94 ± 3.63	0.47 ± 0.45	0.43 ± 0.59	0.65 ± 0.24	0.63 ± 0.55	0.61 ± 1.34
NO_3	33 ± 47	39 ± 39		68 ± 46		47 ± 38	41 ± 45
Ag*	0.33 ± 0.117	0.5 ± 0	0.5 ± 0	0.603 ± 0.85	0.103 ± 0.024	0.775 ± 0.91	0.526 ± 0.666
Al	0.026 ± 0.031	0.015 ± 0.019	0.066 ± 0.083	0.104 ± 0.106	0.024 ± 0.163	0.008 ± 0.019	0.036 ± 0.084
As	0.024 ± 0.103	0.005 ± 0.006	0.055 ± 0.136	0.019 ± 0.023	0.001 ± 0.001	0.011 ± 0.031	0.016 ± 0.062
B	1.679 ± 1.207	0.821 ± 0.403	2.175 ± 2.082	1.697 ± 1.11		1.192 ± 0.812	1.491 ± 1.241
Ba	0.028 ± 0.029	0.057 ± 0.09	0.029 ± 0.024	0.073 ± 0.068	0.044 ± 0.038	0.045 ± 0.041	0.049 ± 0.071
Ce*	0.76 ± 1.726	0.5 ± 0	0.5 ± 0	0.577 ± 0.302	1.686 ± 13.23	0.208 ± 0.219	0.635 ± 5.023
Co	0.005 ± 0.01	0.008 ± 0.018	0.004 ± 0.002	0.011 ± 0.017	0.099 ± 0.574	0.006 ± 0.039	0.018 ± 0.208
Cr	0.011 ± 0.011	0.01 ± 0.009	0.013 ± 0.013	0.025 ± 0.048	0.01 ± 0.006	0.018 ± 0.041	0.015 ± 0.03
Cs*	0.5 ± 0.9	6.34 ± 19.8	17.73 ± 44.23	1.03 ± 1.45	0.8 ± 2.98	0.33 ± 0.71	2.8 ± 15.73
Cu	0.004 ± 0.007	0.003 ± 0.003	0.005 ± 0.021	0.018 ± 0.023	0.006 ± 0.026	0.005 ± 0.009	0.007 ± 0.02
Fe	0.572 ± 2.845	0.233 ± 0.569	0.15 ± 0.394	0.398 ± 1.868	0.494 ± 2.566	0.019 ± 0.072	0.283 ± 1.603
Li	0.167 ± 0.521	0.065 ± 0.174	0.08 ± 0.062	0.022 ± 0.032	0.026 ± 0.037	0.004 ± 0.008	0.057 ± 0.223
Mn	0.344 ± 0.62	0.216 ± 0.392	0.177 ± 0.349	0.525 ± 1.514	0.435 ± 1.642	0.091 ± 0.414	0.271 ± 0.912
Mo*	9.4 ± 24.5	7.4 ± 22.6	11.5 ± 17.2	10.9 ± 18.4	5.5 ± 9.7	14.2 ± 28	10.6 ± 22.6
Ni	0.02 ± 0.03	0.04 ± 0.06	0.03 ± 0.04	0.03 ± 0.08	3.05 ± 18.51	0 ± 0.01	0.41 ± 6.68
Rb	0.02 ± 0.02	0.03 ± 0.04	0.03 ± 0.03	0.14 ± 0.18	0.01 ± 0.01	0.02 ± 0.01	0.03 ± 0.08
Si	21.17 ± 10.91	24.72 ± 12.19	23.57 ± 11.55	31.41 ± 15.07	21.32 ± 4.02	25.52 ± 9.35	24.29 ± 11.17
Sr	0.56 ± 0.73	1.31 ± 3.49	0.94 ± 1.21	3.49 ± 3.26	0.48 ± 0.28	0.62 ± 0.68	1.1 ± 2.05
Th*	0.19 ± 0.21	0.5 ± 0	0.5 ± 0	0.5 ± 0	0 ± 0.01	0.19 ± 0.19	0.28 ± 0.23
U*	1.59 ± 2.48	1.23 ± 0.76	2.43 ± 3.2	13.67 ± 27.9	1.1 ± 2.46	4.74 ± 8.4	4.17 ± 12.23
V	0.02 ± 0.02	0.01 ± 0.01	0.02 ± 0.03	0.05 ± 0.06	0 ± 0	0.01 ± 0.01	0.02 ± 0.03
W*	26.2 ± 60.1	7.1 ± 26	21.1 ± 45.5	3.3 ± 14.5	9.5 ± 30.3	0.7 ± 2.4	12.1 ± 49
Zn	0.027 ± 0.083	0.029 ± 0.093	0.125 ± 0.697	0.254 ± 1.313	0.026 ± 0.078	0.018 ± 0.032	0.127 ± 1.15
Au^c #	2.62 ± 2.65	2.29 ± 3.59	0.83 ± 1.28	1.66 ± 2.4	1.18 ± 2.62		5.04 ± 43.64
Pt^c #	0.99 ± 1.36	3.86 ± 16.73	1.83 ± 3.15	1.55 ± 2.04	0.98 ± 4.22		2.64 ± 9.09
Pd^c #	0.63 ± 0.41	0.54 ± 0.07	0.9 ± 0.88	0.96 ± 1.98	1.92 ± 3.29		1.09 ± 2.06
Ag^c *	9.26 ± 12.7	40.53 ± 169	32.65 ± 74.37	51.1 ± 108.22			37.57 ± 102.74
Bi^c *	1.29 ± 1.51	2.54 ± 6.2	0.46 ± 0.61	0.89 ± 0.7			1.61 ± 4.1

All values in mg/L, except * µg/L and # ng/L.
WT = Water table depth. C = extracted by activated carbon.

5. HARMONY/CAMELOT

5.1 Site description and sampling

The Harmony deposit and Camelot exploration area (Figure 12) are immediately north of Leinster and lie within the Agnew - Wiluna greenstone belt (Figure 2). This belt is highly mineralized, hosting the Mt Keith, Honeymoon Well, Six Mile Well, Perseverance and Rocky's Reward deposits. Originally thought to be an intrusive dunite-hosted deposit (Martin and Allchurch, 1975; Billington, 1984; Marston et al., 1981), Perseverance and Rocky's Reward are now considered to be volcanic-hosted deposits, related to komatiite flows which underlie a large, extrusive dunite body (Barnes *et al*., 1988a,b). The linear structure of the deposit suggests that the NiS accumulated in a rifting fracture zone by hydrothermal processes at the time of tectonic activity, with the Harmony ore body inserted between two large blocks of non-sulphidic felsic volcanics.

The Harmony/Camelot area has undergone extensive folding and faulting activity, with stratigraphic units dipping 70-80°W. The north-south trending Perseverance Fault separates the surrounding granites from the ultramafic/felsic volcanic/sedimentary belts (Figure 12). Harmony was sampled prior to mining and data is combined with the results generated from this study. This area will be discussed in detail as it allows the clearest demonstration of the effectiveness of hydrogeochemistry to delineate sulphide chemistry. The blue shaded areas in Figure 12 delineate groundwaters whose characteristics indicate presence of sulphides: as per the discussion in Section 3.3, this includes groundwaters which have one or more of the following characteristics:

(i) reduced (Eh< 300 mV) – observed for deeper waters due to sulphides at depth
(ii) slightly to very acid (pH < 6.5) – sulphide oxidation, especially when Fe-rich
(iii) Fe present (> 0.1 mg/L) – released from sulphides
(iv) Al clearly above detection (> 0.03 mg/L) – permanent or transient acidity attacking wall rocks

This grouping therefore is independent of sampling depth, as it includes the varying characteristics of waters contacting sulphides (Section 3.3). Sulphide dominated areas include (Figure 12):

A: Most of the Endurance area
B: Parts of the Knights area, particularly associated with the main mineralisation
C: A large, weakly mineralised, area in the middle of Excalibur
D: The main Harmony ore body
E: Sulphidic Cherts west of Harmony
F: Weakly mineralised sulphides east of Harmony

How the properties of these “sulphide” groundwaters relate to NiS exploration are discussed below.

5.2 Lithological Indicators

Several elements have been identified as lithological indicators. The most obvious is Cr (Figure 13), which indicates ultramafic rocks. The higher dissolved Cr concentrations (0.018 -0.310 mg/L) occur over the ultramafic rocks, although some low Cr concentrations were also determined from samples taken from ultramafic rocks. In middle to upper groundwaters (*i*.e., weakly reducing to oxidising) Cr is dominantly released into groundwater in oxidized environments as Cr^{6+}, which is readily reduced by dissolved Fe and Mn to Cr^{3+} (Gray, 2003).

$$CrO_4^{2-} + 3Fe^{2+} + 8H_2O \rightarrow Cr(OH)_3 + 3Fe(OH)_3 + 4H^+$$

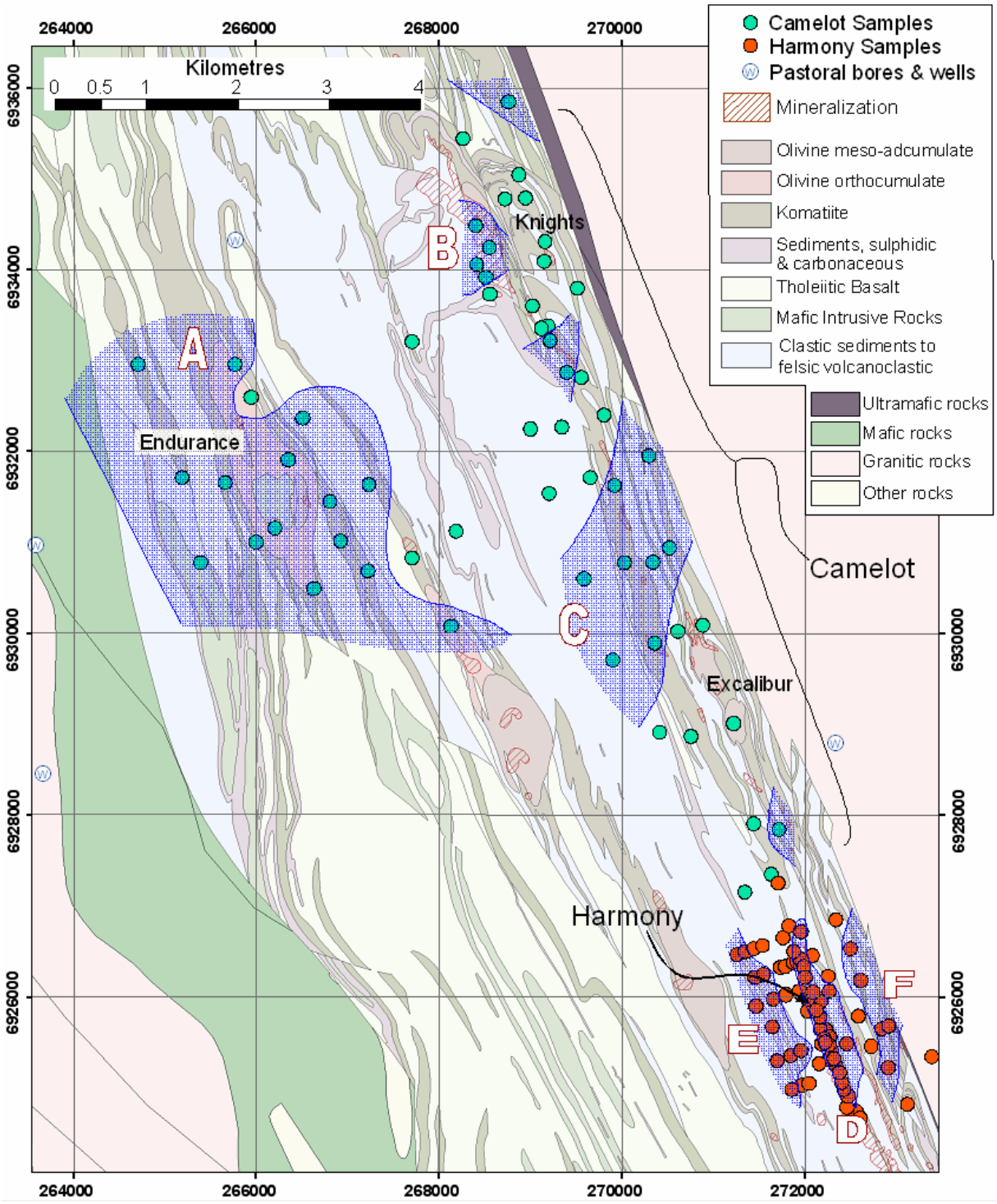

Figure 12: Detailed geology and sample locations of the Harmony/Camelot region. Blue shaded areas A-F are influenced by sulphide chemistry (Eh< 300 mV, &/or pH < 6.5, &/or Fe > 0.1 mg/L, &/or Al > 0.03 mg/L), as described in Section 5.1.

Trivalent Cr has a similar low solubility to Fe^{3+}: thus, mineralised ultramafics would be expected to have lower Cr concentrations due to Cr^{6+} reduction by Fe^{2+} (and possibly Mn^{2+}) released from the weathering of sulfides. Comparing the Cr to the Fe and Mn concentration plots for this region (Figure 18 and Figure 26) shows a slight negative relationship - Mn, and to a lesser degree Fe, have .higher concentrations at the sites where Cr is lower.

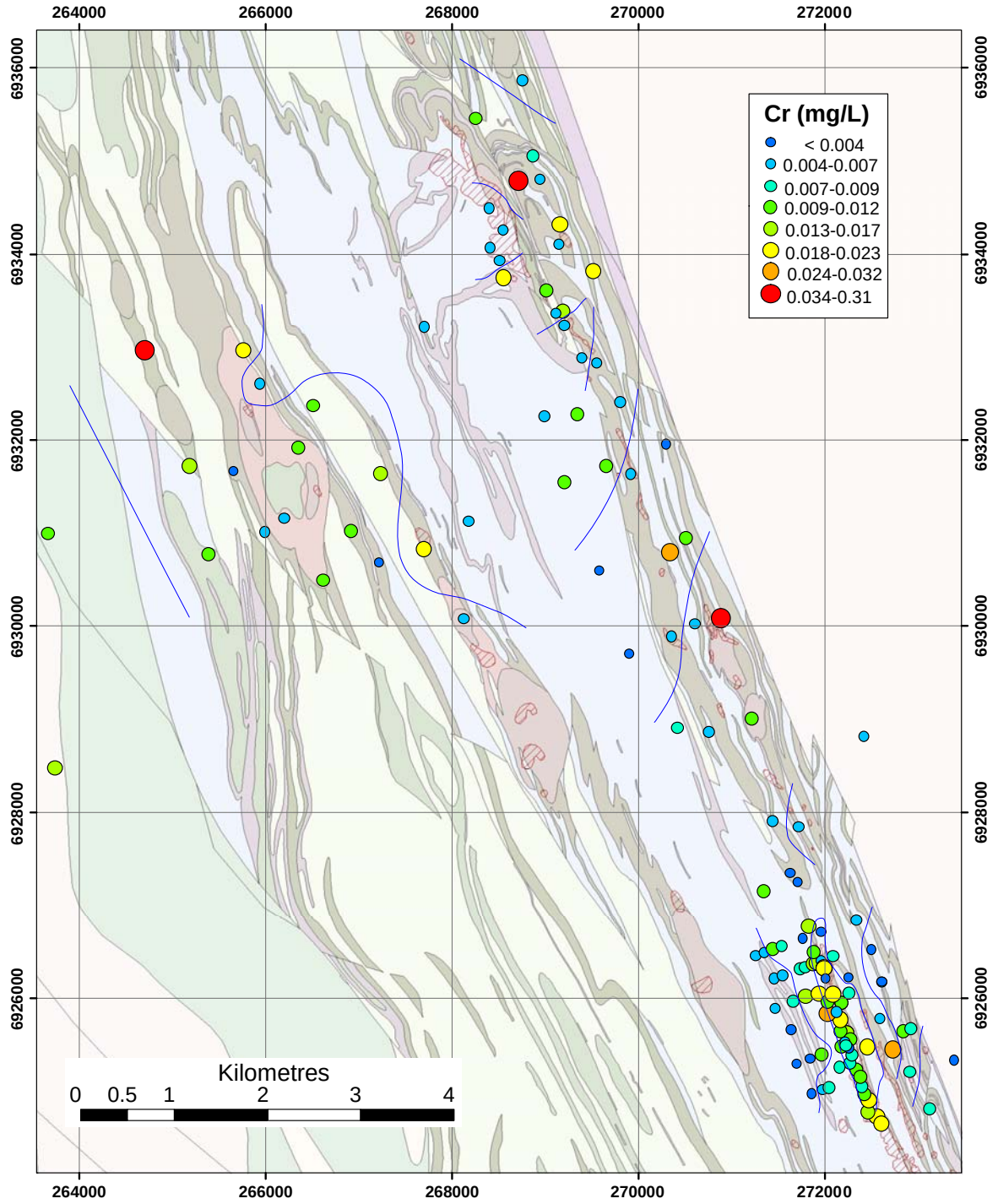

Figure 13: Dissolved Cr distribution at Camelot.

However, the antipathetic relationship between Cr and Fe/Mn does not occur in very reduced waters (Eh < 150 mV; the dark blue circles in Figure 16) such as Endurance where dissolved Cr, Fe and Mn coexist (Figure 13, Figure 18 and Figure 26). This is possibly because in highly reducing, sulphide dominated environments Cr can be reduced below the common valence state of 3+ to soluble Cr^{2+}. Thus, high Cr concentration (> 0.01 mg/L) is a positive indicator of ultramafic rocks, although there can be false negatives. Regionally, low-S ultramafics such as at Lawlers have stronger Cr anomalies, possibly due to low dissolved Fe or to higher Cr in the rocks. The sulphidic sediments and felsics immediately to the west of Harmony, Excalibur and Knights are generally low in dissolved Cr (< 0.01 mg/L) (Figure 13), consistent with lithological control.

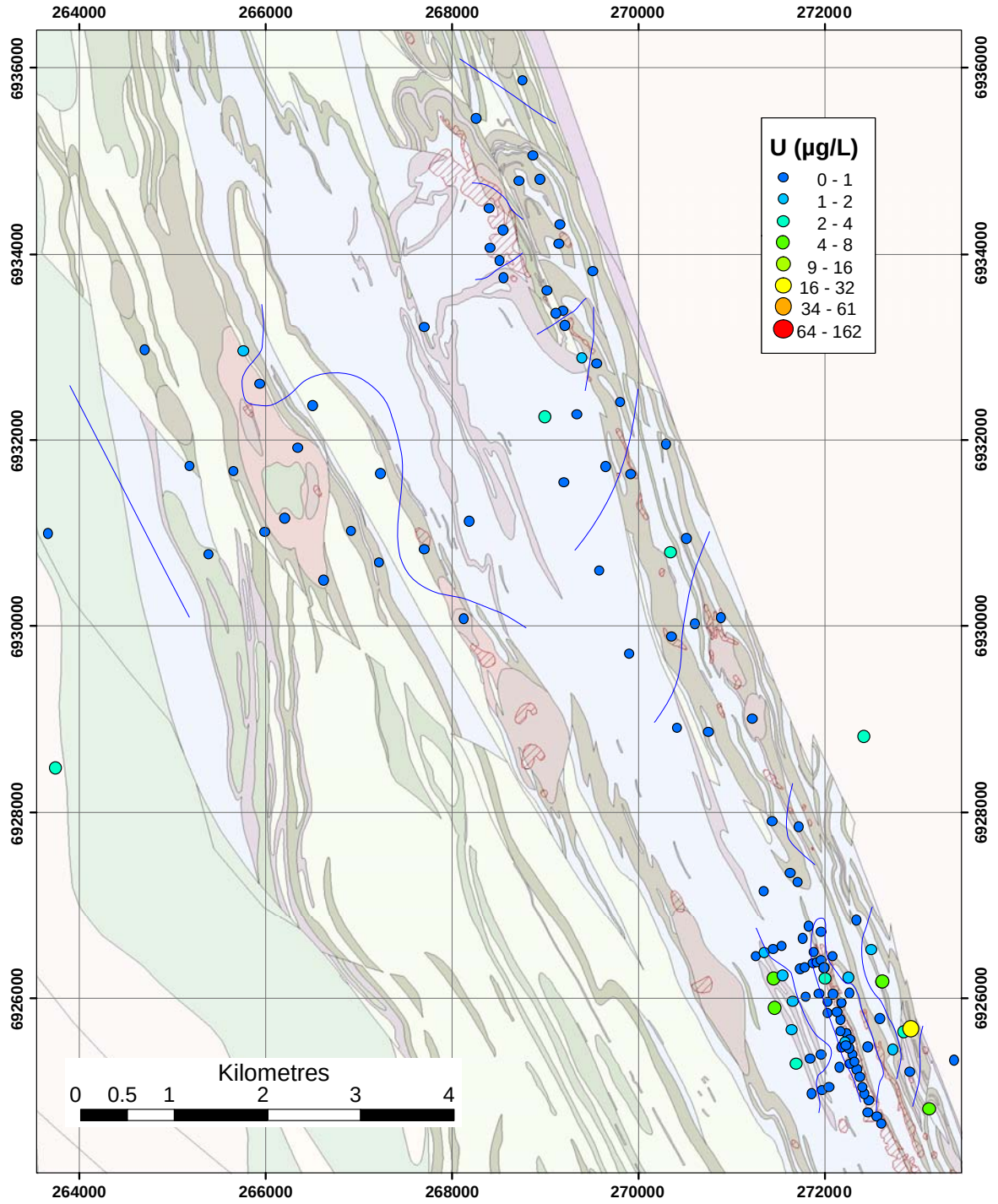

Figure 14: Dissolved U distribution at Camelot.

Another lithological indicator is U, which appears to be higher over granitic rocks east of Harmony/ Camelot (Figure 14), although the contrast appears subdued. This may be due to pH, phosphate and carbonate controls on U solubility influencing absolute concentrations. One strategy to correct for this effect is to calculate saturation of groundwaters with respect to relevant secondary minerals (Section 2.2). This ensures a much better lithological correlation: groundwaters are close to rutherfordine (UO_2CO_2) saturation in or immediately adjacent to the granites east and west of the Camelot area (Figure 15). Most probably this does not reflect control by rutherfordine itself, but more likely by more common and less soluble U minerals such as autinite or carnotite. However, SI data for these minerals are not shown here as they are more problematic due to P and V concentrations commonly being close to or below detection at Camelot.

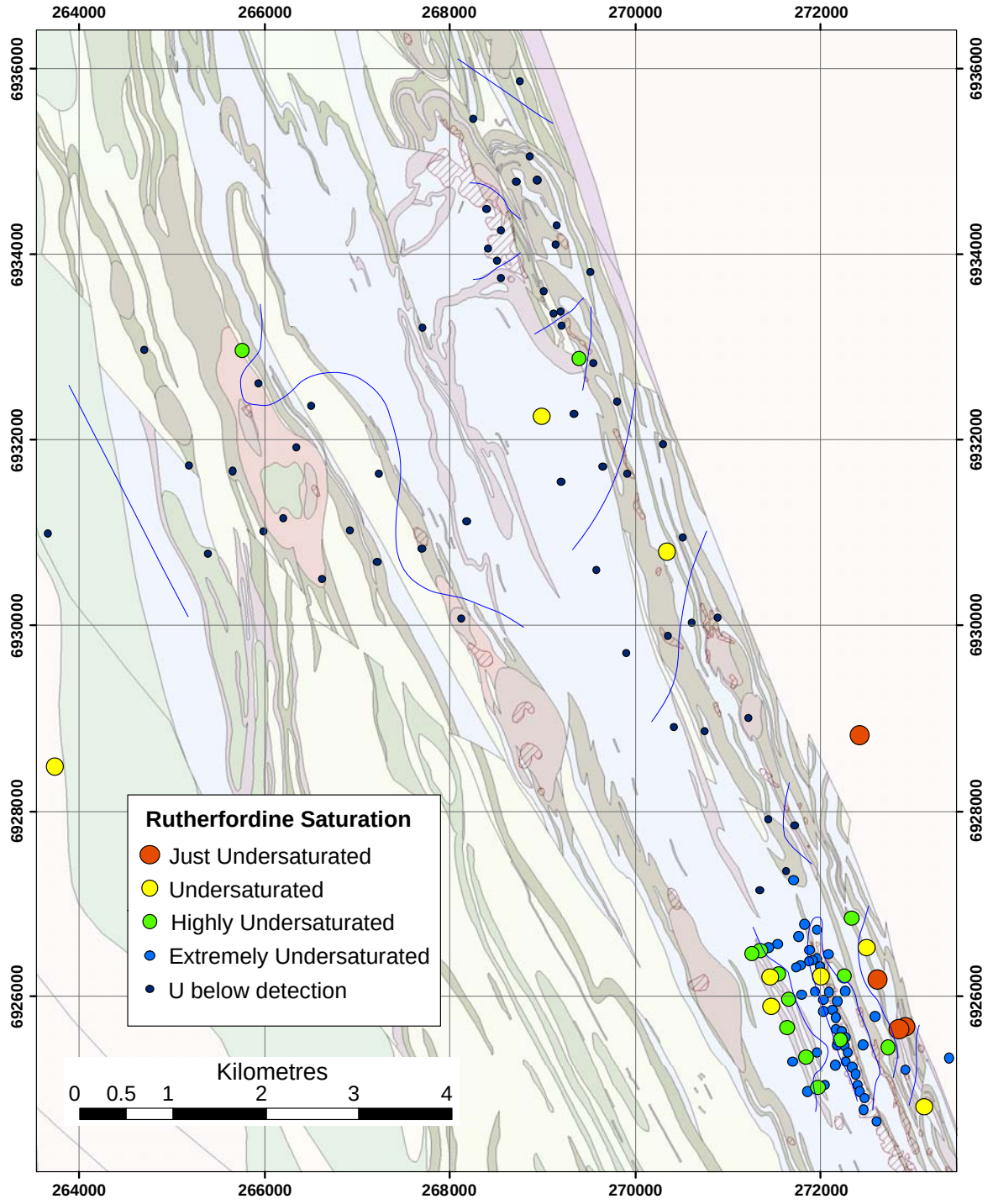

Figure 15: Distribution of Rutherfordine (UO_2CO_3) SI at Camelot.

5.3 Sulphide Indicators

Although several parts of the Camelot area are affected by sulphides (Figure 12), the groundwater effects differ because of varying depths of groundwater relative to the depth of weathering, and due to the sulphide mineralogy. Groundwaters at the Harmony deposit (Area D) are more oxidised than other sites (dominantly > 360 mV; Figure 16), with relatively shallow sampled groundwaters (less than 50 m depth) intersecting deeply weathered mineralisation. Harmony groundwaters are also subtly but clearly more acidic (commonly < pH 6.8 and down to pH 5, with surrounding groundwaters commonly > pH 7.0; Figure 17).

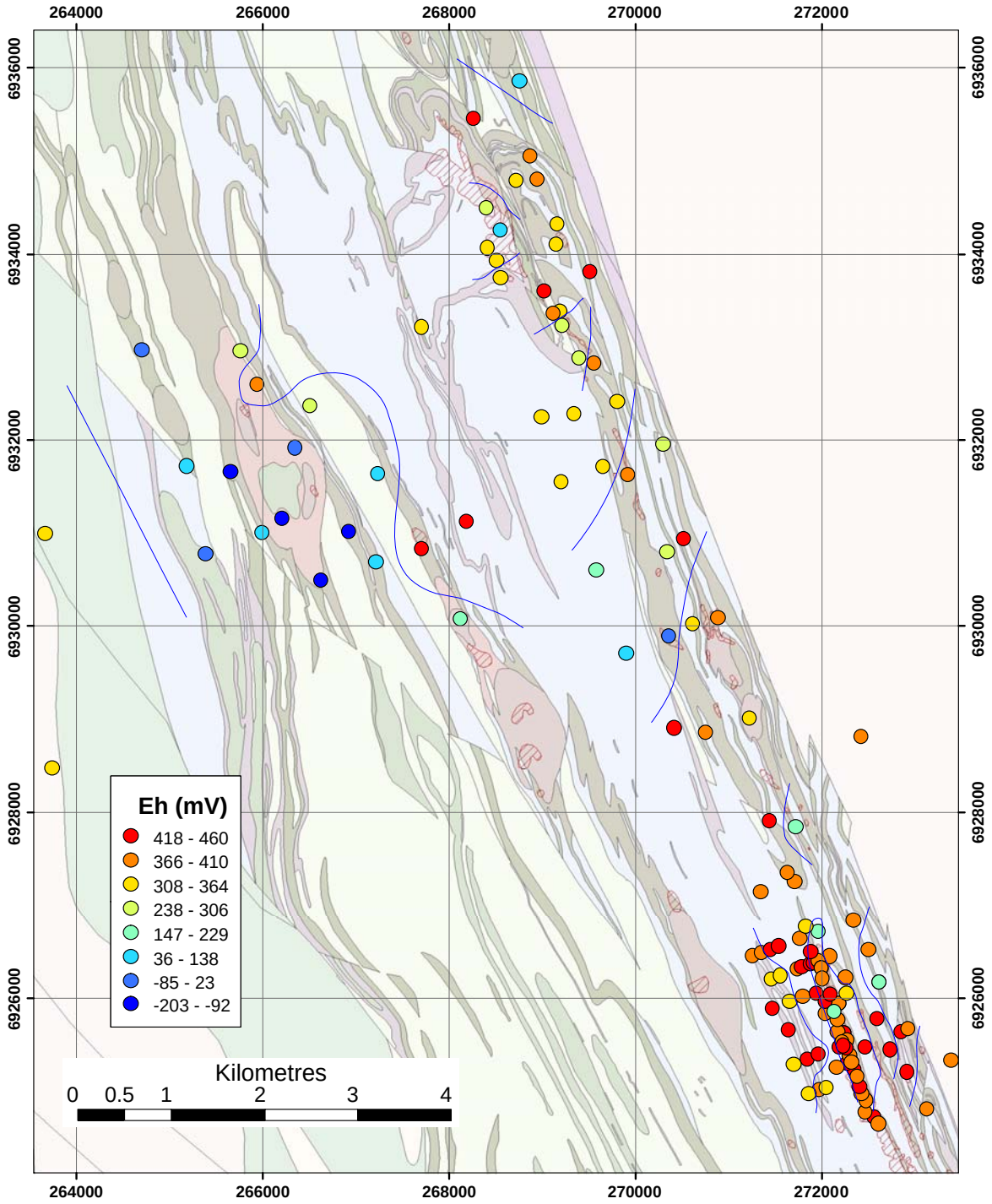

Figure 16: Groundwater Eh values at Camelot. Reduced zones are shown in blue.

In contrast, Endurance (Area A) is commonly highly reduced (Figure 16), reflecting greater regolith truncation and a greater proportion of groundwaters sampled from deeper bores. Area C shows similar Eh and pH characteristics to Endurance, though, as will be discussed later, its minor element composition is different. Properties of groundwaters from the Knights area are intermediate to these two regions.

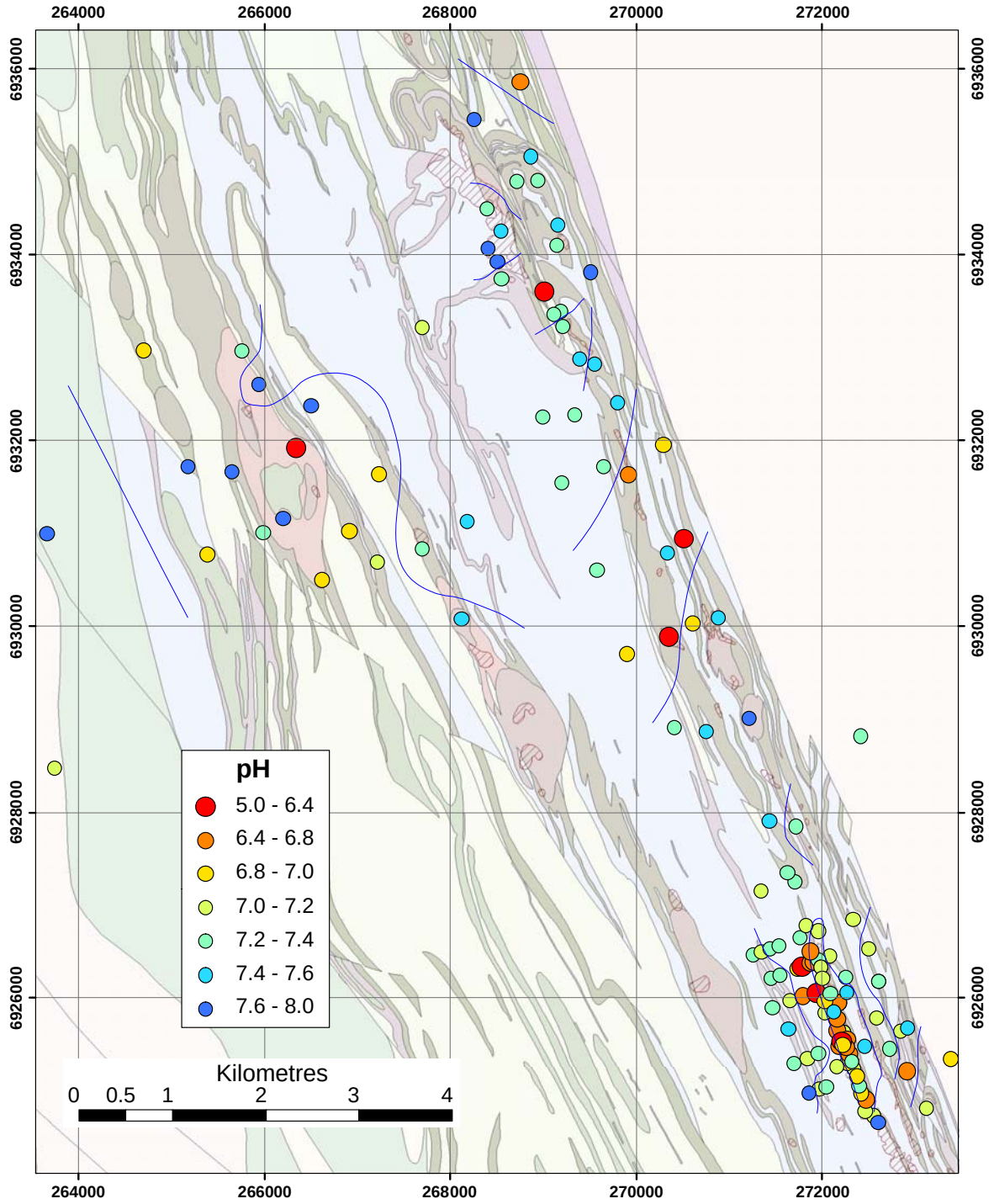

Figure 17: Groundwater pH values at Camelot.

The regions influenced by sulphide chemistry are also well defined by Fe concentrations (Figure 18). Dissolved Fe is highest around the Endurance area, suggesting Fe release from sulphides. With one exception, Harmony and Knights have only moderate Fe concentrations. As with U (Section 5.2), SI analyses show additional properties. Groundwaters at and around Harmony are all oversaturated with respect to ferrihydrite (*i.e*, ferric hydroxide; Figure 19) reflecting deep oxidization, whereas there is a greater tendency to saturation with respect to $Fe_3(OH)_8$ (a mixed valence Fe hydroxide; Figure 20), , in the sulphidic cherts west of Harmony (Area E) and the mineralised zone at Knights, suggesting these areas are less strongly oxidized than Harmony. As expected, sulphidic groundwaters at Endurance and Excalibur are mainly undersaturated with respect to these Fe minerals, indicating reduced groundwaters.

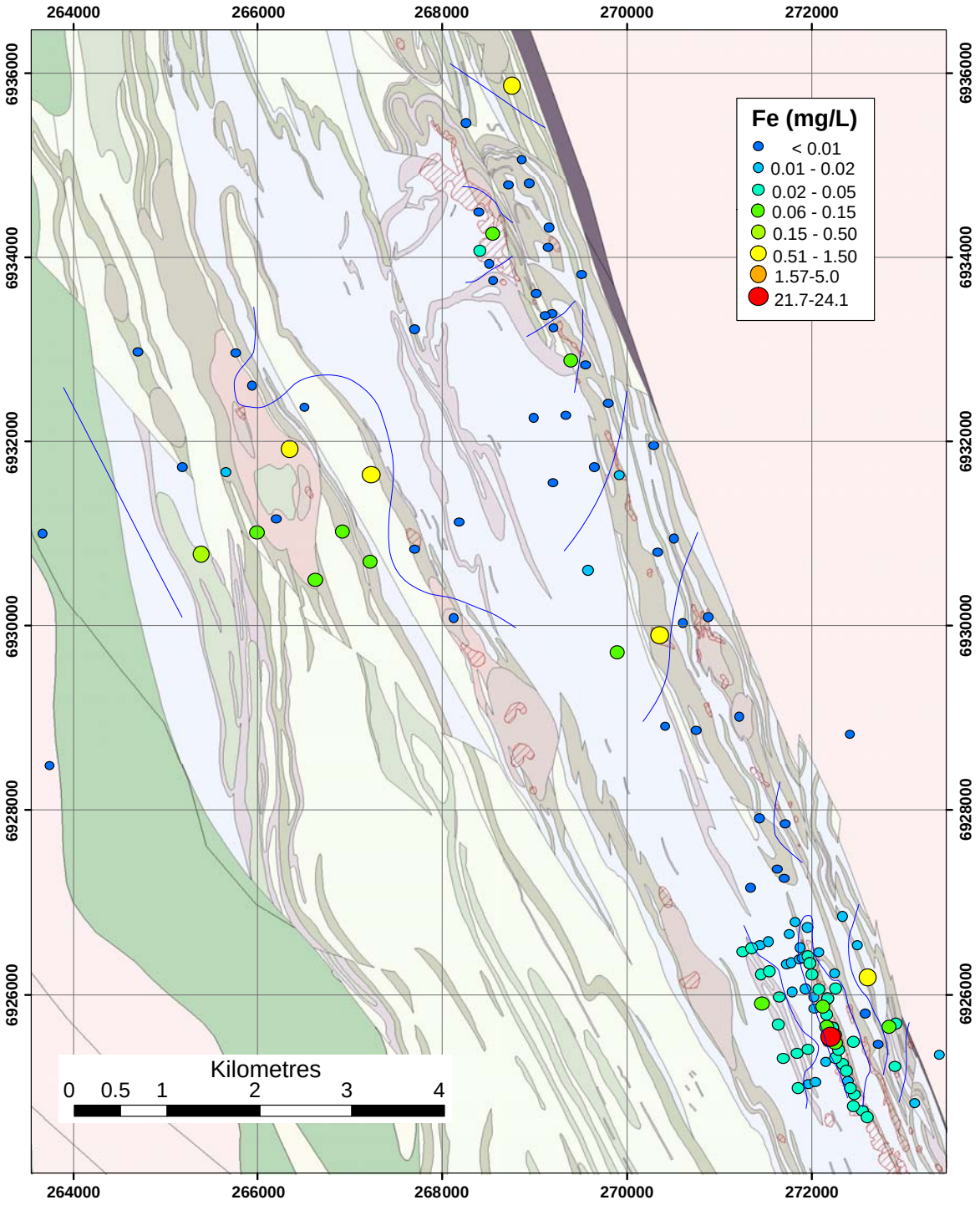

Figure 18: Dissolved Fe distribution at Camelot.

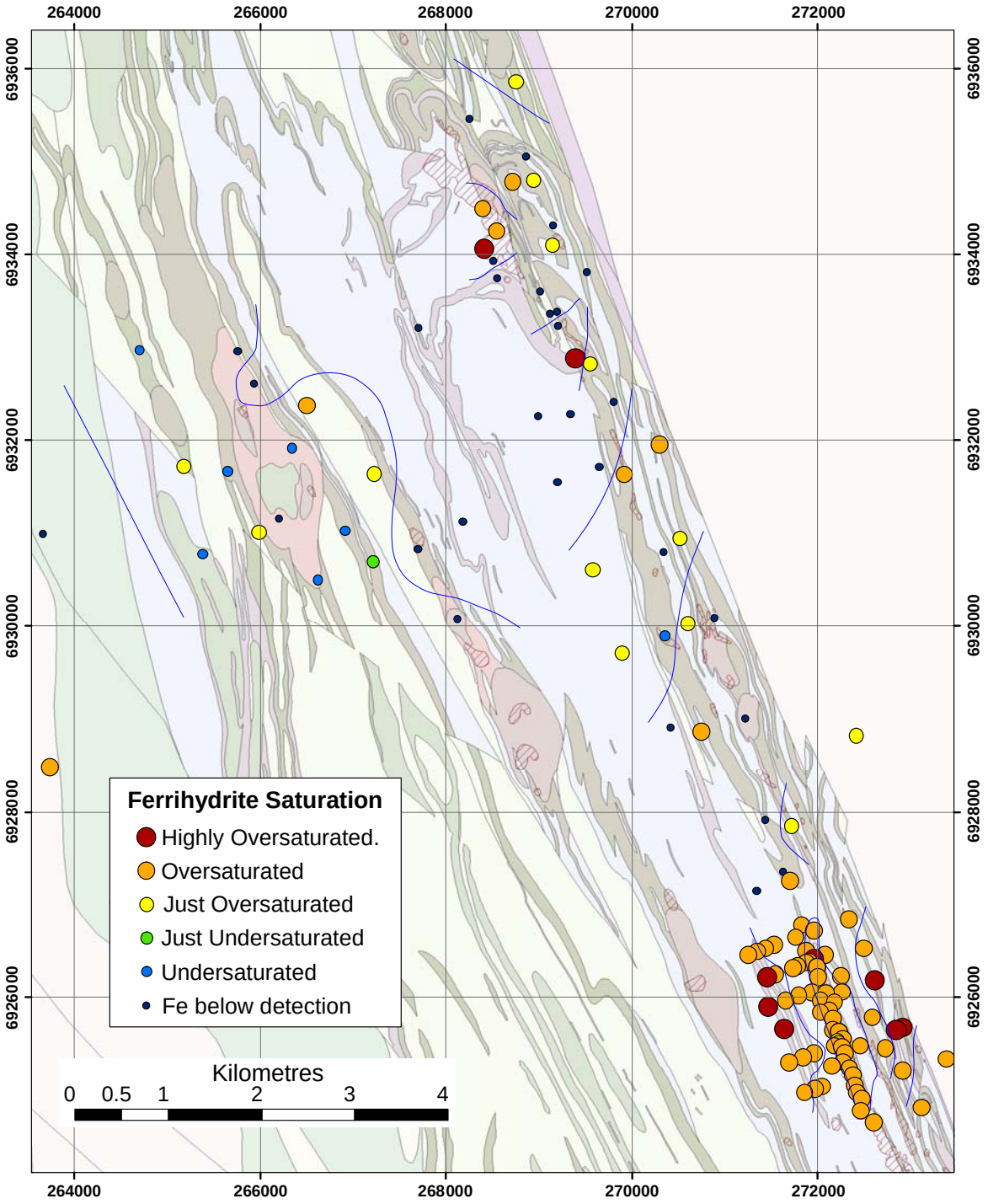

Figure 19: Distribution of groundwater saturation index of ferrihydrite [$Fe(OH)_3$] at Camelot.

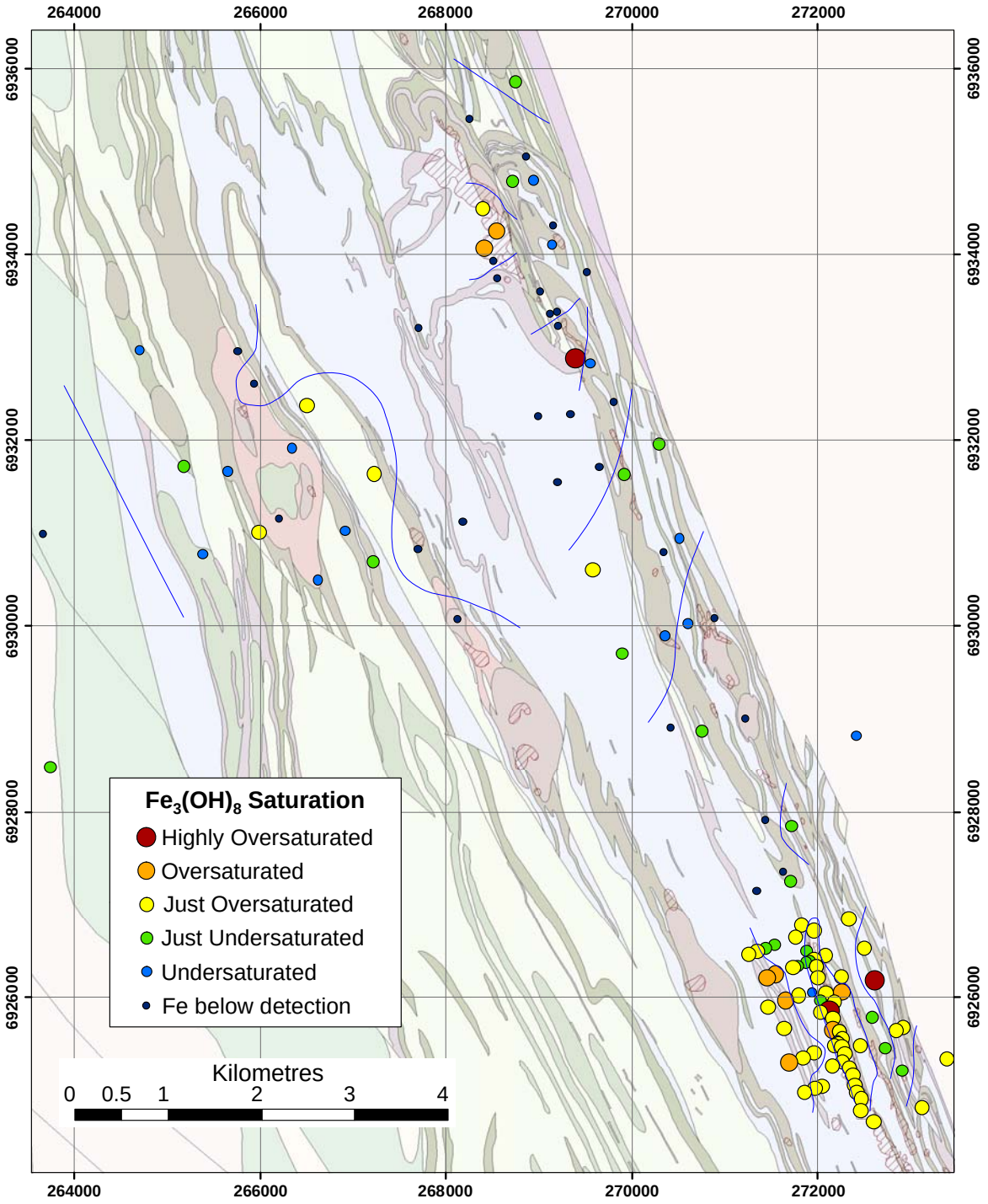

Figure 20: Distribution of groundwater saturation index of $Fe_3(OH)_8$ at Camelot.

Apart from one high dissolved Al (> 0.5 mg/L; Figure 21) and Ce (> 0.1 mg/L: Figure 22) groundwater at Harmony due to acid (< pH 5.5) water, Al and REE values are low in the Harmony/Camelot area, as expected in groundwaters with pH > 6. However, dissolved Al does show a subdued (0.01 – 0.1 mg/L) halo around the Knights mineralisation as well as spot highs at Endurance and Excalibur (Figure 21). While some of the higher Al concentrations at Endurance and Excalibur can be related to specific low pH groundwaters, dissolved Al at Knights is highly anomalous for the observed pH. The disequilibrium is indicated by the solutions being over-saturated with respect to Al-phases such as kaolinite and alunite and saturated with respect to amorphous alumina - these minerals should be precipitating and removing Al from solution.

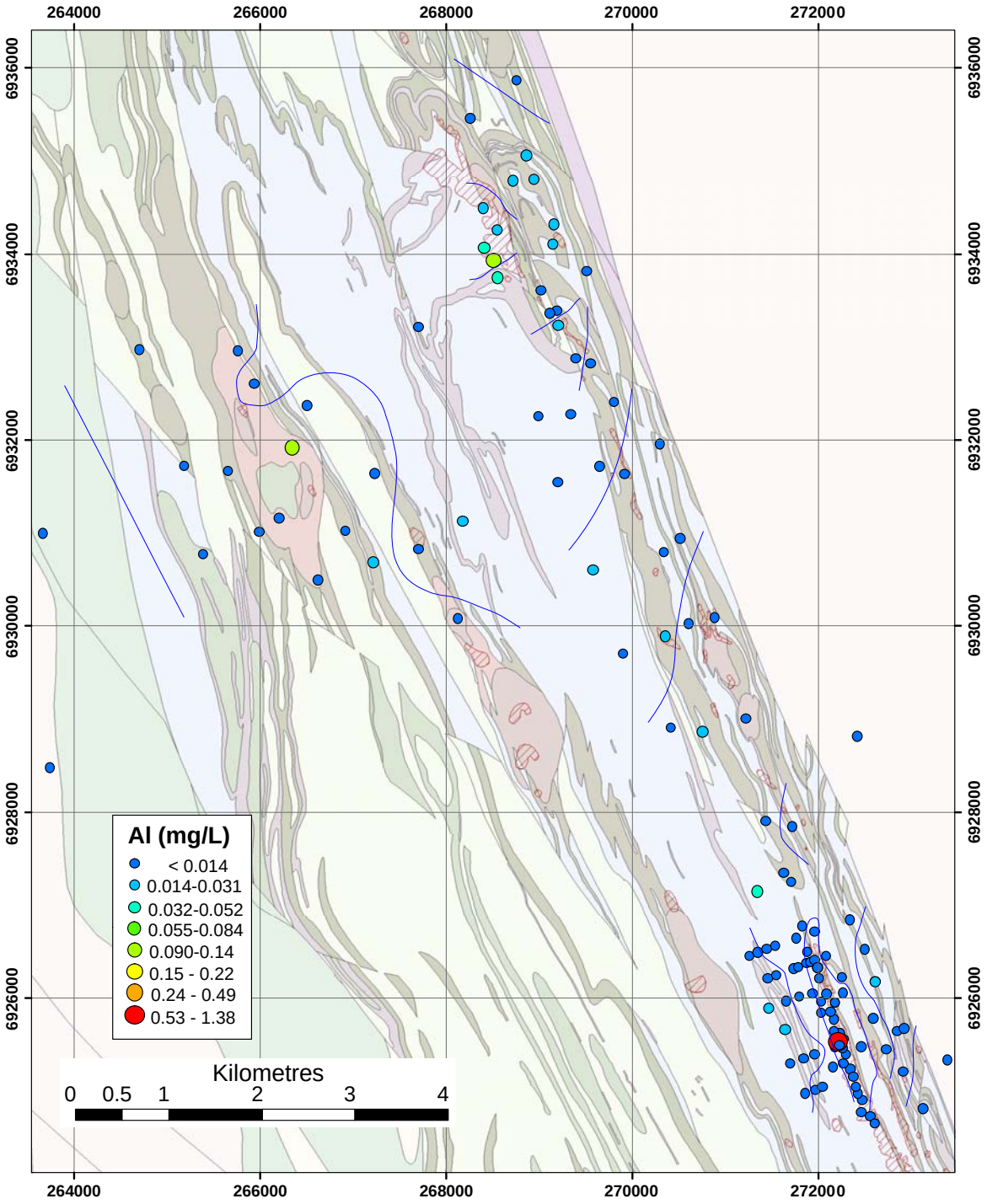

Figure 21: Dissolved Al distribution at Camelot.

Anomalously high dissolved Al can be explained by release from acid-initiated dissolution of primary minerals such as chlorite, with Al occasionally remaining in solution due to kinetic factors when the waters are neutralised by contact with carbonates or other phases.

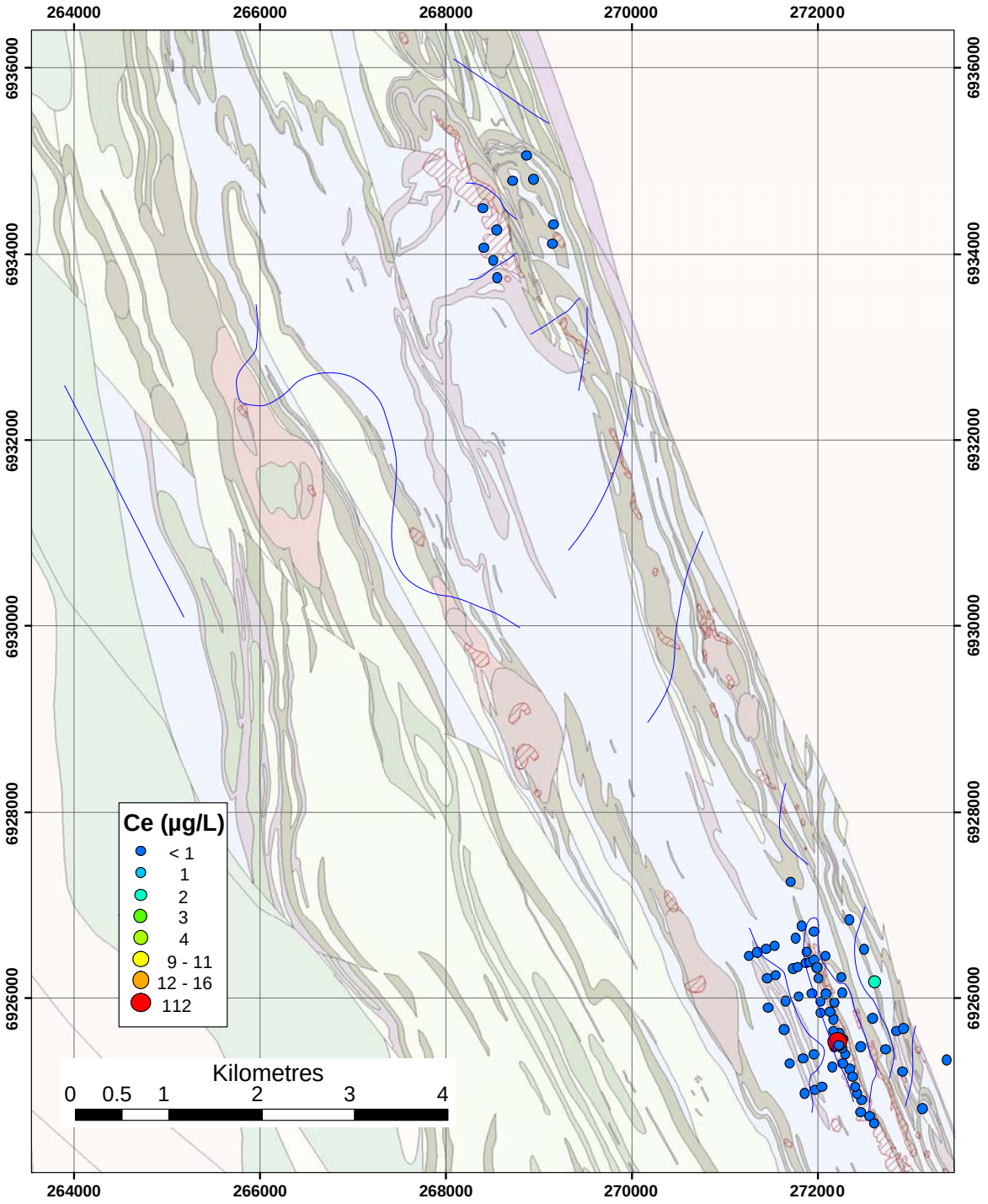

Figure 22: Dissolved Ce distribution at Camelot.

Depending on the depth of oxidation of the sulphides, and the mineralogy of the wall rocks, any acid production will potentially cause release of various minor elements. The Endurance area differs dramatically from other areas of Camelot, with a wide range of "felsic/granitic" elements elevated in the groundwaters. This includes Li (Figure 23), Ba (Figure 24), F (Figure 25), V and possibly Mn (Figure 26). These results suggest that weathering of sulphides at Endurance is producing significant acidity, *i.e.*, sulphides tend to be Fe- and/or pyrite-rich and acid groundwaters are attacking wall rocks and dissolving various elements, including Al and REE, which are mainly reprecipitated, and Li, Mn, Ba, F, V etc, which are generally conservative and give more well-defined anomalies.

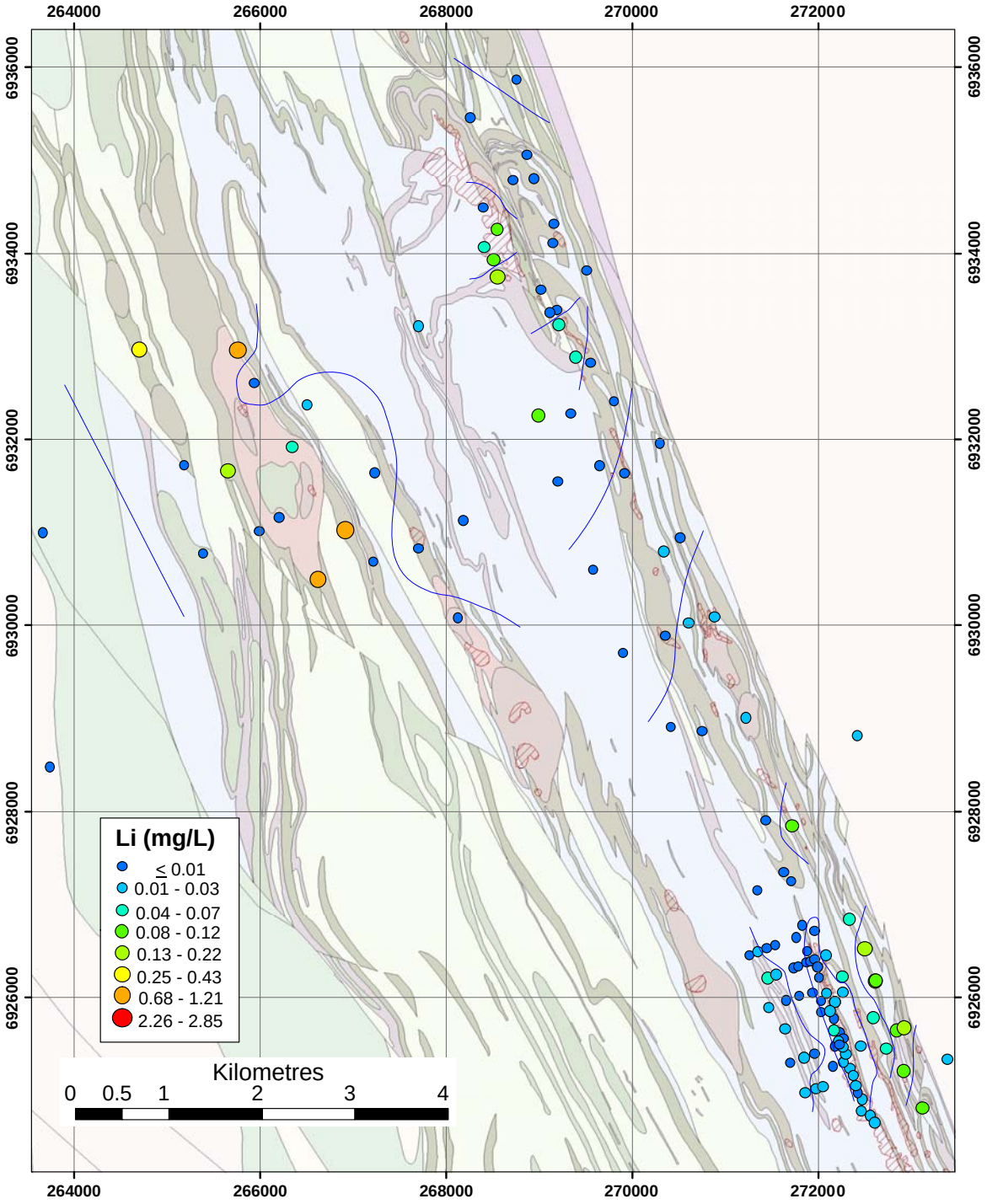

Figure 23: Dissolved Li distribution at Camelot.

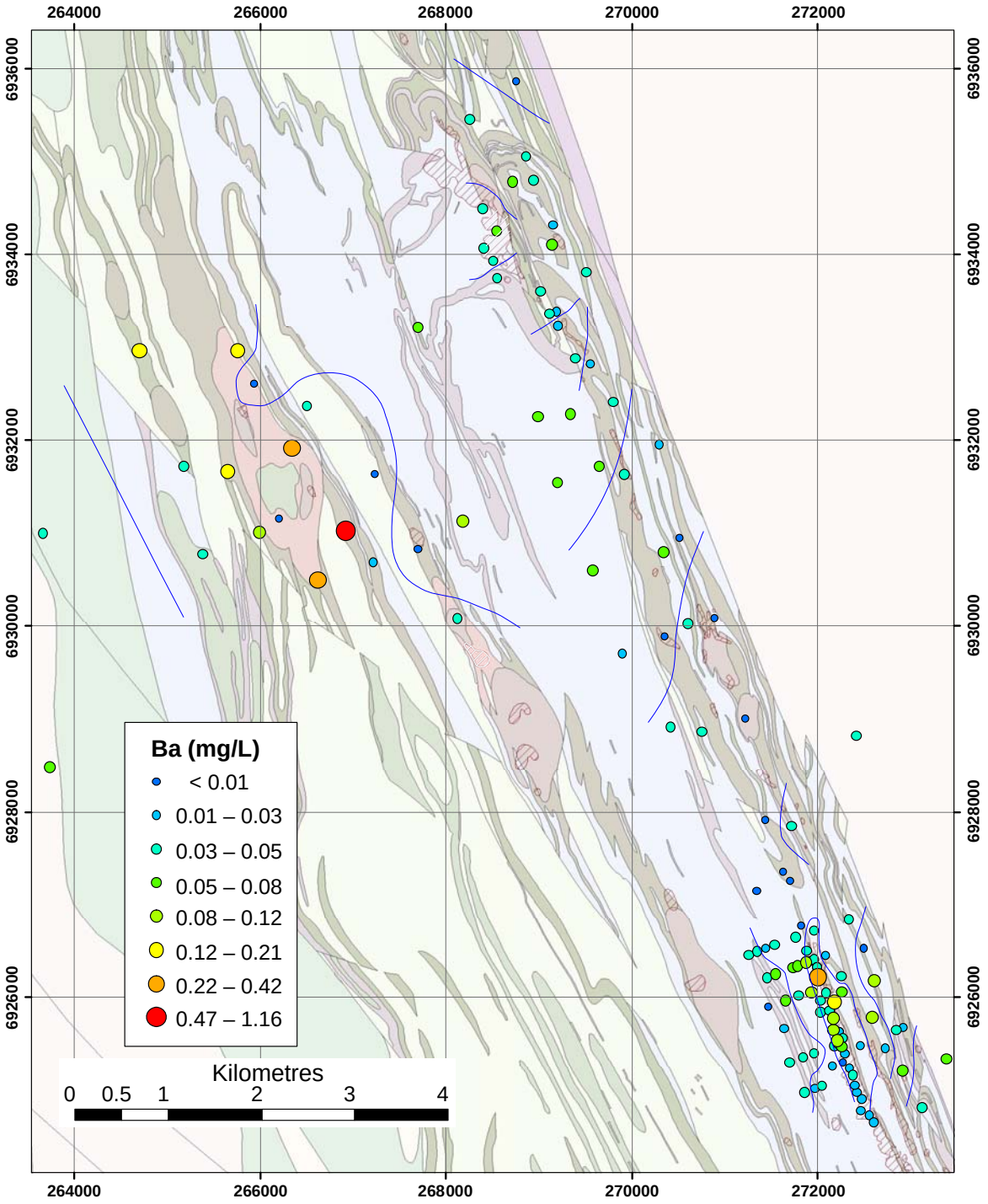

Figure 24: Dissolved Ba distribution at Camelot.

Thus, Li (Figure 23) and Mn (Figure 26) gave different responses to Al (Figure 21). Lithium concentration is much greater in the Endurance region relative to other areas; in particular, Li concentrations in the groundwater over Harmony are low, typically <0.03 mg/L. Reasons for the higher Li concentrations at Endurance could be related to the higher Fe concentration and in turn the metal:S ratio (Section 3.3). The Knights region contains a cluster of four moderate Li concentrations (~0.1 mg/L) directly over the mineralisation. A similar cluster of results occurs in groundwater approximately 1 km to the east of Harmony and trending parallel.

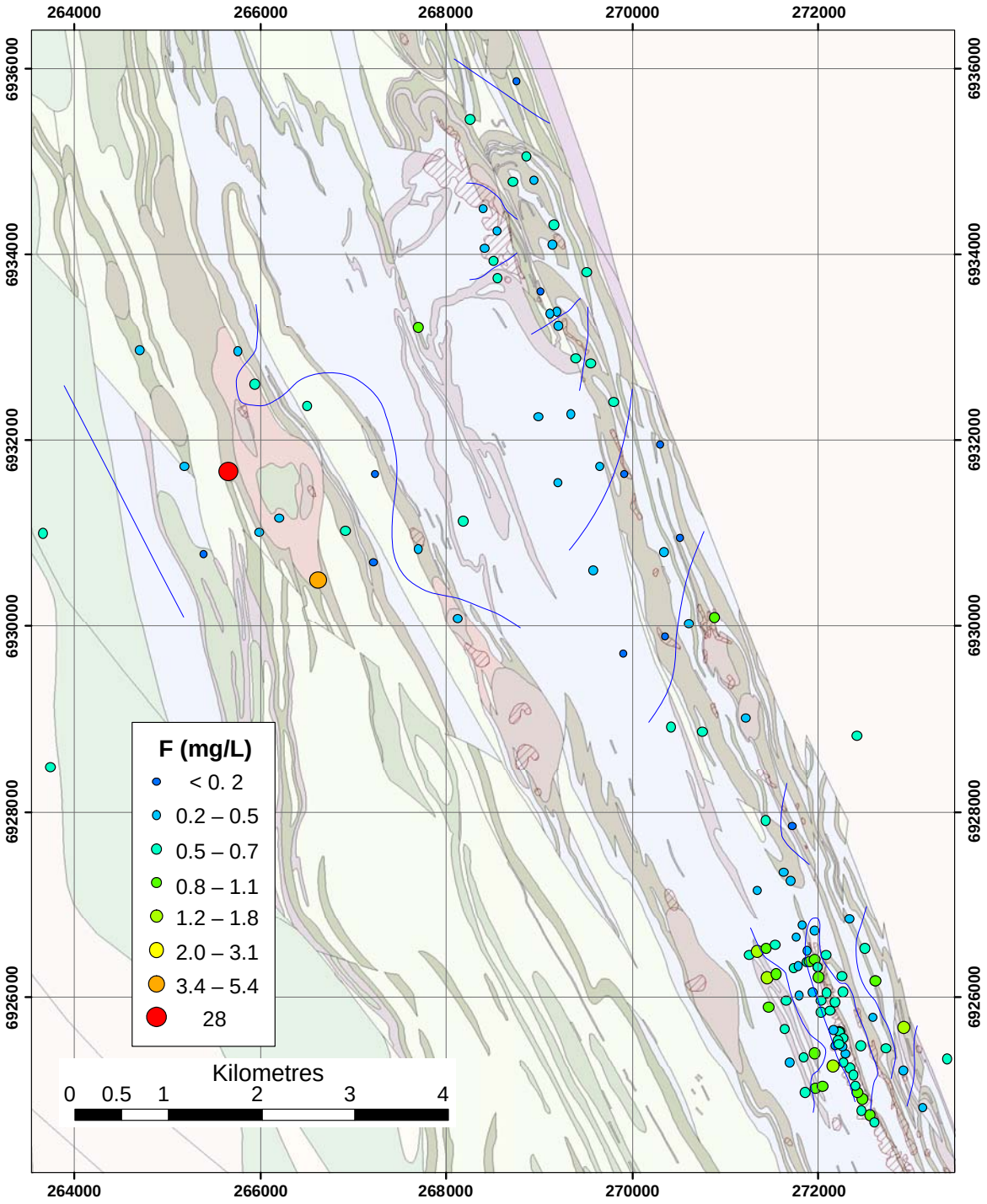

Figure 25: Dissolved F distribution at Camelot.

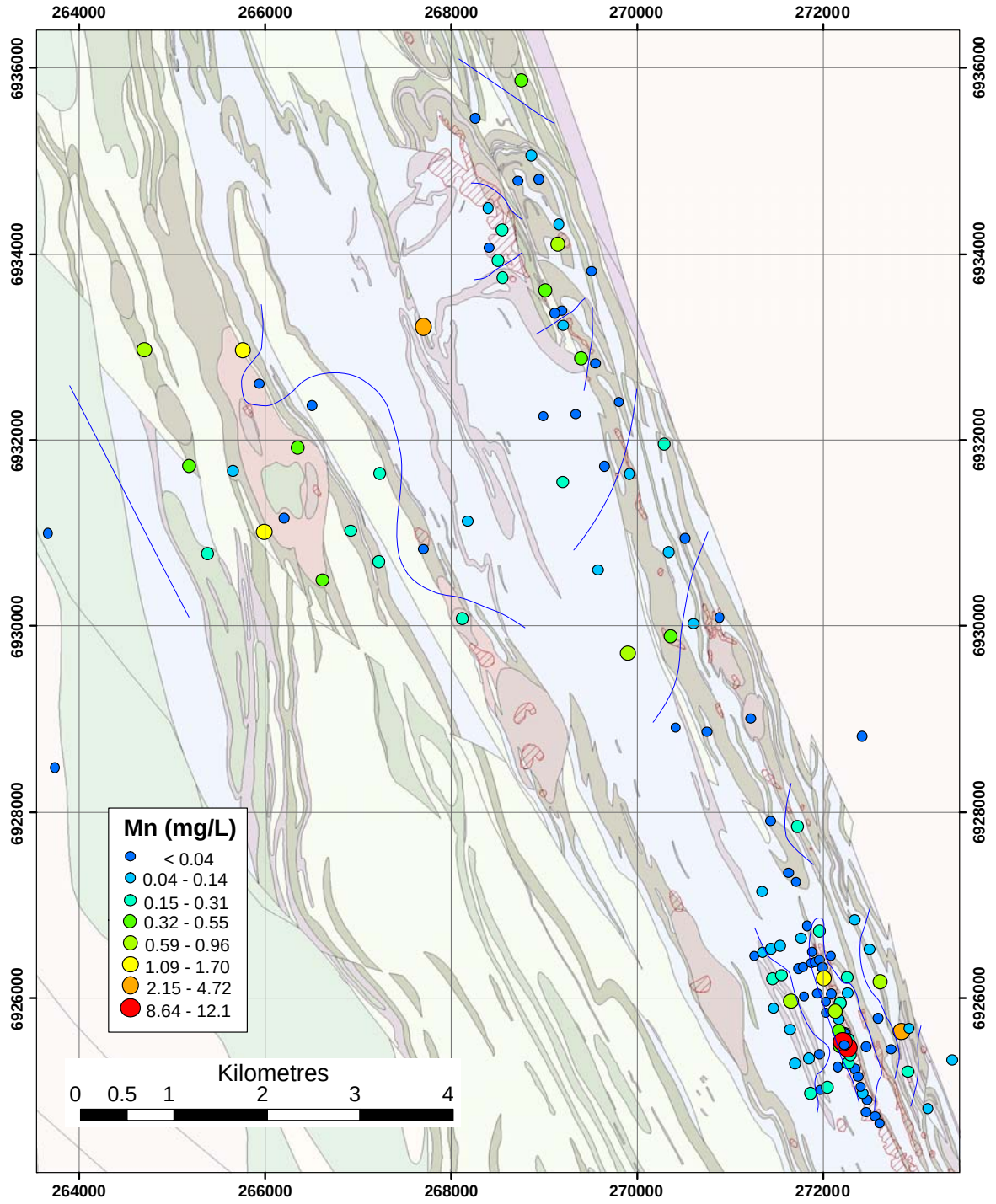

Figure 26: Dissolved Mn distribution at Camelot.

5.4 NiS Mineralisation Indicators

Results from the Harmony Ni deposit indicate that Ni and Co are effective groundwater indicators for mineralisation. These two elements have highly anomalous concentrations (> 0.07 mg/L Ni and > 0.01 mg/L Co) in the Harmony area with lower background values east and west (Figure 27 and Figure 28). Sporadic dissolved Ni highs around Harmony may represent minor NiS pods. The surrounding areas (*i*.e., Knights, Endurance, Excalibur) have lower dissolved Ni than at Harmony, though still commonly greater than 0.03 mg/L and regionally anomalous However, as will be discussed below, it becomes critical to distinguish Ni dissolved from NiS from that derived from acidic conditions caused by sub-economic or barren sulphides.

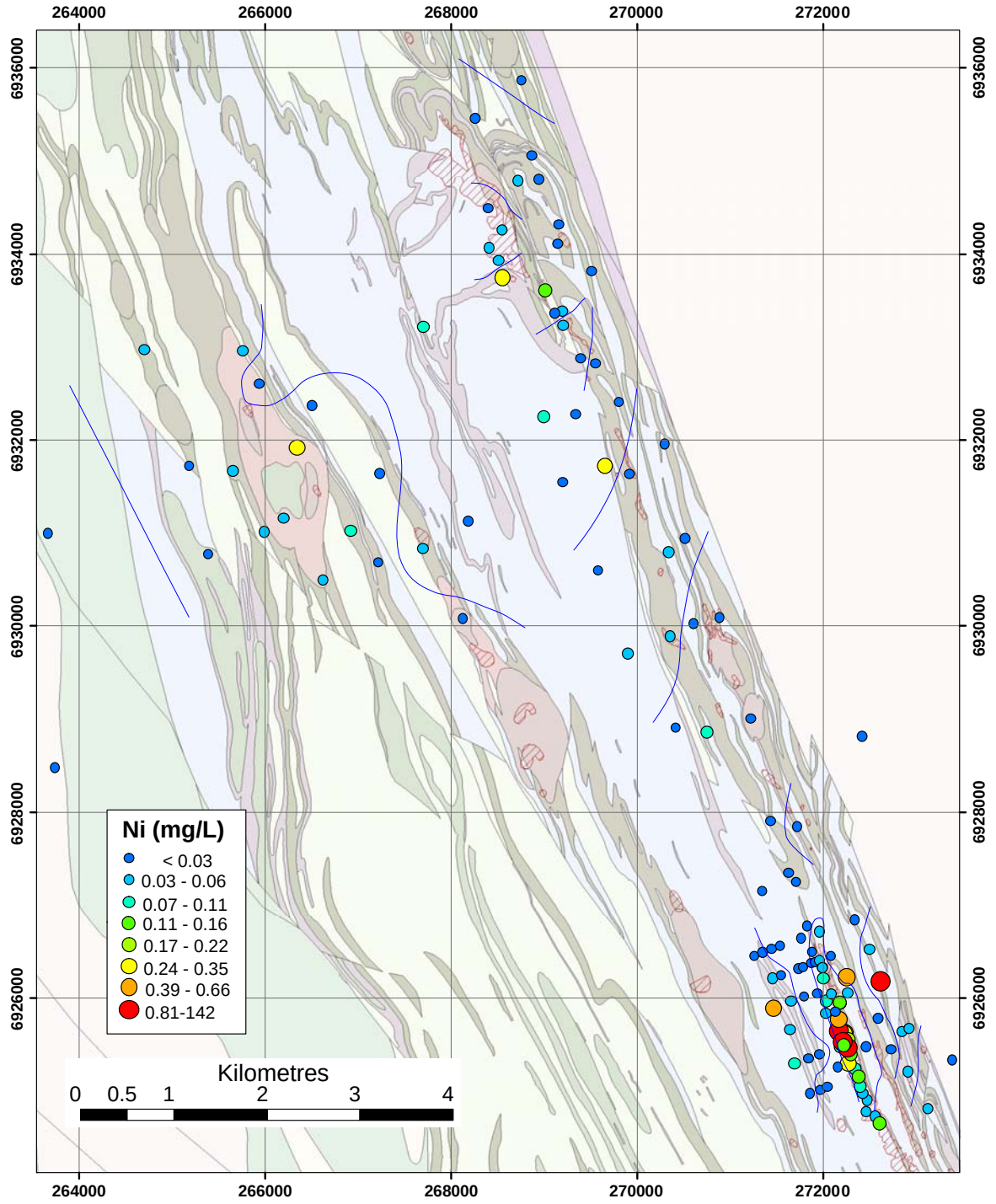

Figure 27: Dissolved Ni distribution at Camelot.

Higher dissolved Ni groundwater does not always have higher Co concentrations. Cobalt has a large halo of concentrations > 0.006 mg/L around Knights, and a few higher values through the Excalibur region (Figure 28). At Harmony there is a very clear delineation of the mineralisation: most Harmony groundwaters have greater than 0.006 mg/L Co, with < 0.002 mg/L Co in most outlying waters. The Endurance area contains both high and low concentrations of Co, with no distinct pattern.

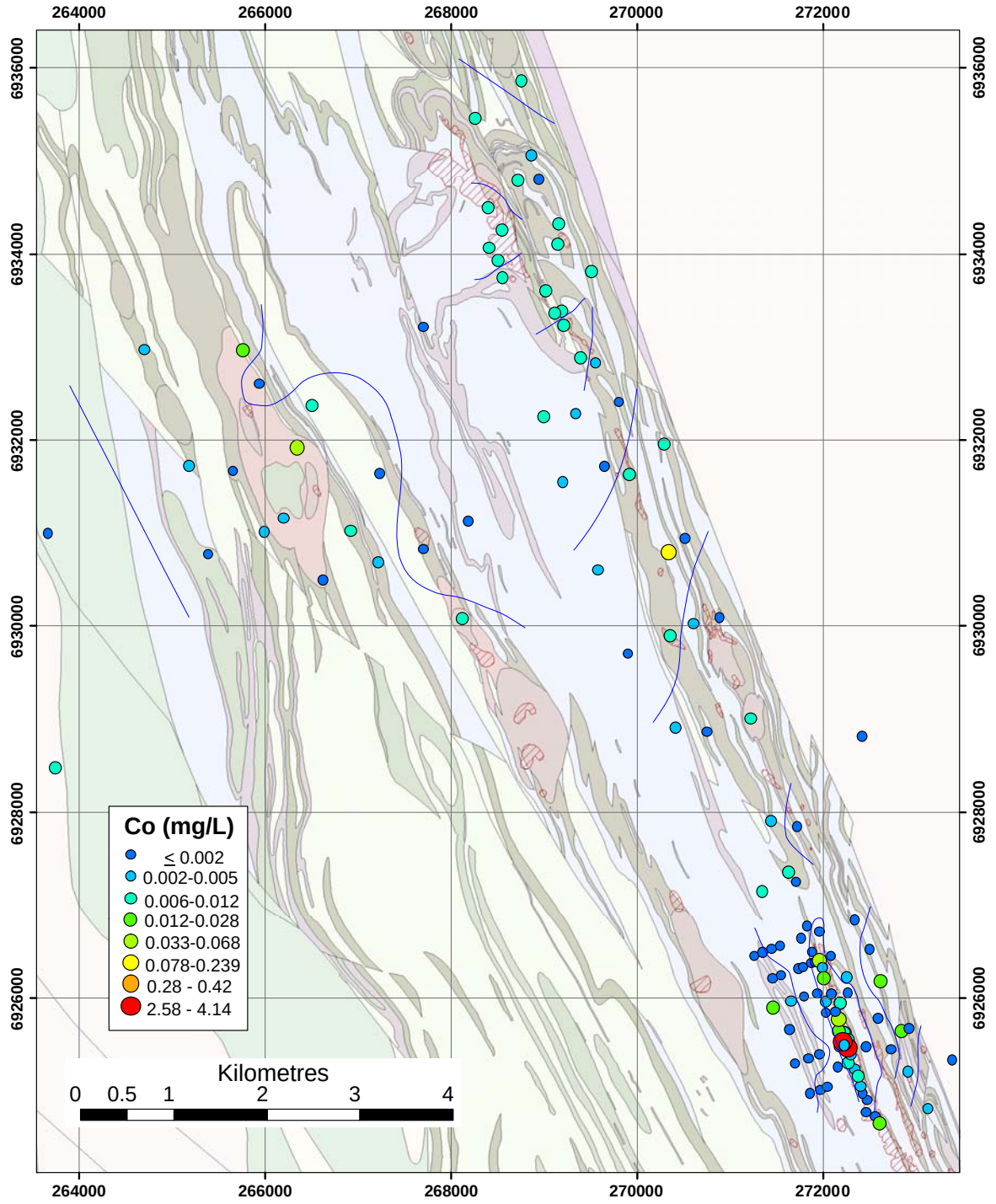

Figure 28: Dissolved Co distribution at Camelot.

5.5 Use of indices

Derived indices (Section 2.3) and their linear combinations greatly improve the delineation of the mineralised zones, particularly for pathfinders such as Co and Pt that are not consistently distributed or detectable. Additionally, these transforms scale data relative to all sites, giving a sense of the "camp scale" anomaly of Harmony/Camelot. The Harmony ore body is indicated by Ni and Co indices (Figure 29 and Figure 30) to be highly anomalous (index scores commonly > 0.75). Also most other Harmony/Camelot groundwaters had Ni and/Co index scores > 0.56, indicating the area to be highly prospective. These higher scores may correspond to mineralized, or sub-economic, sulphides.

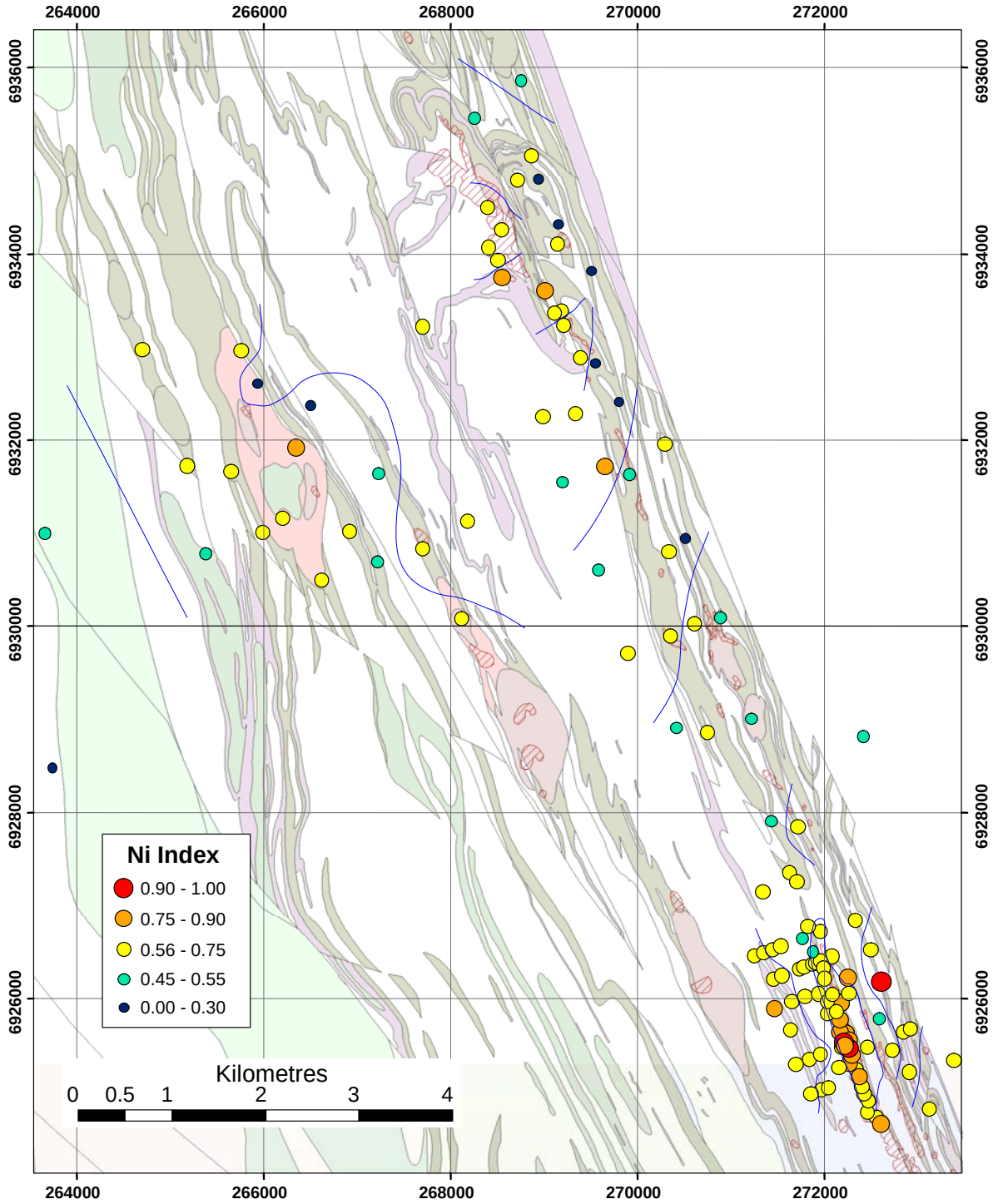

Figure 29: Ni Index distribution at Camelot.

The index normalization also enables individual element indices to be added or subtracted from each other. Thus, adding the Ni, Co W and Pt indices – giving a "Mineralisation" index (Figure 31), increases the contrast of anomalies compared to the individual elements. This treatment is very beneficial for some of the more moderately mineralised areas, particularly elsewhere in the NE Yilgarn (Sections 6 - 9).

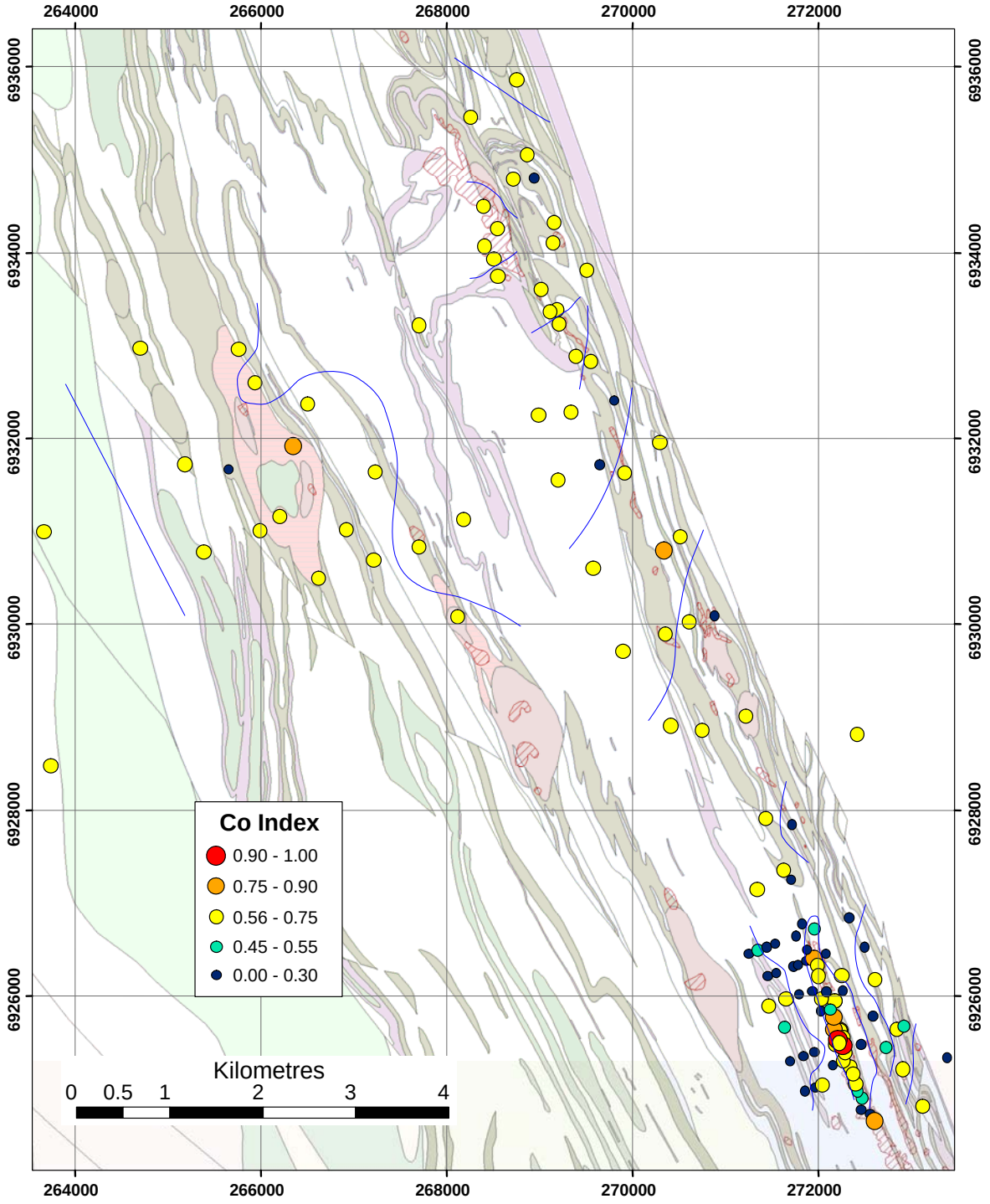

Figure 30: Co Index distribution at Camelot.

Using geochemical parameters based on the model for groundwater evolution around weathering sulphides (Section 3.3), two indices for sulphides (barren or mineralised) were created:

1) The "FeS" index (pH-Eh+Fe+Mn; Figure 32) includes major parameters associated with the oxidation of Fe-rich sulphides;
2) The "AcidS" index (Mo+Ba+Li+Al; Figure 33) uses accessory metals that may be released, possibly from wall rocks, because of acid generation around sulphides.

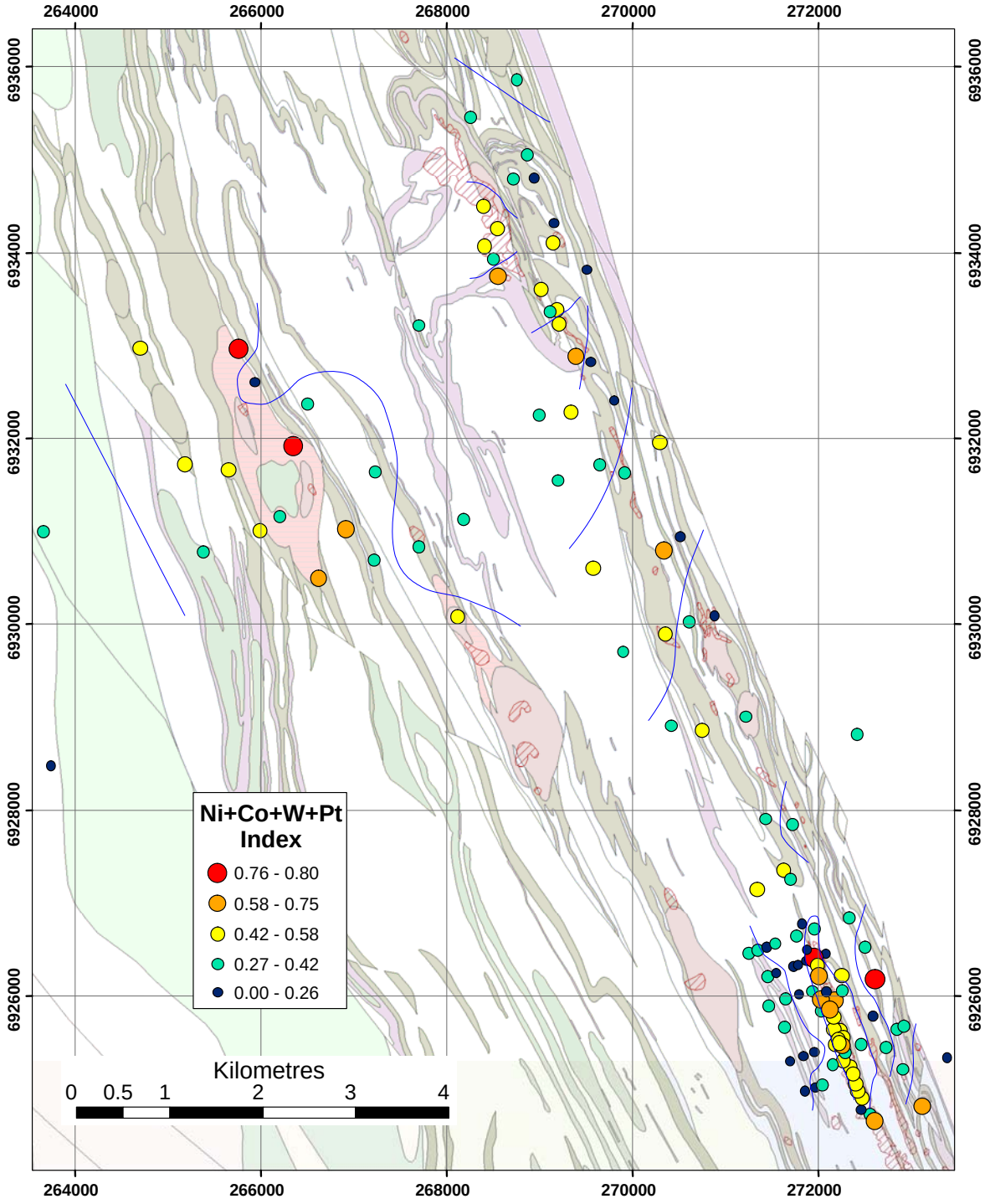

Figure 31: Mineralisation (Ni+Co+W+Pt) Index at Camelot.

Barren sulphides are generally dominated by Fe rather than Ni, and oxidation would be expected to create greater acidity than for mineralised sulphides (Section 3.3). The FeS index (Figure 32) may preferentially indicate sulphides that have a higher Fe:Ni ratio, potentially assisting in distinguishing barren from mineralised sulphides. This index score is higher (> 0.59) around the Endurance region and also to the east of Excalibur, whereas Harmony scores < 0.58 in all samples except two – one of which is west of the known mineralisation. The high scores for Endurance and Excalibur suggest that these areas probably contain more Ni-poor sulphides than Harmony and Knights.

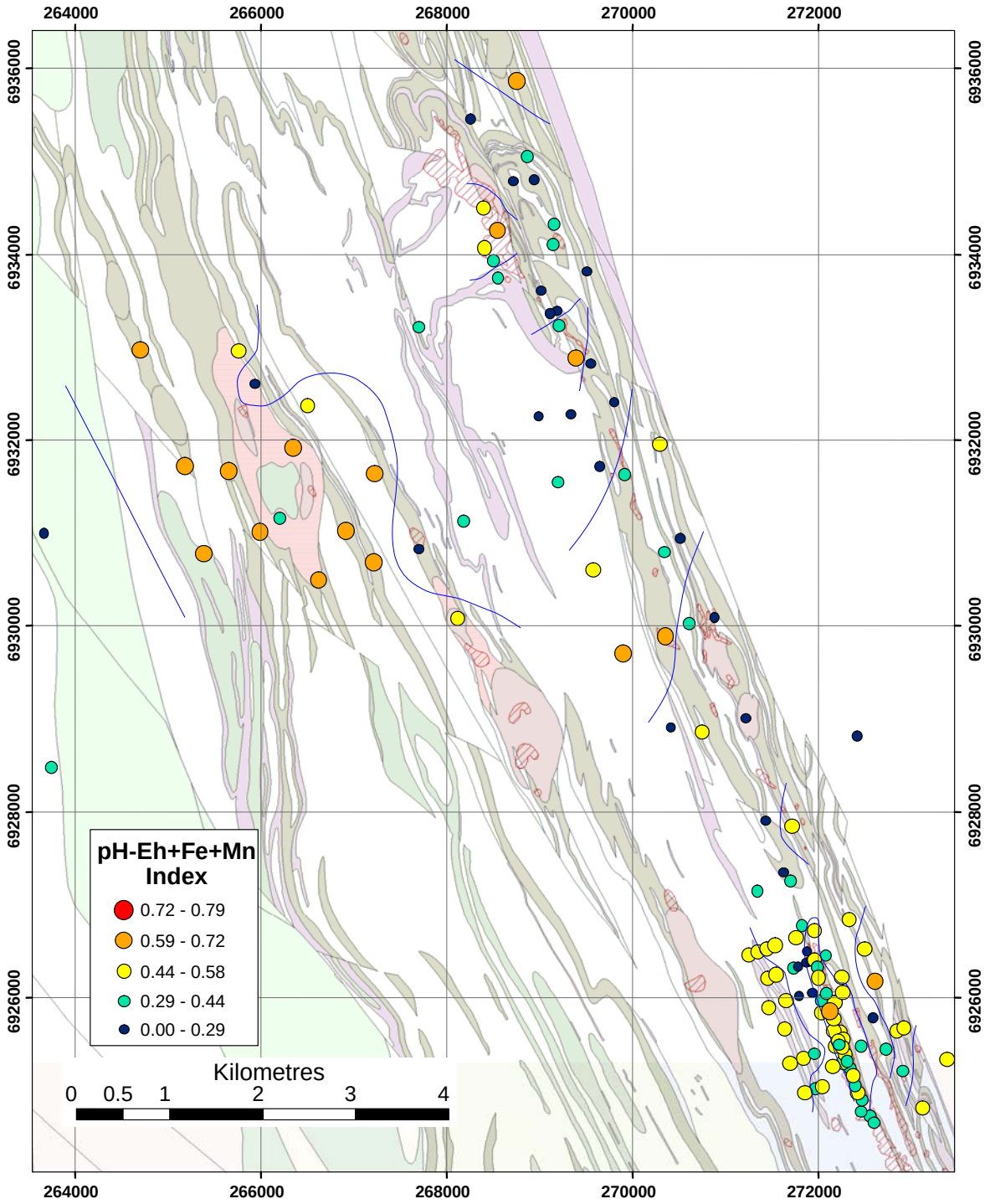

Figure 32: FeS (pH-Eh+Fe+Mn) Index at Camelot.

The AcidS index (Figure 33) is similar to the FeS index (Figure 32) in showing higher values in the Endurance region, and also east of Harmony, again consistent with extensive unmineralised sulphides. The high scores in a small cluster on the southern edge of the Knights mineralisation (Figure 33) is consistent with the previously discussed dissolution of wall rocks, the transient acidity and the high SI of Mg minerals (Section 5.2). The similarity between results for the FeS and AcidS indices supports the groundwater evolution model (Section 3.3).

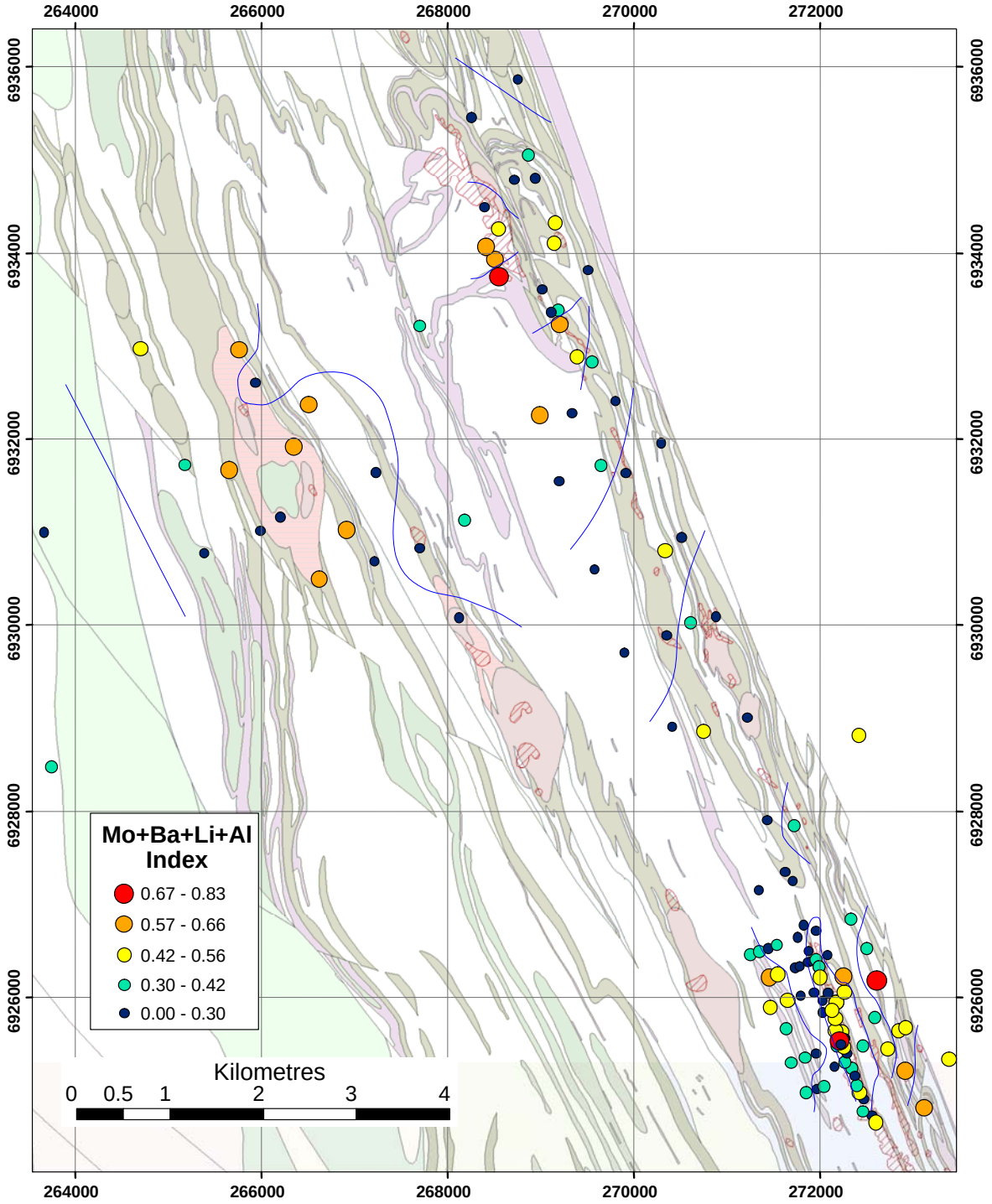

Figure 33: AcidS Index (Mo+Ba+Li+Al) at Camelot.

Subtracting the two sulphide indices from the Mineralisation index, giving the "Min-FeS" (Figure 34) and "Min-AcidS" (Figure 35) indices, may increase contrast between the mineralised and barren sulphides. These enhanced indices show numerous anomalies along the ultramafic belt between Harmony and Camelot, possibly reflecting pockets of NiS. Immediately adjacent to the Harmony deposit, samples that appear to be positive anomalies when using only the individual elements, are suppressed to background by this combination, resulting in a good delineation of the Harmony deposit (Figure 34 and Figure 35). Camelot shows many anomalous samples, suggesting that this area has a much stronger signature of mineralised sulphides than the other regions studied.

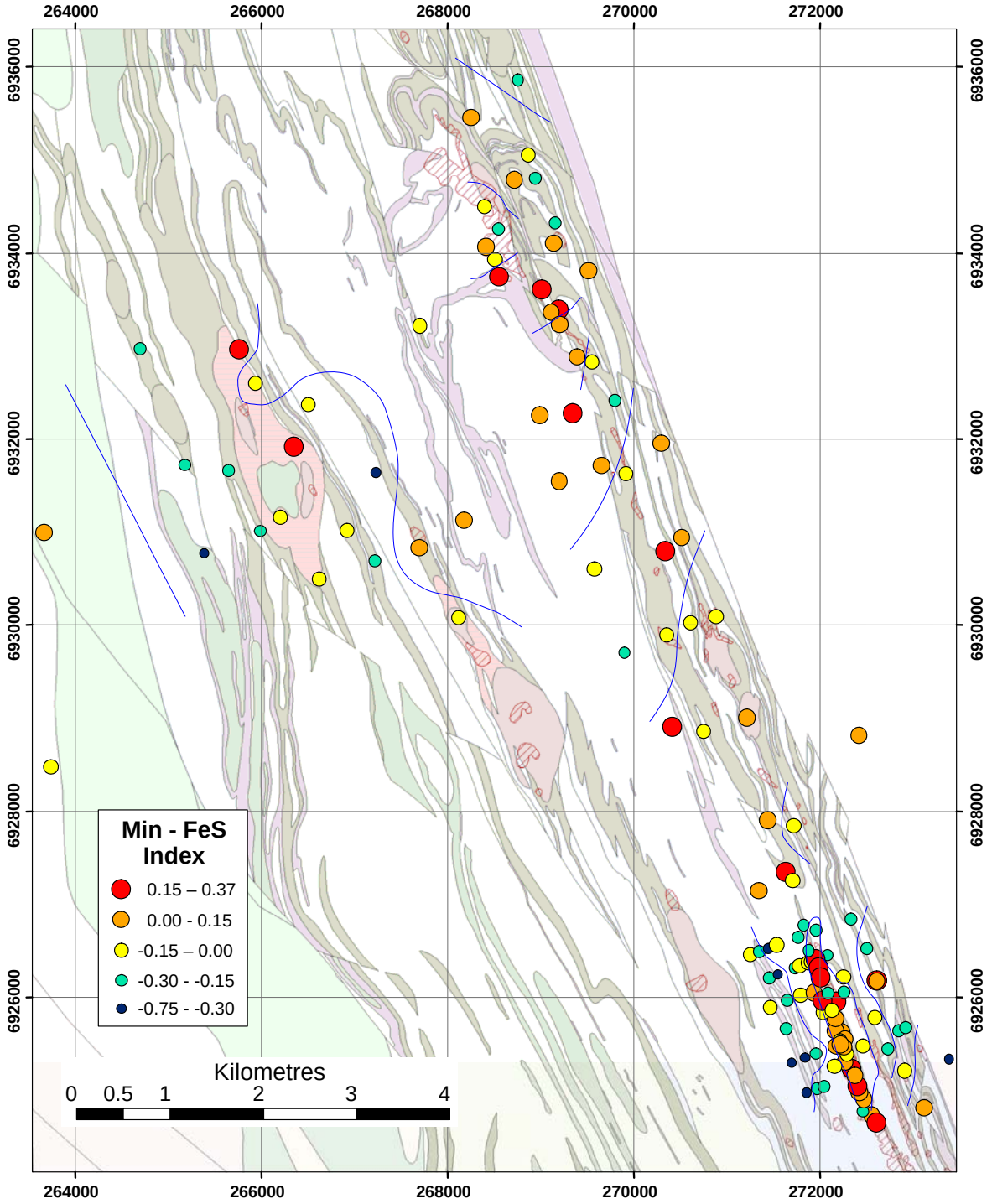

Figure 34: Min–FeS Index at Camelot.

Although the Endurance region also has a few high scores for the Min-FeS and Min-Acid S indices (Figure 34 and Figure 35), it does not appear as prospective as the other regions of Camelot/Harmony. Use of these indices has reduced the Endurance anomaly, relative to the mineralized sites at Harmony and Knights, compared with the use of a straight mineralisation index, such as Ni, Co or combined Ni+Co+W+Pt (Figure 29 to Figure 31). Overall, Harmony stands out as the major NiS zone: however the entire Camelot region also contains numerous mineralised sulphide pods and is more prospective than many other sites investigated in this research.

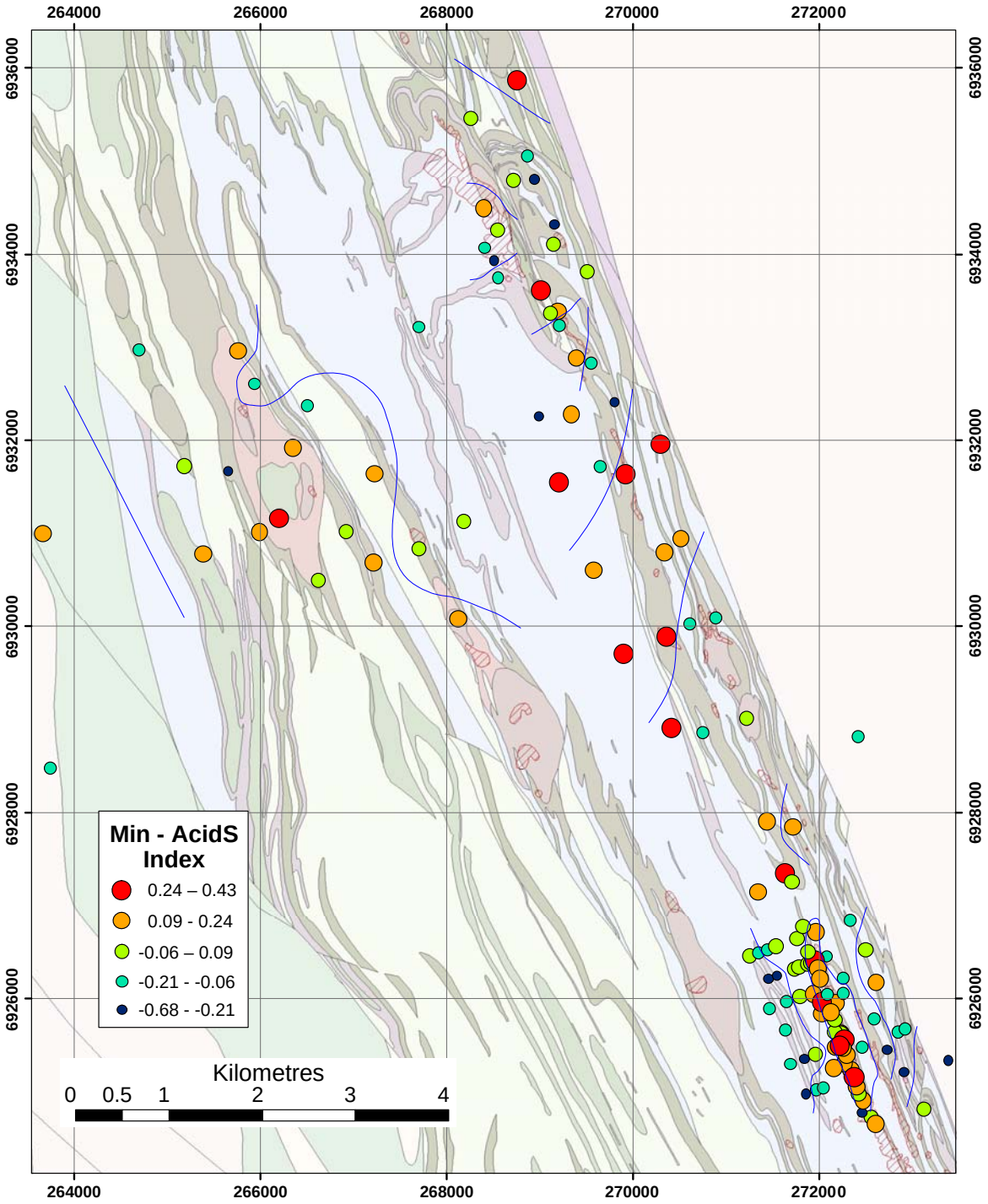

Figure 35: Min–AcidS Index at Camelot.

A similar, though less well defined, distribution pattern is observed for the "Min–Cr" index (Figure 36), which subtracts away a lithological indicator for ultramafics. This index is designed to remove lithological effects and produces less anomalously high scores (> 0.30) than the other mineralised indices. Using this index (Figure 36) the Harmony deposit is weakly identified, along with three regions characterised by sulphide chemistry: east of Harmony, Excalibur, and two points in the Endurance area.

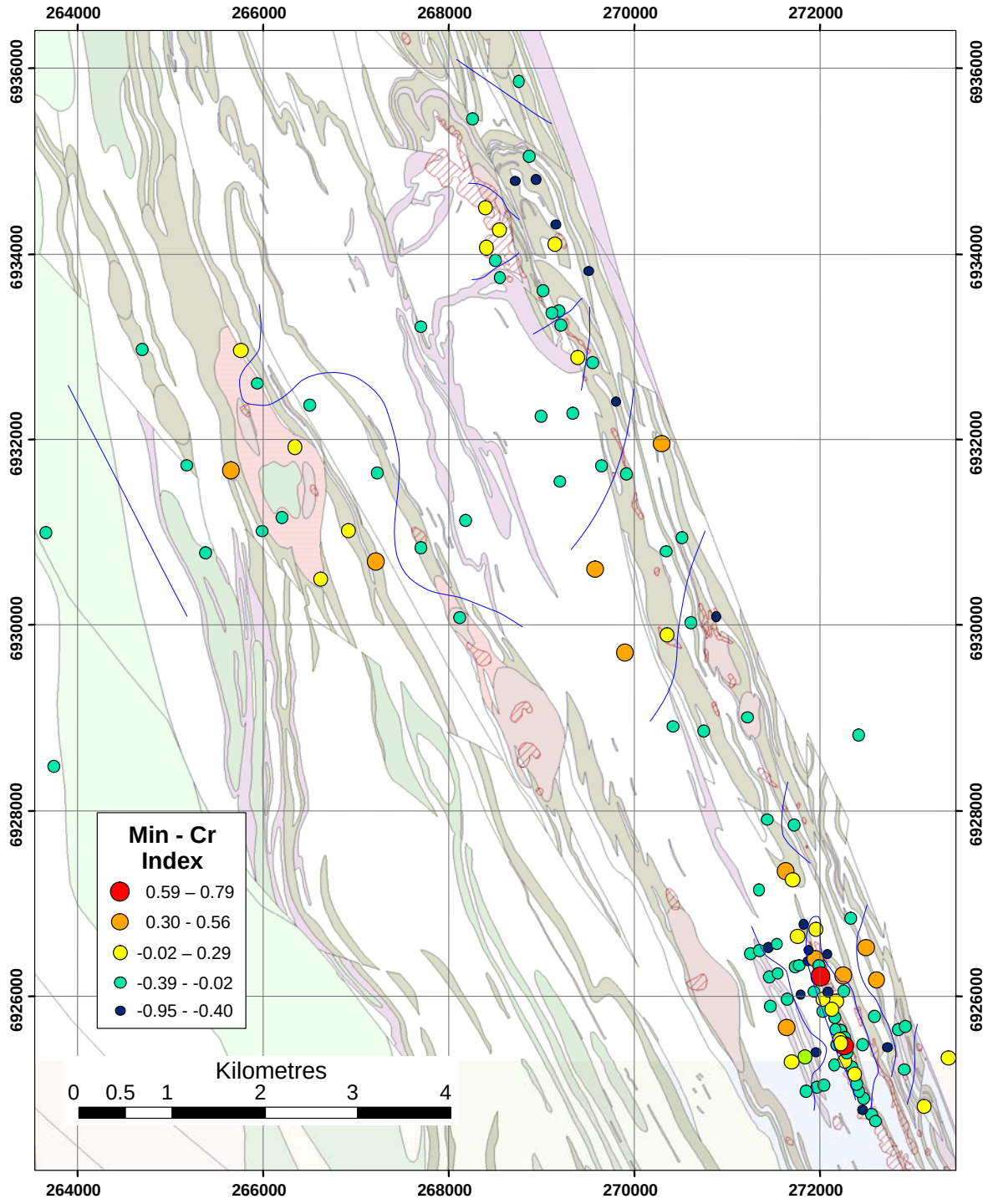

Figure 36: Min-Cr Index at Camelot.

Other single element indices (Pt; Figure 37 and W; Figure 38) show fewer anomalous responses and are more subdued than the mineralised combination indices. In particular, Pt has is commonly below detection, and the index responses have only eight anomalous values (> 0.56), of which three occur directly over mineralisation in the Harmony region. Other high Pt index scores occur in the Excalibur region over ultramafic rocks that may hold isolated pods of mineralised sulphides (Figure 37). All except one of the anomalous Pt index scores (> 0.56) occur in the regions that are influenced by sulphide chemistry (blue lines; Figure 37). The Pt index did not indicate anomalous scores in the Endurance area, which has no known significant NiS. When Pt is detected it is in area of known sulphides, however the more subtle expressions of undiscovered ore bodies may be overlooked. Improved detection limits will strongly enhance the potential of Pt as a hydrogeochemical pathfinder.

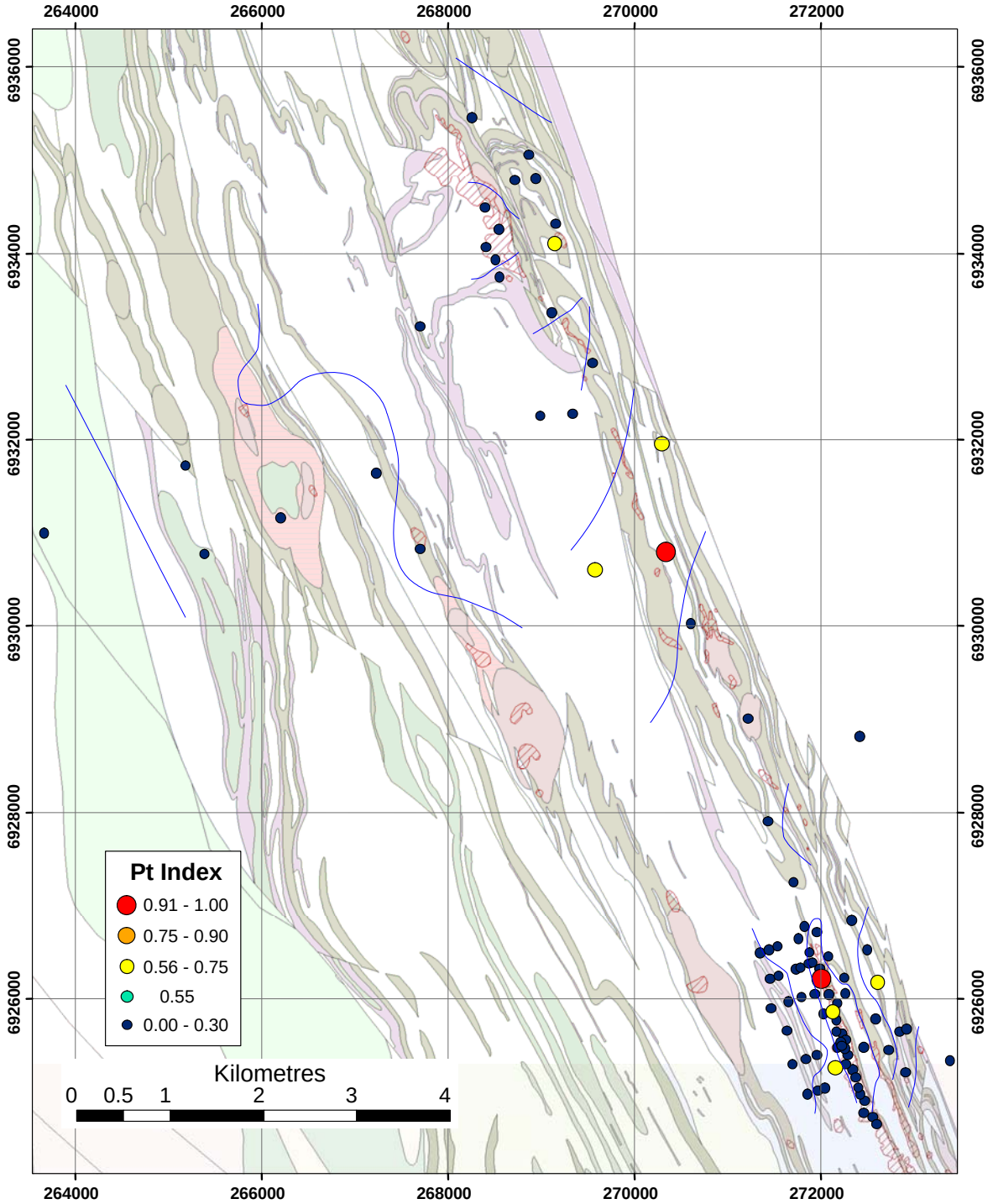

Figure 37: Pt Index at Camelot.

In contrast, W is commonly well above detection. The Harmony area is very well delineated by the high scores of the W index (> 0.55; Figure 38). Unlike Pt, the W index scores are high at Knights, and have some higher scores in the Endurance area (Figure 38). The association between W and sulphides is unexpected, and should be investigated further. Dissolved W is potentially a good pathfinder in the NE Yilgarn as the anionic WO_4^{2-} is not readily adsorbed by minerals such as Fe oxides in neutral to alkaline conditions. In contrast, W is not expected to be mobile in saline and acidic conditions, such as the Kalgoorlie area (Gray, 2001). Other common oxyanions such as As and Sb were not observed to be valuable pathfinder elements for NiS, with many samples being near or below detection limits for these metalloids.

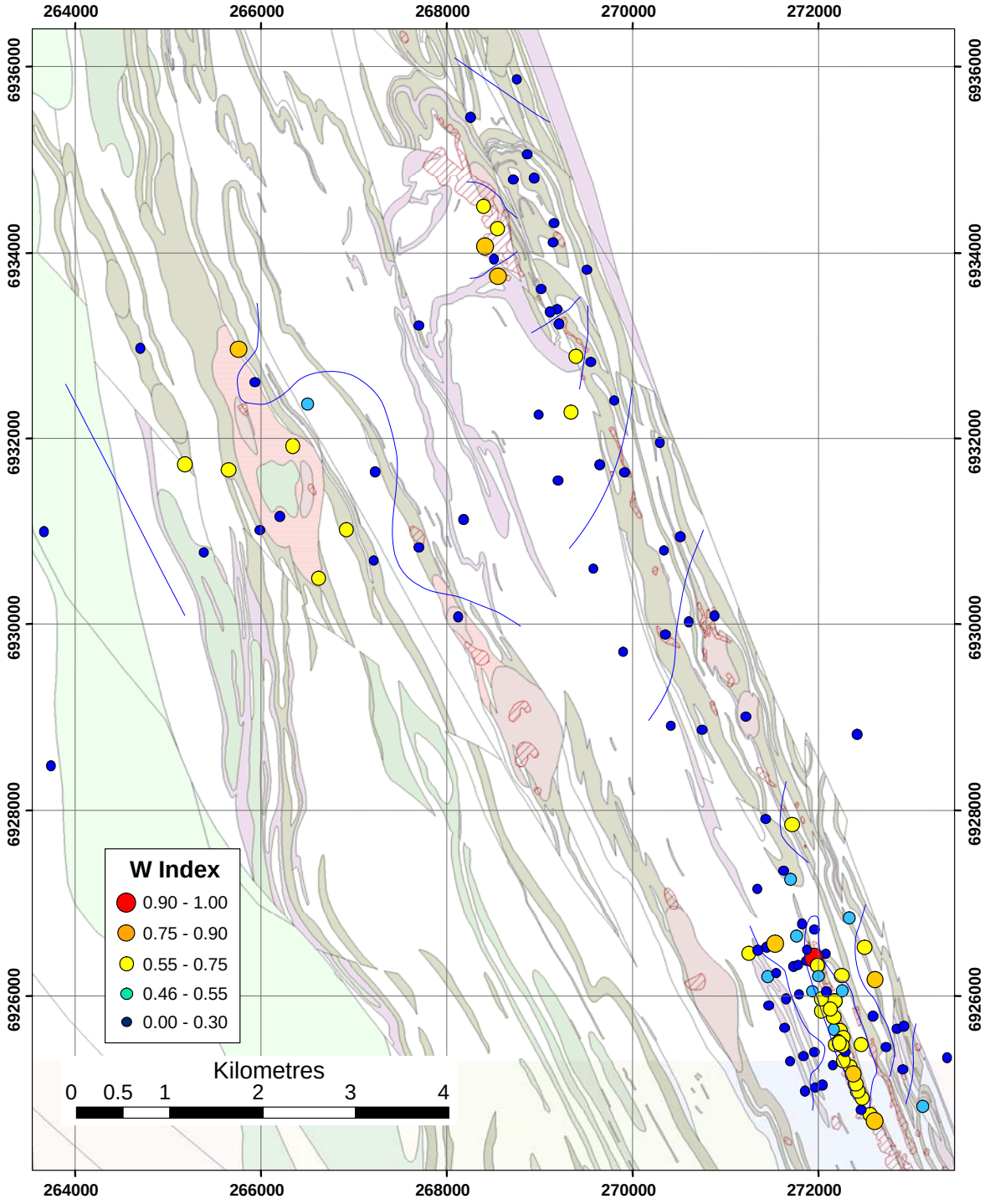

Figure 38: W Index at Camelot.

6. WILDARA/WATERLOO

6.1 Site description and sampling

The Wildara region is located approximately 40 km south of Leinster (Figure 2) and includes the Waterloo (LionOre) and Weebo (BHP Billiton) Ni occurrences (Figure 39). The climate is arid, with annual rainfall of approximately 230 mm annually. The watertable in the region is typically 20-50 m below surface. The regional geology consists of greenstone belts containing ultramafic rocks, enclosed within granitic and felsic rocks. NiS mineralisation at Waterloo is associated with the basal contact of a serpentinised ultramafic unit. Main mineralisation styles include massive, matrix, disseminated, and remobilized stringer and breccia sulphide mineralisation. The sulphides also contain significant levels of Cu and PGE's.

6.2 Lithological Indicators

At Wildara dissolved Cr (Figure 40) indicates ultramafic rocks. The highest Cr concentrations were observed for the central area, where the sulphide signature is lower, similarly to barren ultramafics in the Lawlers/Agnew area, which give extremely high (up to 0.33 mg/L) dissolved Cr (Figure 110). At the closer scale at Waterloo (insert in Figure 40) there is a weaker correlation of dissolved Cr with the ultramafic units. Many of the holes are angled and may intersect the groundwater of adjacent geological units. On the other hand, higher dissolved U (Figure 41) represents granitic rocks, although there are very few samples taken from granitic rock in this area.

6.3 Sulphide Indicators

The groundwaters in contact with sulphides at Wildara exhibit the same characteristics as those from other parts of the NE Yilgarn. The waters can be highly variable, but can be clearly delineated from background waters due to the low Eh or pH and comparably high concentrations of some of the following elements Al, Ba, Ce, Fe, La, Li, Mn, Mo, V and W. Reduced waters are observed for the Weebo BHP Billiton tenements, Waterloo LionOre tenements and the west-central region of Wildara (Figure 42). Four groundwaters have pH values below 6.5 (Figure 43), consistent with acid generation from the oxidation of sulphides.

The observed high concentrations of elements characteristic of acid lithologies in other parts of the Agnew Wiluna greenstone belt (Ba, Li, Mn, Mo, V, W), are not so evident in the Wildara region. Aluminium and Ce have a few high values at Waterloo, but not prominent at Weebo or other sulphide pods (Figure 44 and Figure 45). Lithium exhibits some high concentrations (0.25 – 2.85 mg/L) at Waterloo (Figure 46), whereas Mn is above background in the close vicinity of Waterloo and Weebo (Figure 47).

In the Waterloo area, reduced waters are common throughout (insert in Figure 42). Two groundwaters with pH values below 6 are observed (Figure 43), consistent with acid-forming reactions by the oxidation of sulphides and Fe at Waterloo. Other sulphide indicators are also observed, with higher than expected concentrations of dissolved Al (Figure 44) and REE (*e*.g. Ce, Figure 45) which are out of equilibrium when waters are neutral, indicating the Al and REE were released under acid conditions, and then remained in solution due to kinetic factors when the waters were neutralized. The relict low pH conditions might also explain the higher concentrations of elements such as Ba, Li (Figure 46), Mn (Figure 47), Mo, V and W. These elements are generally higher in the southern part of the Waterloo deposit

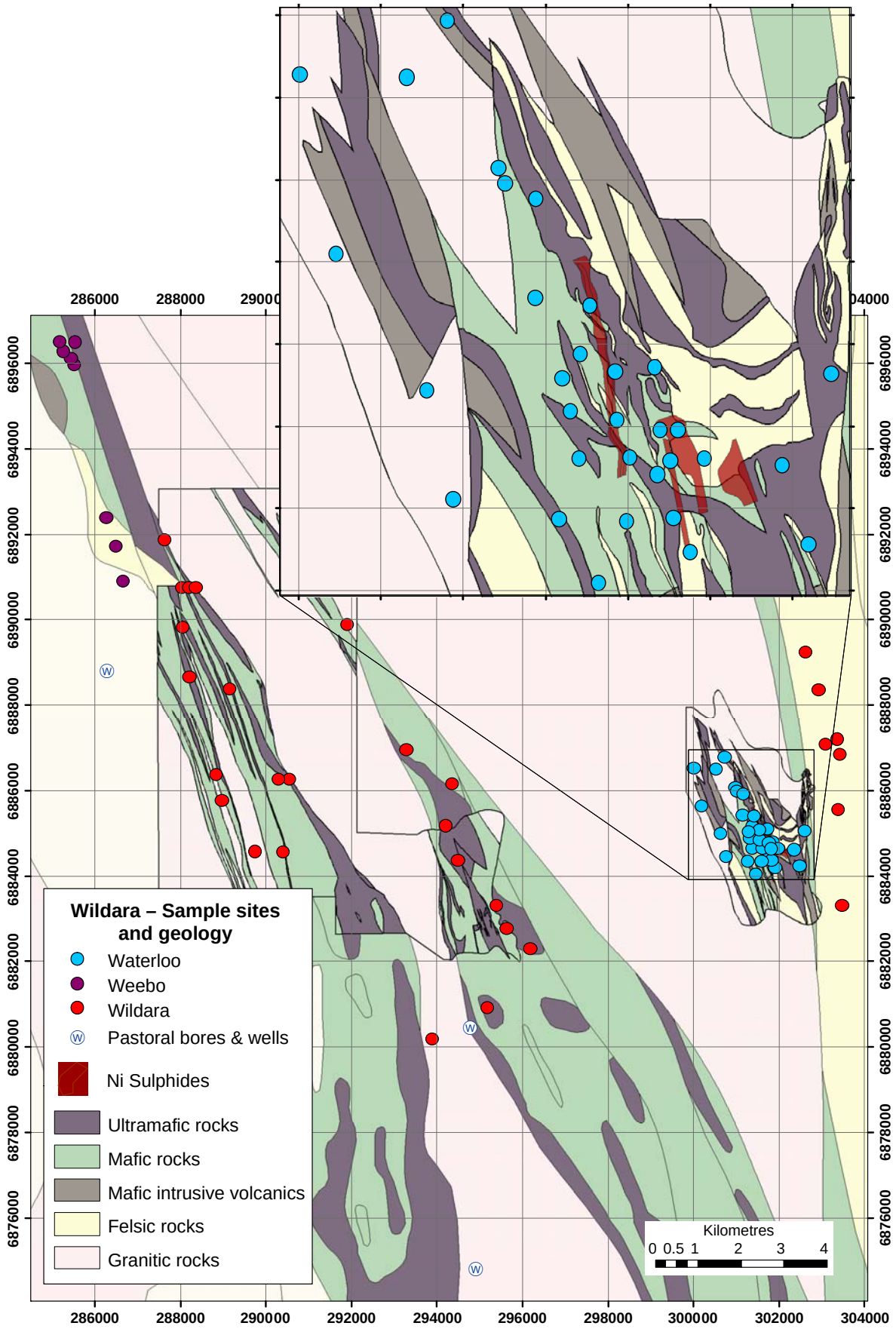

Figure 39: Detailed geology and sample locations of the Wildara (Weebo and Waterloo) region.

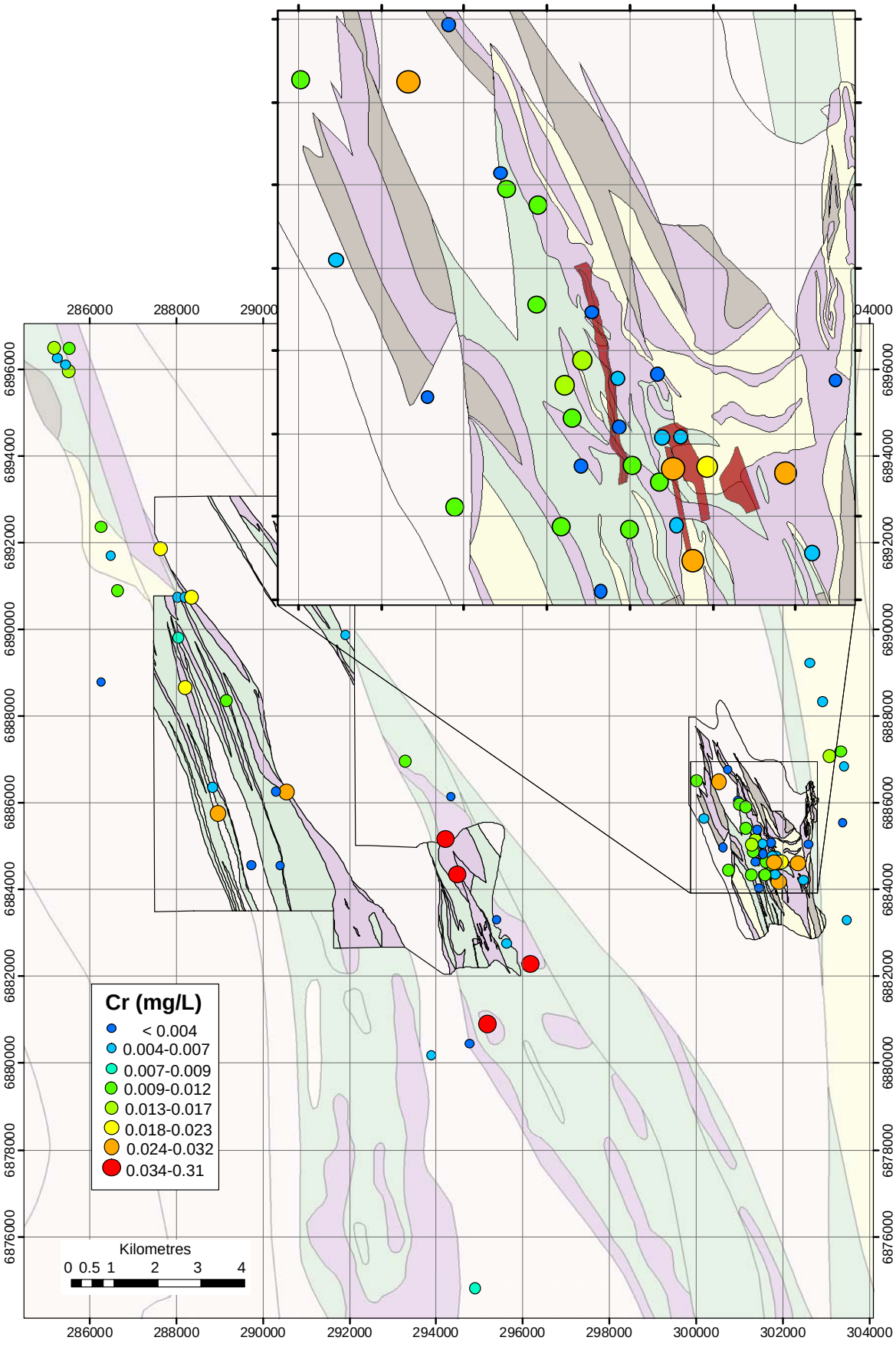

Figure 40: Dissolved Cr distribution at Wildara.

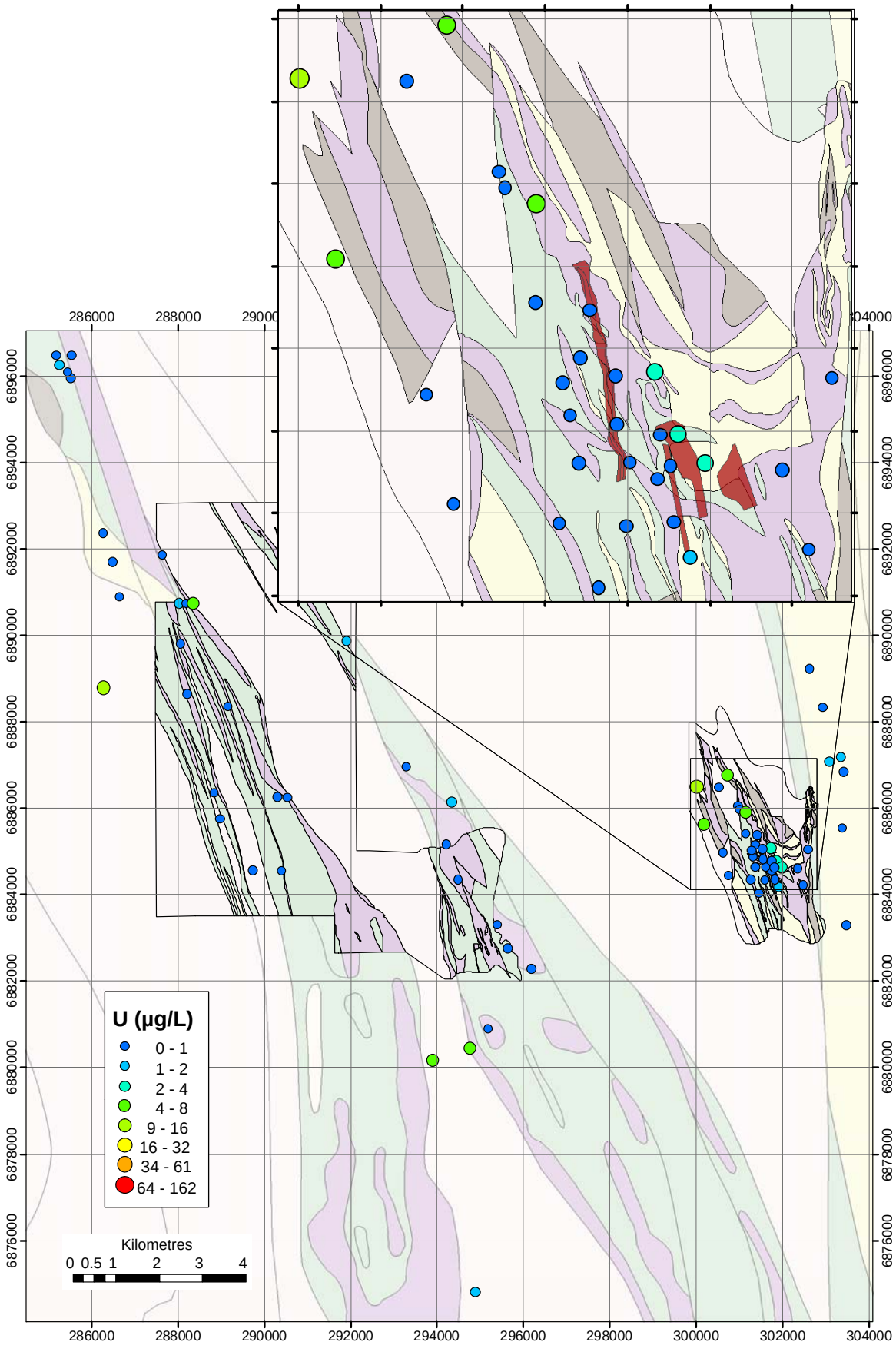

Figure 41: Dissolved U distribution at Wildara.

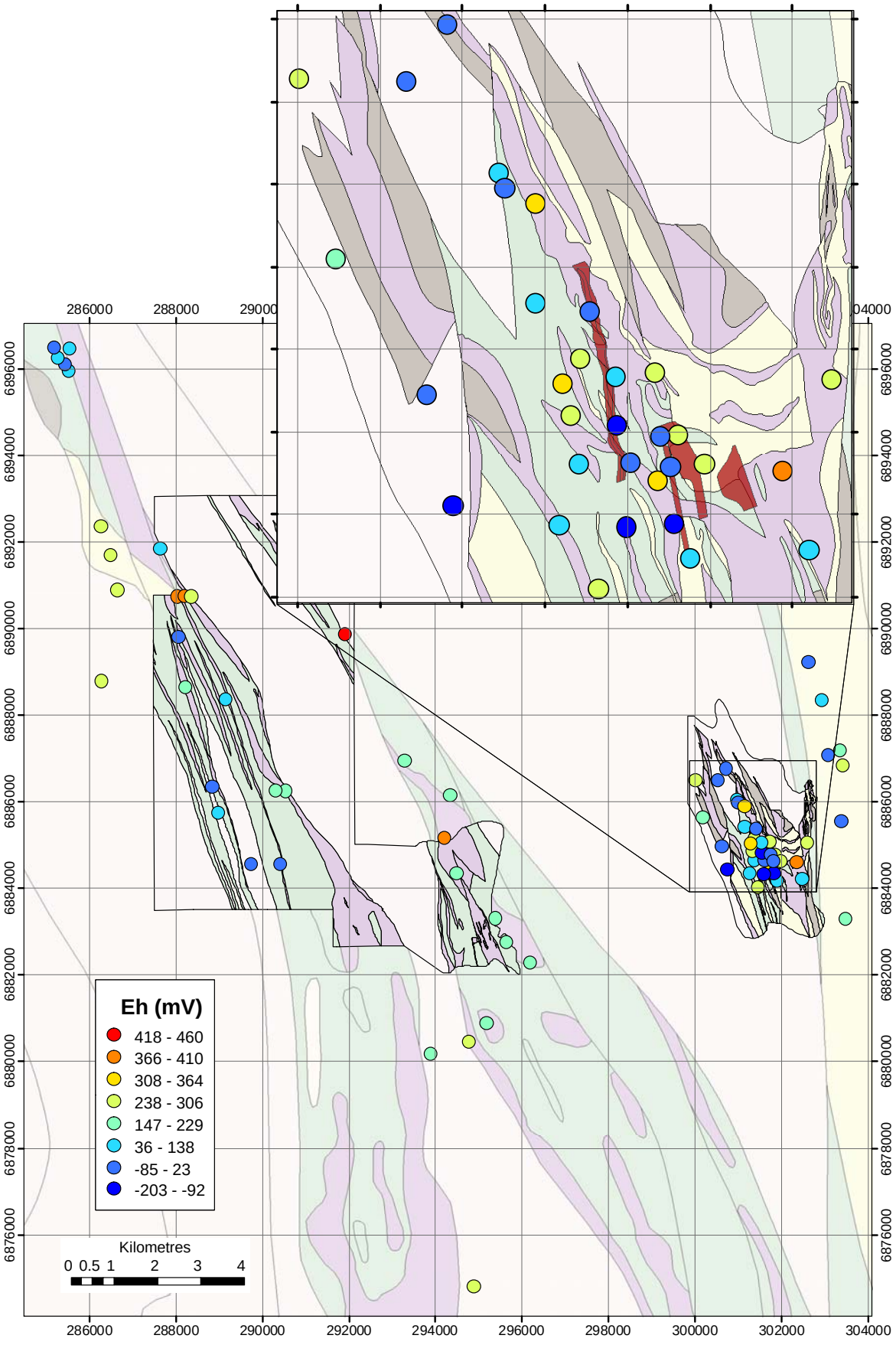

Figure 42: Groundwater Eh values at Wildara. Reduced zones are shown in blue.

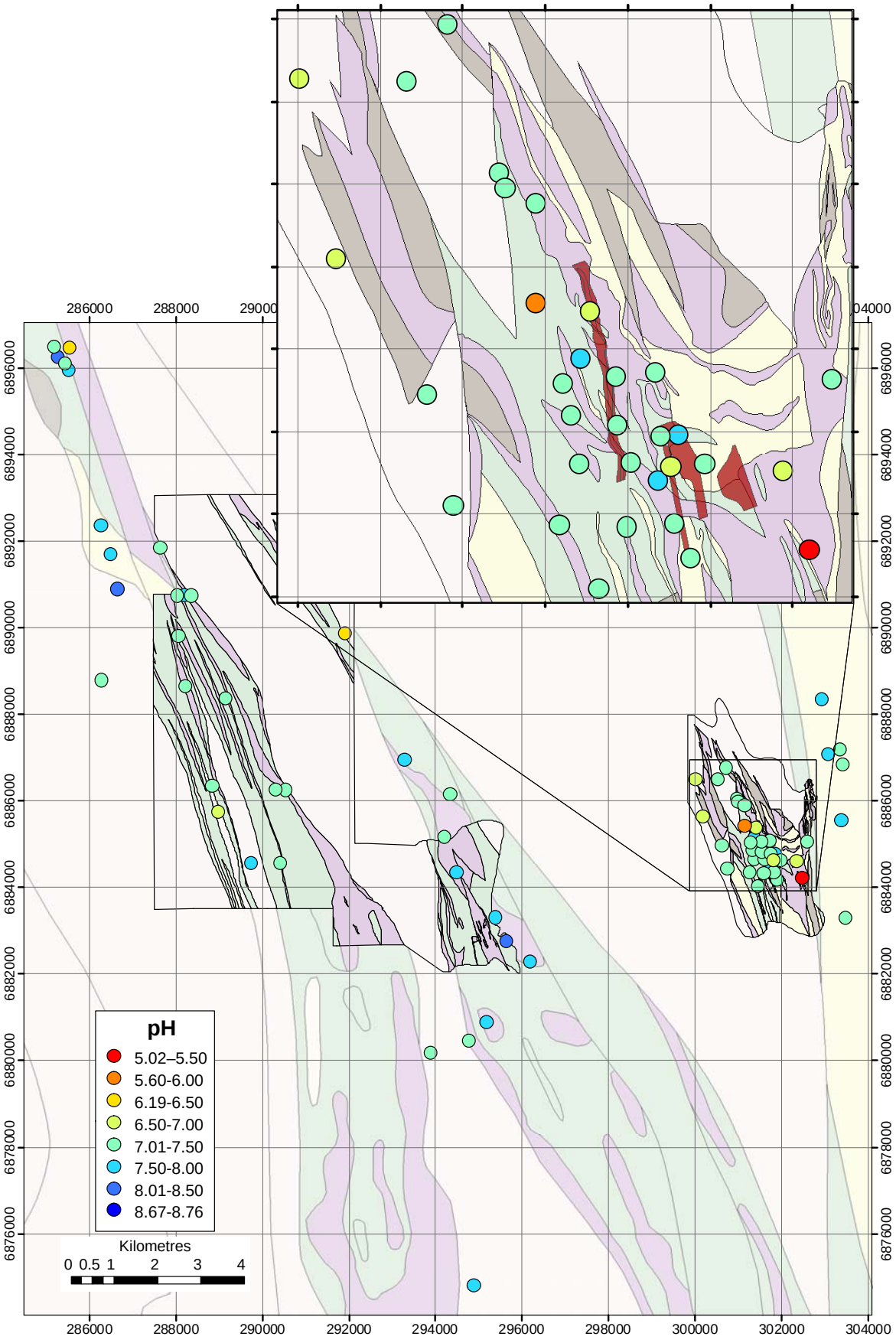

Figure 43: Groundwater pH values at Wildara.

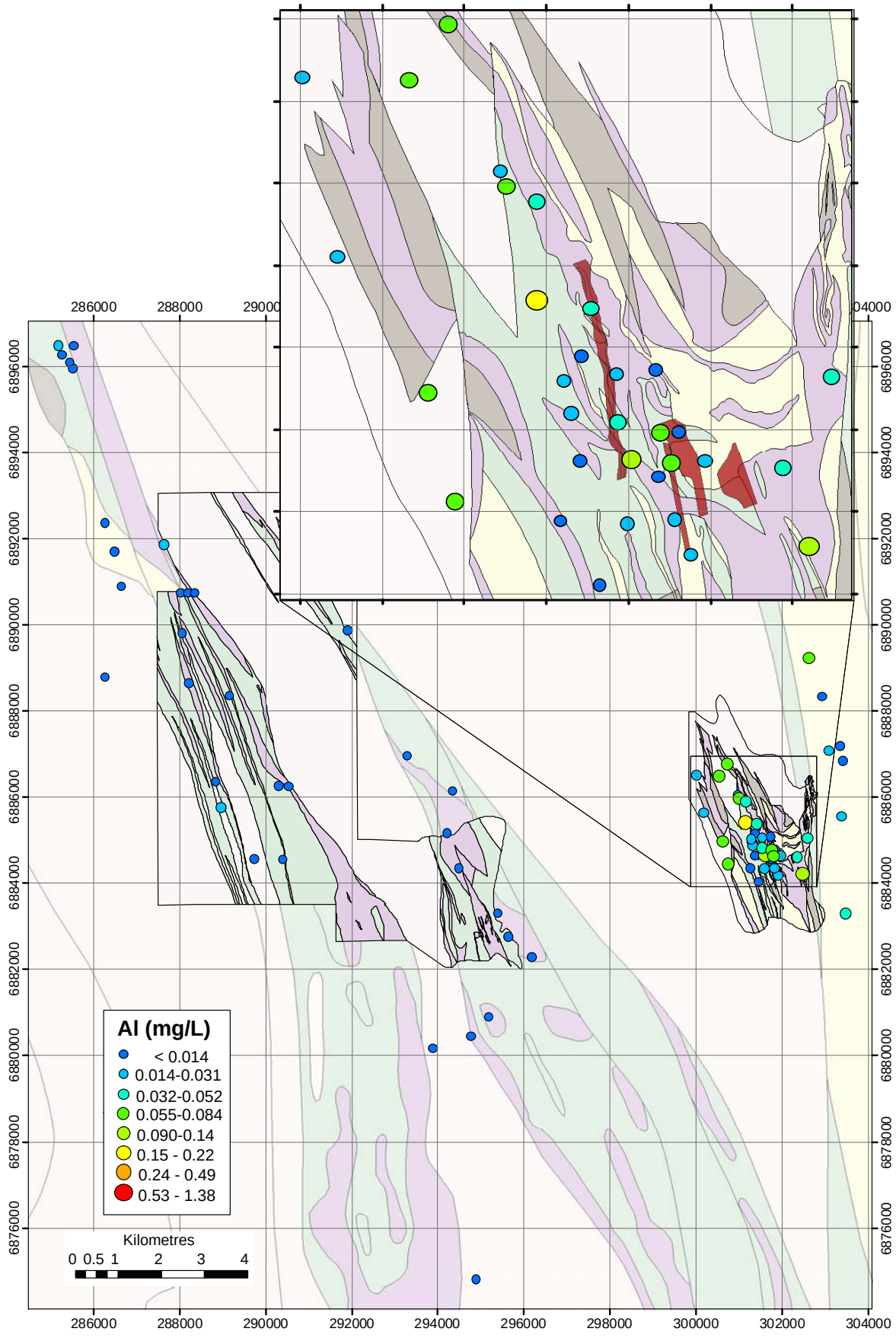

Figure 44: Dissolved Al distribution at Wildara.

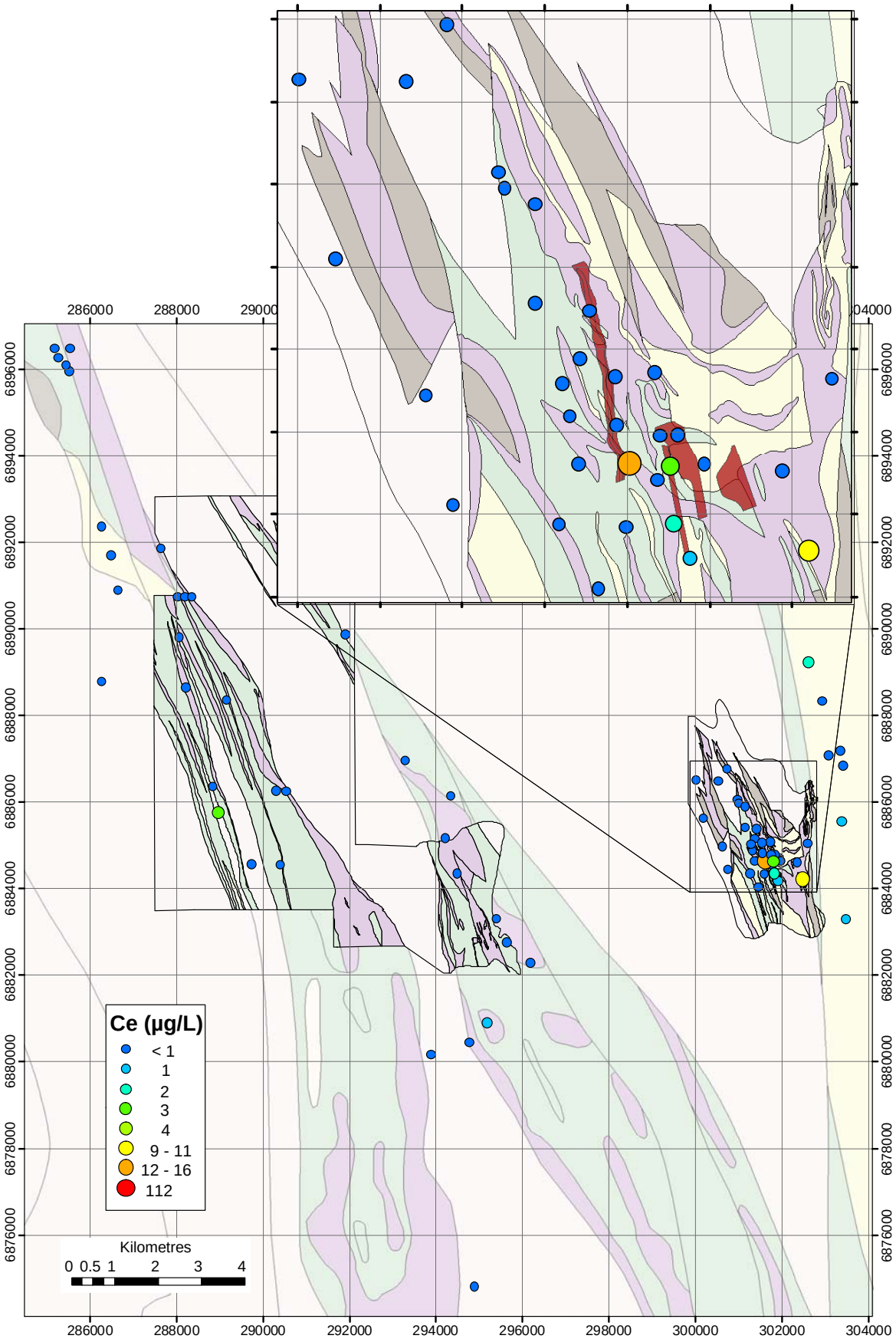

Figure 45: Dissolved Ce distribution at Wildara.

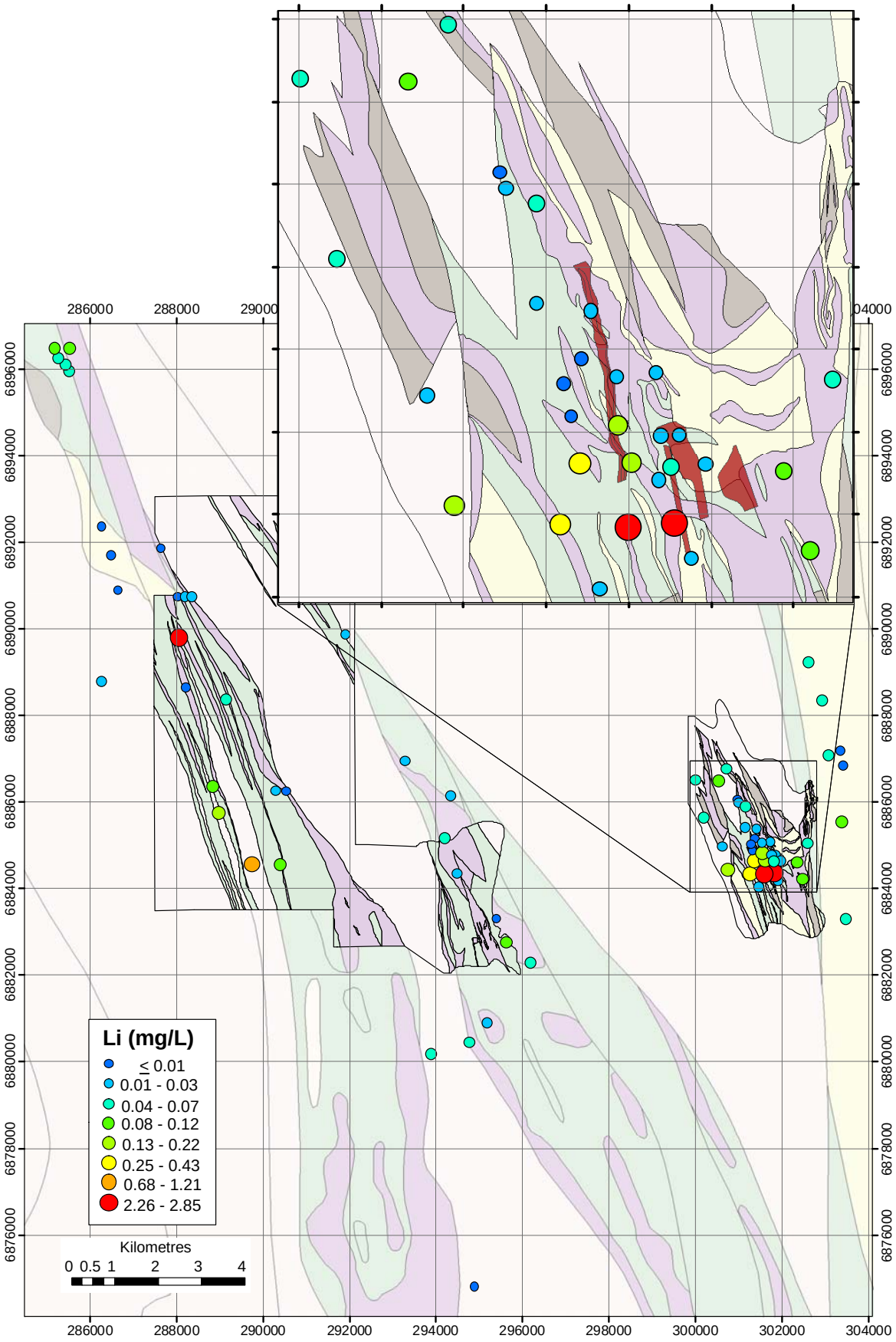

Figure 46: Dissolved Li distribution at Wildara.

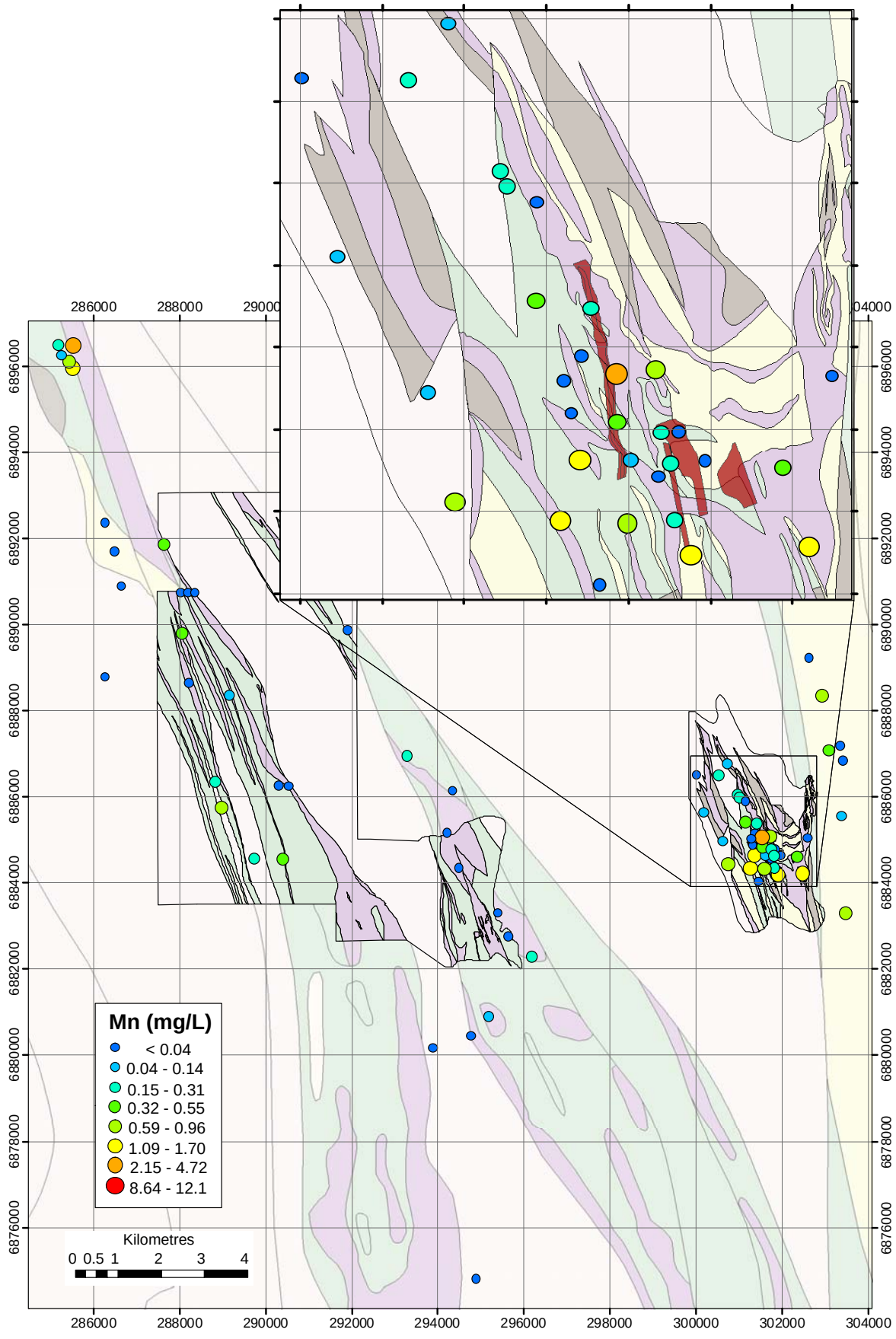

Figure 47: Dissolved Mn distribution at Wildara.

6.4 NiS Mineralisation Indicators

Nickel (Figure 48) and Co (Figure 49) are the best single element groundwater indicators for NiS in this area, although the anomalies are much weaker than at Harmony/Camelot (Figure 27 and Figure 28). These two elements are higher at Waterloo and at the Weebo (BHP Billiton) exploration sites, but show no enrichment in the third anomalous Eh zone in the west-central region (Figure 42).

6.5 Use of indices

Derived indices of Ni (Figure 50) and Co (Figure 51) were moderately effective singularly. Dissolved W (Figure 52) delineates the main areas of mineralisation, as well as two high points NE of Waterloo possibly related to Au mineralisation which can also give high dissolved W. In contrast, Pt has some anomalous values over Waterloo, but none in the other areas of Wildara (Figure 53).

Combination element indices proved more effective than any individual element. The Mineralisation index (Ni+Co+W+Pt; Figure 54) gives a stronger and more localised anomaly than any of the individual elements for the Wildara area. General sulphide parameters (FeS and AcidS index; Figure 55 and Figure 56) also delineate the two Weebo and Waterloo NiS occurrences, as well as the west-central region, which possibly represents relatively barren sulphides. Subtracting the major parameters of mineralised vs. barren sulphides enhances the hydrogeochemical signature (Figure 57 and Figure 58), giving more specific anomalies at the two mineralised areas. Similar results are observed for the Mineralisation –Cr index (Figure 59).

Other element combinations were also tested for this area. Based on regolith signatures above Ni mineralisation (Brand, 1997), the use of Cu+Fe+Pt index was used (Figure 60). Palladium would also have been used if the very small concentrations in these NE Yilgarn groundwaters could have been consistently determined. The Kambalda ratio [(Ni:Cr)+(Cu:Zn)] was also adapted to a hydrogeochemical index: (Ni+Cu)-(Cr+Zn) (Figure 61). These element indices proved relatively effective as vectors towards mineralisation, although as with the Ni index, Weebo did not show a strong anomaly using the Kambalda index (Figure 61).

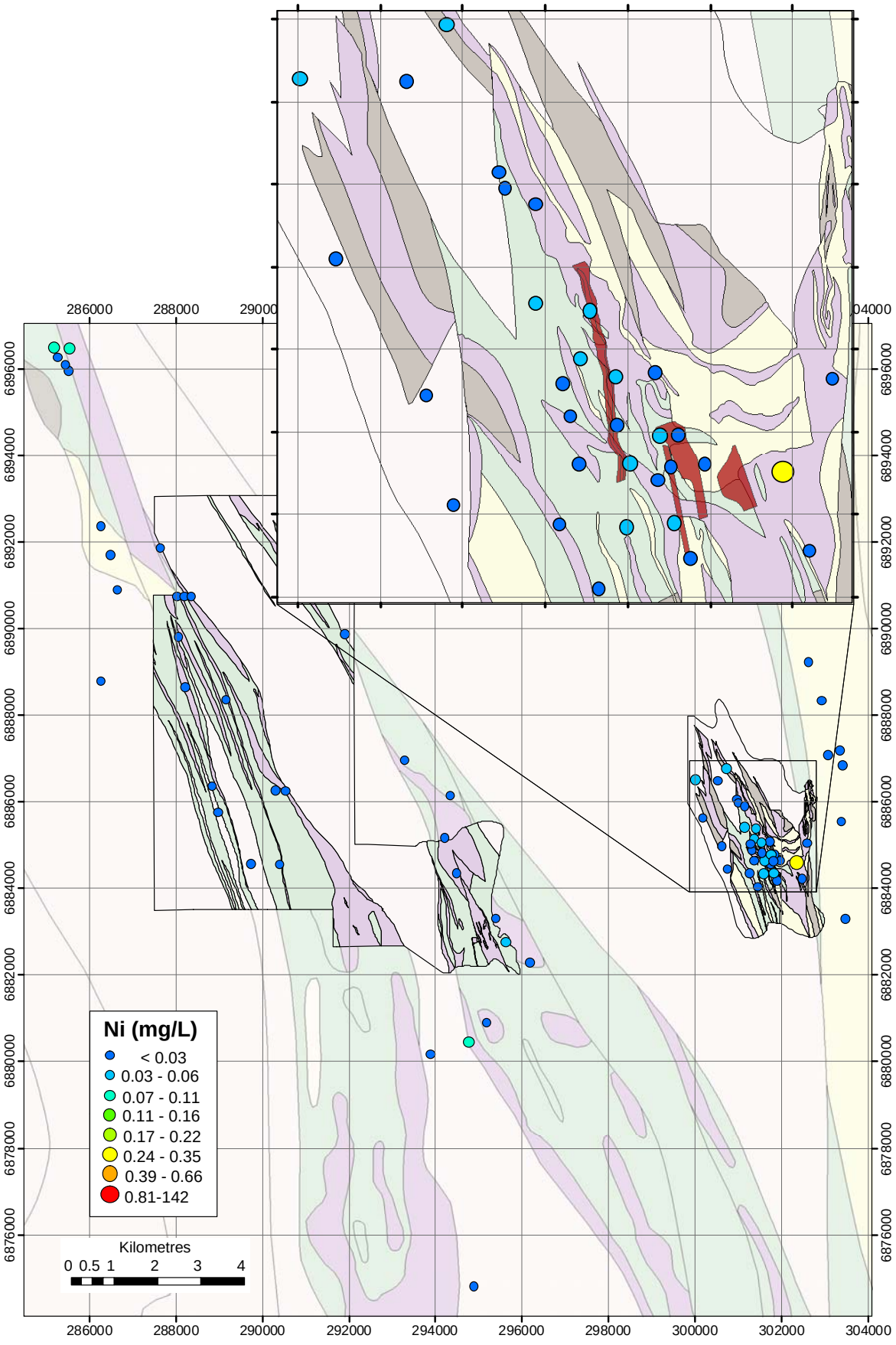

Figure 48: Dissolved Ni distribution at Wildara.

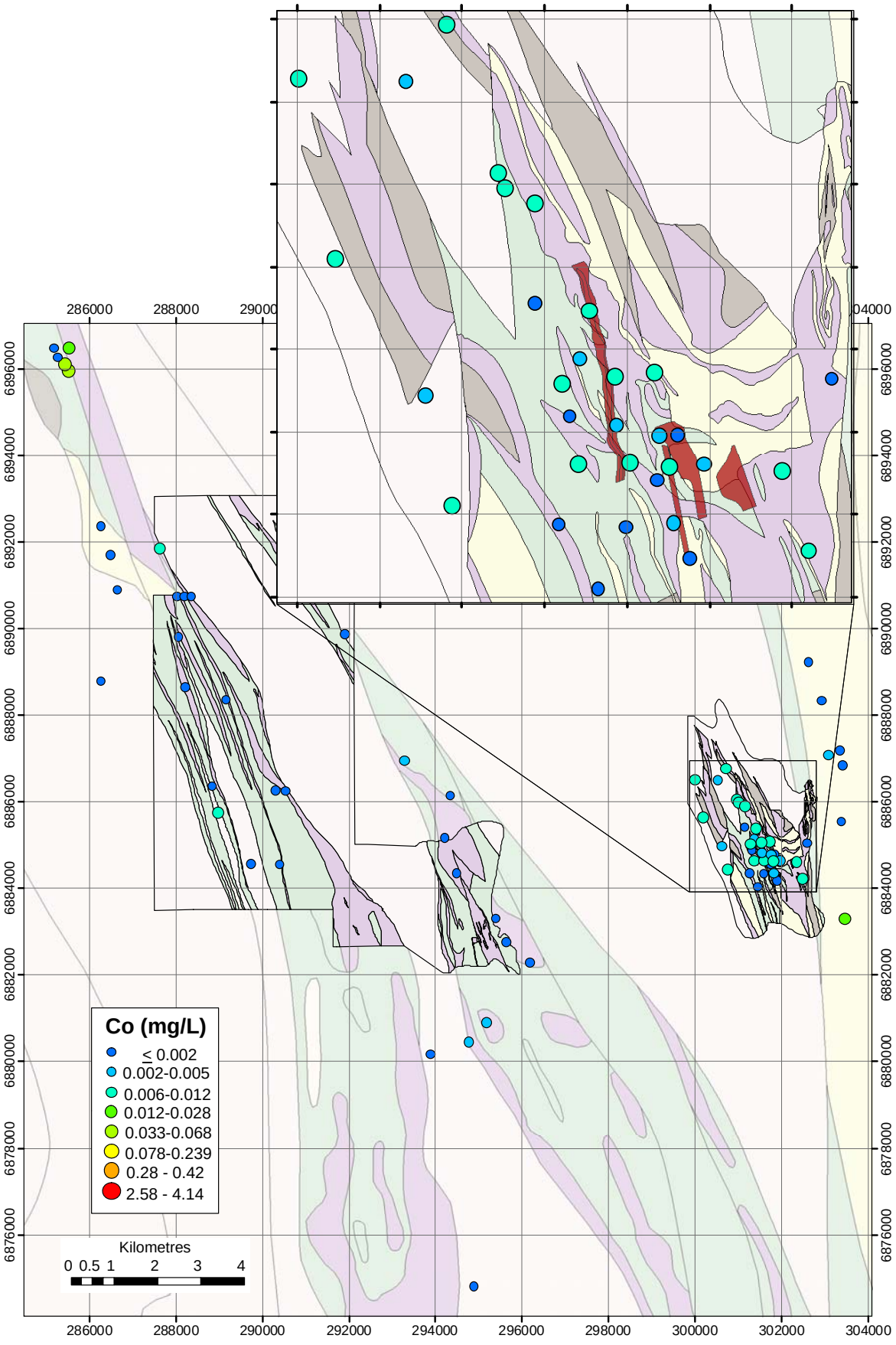

Figure 49: Dissolved Co distribution at Wildara.

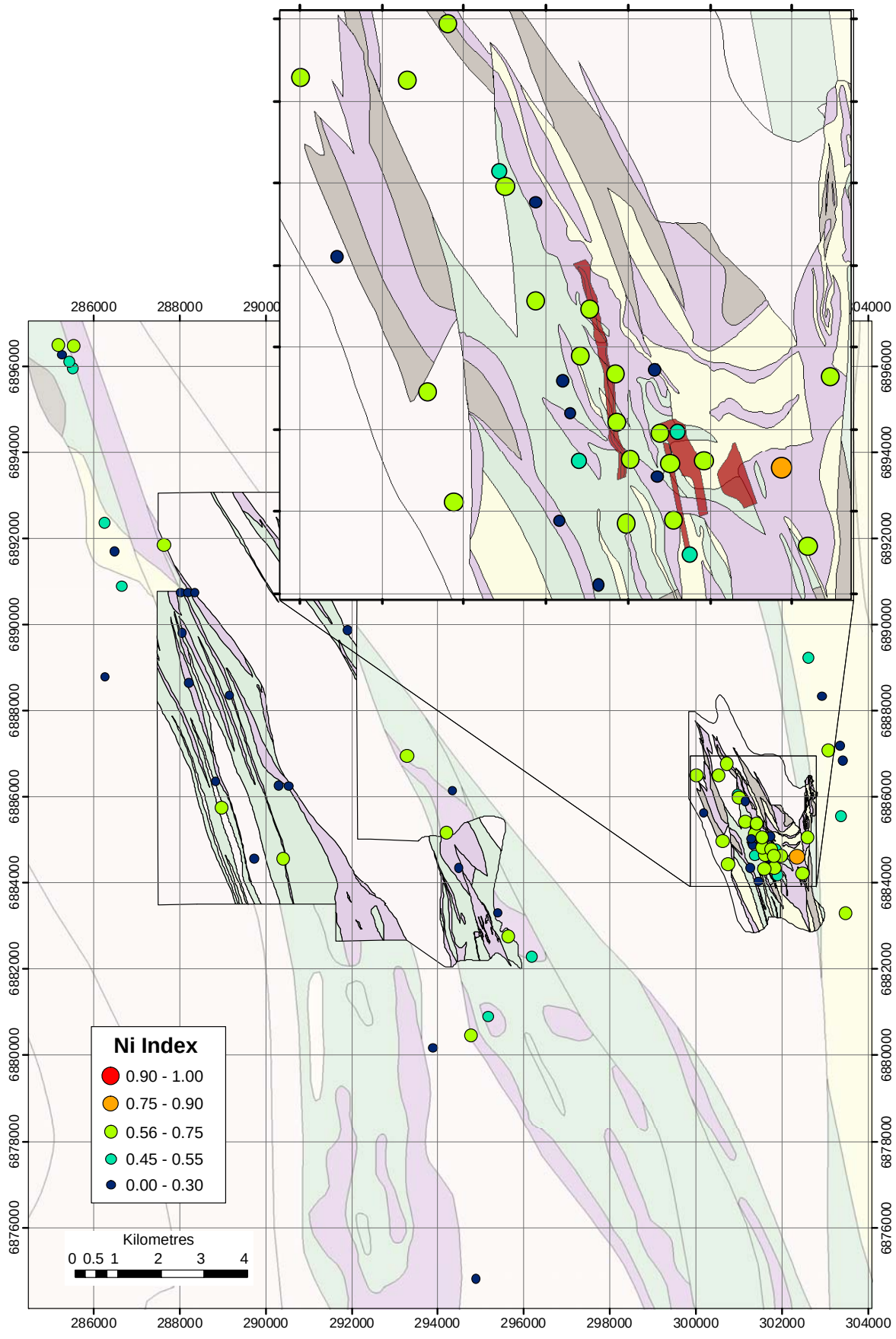

Figure 50: Ni Index distribution at Wildara.

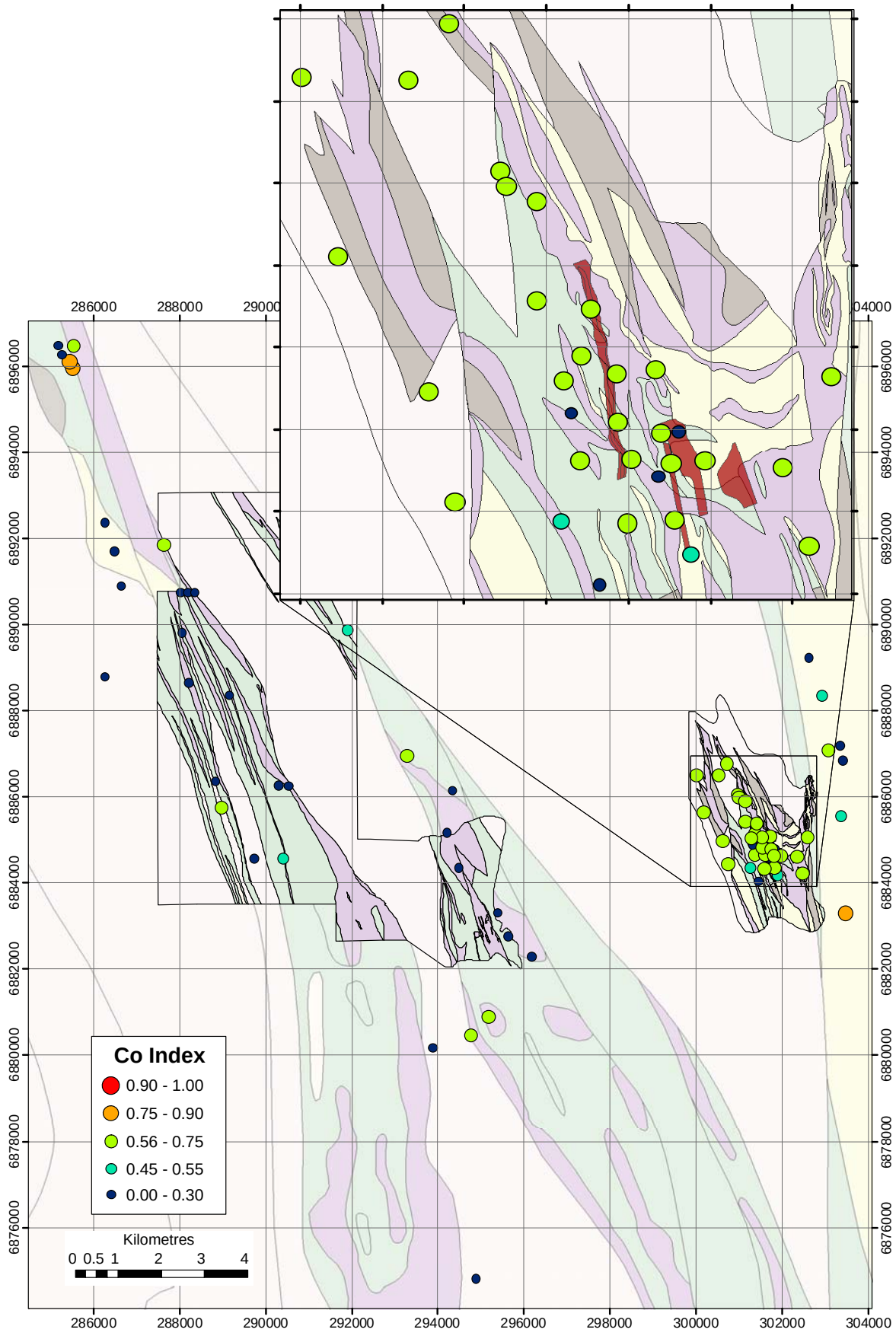

Figure 51: Co Index distribution at Wildara.

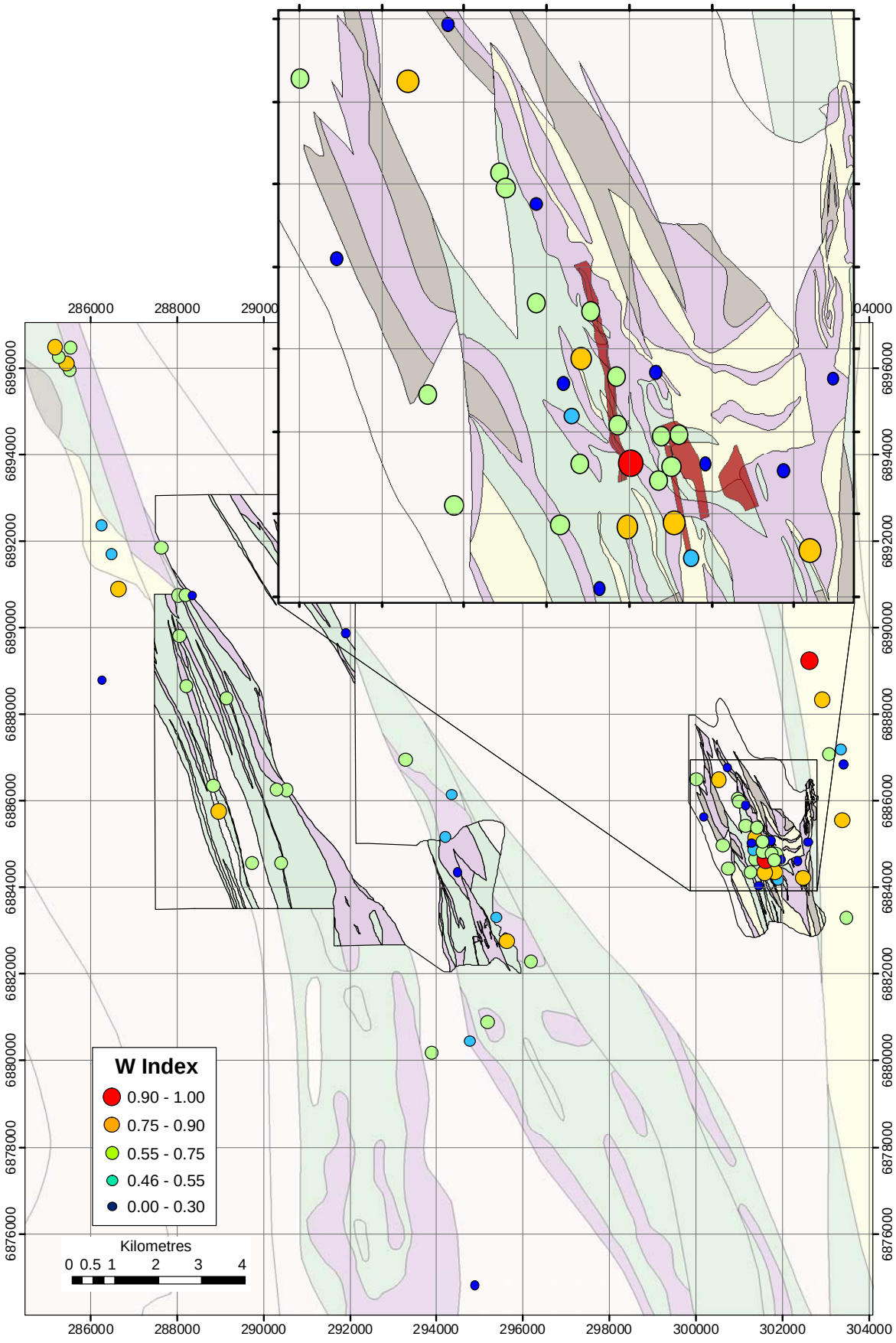

Figure 52: W index at Wildara.

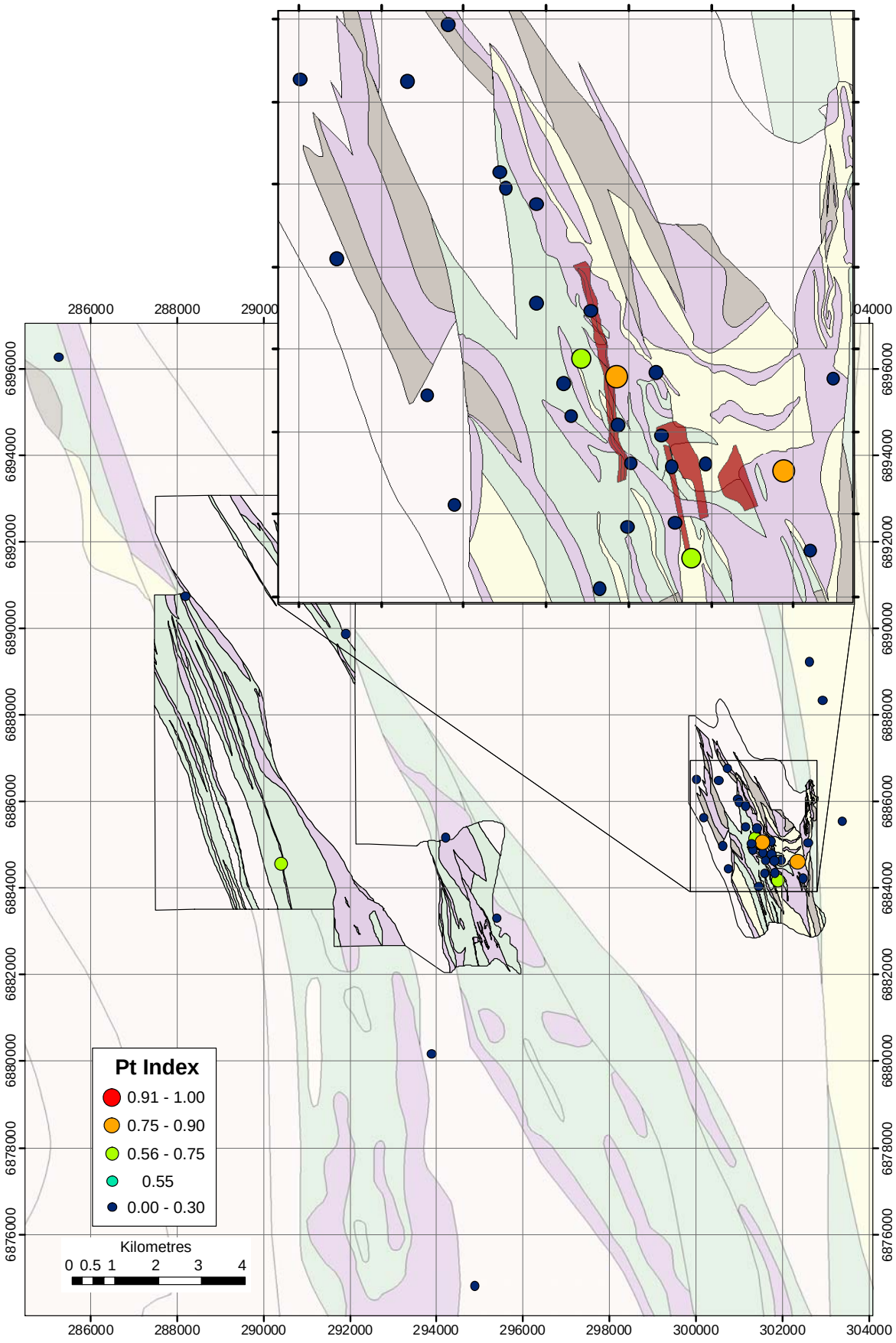

Figure 53: Pt Index at Wildara.

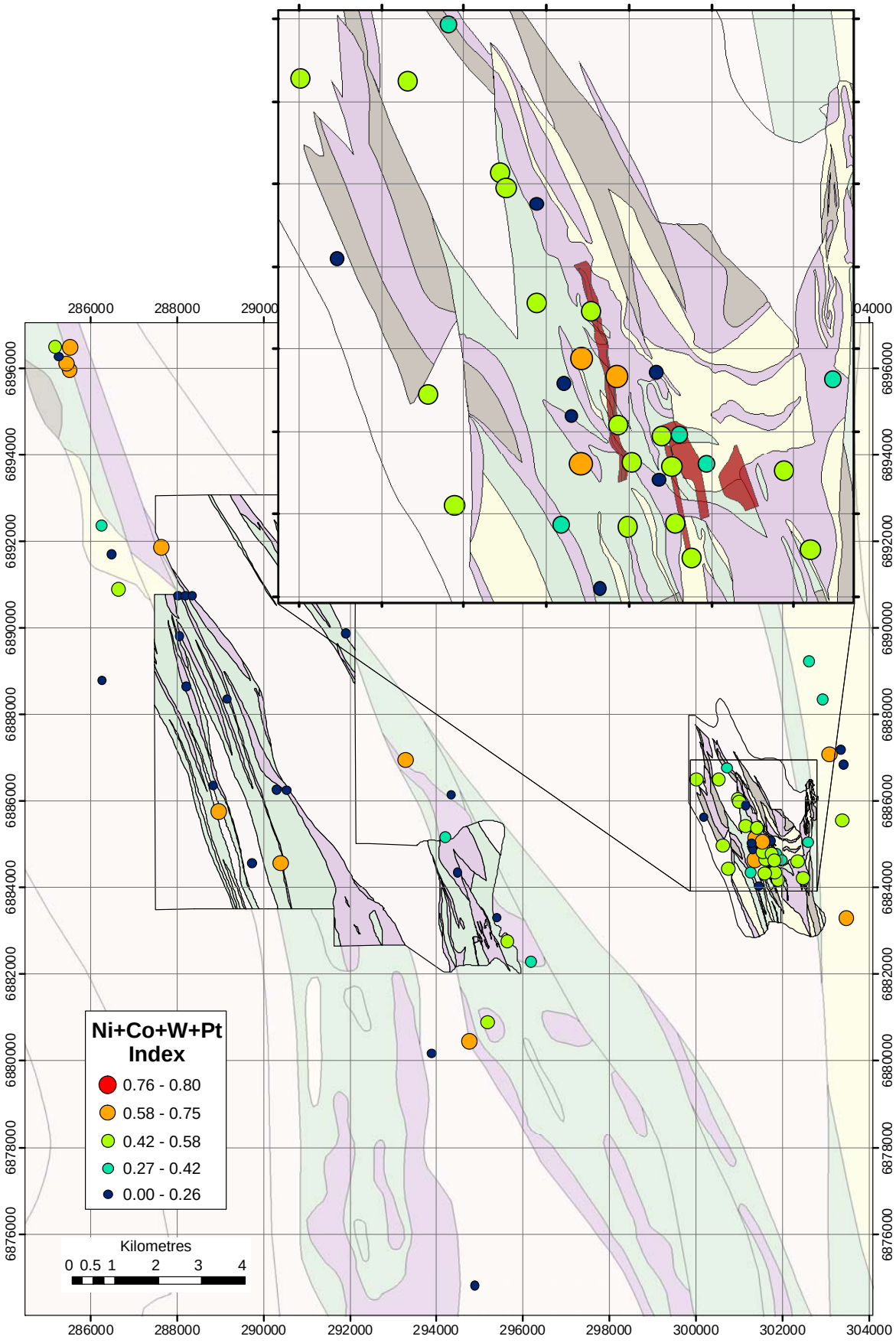

Figure 54: Min (Ni+Co+W+Pt) Index at Wildara.

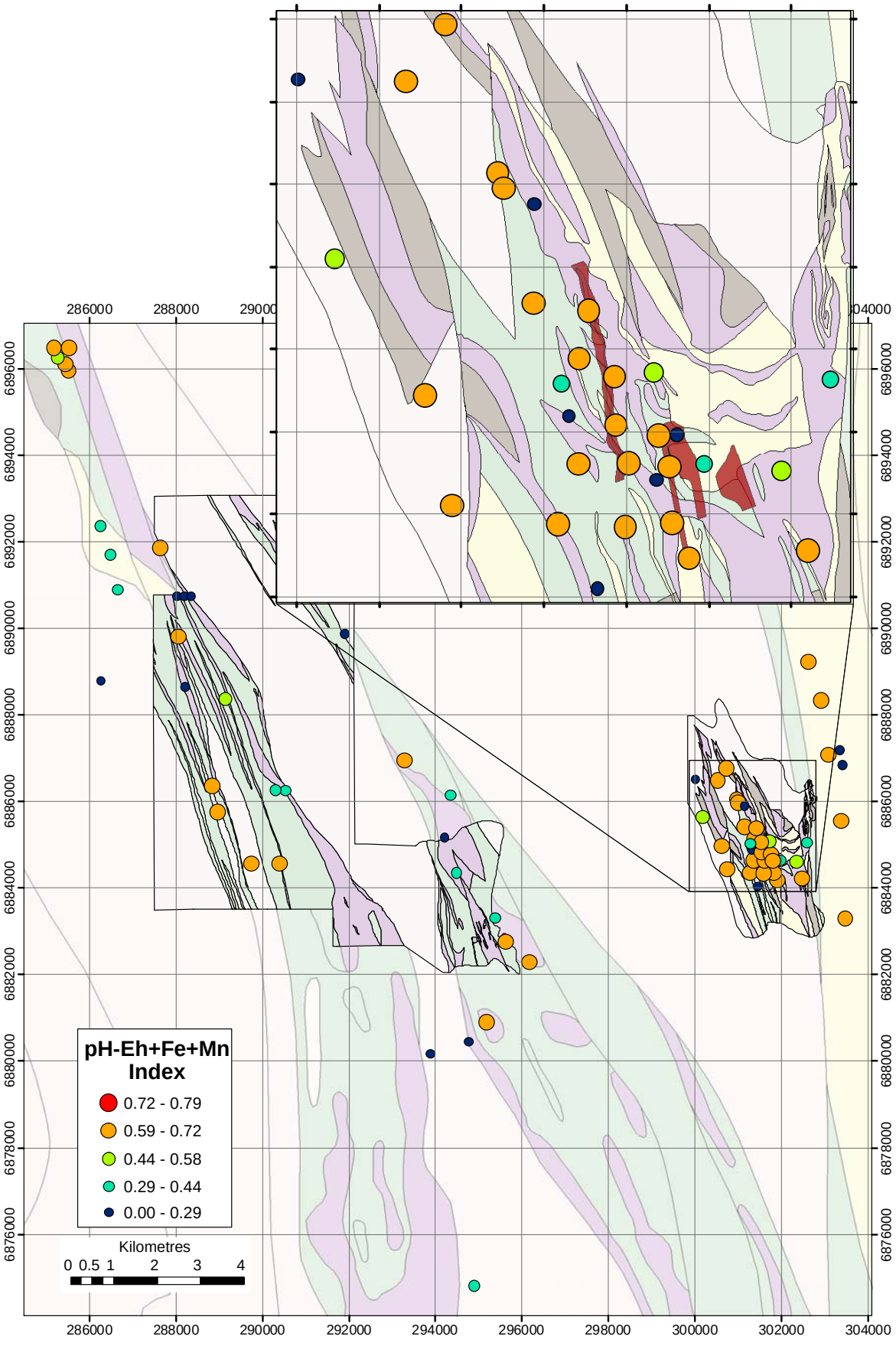

Figure 55: FeS (pH-Eh+Fe+Mn) Index at Wildara.

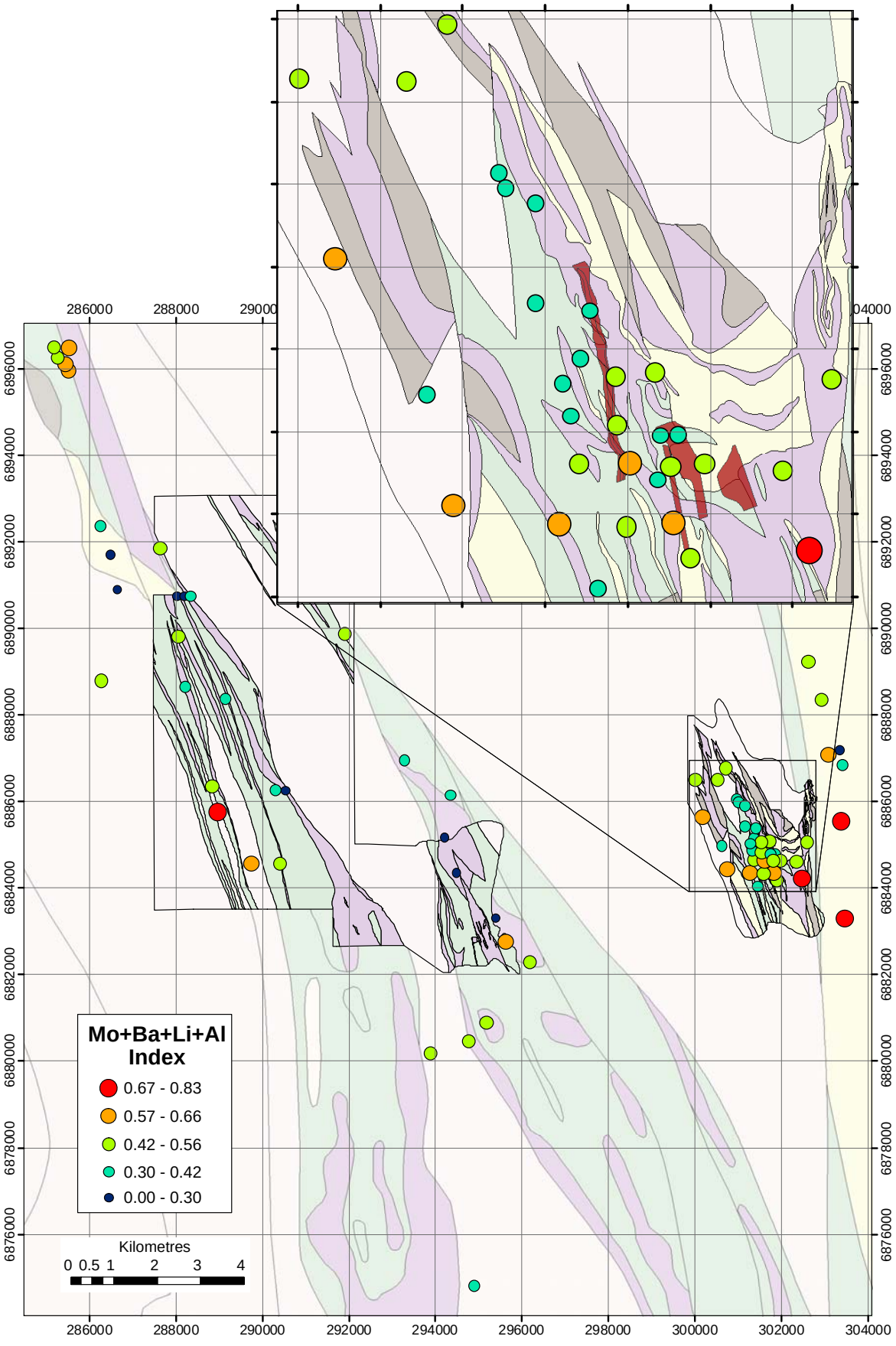

Figure 56: AcidS (Mo+Ba+Li+Al) Index at Wildara.

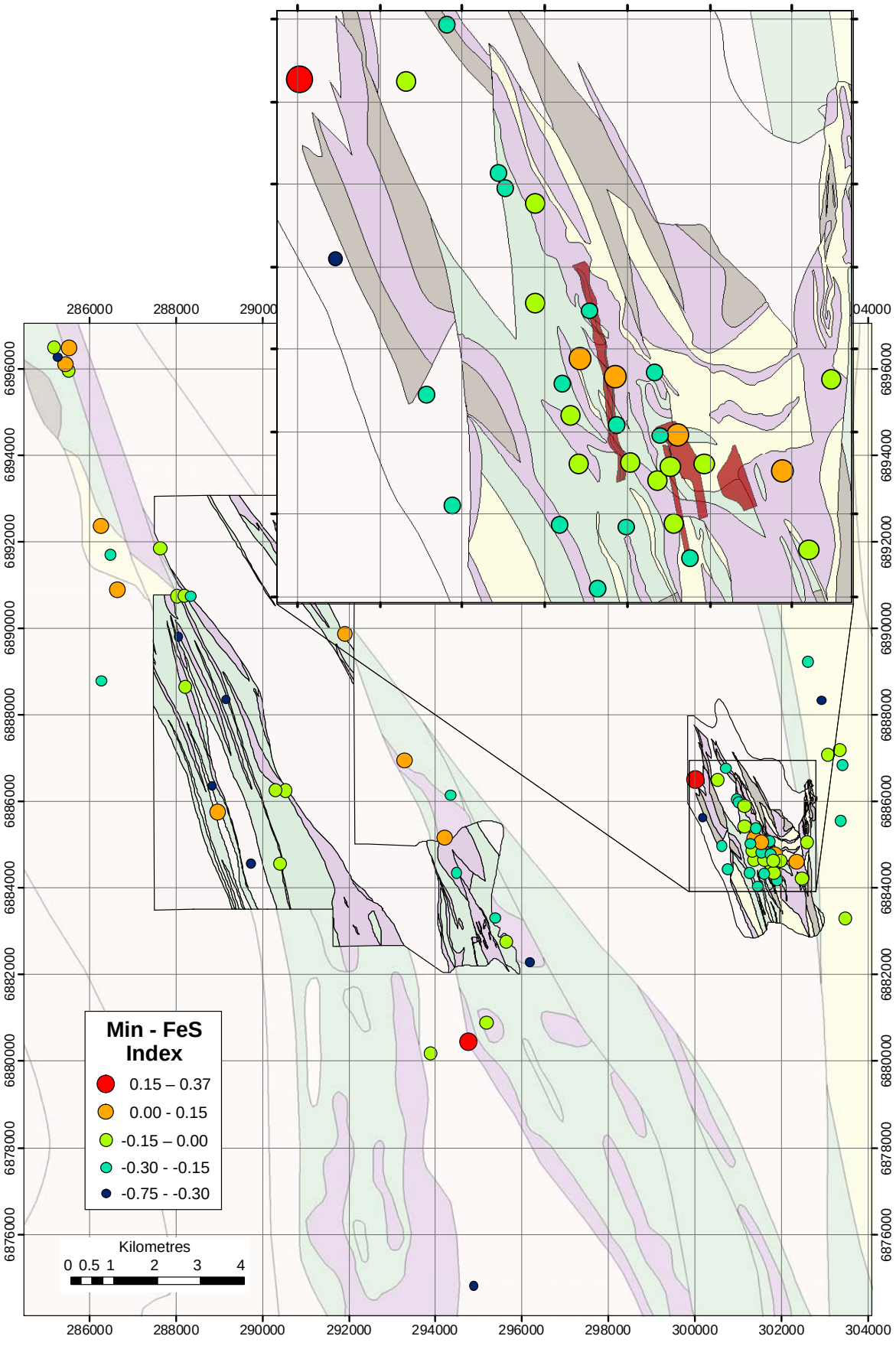

Figure 57: Min –FeS Index at Wildara.

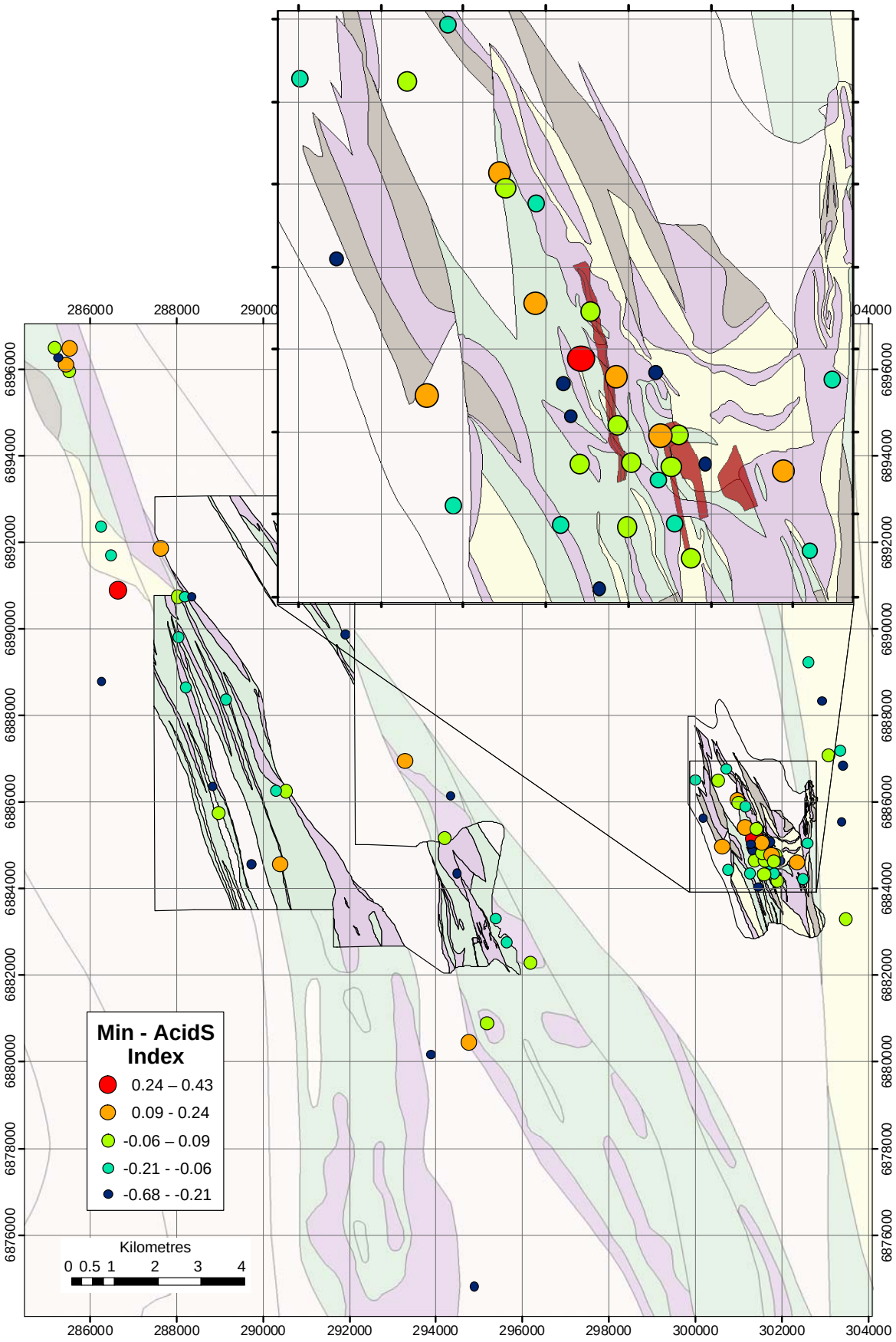

Figure 58: Min – AcidS Index at Wildara.

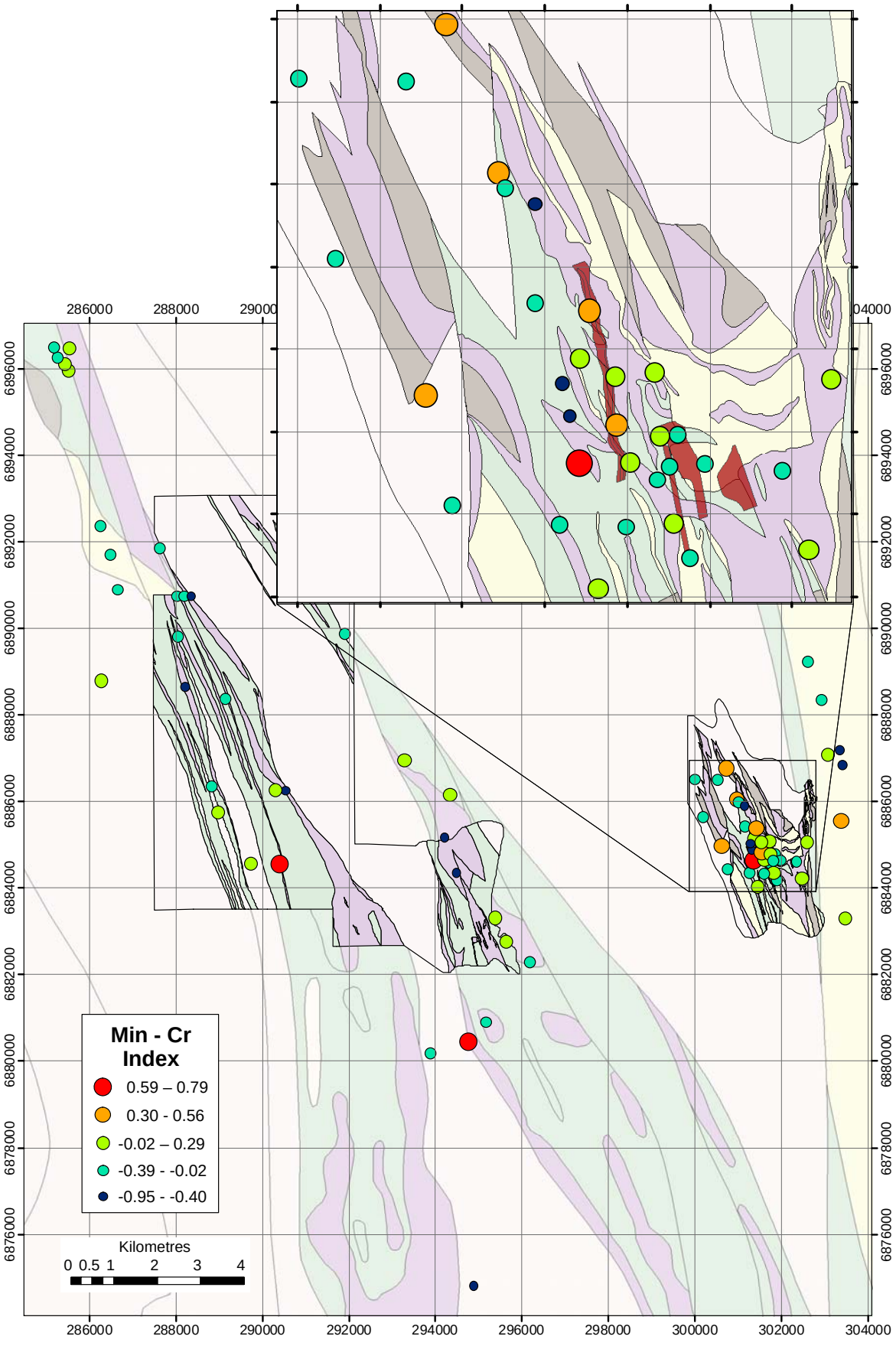

Figure 59: Min - Cr Index at Wildara.

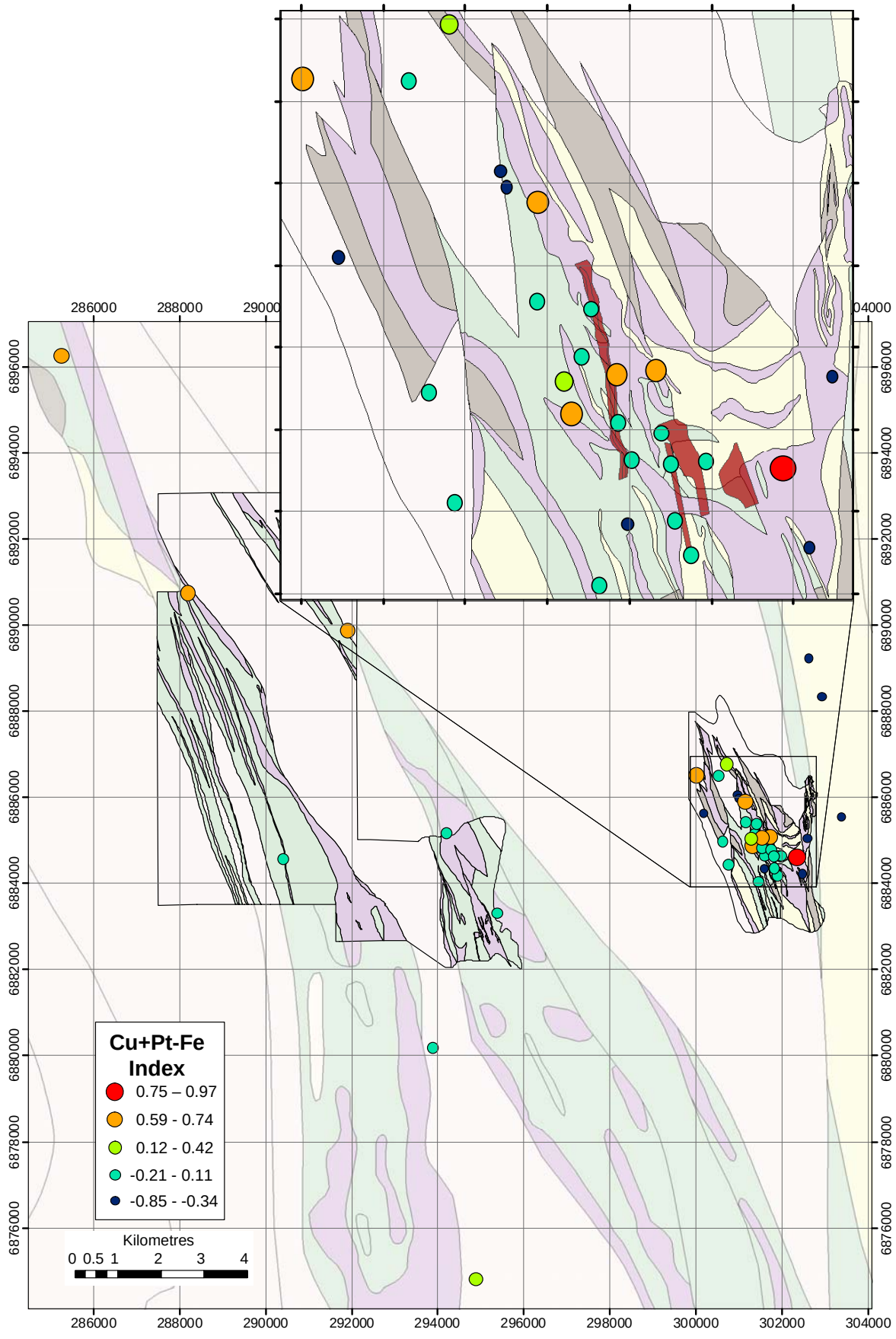

Figure 60: Cu+Pt-Fe Index at Wildara.

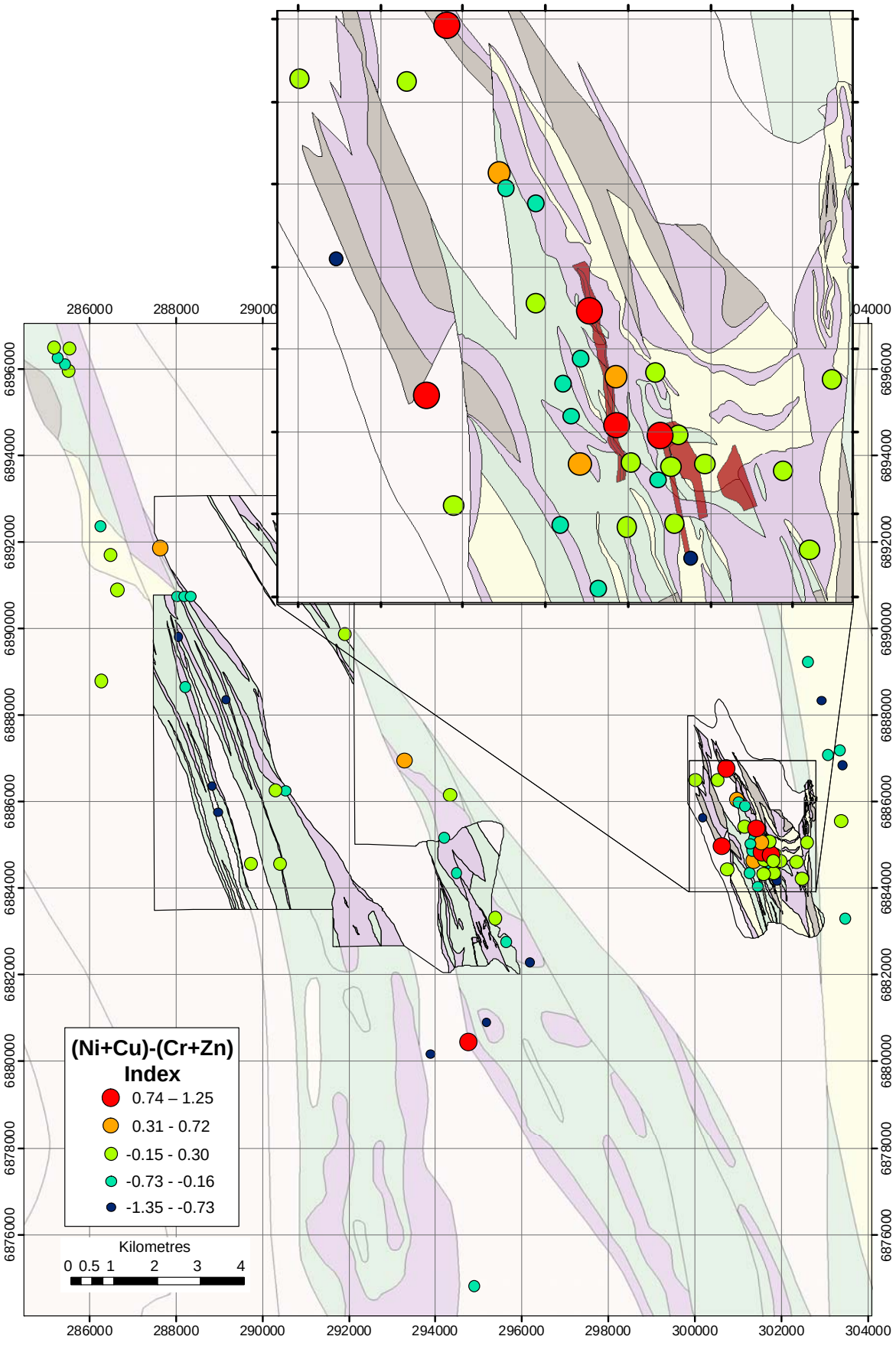

Figure 61: Modified Kambalda Ratio Index at Wildara.

7. YAKABINDIE

7.1 Site description and sampling

Yakabindie (BHP Billiton) is located approximately 60 km north of Leinster and 40 km south of the Mt.Keith Ni mine (Figure 2). The area sampled at Yakabindie comprised four main prospects, Six Mile, Serpentine Hill, Goliath North and David (Figure 62). The water table is 10-30 m below the surface. The regional geology is similar to that of the other prospects. Regolith is generally highly truncated.

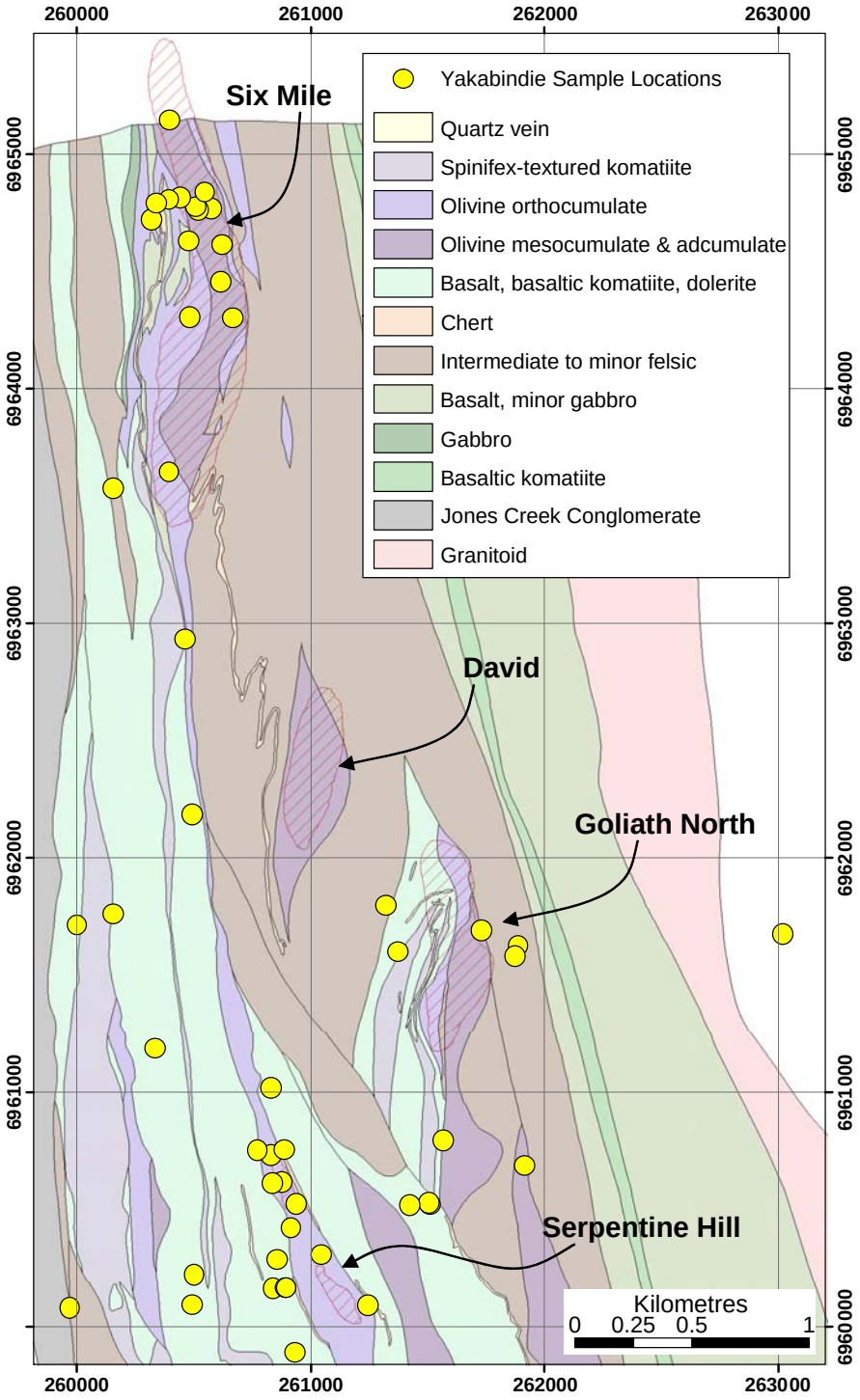

Figure 62: Detailed geology and sample locations of the Yakabindie region.

7.2 Lithological Indicators

Lithological indicators evident at the previous sites were not as clear at the Yakabindie site. Higher dissolved Cr seems to relate to the ultramafics in the north (Six Mile deposit), but is more subdued in the central southern ultramafics (Serp Hill deposit) and those in the central east (David and Goliath North deposits). Uranium was also inconsistent in identifying the granitic rocks (Figure 64).

7.3 Sulphide Indicators

The groundwaters at Yakabindie are very typical of the NE Yilgarn, being fresh and neutral. Those waters sampled from the sulphides in the area are moderately to highly reduced (Figure 65), possibly reflecting the major regolith truncation. Unlike other areas sampled in this study, none of the samples have acidic pH values (Figure 66), possibly because of regolith truncation and that all of the sulphides are disseminated. This might also explain why the previously observed high concentrations of elements characteristic of acid S lithologies (Al, Ba, Ce, Li, Mn, Mo, W) are not as strong in this area. Some high concentrations of Al occur in the Six Mile sulphides, but not elsewhere (Figure 67). Another interesting observation in the region is the significant difference between As and V concentrations. Dissolved As and V are almost undetectable to the north, but high in the southern mineralised zones (Figure 68 and Figure 69), possibly because of hydrothermal alteration over printing the highly structurally deformed southern section of Yakabindie.

7.4 NiS indicators

There is a moderate geochemical response for pathfinder elements in the groundwaters from Yakabindie. The Ni response (Figure 70) is less than for Harmony/Camelot (Figure 27), though greater than for Wildara (Figure 48). Dissolved Co values did not exceed 0.012 mg/L (Figure 71), which is lower than for Harmony/Camelot (Figure 28) and similar to Wildara (Figure 49).

7.5 Use of indices

Nickel (Figure 72) and Co indices (Figure 73) are above background across much of Yakabindie. The highest Ni signature is at Six Mile and Serpentine Hill, with a weaker anomaly over the Goliath area (Figure 72). The Co index shows little local scale discrimination across the Yakabindie area (Figure 73). Other single element indices used included Pt and W. The three anomalous Pt samples at Yakabindie are all associated with mineralisation (Figure 74). Likewise, W appears to have a similarly successful signature above mineralisation, but it has more anomalous sample points, and possibly a false positive result in central Yakabindie (Figure 75).

The element combination indices proved more effective in detecting the mineralisation at Yakabindie. The mineralisation index (Figure 76) had moderate to high scores over most of the mineralisation, with two points that would be considered outside of the known mineralised zones (central and the central west Yakabindie points; Figure 76). Using parameters that are affected by sulphides in general (the FeS and AcidS indices; Figure 77 and Figure 78) delineates the major sulphide bodies around Yakabindie. The Min-FeS index (Figure 79) improves the detection, but not the Min-AcidS index (Figure 80). The Min-Cr Index (Figure 81) is designed to remove lithological effects and appears to produce results similar to the Min-AcidS index (Figure 80).

Just as at Wildara (Section 6.5; Figure 60 and Figure 61), the Cu+Pt-Fe (Figure 82) and modified Kambalda ratio index [(Ni+Cu)-(Cr+Zn)] (Figure 83) showed utility in delineating NiS mineralisation.

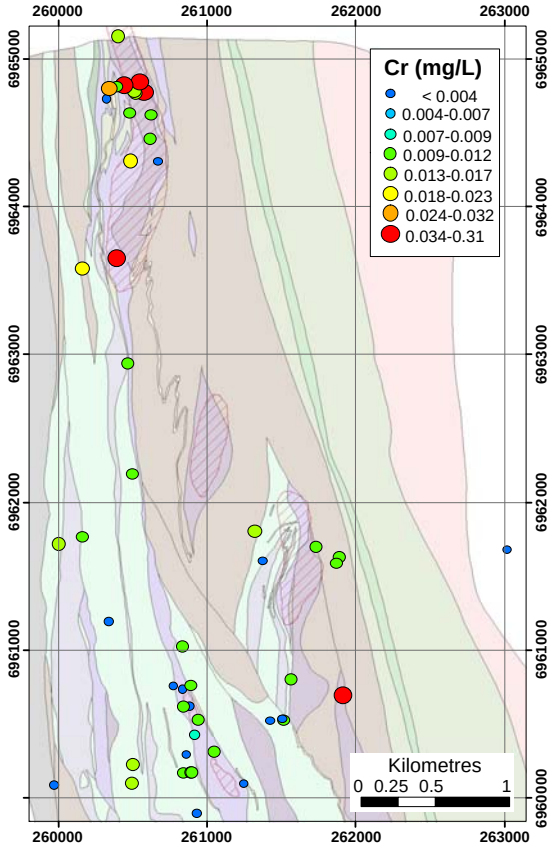

Figure 63: Dissolved Cr distribution at Yakabindie.

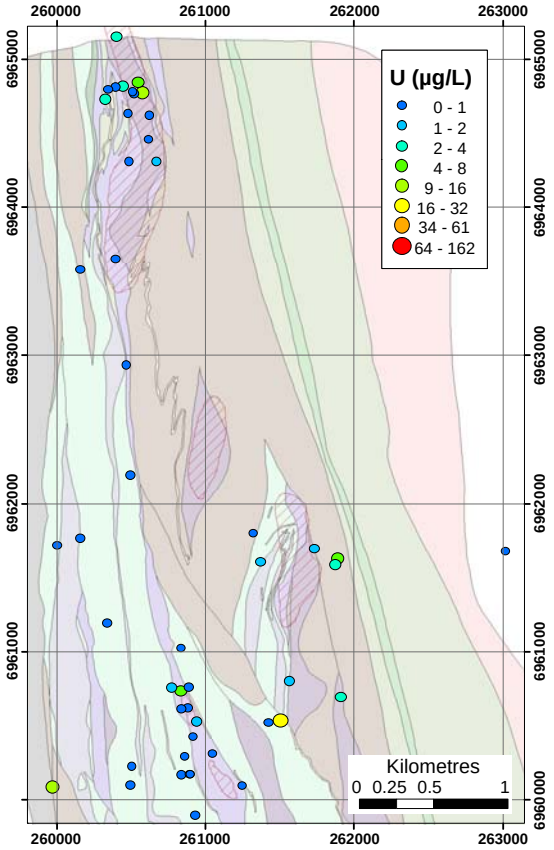

Figure 64: Dissolved U distribution at Yakabindie.

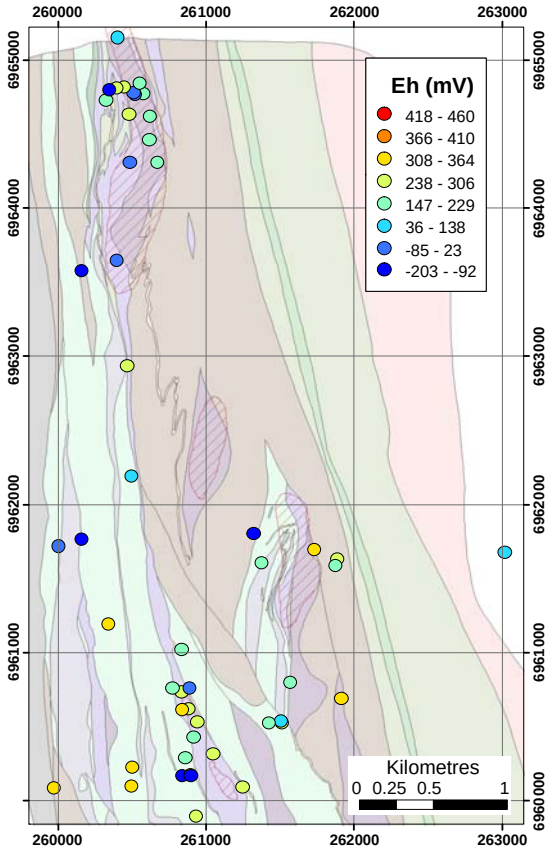

Figure 65: Groundwater Eh values at Yakabindie.

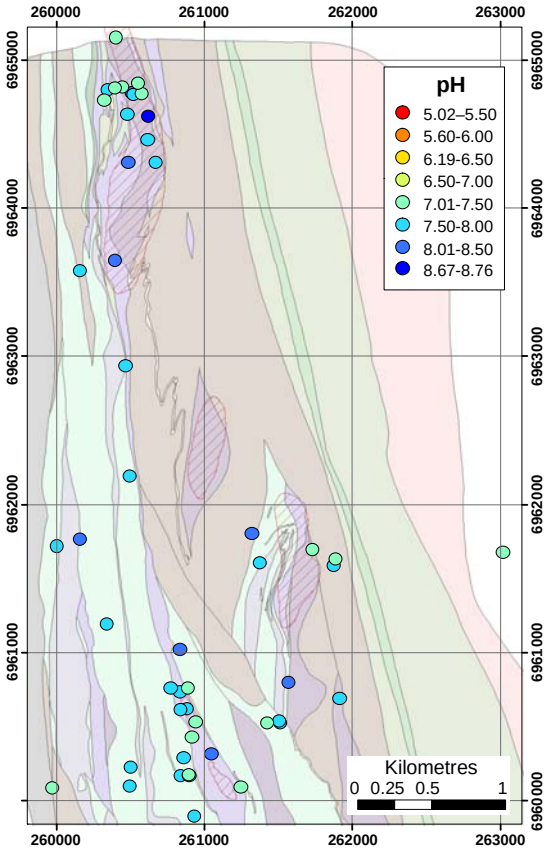

Figure 66: Groundwater pH values at Yakabindie.

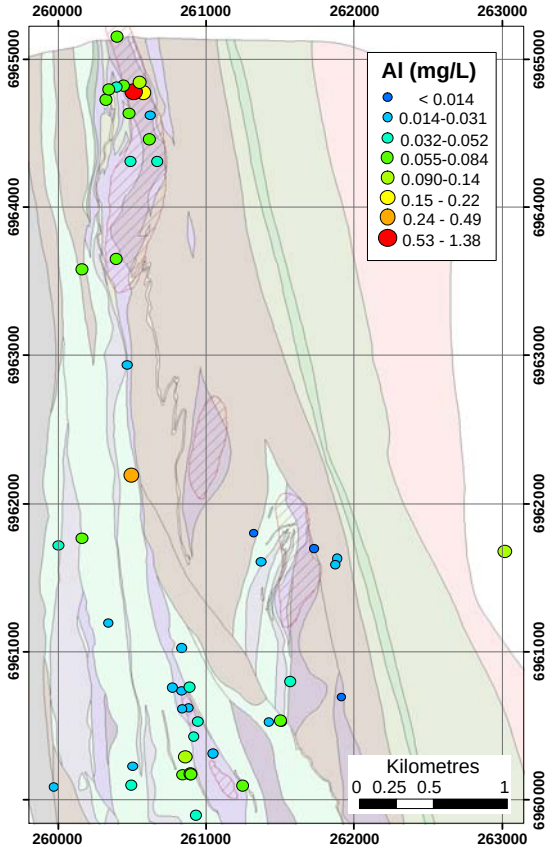

Figure 67: Dissolved Al distribution at Yakabindie.

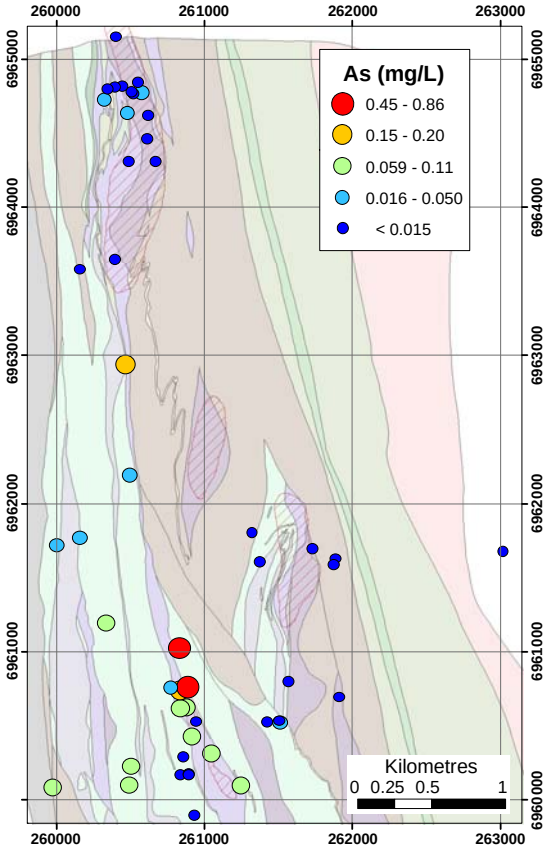

Figure 68: Dissolved As distribution at Yakabindie

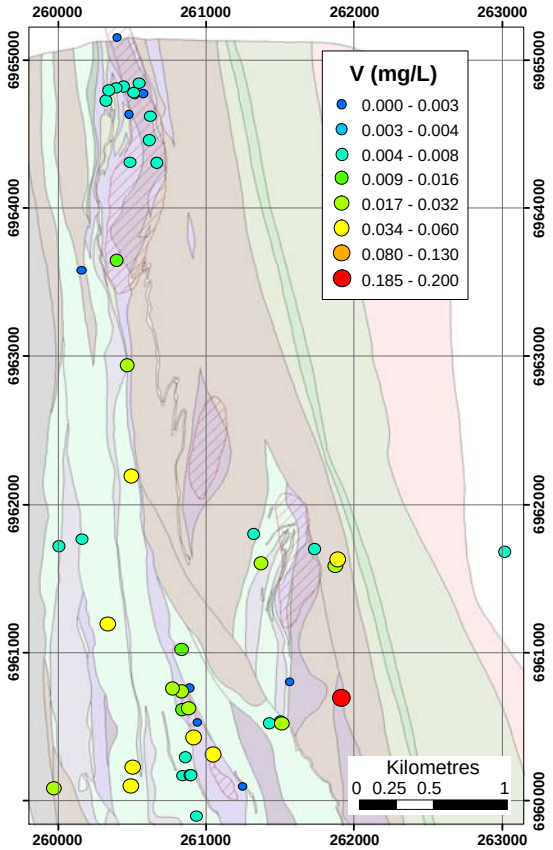

Figure 69: Dissolved V distribution at Yakabindie.

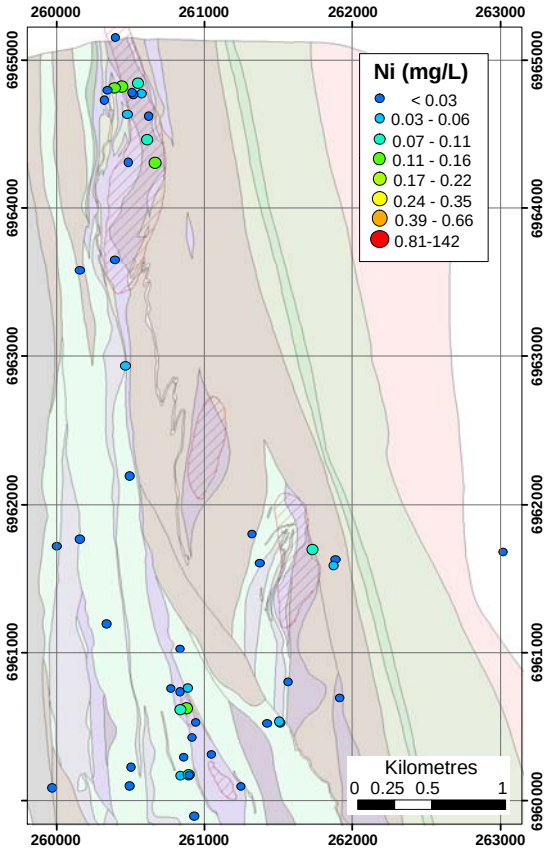

Figure 70: Dissolved Ni distribution at Yakabindie.

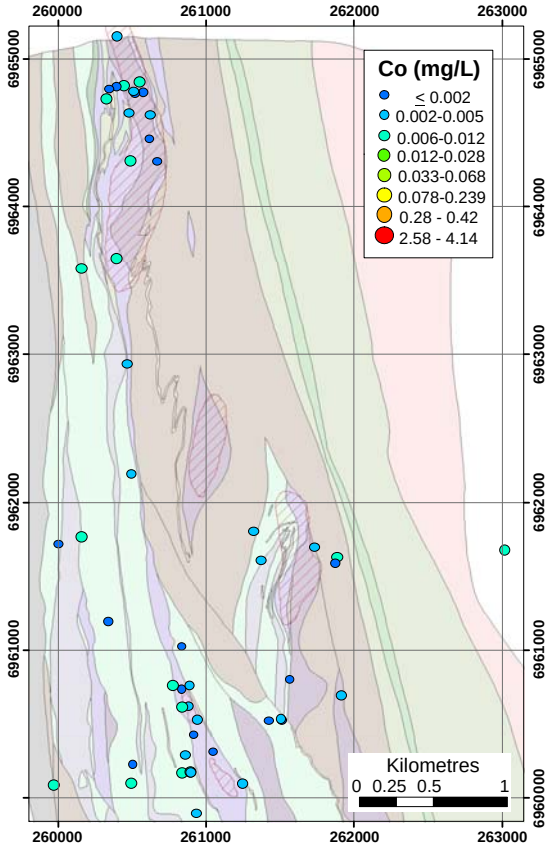

Figure 71: Dissolved Co distribution at Yakabindie.

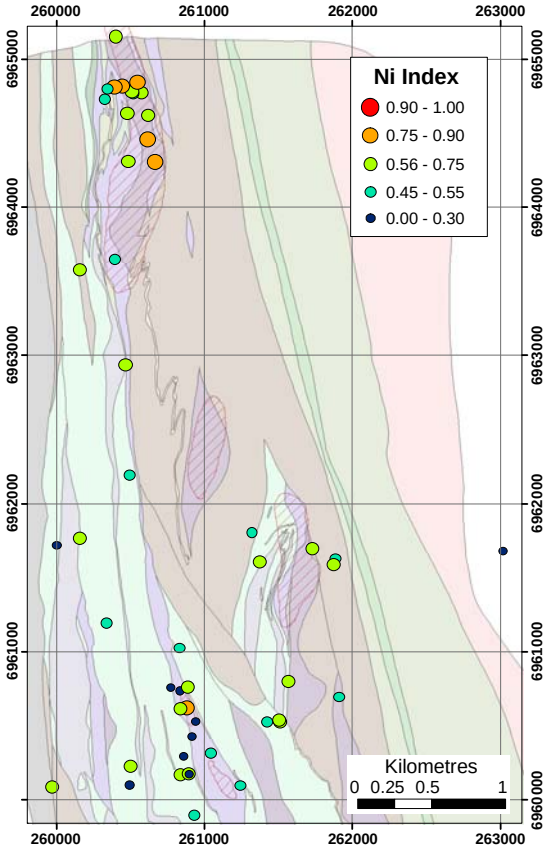

Figure 72: Ni Index distribution at Yakabindie.

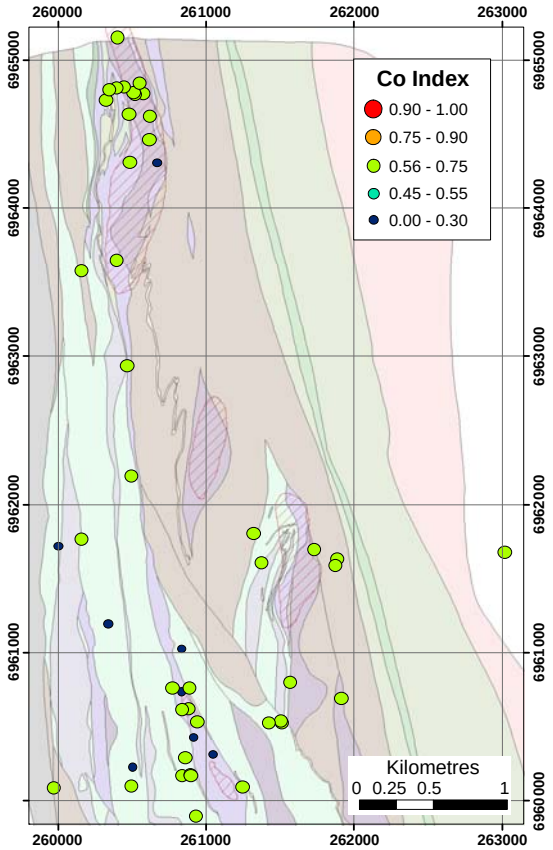

Figure 73: Co Index distribution at Yakabindie.

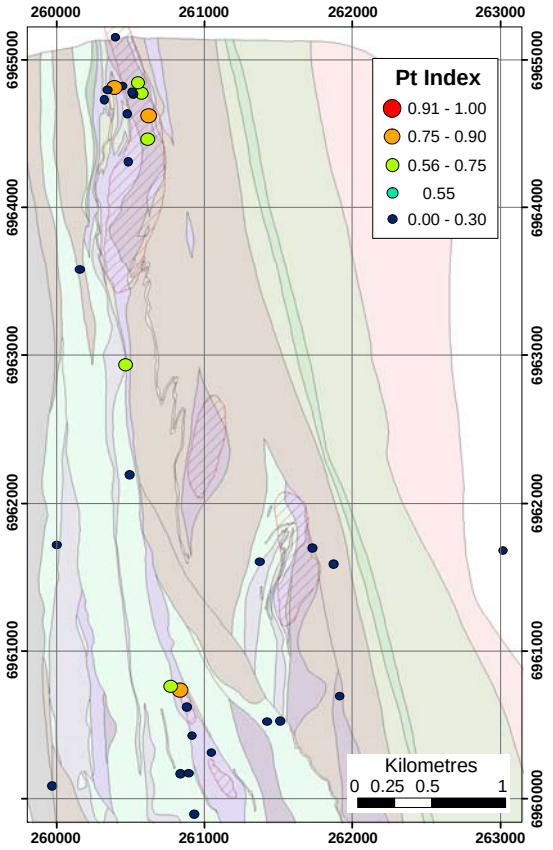

Figure 74: Pt Index at Yakabindie.

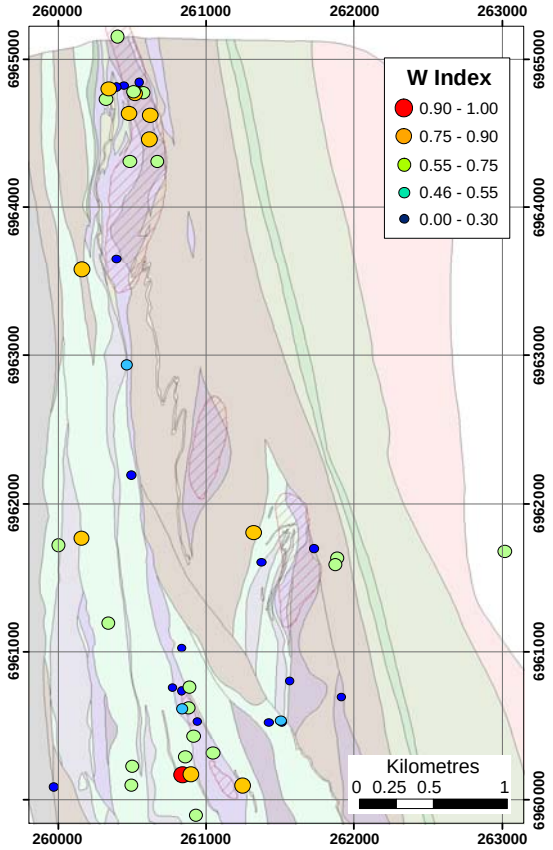

Figure 75: W Index at Yakabindie.

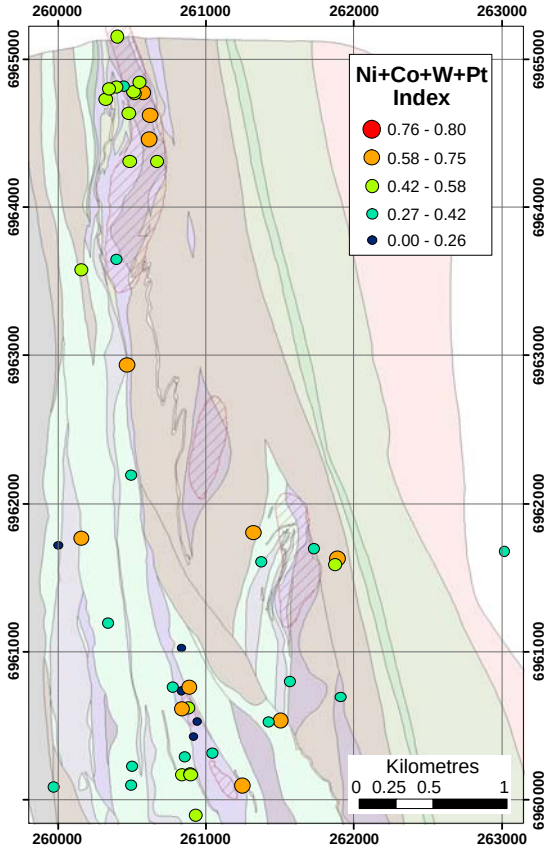

Figure 76: Min (Ni+Co+W+Pt) Index at Yakabindie.

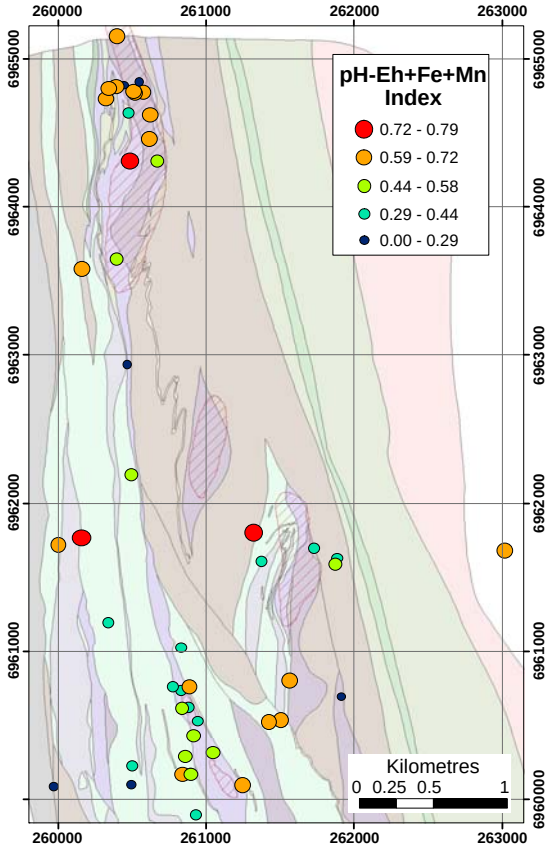

Figure 77: FeS (pH-Eh+Fe+Mn) Index at Yakabindie.

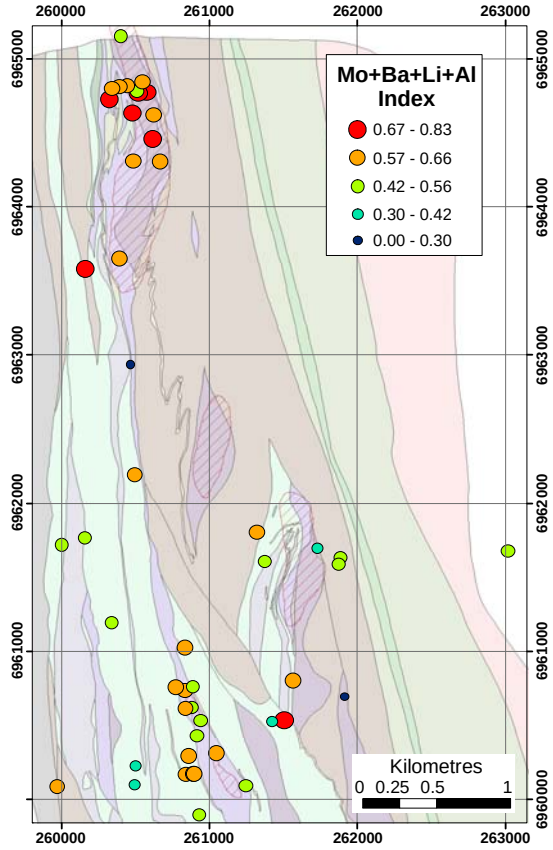

Figure 78: AcidS Index (Mo+Ba+Li+Al) at Yakabindie.

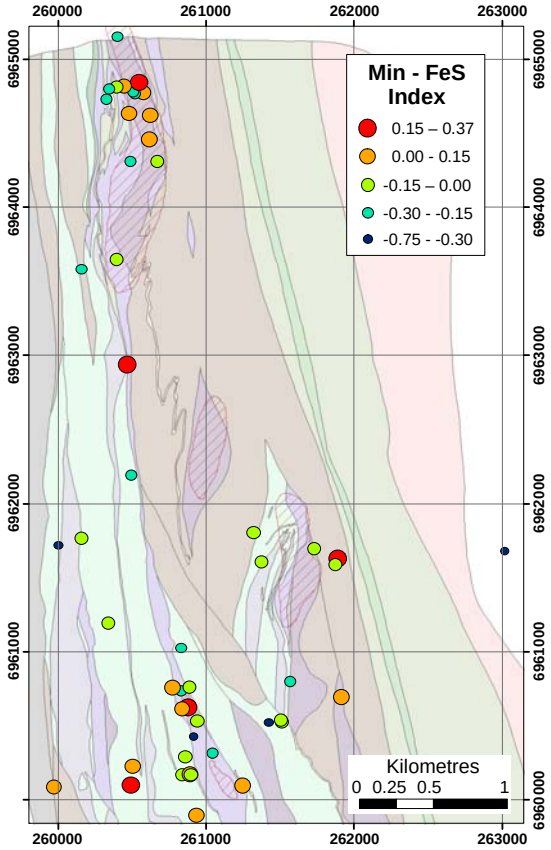

Figure 79: Min –FeS Index at Yakabindie.

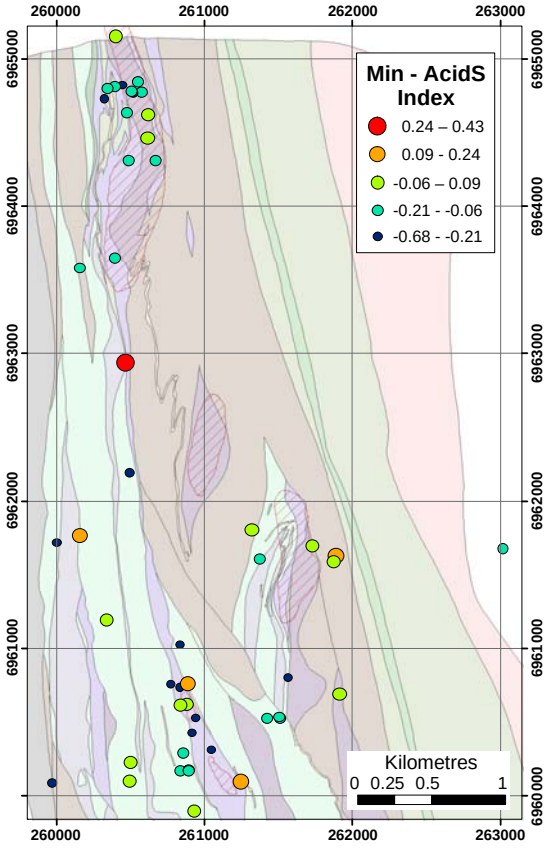

Figure 80: Min – AcidS Index at Yakabindie.

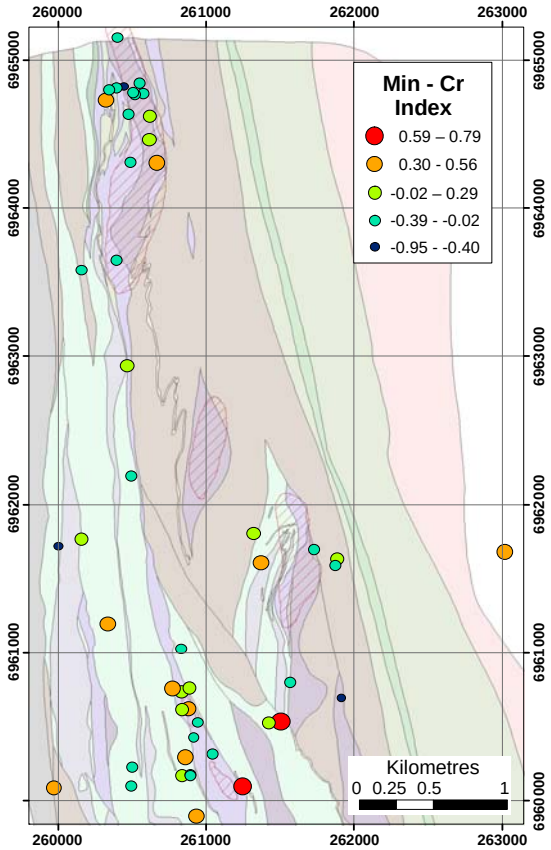

Figure 81: Miner-Cr Index at Yakabindie.

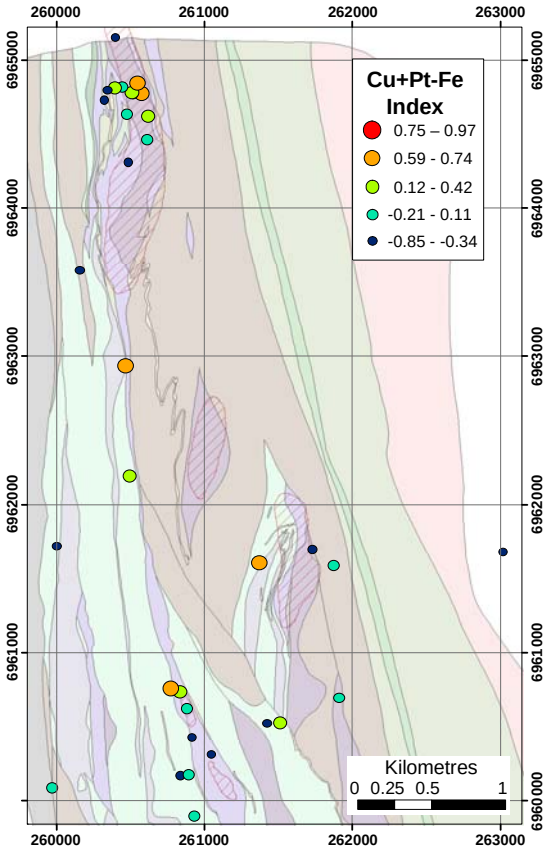

Figure 82: Cu+Pt-Fe Index at Yakabindie.

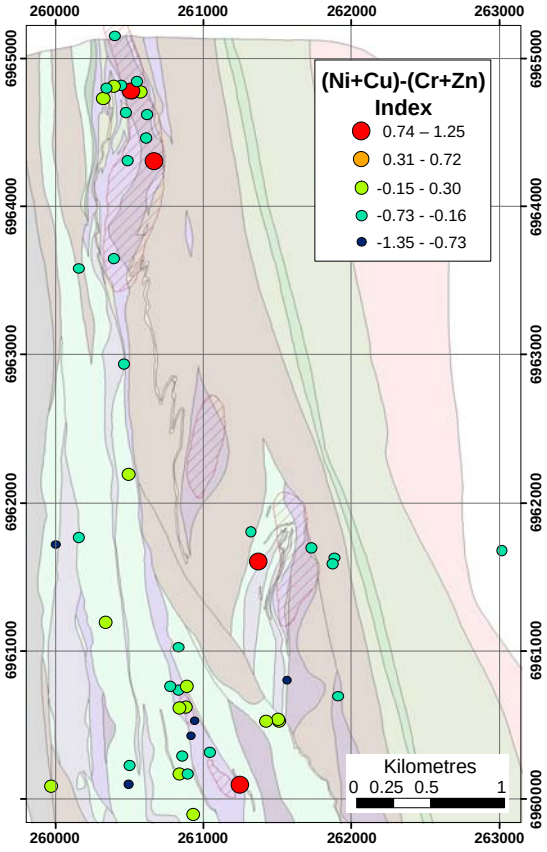

Figure 83: Kambalda ratio Index at Yakabindie.

8. HONEYMOON WELL

8.1 Site description and sampling

The Honeymoon Well Ni prospect (LionOre) is the most northern region sampled. It is located in the Agnew-Wiluna greenstone belt, approximately 90 km north of Leinster. The topography is broadly flat with ancient alluvial transported cover. The area is generally covered by low lying native shrubs and grasses with limited tree cover. The primary land use of the area is cattle grazing and mining. The climate is arid, with an annual rainfall of 256 mm y^{-1} and average daily maximum temperature of 29°C. There are four known prospects: Wedgetail, Corella, Hannibal and Harrier. Wedgetail is the only prospect that contains massive NiS, with disseminated NiS in the other deposits. The disseminated and massive sulphides are hosted in an ultramafic sequence of diverse metamorphosed komatiite lithologies (Gole and Woodhouse, 2000). The regolith in the study site comprises a 15-40 m thickness of mixed transported material (Noble, Unpublished) with a watertable depth of approximately 1-10 m. The Wedgetail deposit is the most northerly site at Honeymoon Well and is situated on a gradual slope towards Lake Way (Figure 84).

Sample numbers at Honeymoon Well are greater than other areas, due to easy access and a good database of regional bores. Honeymoon Well was the site for testing of sampling methodology. The region is slightly different to other areas of the NE Yilgarn, primarily due to the groundwater comprising a range of salinities (Figure 85) from fresh to hypersaline adjacent to Lake Way.

8.2 Lithological Indicators

The lithological indicator Cr clearly distinguishes ultramafic rocks from other lithologies at Honeymoon Well (Figure 86). In contrast, dissolved U is a poor lithologic indicator in this region, although it is a potential pathfinder for U mineralisation. The highest U concentrations (Figure 87), index scores (Figure 88) and uraninite SI (Figure 89) all correlate with the palaeochannel drainage at the north end of Honeymoon Well flowing towards Lake Way. Other mineral SI indices such as carnotite (Figure 90) and rutherfordine (Figure 91) show high values in the area, indicating U may well be actively precipitating.

8.3 Sulphide Indicators

The Honeymoon Well samples are commonly reduced (Figure 92) and pH neutral (Figure 93). Many of the regional farm bores had mid range Eh values, and the most reduced waters all occur near known sulphides (Figure 92). The two exceptions occur to the east and the SE of Honeymoon Well in areas mapped as granitic rocks and these samples had the characteristic smell of waters collected near sulphides. The large mapping scale may account for the discrepancy in the data, with sulphides too small to include, or not discovered. Further investigation and possible use of other techniques such as EM or drilling may clarify this in the future. Only one sample at the Wedgetail deposit in the northern part of Honeymoon Well had a pH < 6.5 (Figure 93). All other samples have not been readily oxidized or more likely are adequately buffered by surrounding minerals.

If the waters are being acidified then buffered (Section 3.3), some of the other elements that have been used in other sites to indicate groundwater evolution should produce significant anomalies. Dissolved Al and Mn agree with the model, having anomalous concentrations over the mapped sulphides (Figure 95 and Figure 96). Dissolved Ce (Figure 97) shows some anomalous values, and Li concentrations are highest at the Wedgetail massive sulphide site (Figure 98).

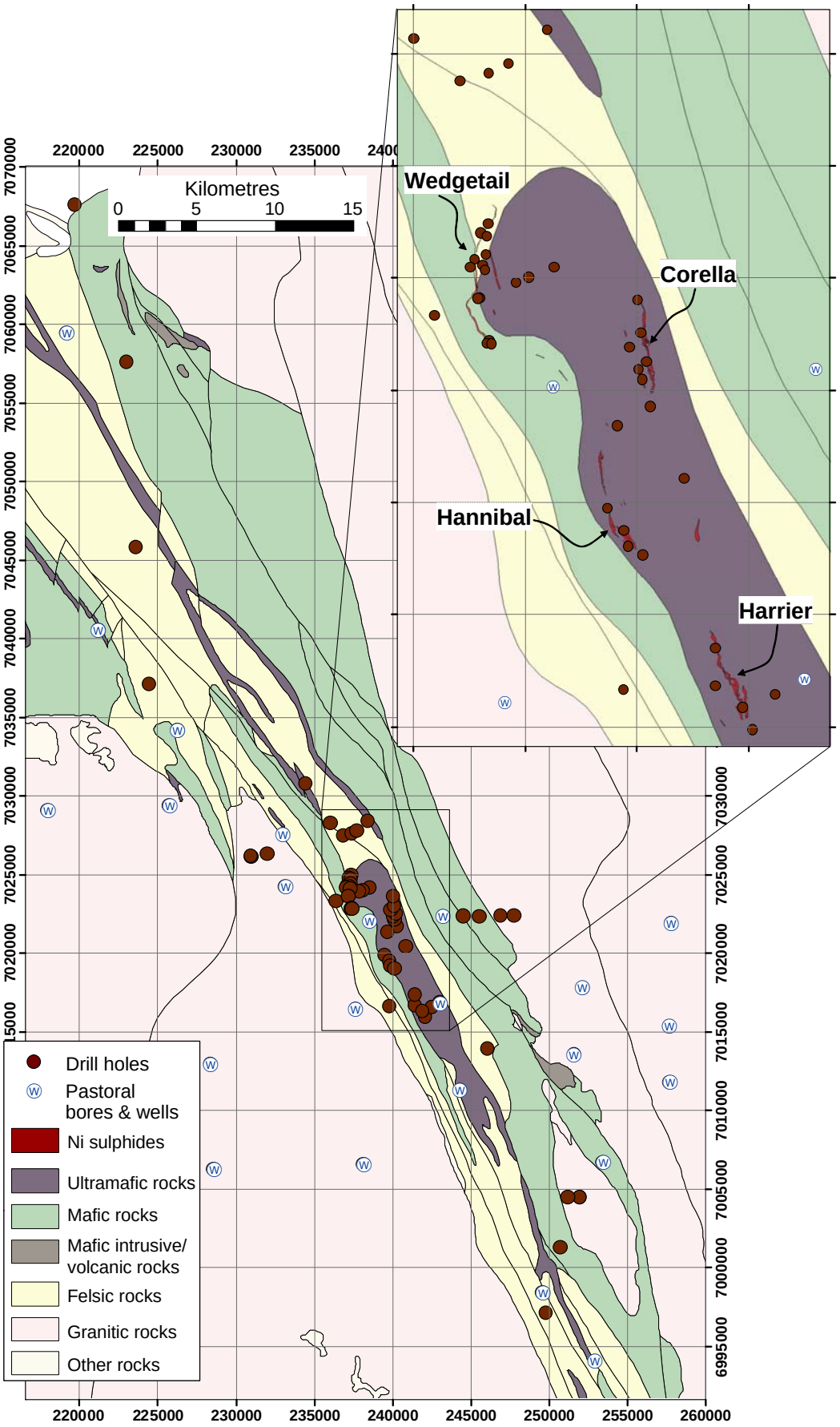

Figure 84: Detailed geology and sample locations of the Honeymoon Well region.

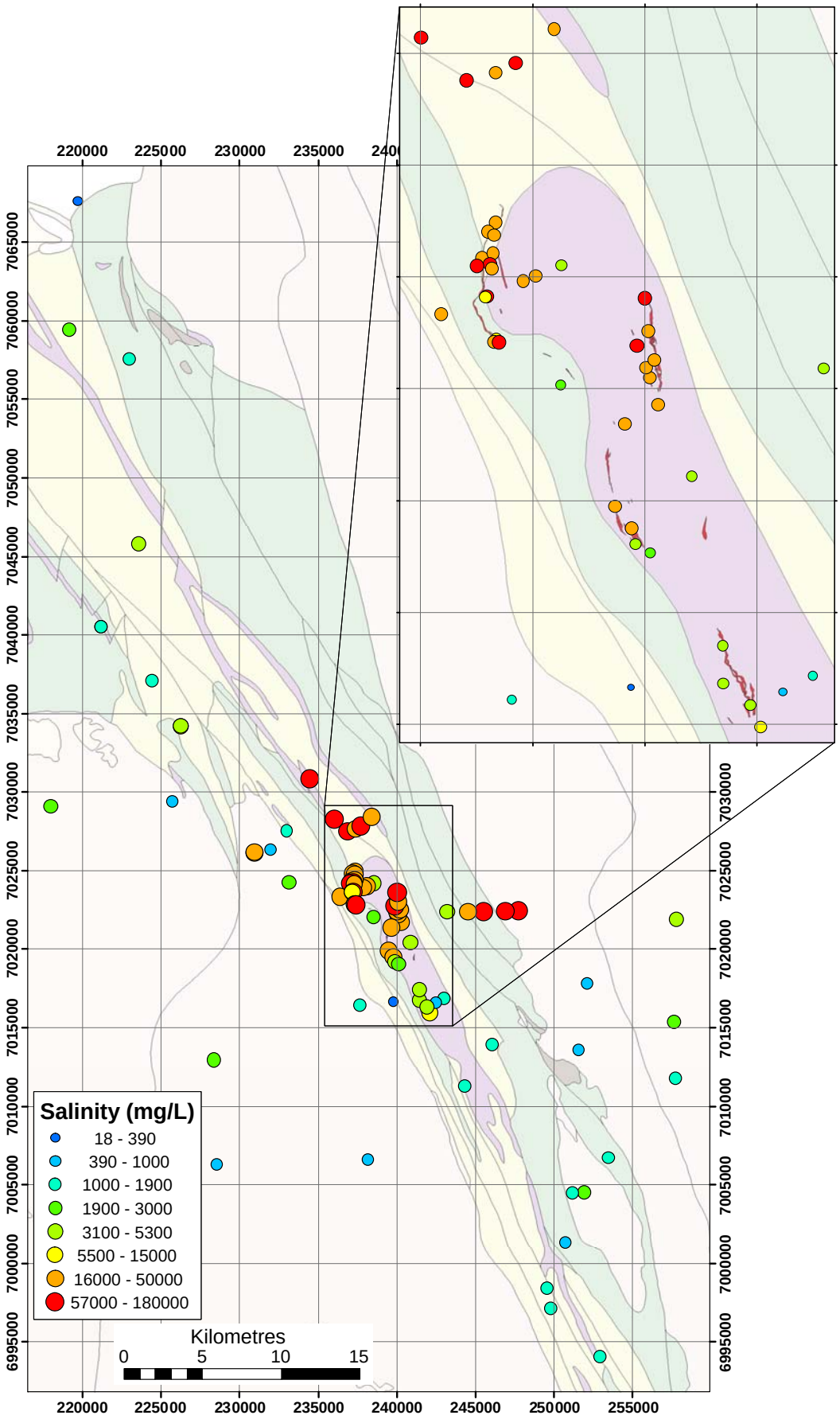

Figure 85: Total Dissolved Solids distribution at Honeymoon Well.

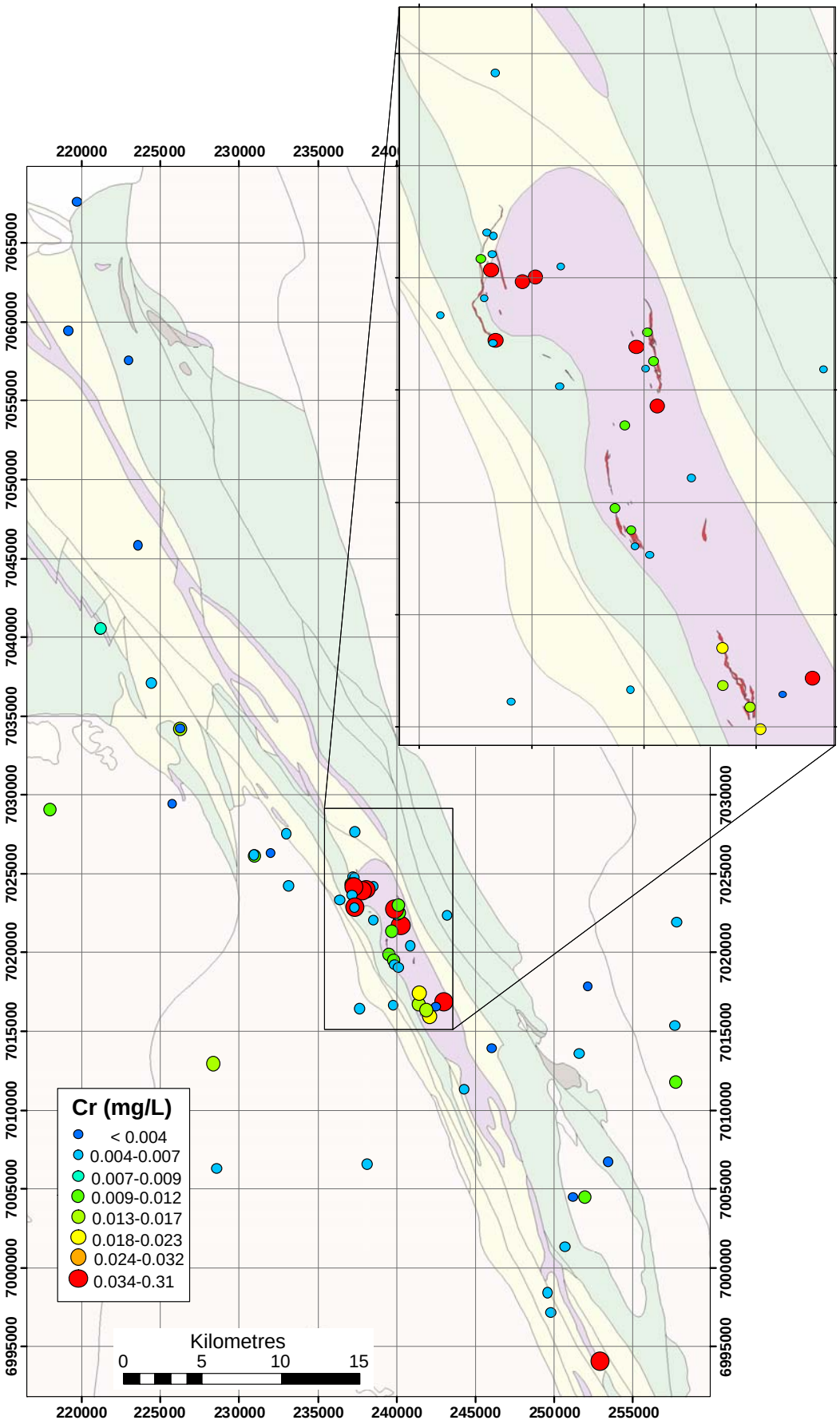

Figure 86: Dissolved Cr distribution at Honeymoon Well.

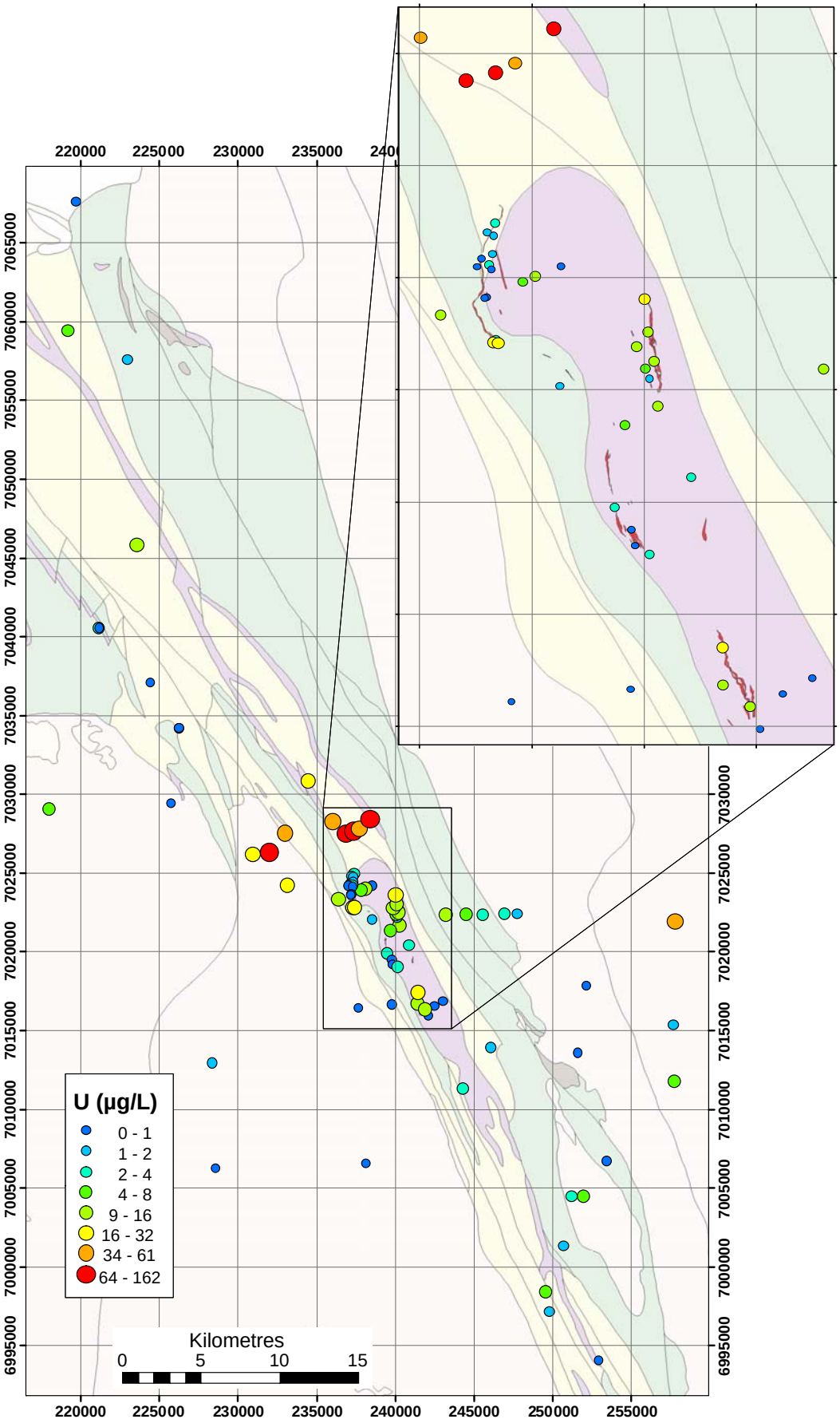

Figure 87: Dissolved U distribution at Honeymoon Well.

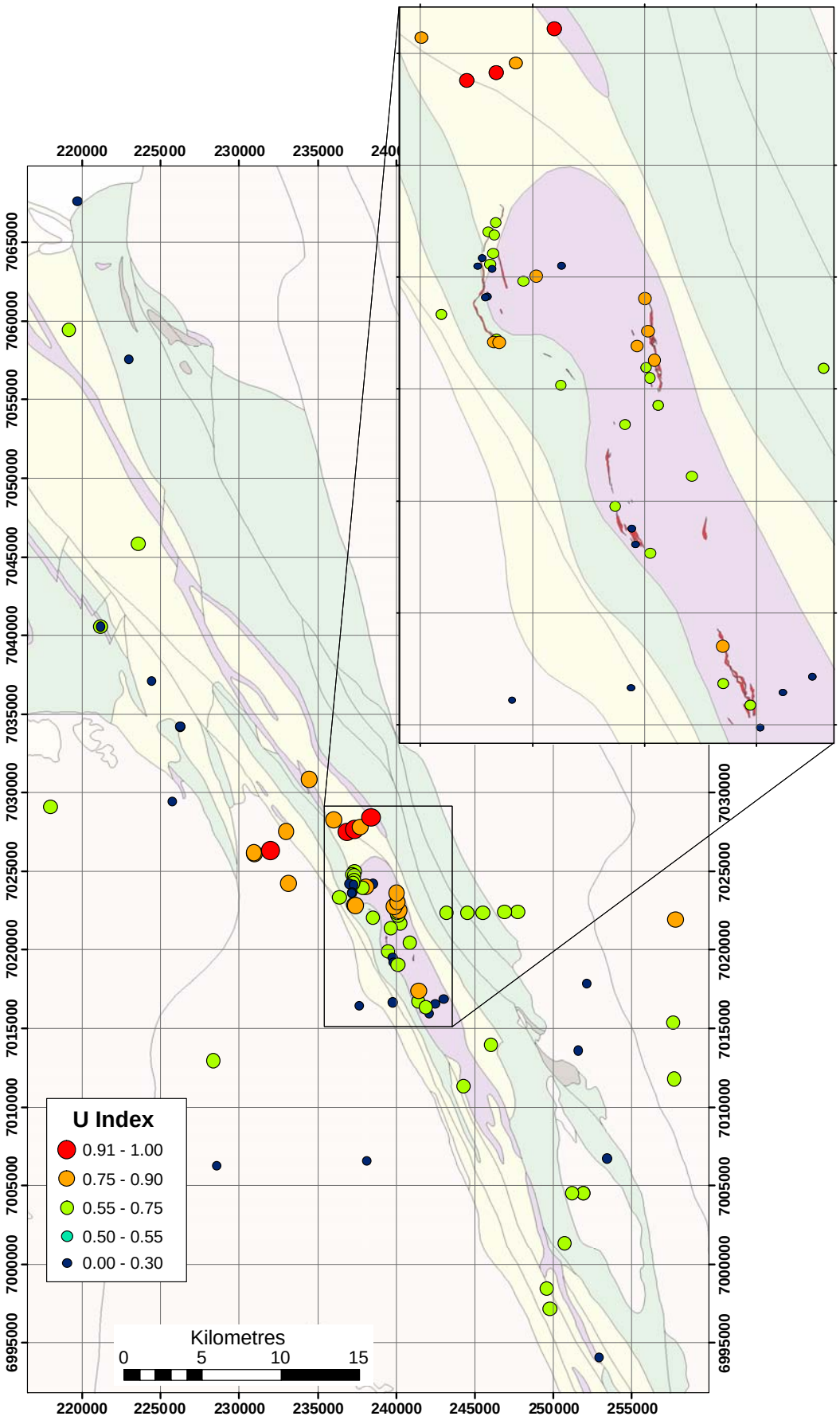

Figure 88: U Index distribution at Honeymoon Well.

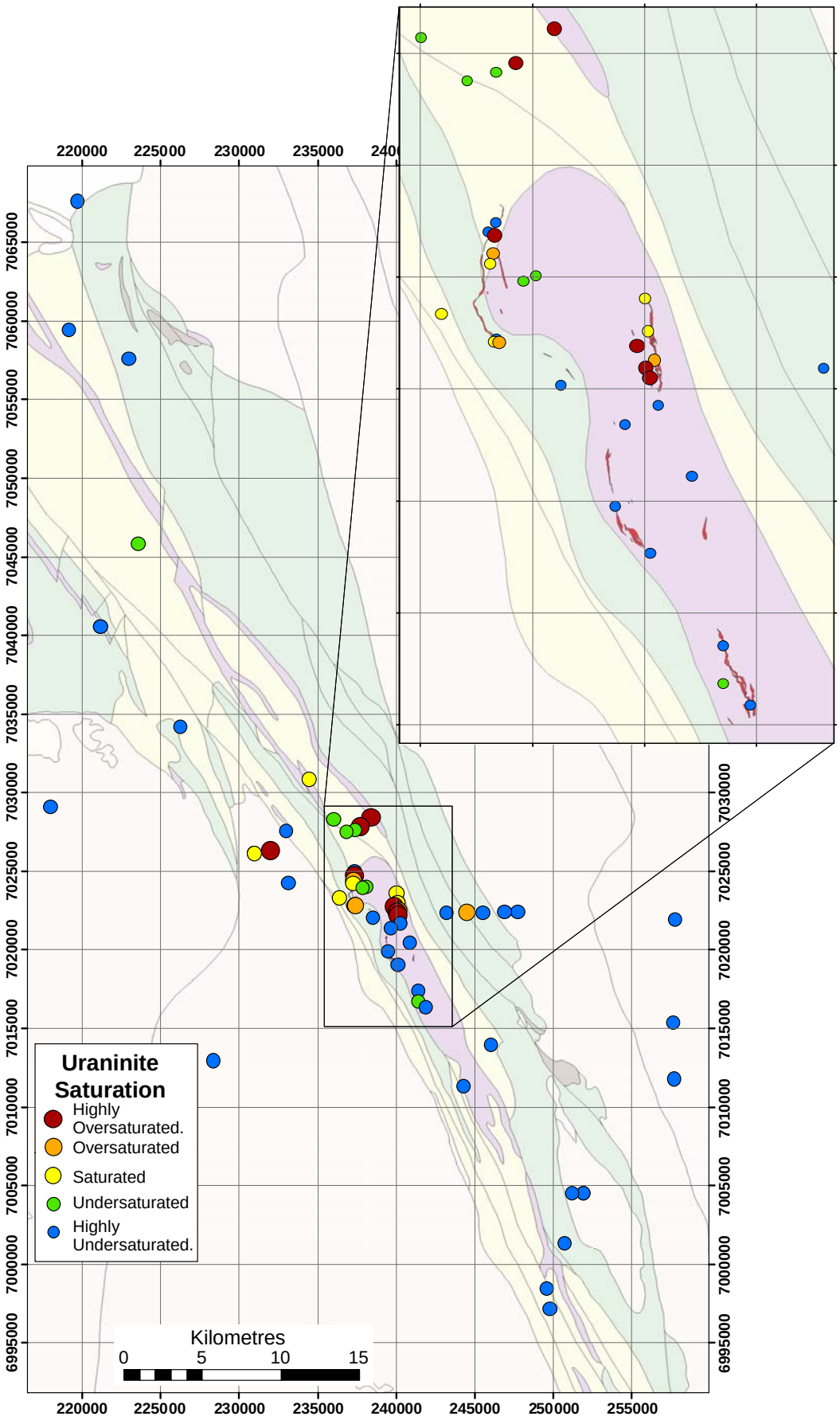

Figure 89: Uraninite SI distribution at Honeymoon Well.

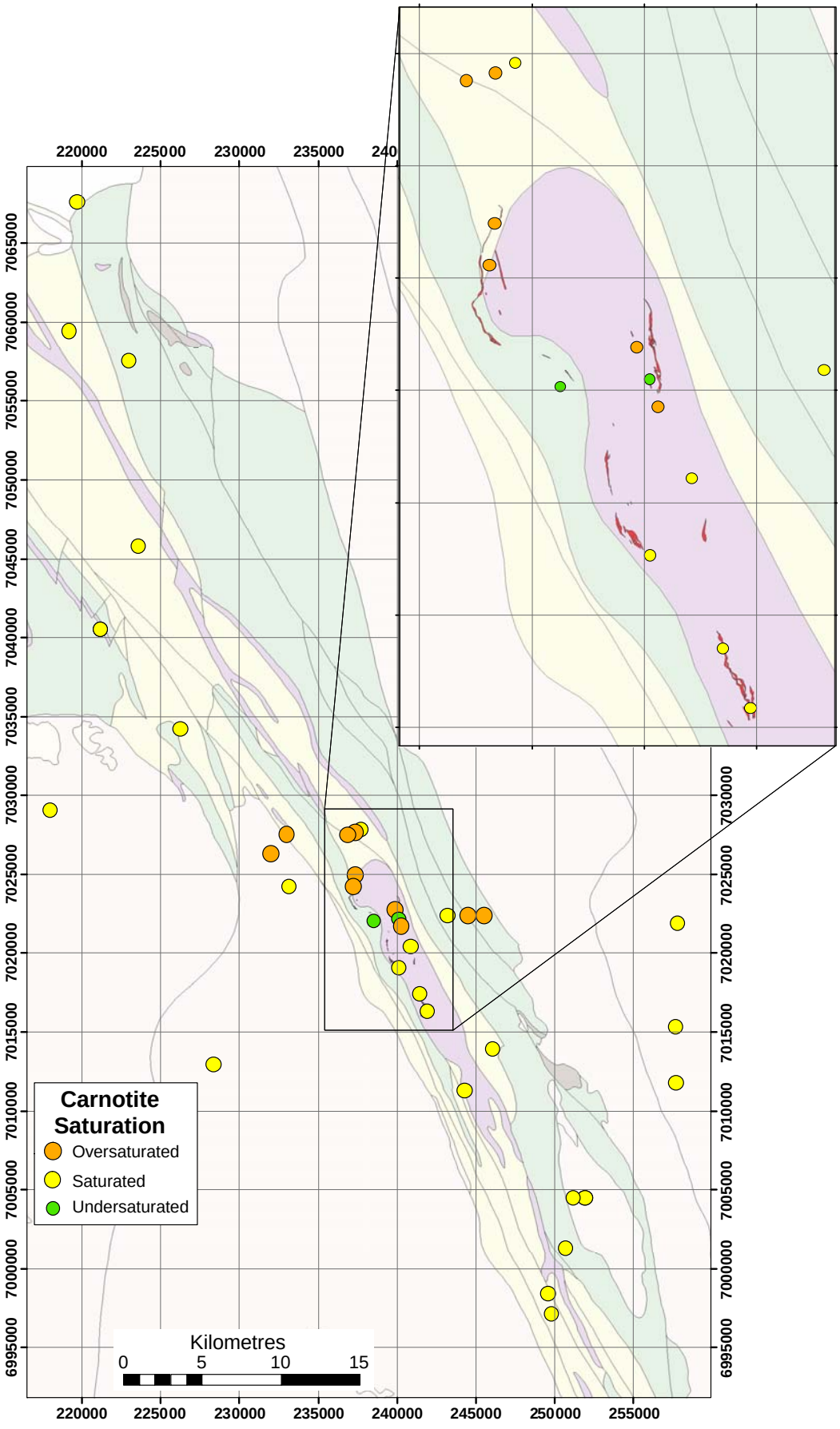

Figure 90: Carnotite SI distribution at Honeymoon Well.

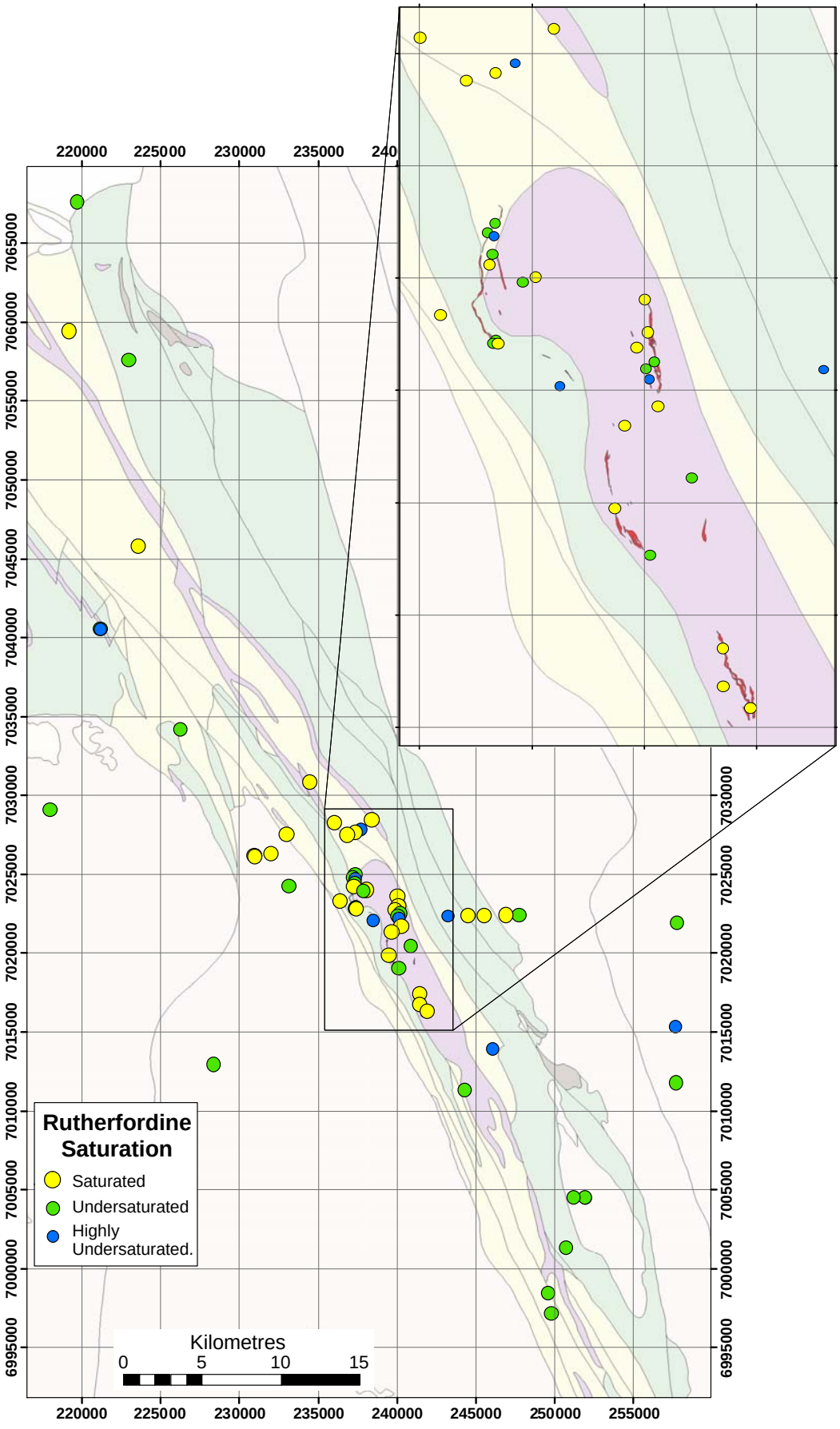

Figure 91: Rutherfordine SI distribution at Honeymoon Well.

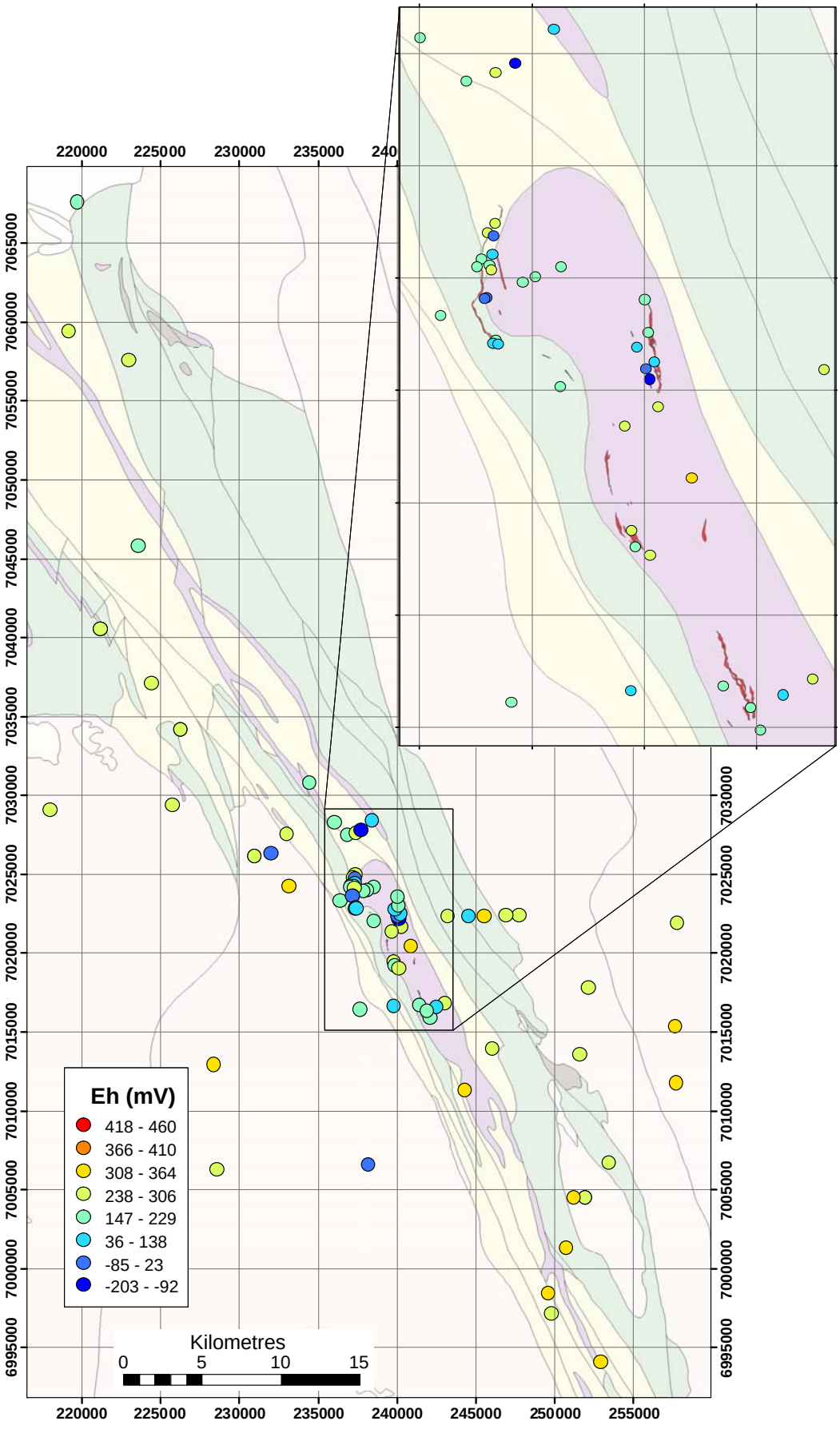

Figure 92: Groundwater Eh distribution at Honeymoon Well.

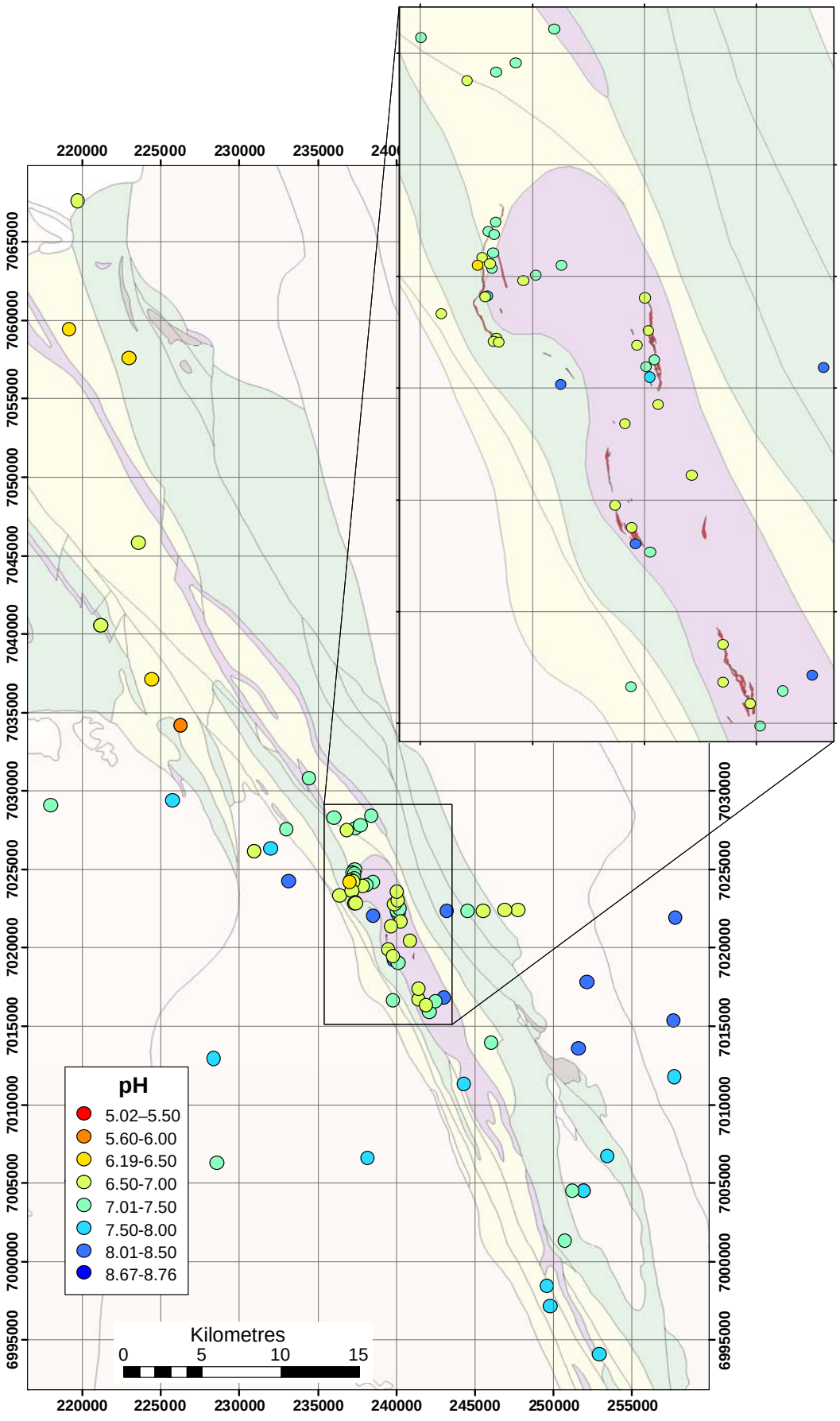

Figure 93: Groundwater pH distribution at Honeymoon Well.

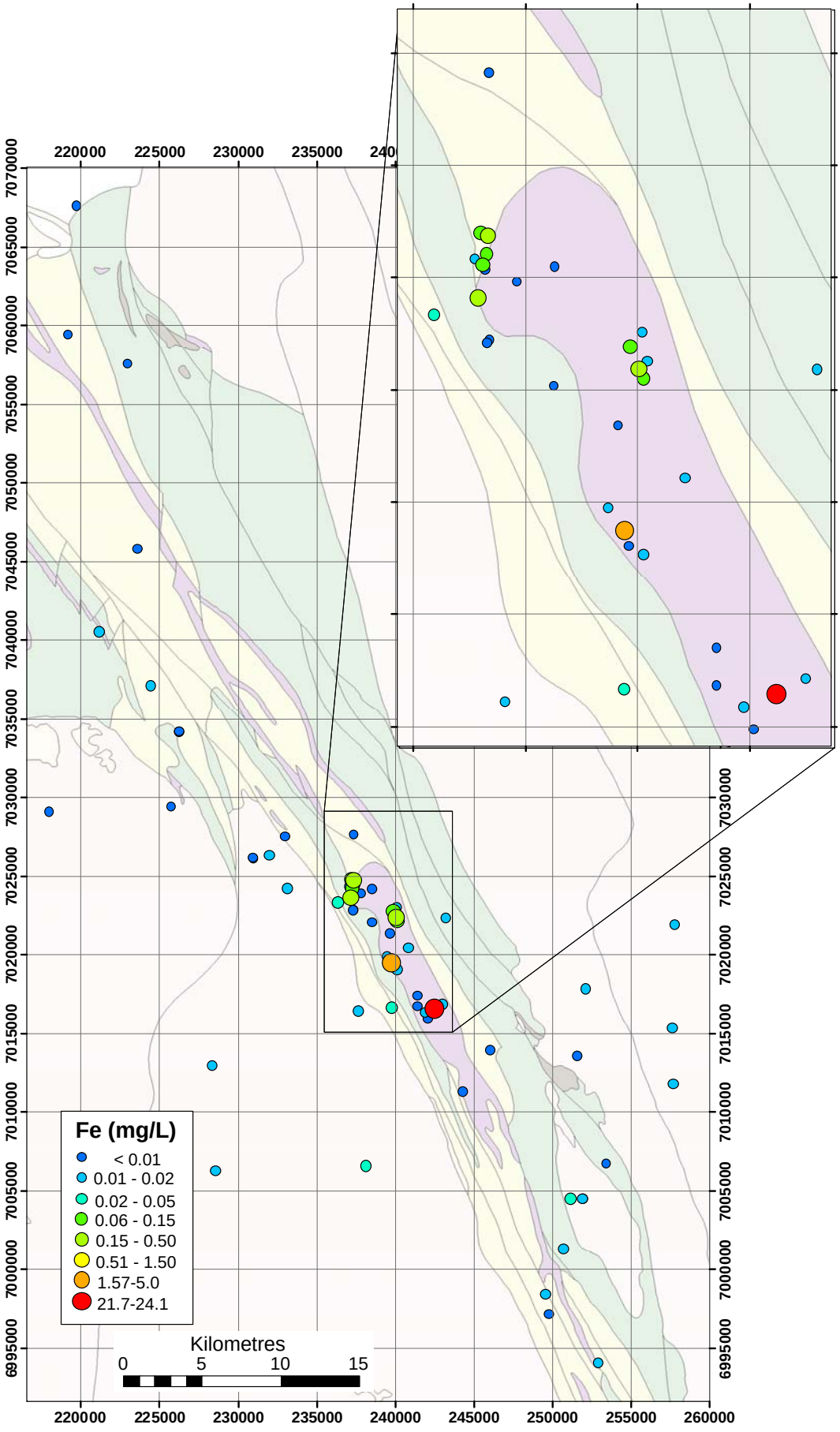

Figure 94: Dissolved Fe distribution at Honeymoon Well.

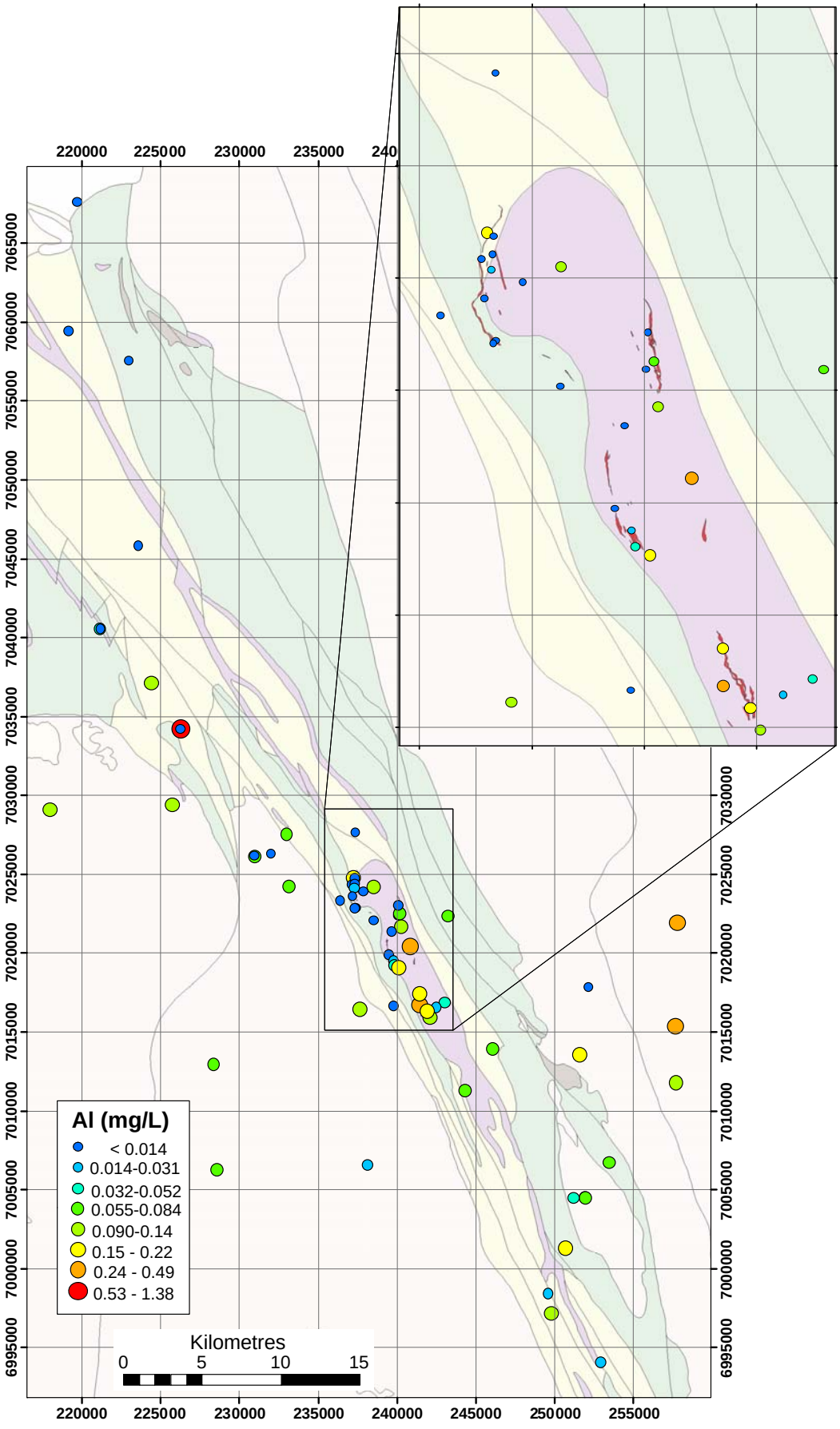

Figure 95: Dissolved Al distribution at Honeymoon Well.

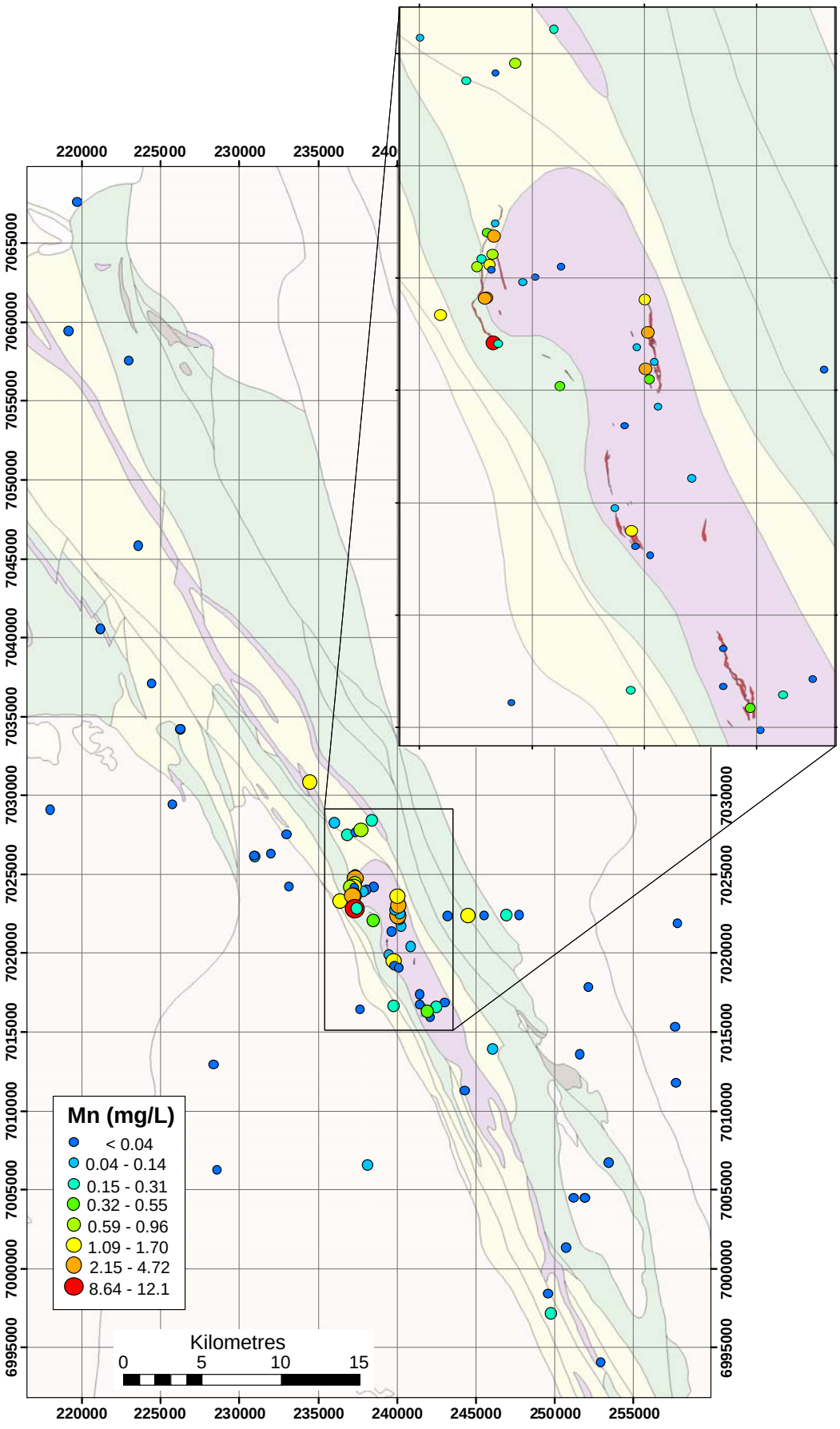

Figure 96: Dissolved Mn distribution at Honeymoon Well.

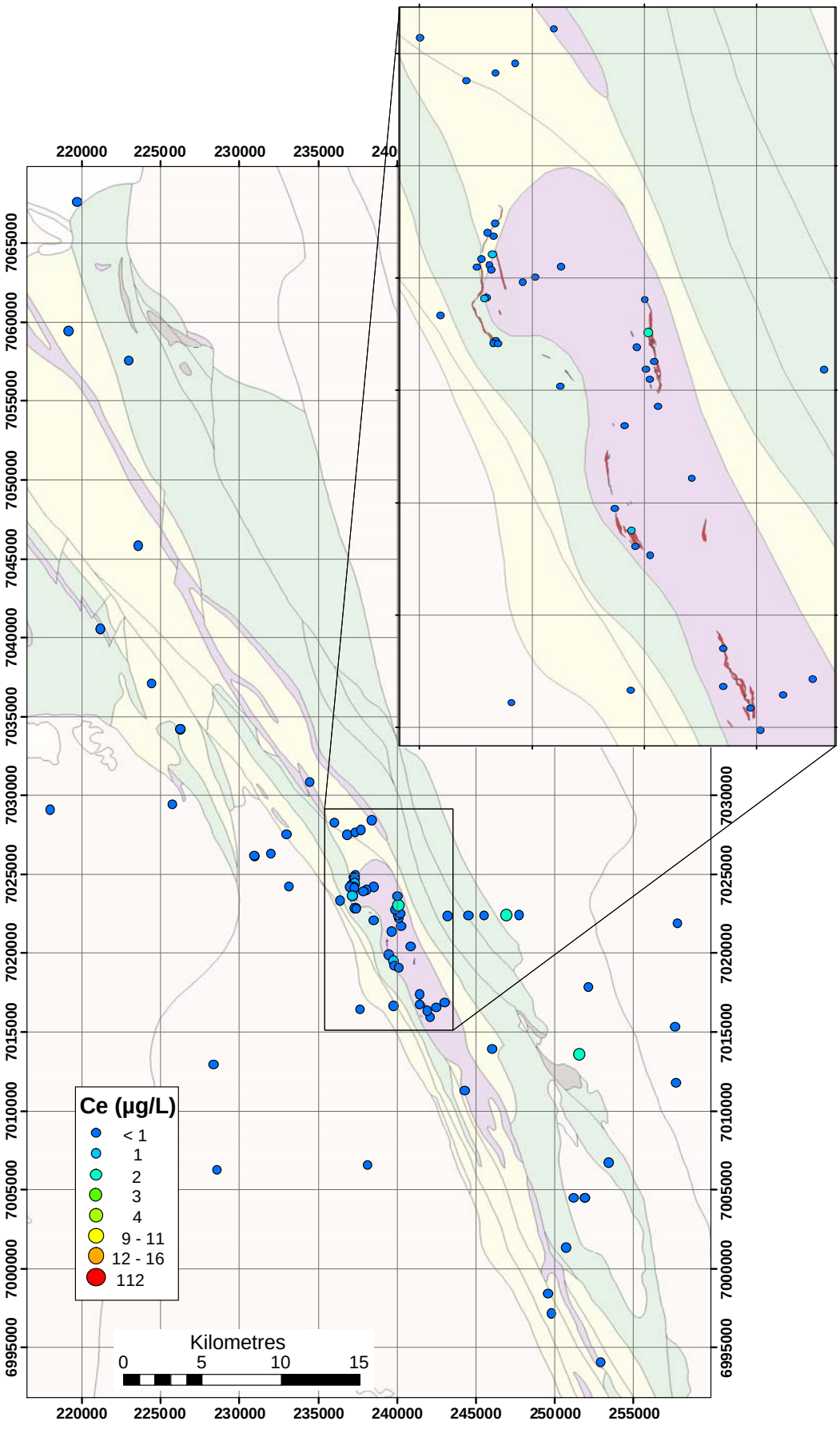

Figure 97: Dissolved Ce distribution at Honeymoon Well.

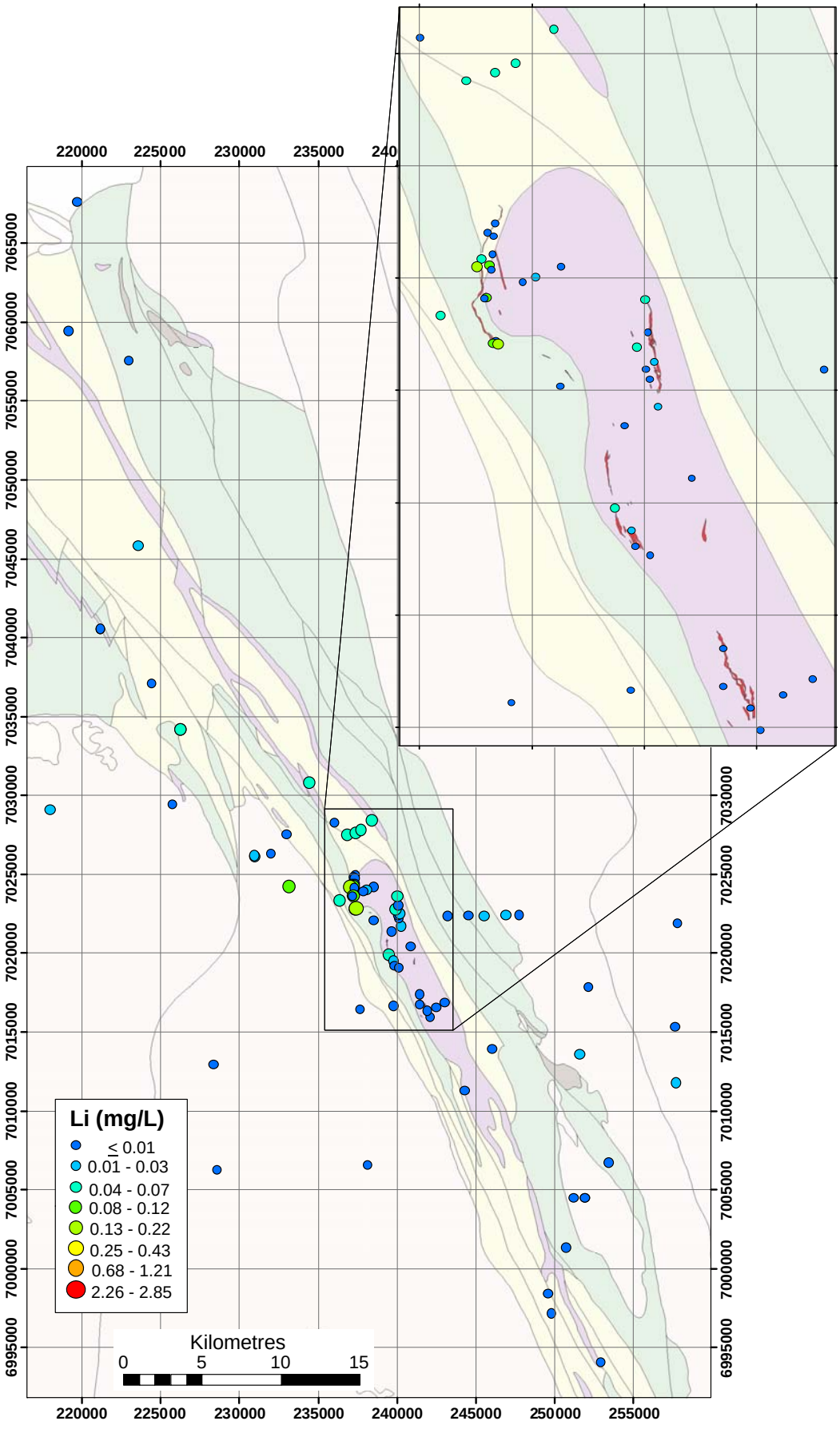

Figure 98: Dissolved Li distribution at Honeymoon Well.

8.4 NiS indicators

Dissolved Ni (Figure 99) and Co (Figure 100) are moderate at Wedgetail and high at Corella, but generally close to background for the southern Hannibal and Harrier prospects. This supports the previous observation at Yakabindie (Section 7) that individual Ni and Co data may not be able to consistently delineate disseminated NiS.

8.5 Use of indices

Use of derived indices for the NE Yilgarn water samples has improved targeting of mineralisation at Honeymoon Well. The Ni (Figure 101) and Co (Figure 102) indices indicated a broad low-level anomaly for the entire area, with highest index scores at Wedgetail and Corella. Other single element indices that have been useful in detecting mineralisation in the Agnew Wiluna Greenstone belt are Pt and W (Figure 103 and Figure 104). These indices only showed higher values directly surrounding the NiS mineralisation, particularly the northern prospects which had good Ni and Co response. However, Pt also showed some response at Hannibal, in addition to Wedgetail and Corella.

The combination indices used to differentiate mineralised and unmineralised sulphides were employed to some benefit. The Mineralisation index of Ni+Co+W+Pt produced results similar to that of the single element Ni index, delineating the northern section of Honeymoon Well, but only weakly showing the southern disseminated mineralised zones. This result is similar to Yakabindie (Section 7.5), where disseminated NiS also had a poor groundwater response. The sulphide discrimination indices were effective in observing sulphides: the FeS index shows many anomalous values over the Honeymoon Well ultramafics (Figure 106), as does the AcidS index (Figure 107). These combination indices show a consistent anomaly in the SW of Honeymoon Well and also to the north of the mineralised areas, over conglomerate and felsic rocks. The signatures of these water samples are not consistent with the mapped geology and are representative of sulphides, possibly Ni-poor.

To emphasize mineralised vs. barren sulphides, the FeS and AcidS indices are subtracted from the mineralisation index. The Min – FeS (Figure 108) and Min – AcidS index (Figure 109) are better than the single indices or the Mineralisation index, in that even the southern disseminated NiS appear to show (albeit minor) anomalies. The lower scores of this index correspond to mineralisation at Honeymoon Well or the unusual areas of interest previously mentioned that relate to low Eh values. Index values between -0.06 and 0.09 are not anomalous for most of the NE Yilgarn using the mineralised-acid S index, but at Honeymoon Wells values >-0.06 seem to be important as potential pathfinding scores. The suppressed contrast in this region may be an influence of the increased salinity of these samples compared to other regions of this study.

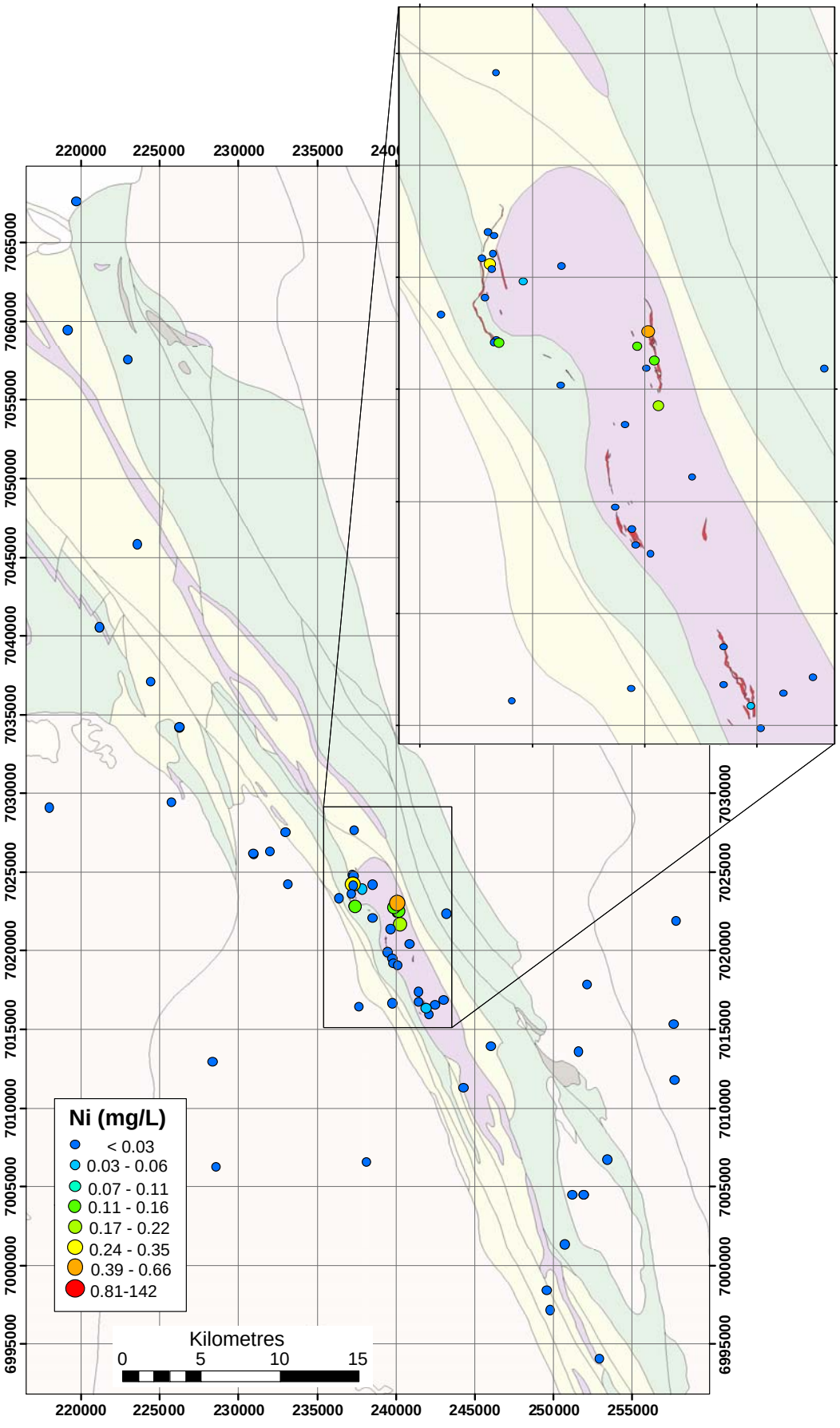

Figure 99: Dissolved Ni distribution at Honeymoon Well.

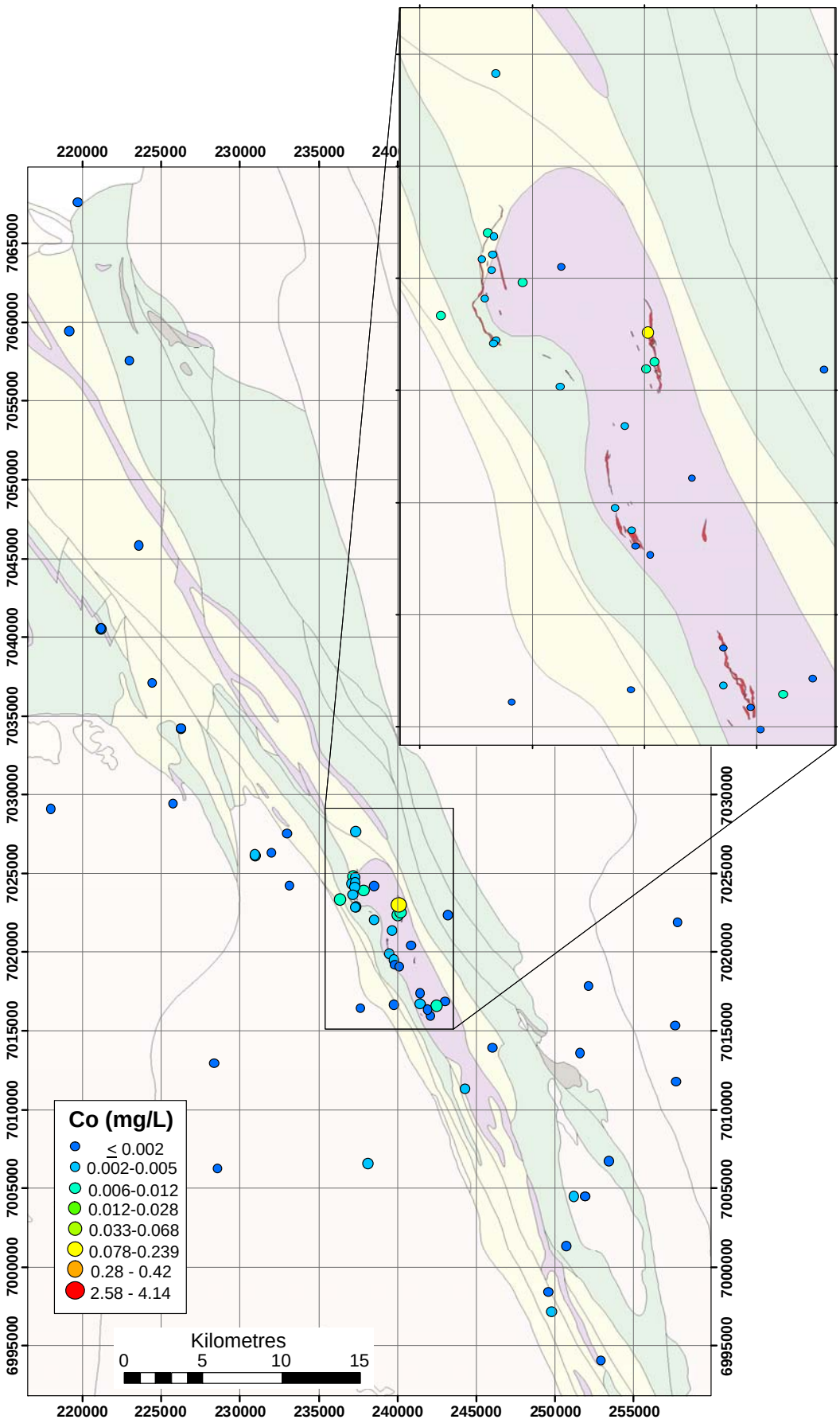

Figure 100: Dissolved Co distribution at Honeymoon Well.

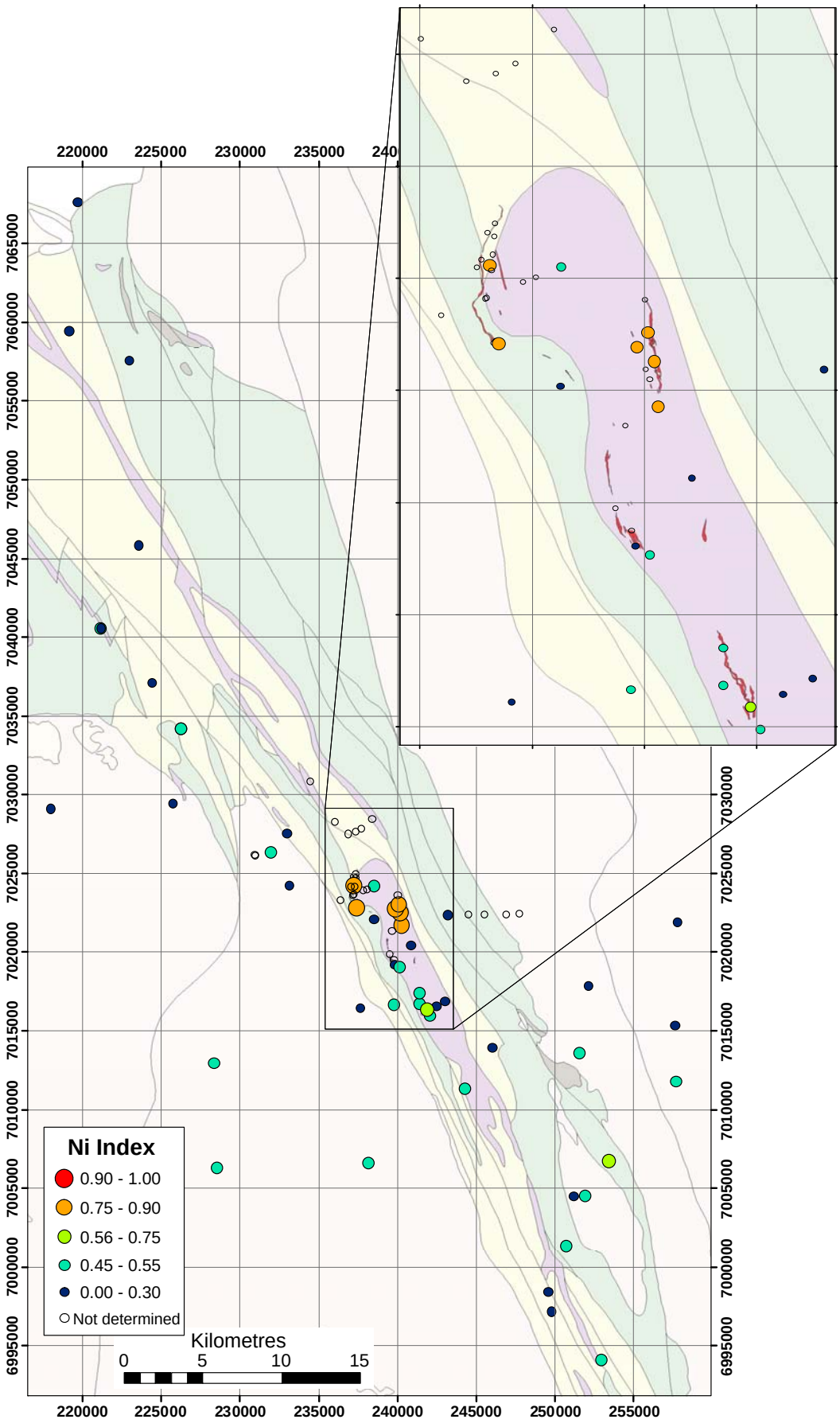

Figure 101: Ni Index distribution at Honeymoon Well.

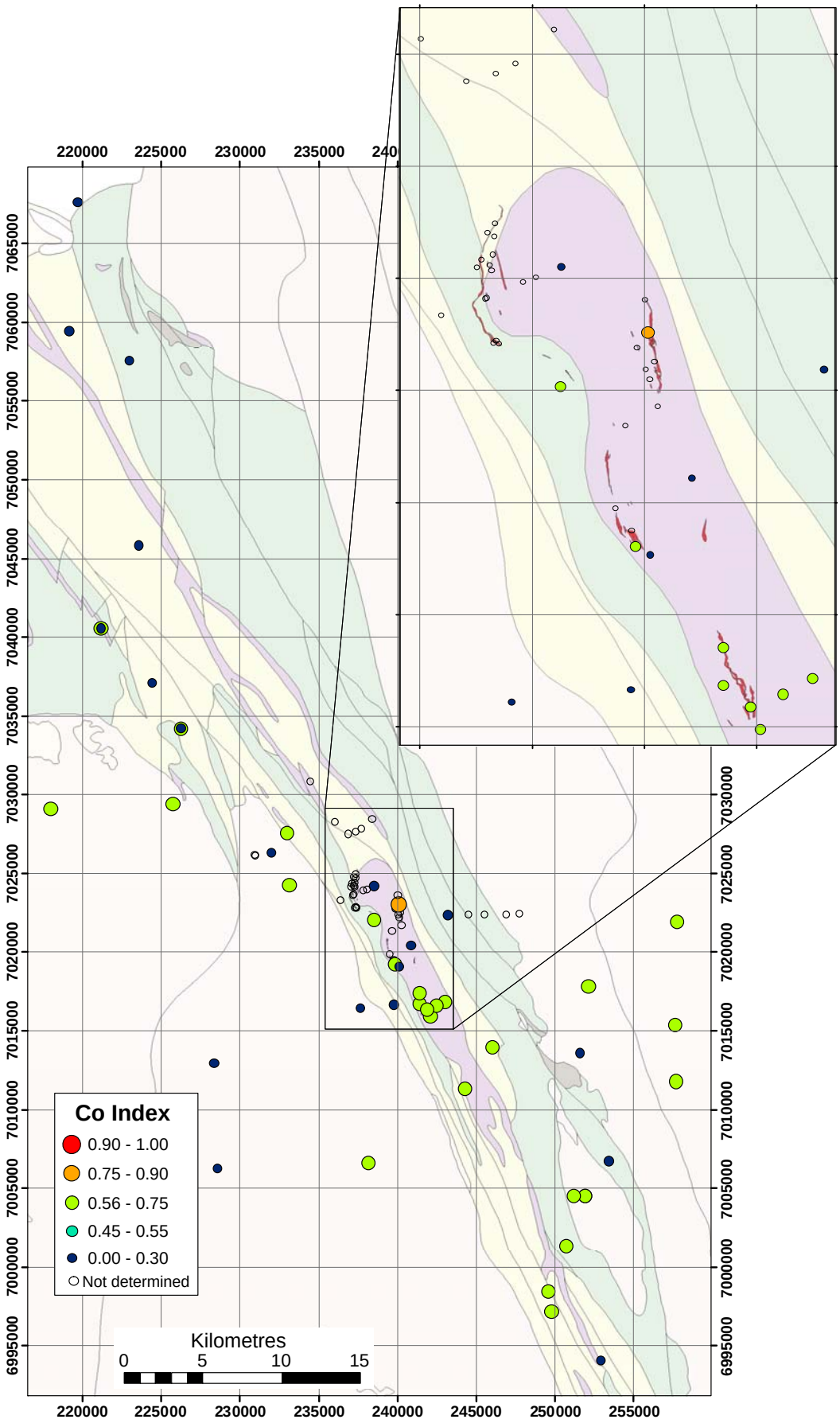

Figure 102: Co Index distribution at Honeymoon Well.

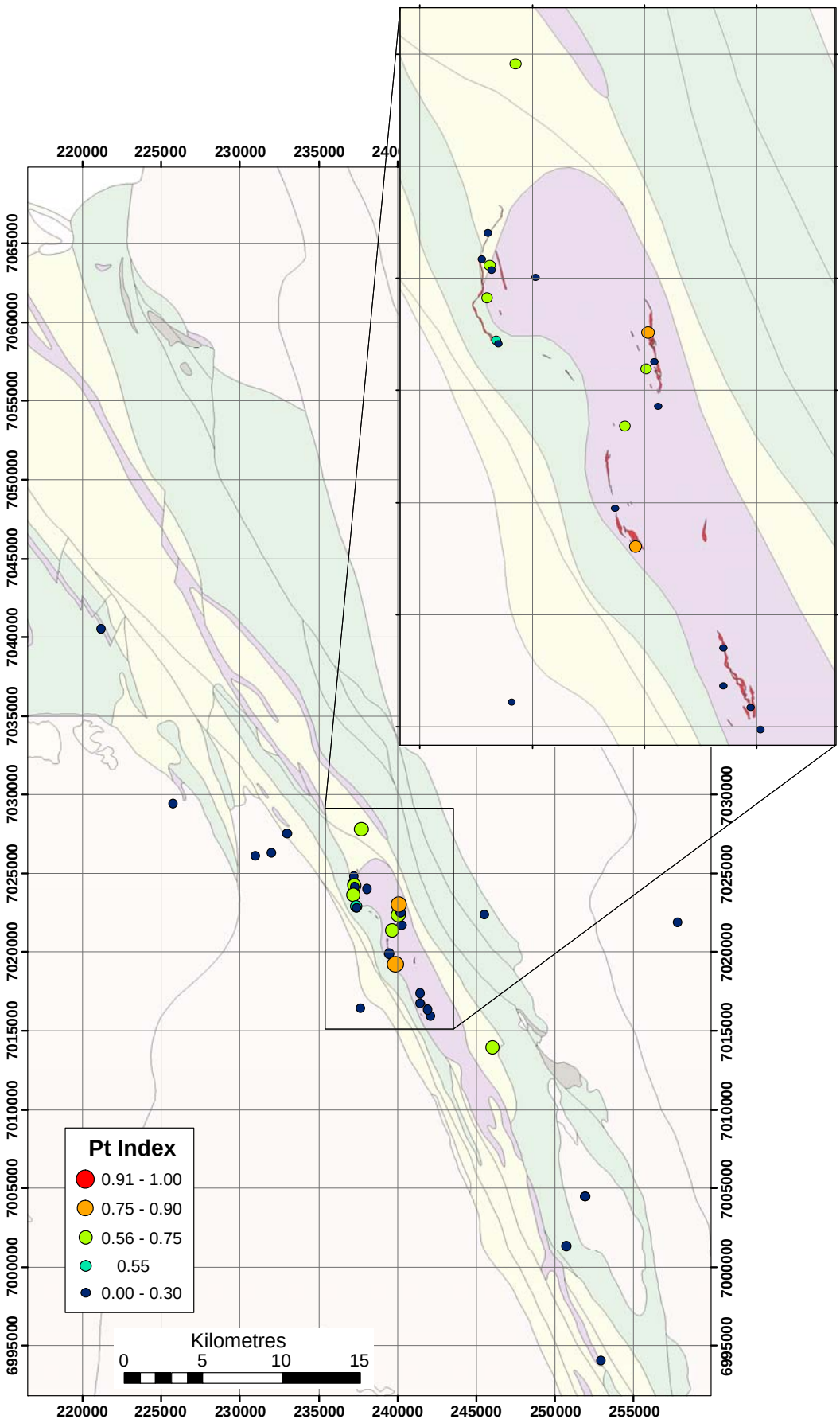

Figure 103: Pt Index distribution at Honeymoon Well.

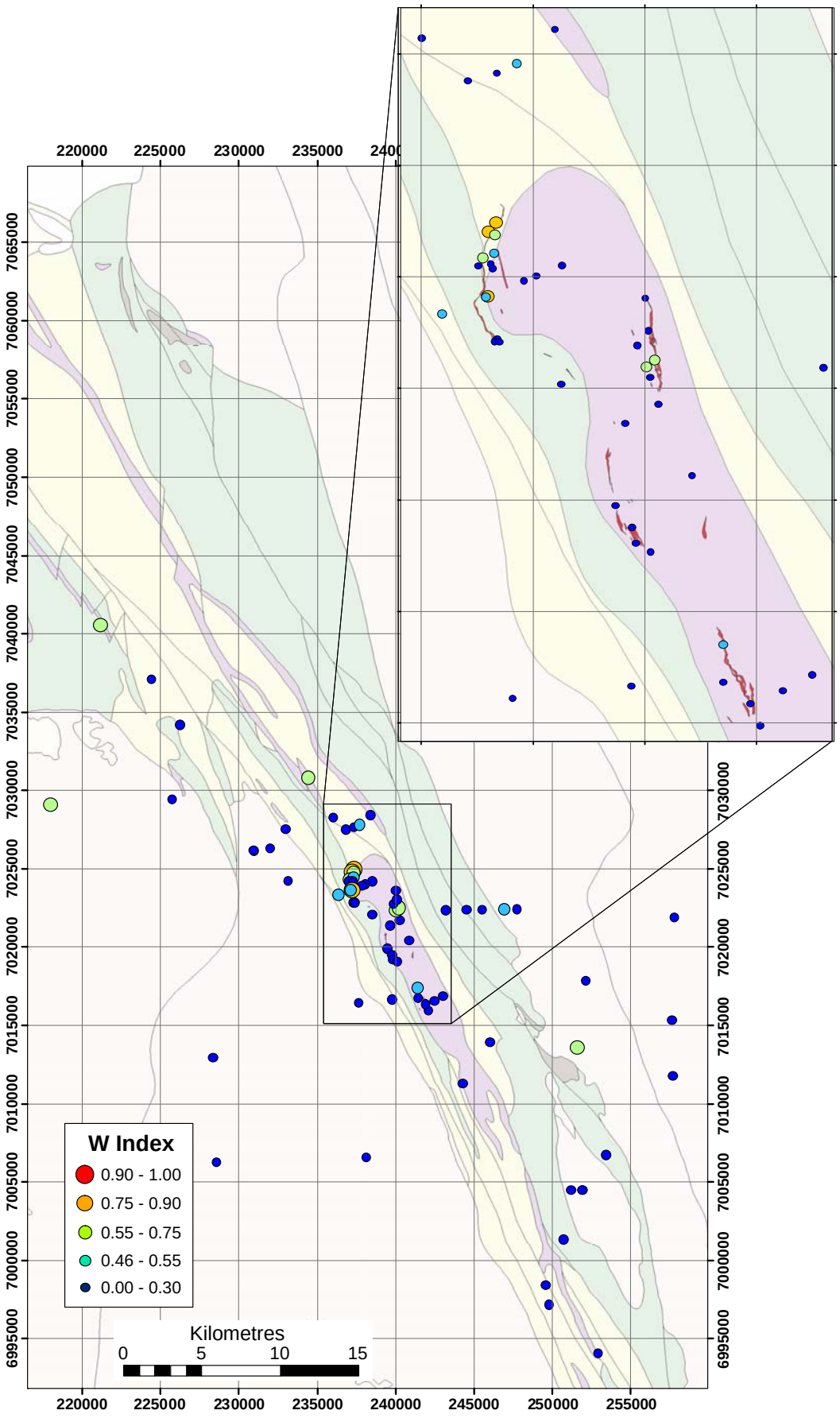

Figure 104: W Index distribution at Honeymoon Well.

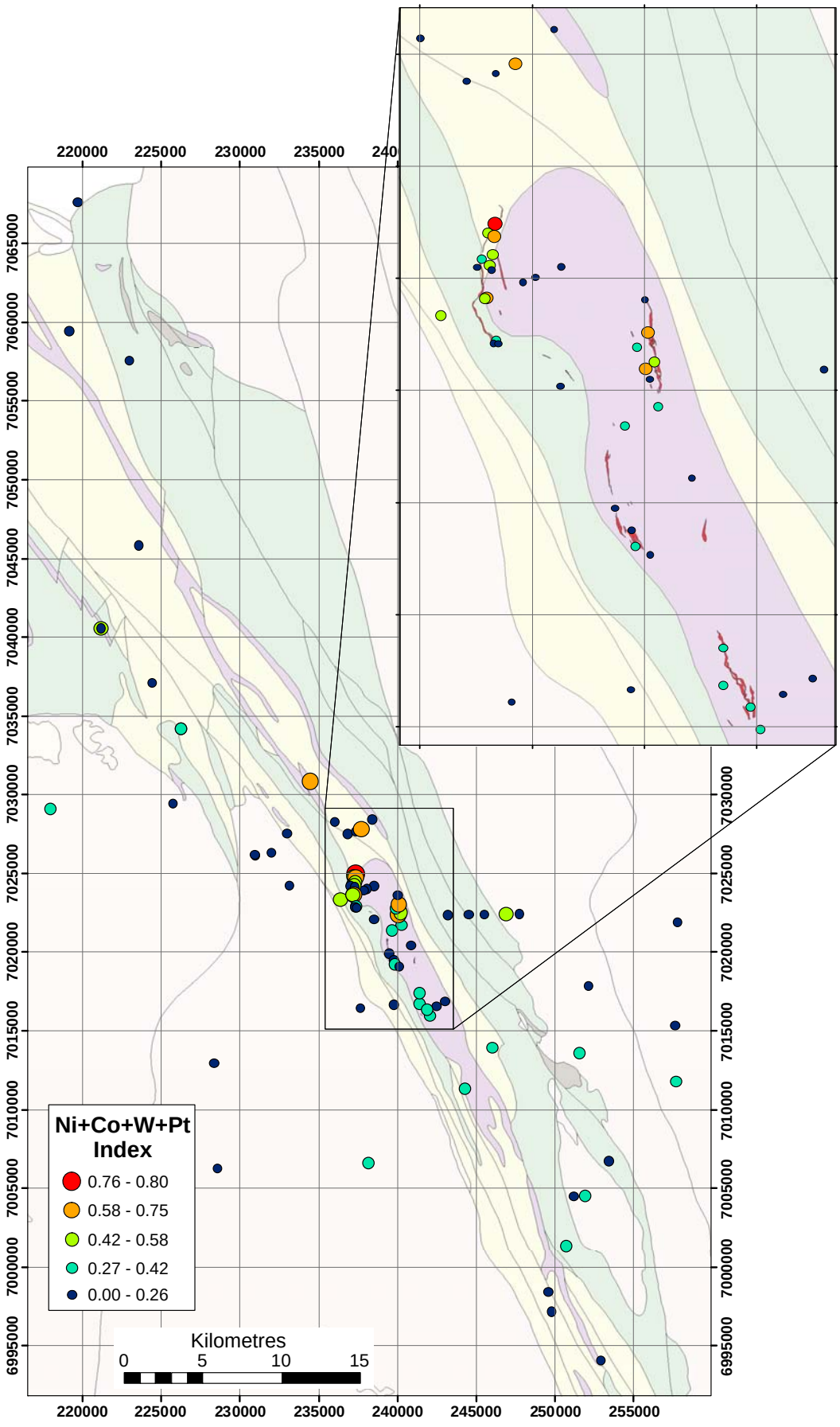

Figure 105: Min (Ni+Co+W+Pt) Index distribution at Honeymoon Well.

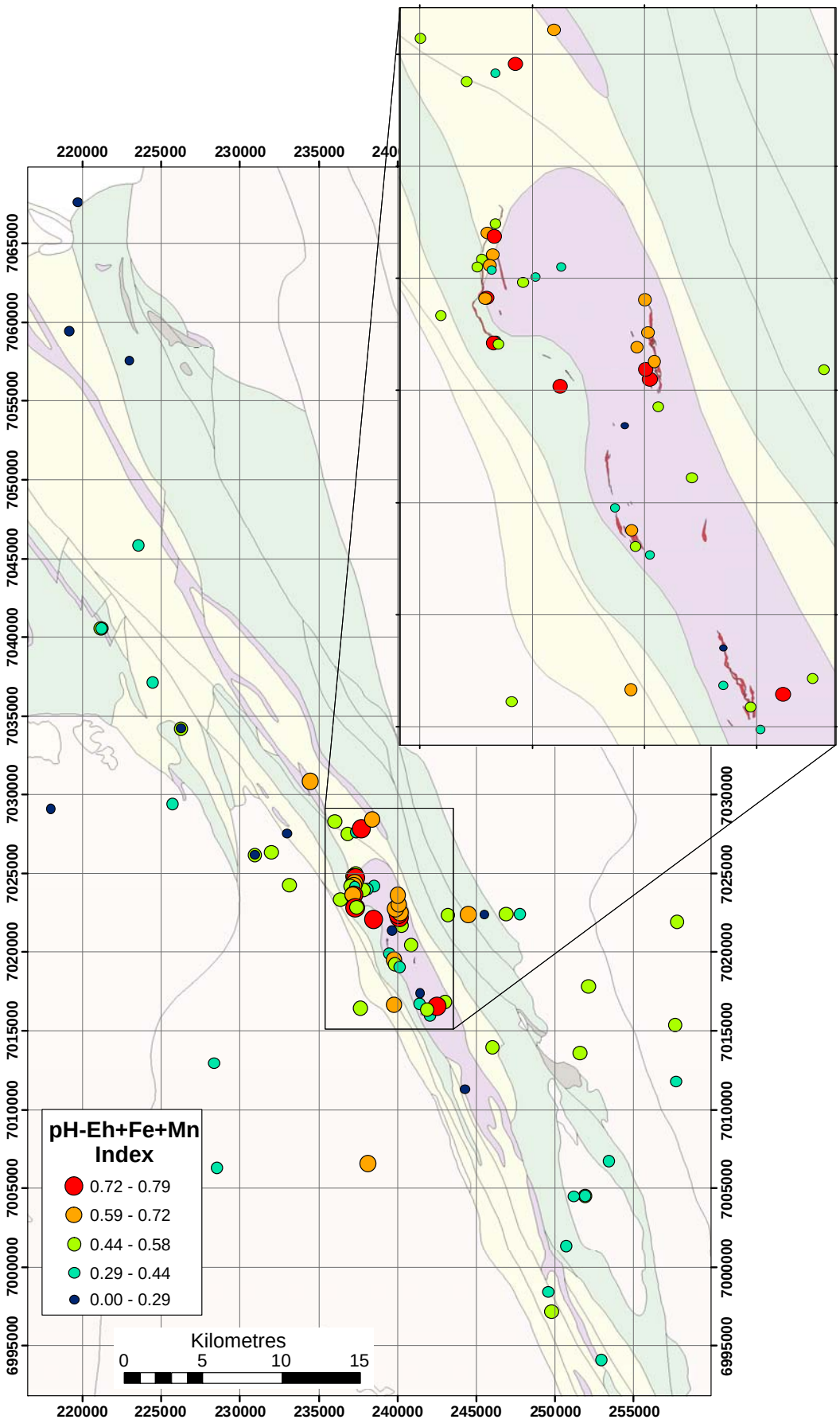

Figure 106: FeS (pH-Eh+Fe+Mn) Index distribution at Honeymoon Well.

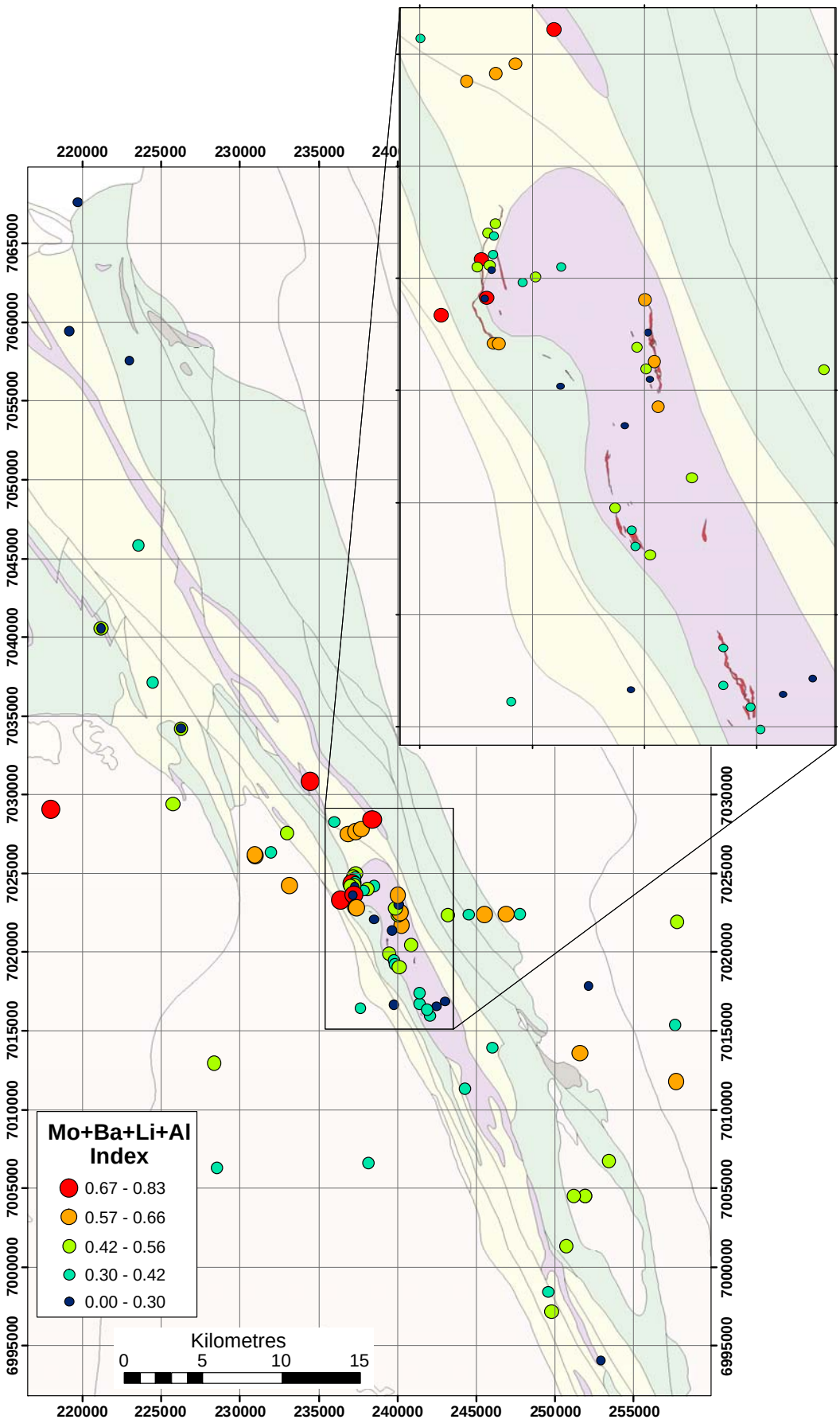

Figure 107: AcidS (Ba+Li+Mo+Al) Index distribution at Honeymoon Well.

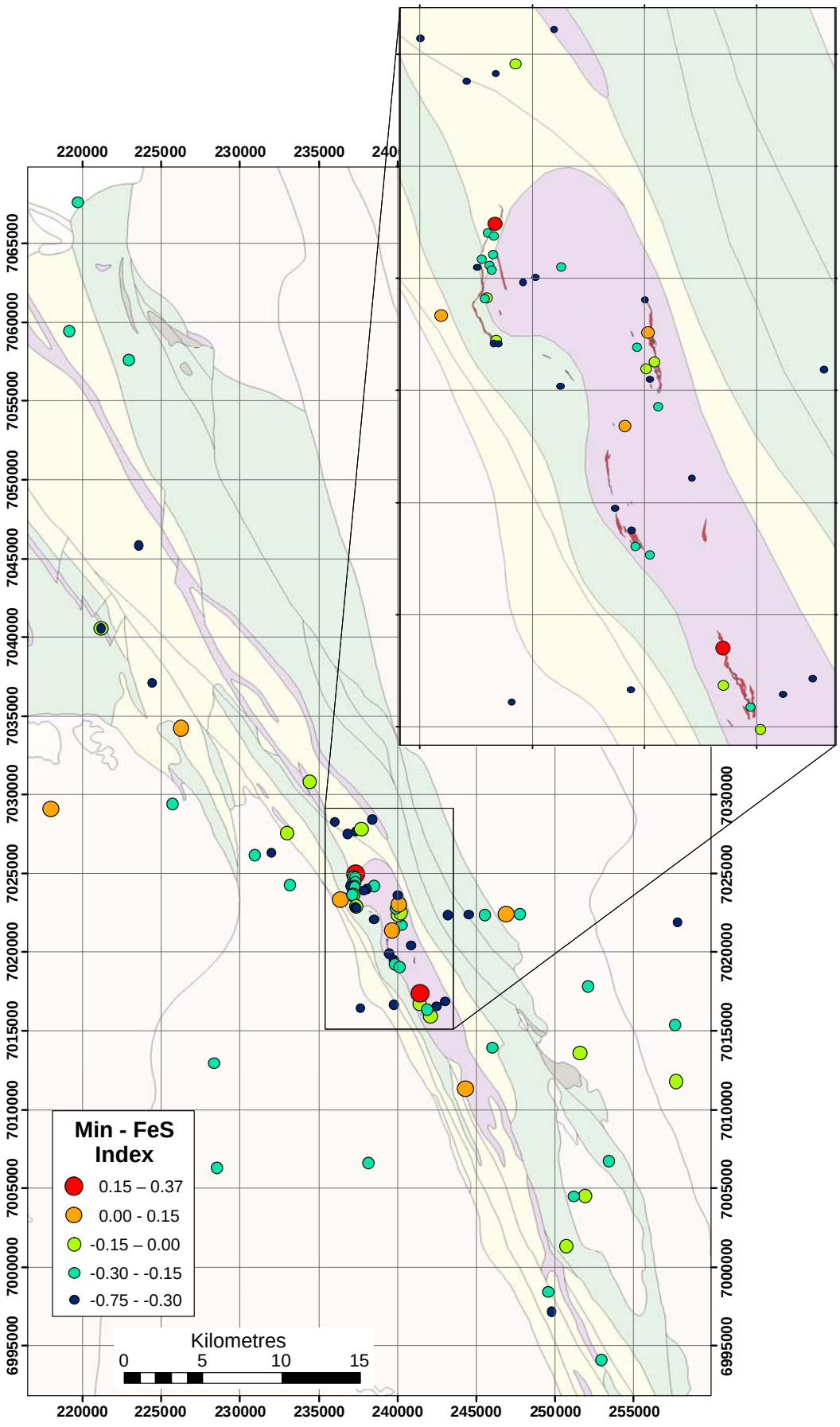

Figure 108: Min – FeS Index distribution at Honeymoon Well.

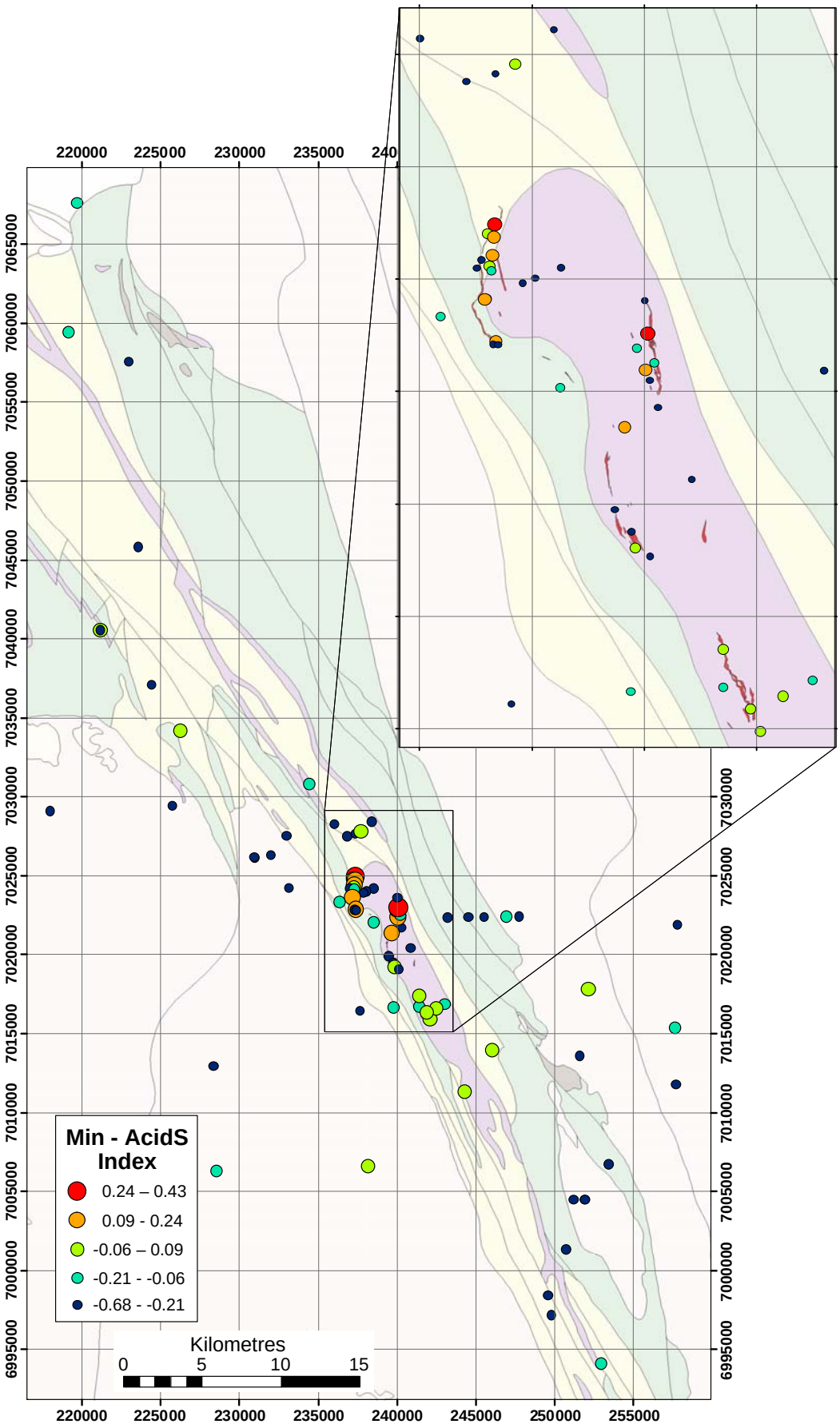

Figure 109: Min – AcidS Index distribution at Honeymoon Well.

9. REGIONAL OVERVIEW

9.1 Lithological indicators

The most obvious lithological indicator is Cr (Figure 110), which indicates ultramafic rocks. At a regional scale. Barren ultramafics in the Lawlers/Agnew area give extremely high (up to 0.31 mg/L) dissolved Cr. Lower Cr concentrations for NiS ultramafics are possibly due to lower Cr concentration in the rocks or to dissolved Cr being dominantly Cr^{6+}, which is reduced and precipitated by products of weathering sulphides such as Fe^{2+}, Mn^{2+} or possibly S^{2-}. On the other hand, higher dissolved U (Figure 111) commonly indicate granitic rocks, except at Honeymoon Well (Section 8.2), where this effect is masked by high U concentrations NW of Lake Way.

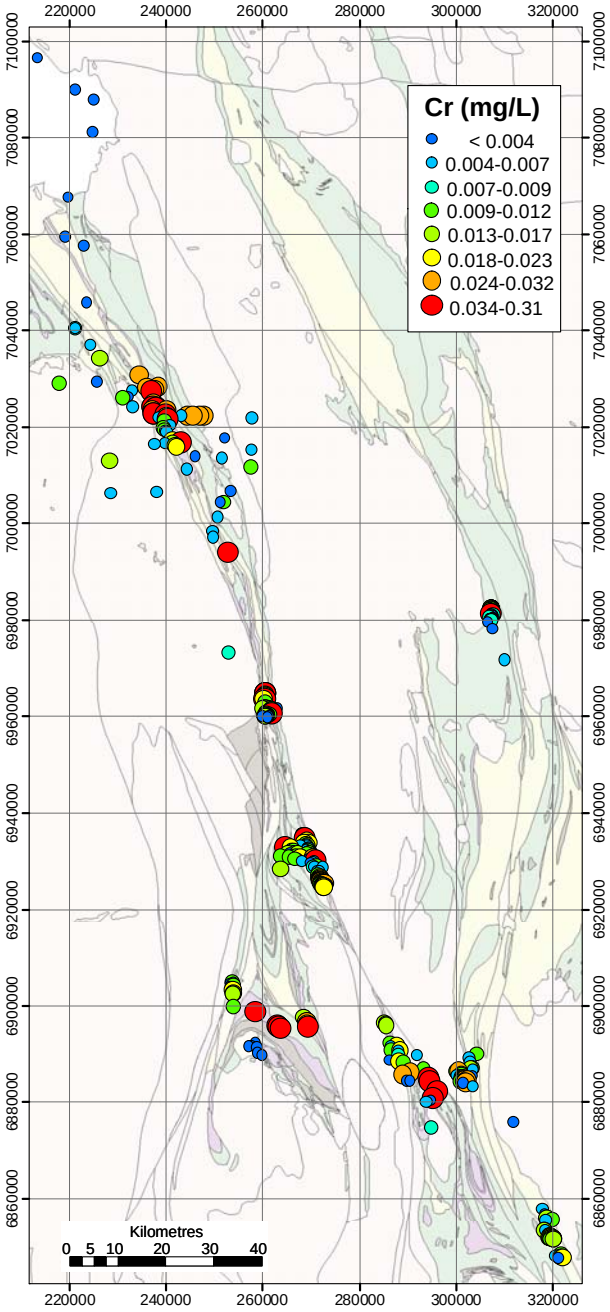

Figure 110: Dissolved Cr distribution for groundwaters from the NE Yilgarn Craton.

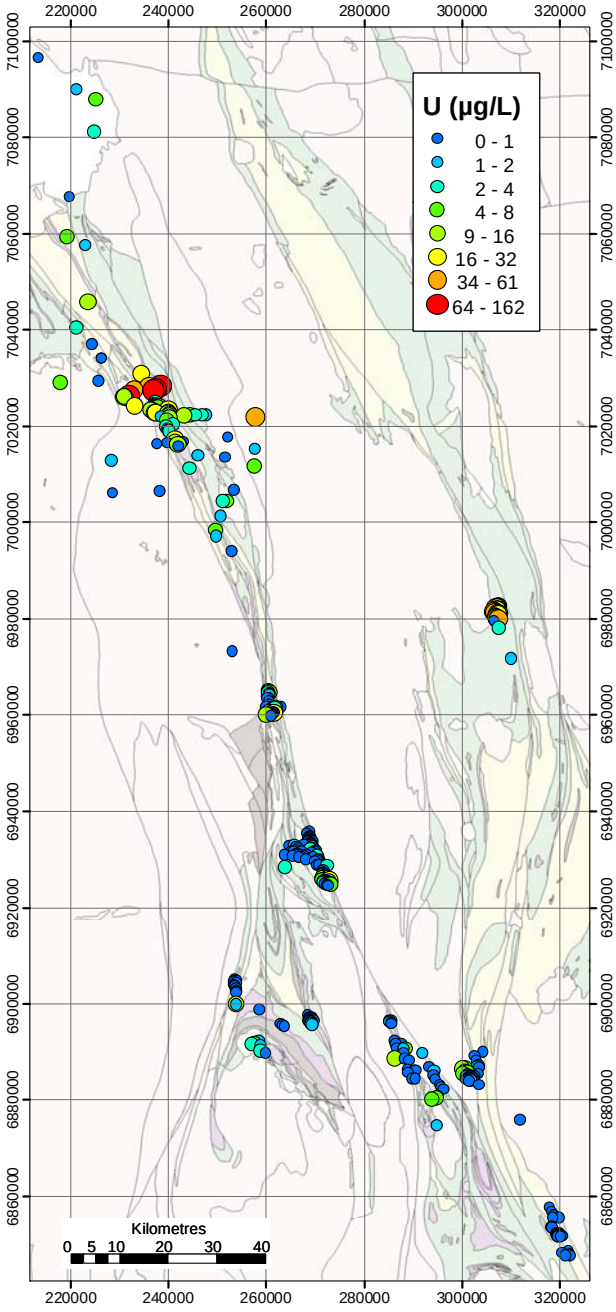

Figure 111: Dissolved U distribution for groundwaters from the NE Yilgarn Craton.

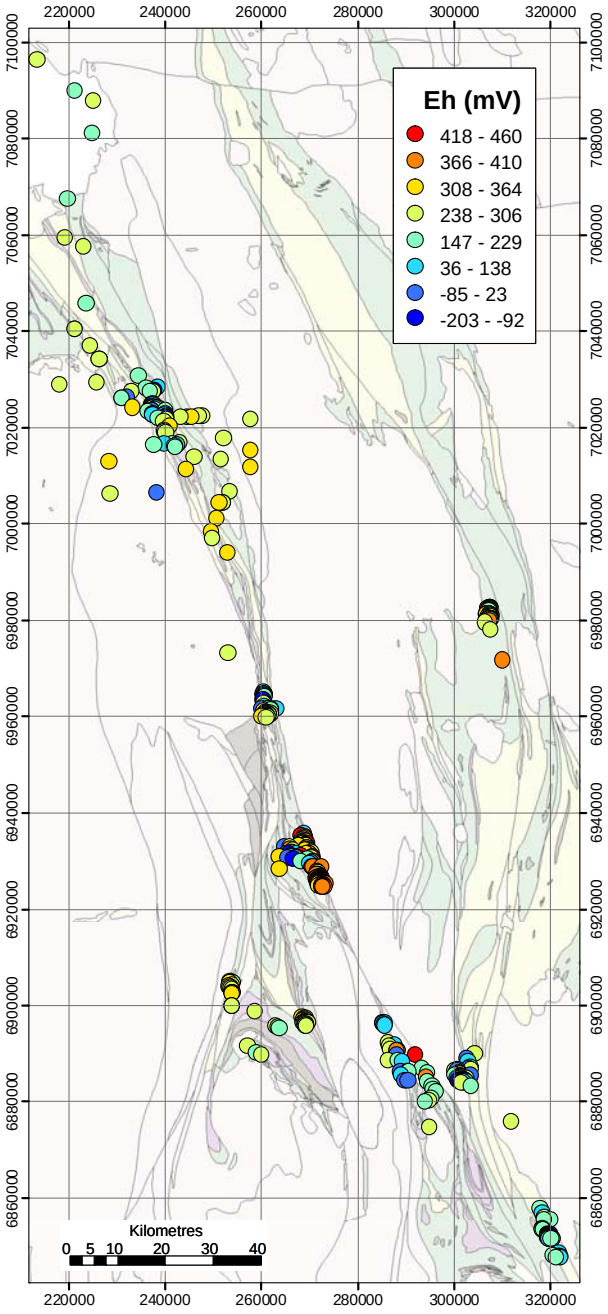

Figure 112: Groundwater Eh values for the NE Yilgarn Craton.

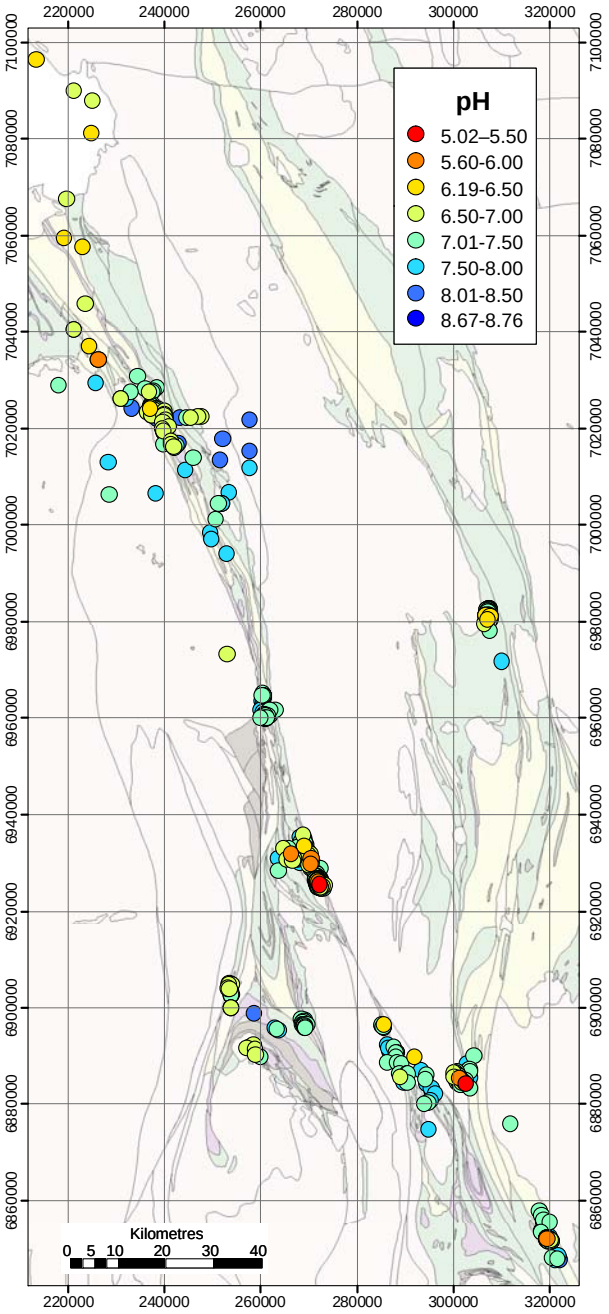

Figure 113: Groundwater pH values for the NE Yilgarn Craton.

9.2 Sulphide Indicators

Weathering sulphides can result in reduced groundwaters (Figure 112) and sporadic acidity (Figure 113). Concomitant potential wall rock attack (Section 3.3) may result in distinct groundwater signatures. Appreciable dissolved Al (Figure 114) and REE (*e*.g. Ce, Figure 115) are out of equilibrium in these neutral groundwaters, which are over-saturated (*i*.e., the mineral should be precipitating) with respect to Al-phases such as kaolinite and alunite and saturated with respect to amorphous alumina (Figure 116). One feasible explanation is that the Al and REE were released under acid conditions, and then remained in solution due to kinetic factors when the waters were neutralized by contact with carbonates or other phases.

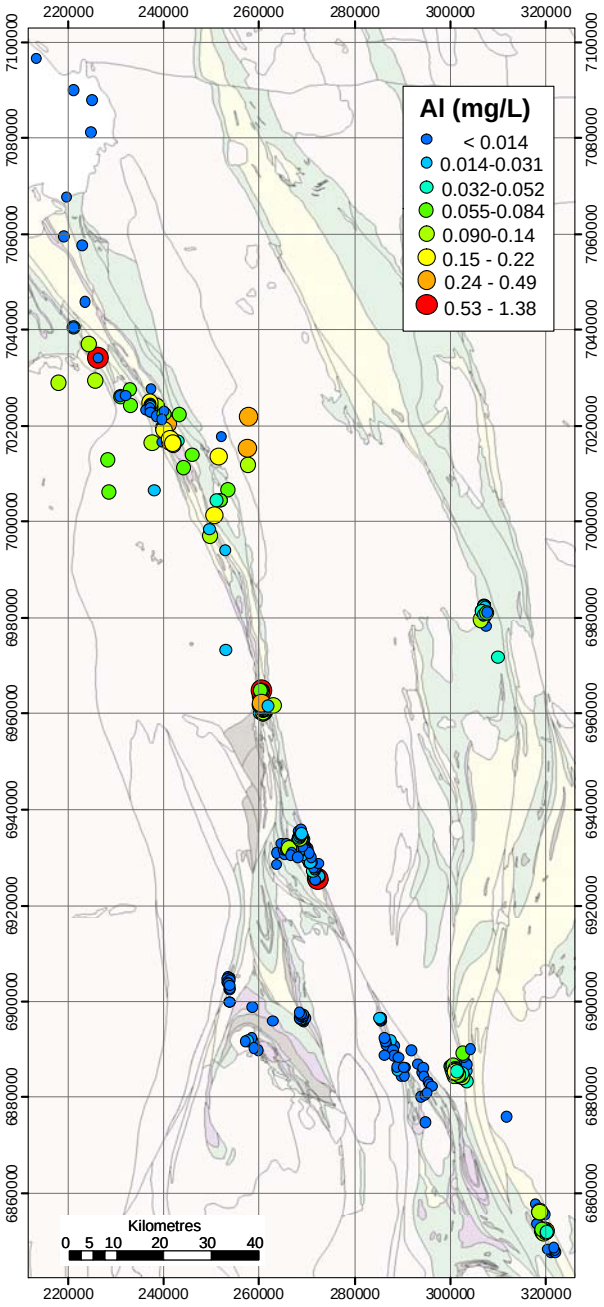

Figure 114: Groundwater Al distribution for the NE Yilgarn Craton.

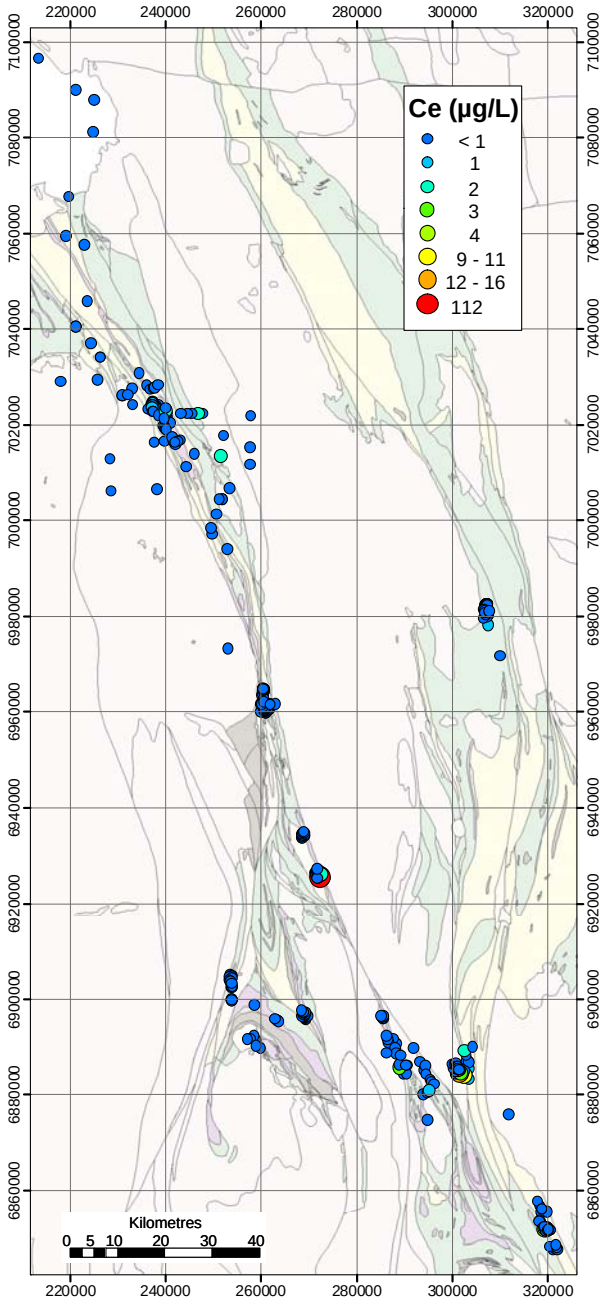

Figure 115: Groundwater Ce distribution for the NE Yilgarn Craton.

These hypothesized transient low pH conditions could also explain the higher concentrations of elements such as Ba, Li (Figure 117), Mn (Figure 118), Mo, V and W, which may well have enhanced dissolution in acid conditions. Once dissolved, these elements are, unlike Al and REE, generally conservative and give more well-defined anomalies with sulphide bodies.

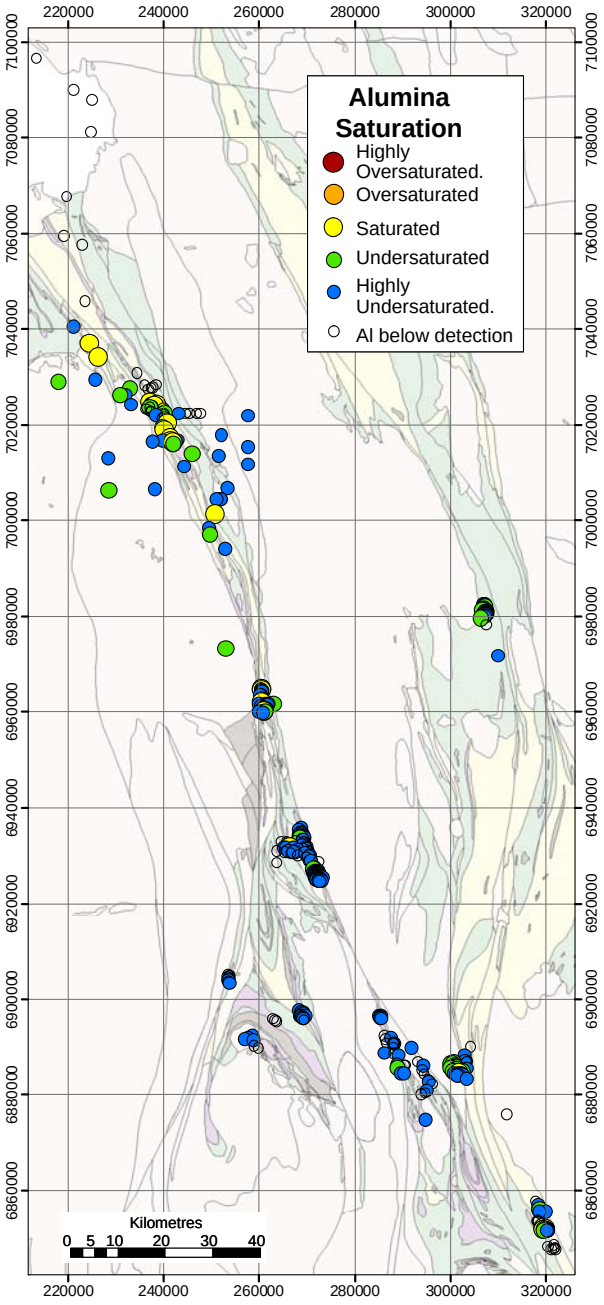

Figure 116: Groundwater amorphous alumina SI distribution for the NE Yilgarn Craton.

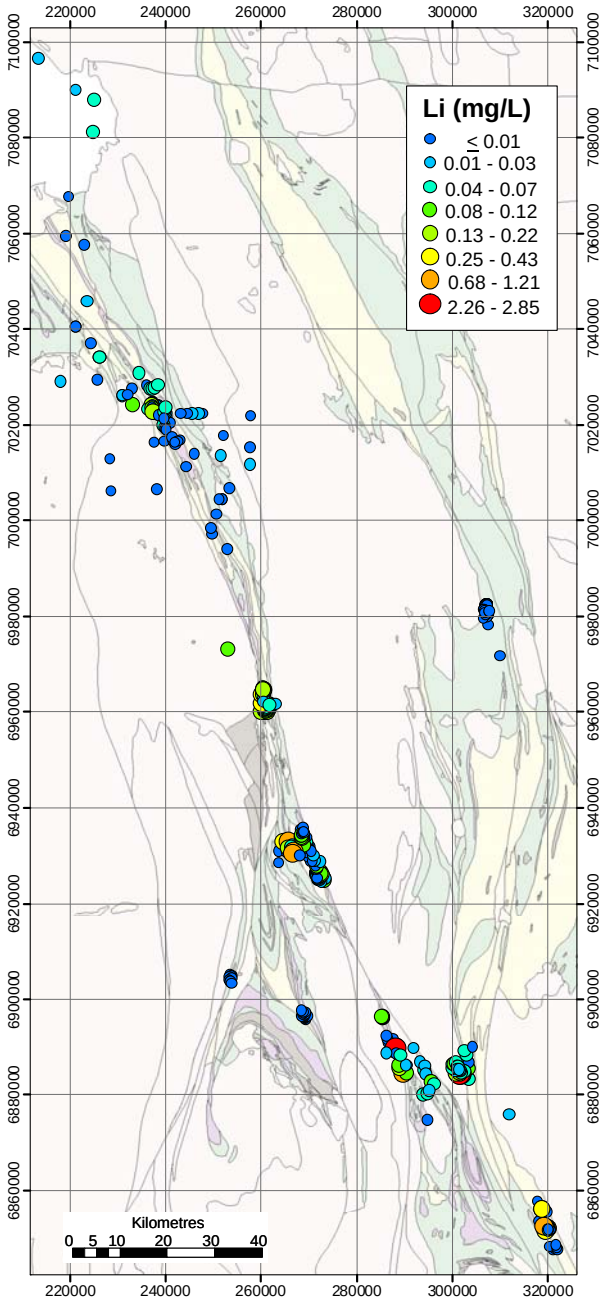

Figure 117: Groundwater Li distribution for the NE Yilgarn Craton.

9.3 NiS Indicators

Results from the NiS deposit studies (Sections 5 - 8) indicate that Ni and Co are the best positive groundwater indicators for mineralisation at the 10-100 m scale. These results are matched at a regional scale, with these two elements typically higher in NiS areas (Figure 119 and Figure 120). Groundwater Ni above 0.2 mg/L is highly anomalous. The response for Co is more subdued and although some anomalous sites show strong contrast, detection issues present difficulties in using Co data alone as a vector to mineralisation. It is possible for barren sulphides to produce positive Ni anomalies due to acidity even if Ni is present at sub-economic levels. However, many other elements will also be present (Section 9.2), and this effect can be corrected for (Section 9.4).

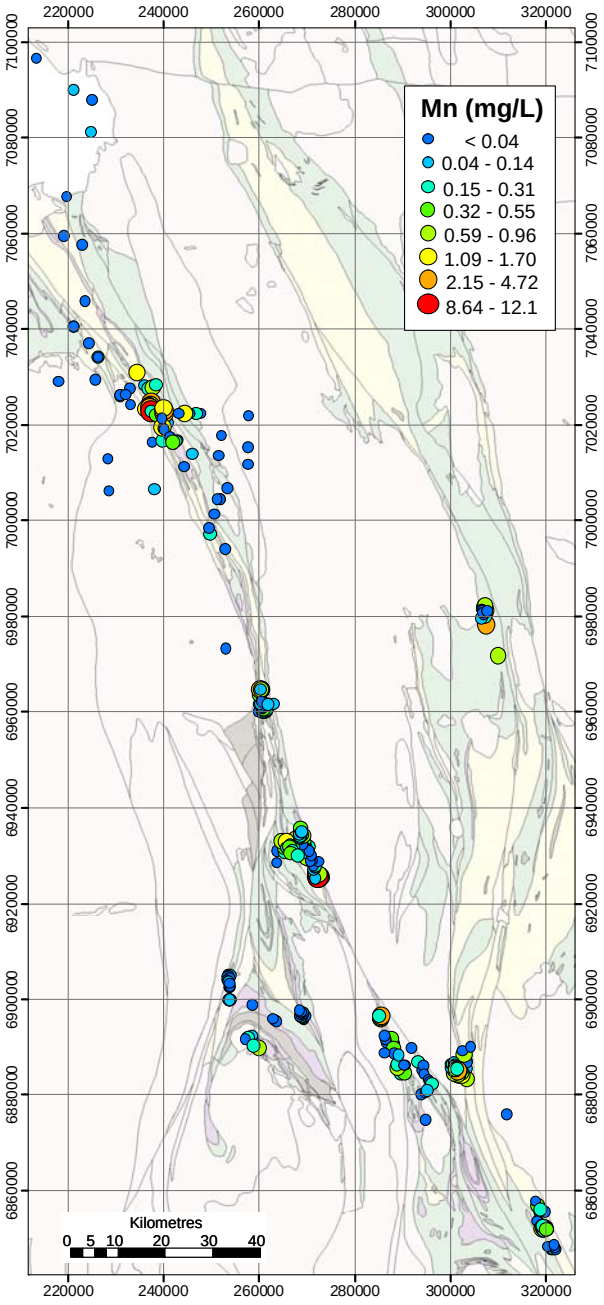

Figure 118: Groundwater Mn distribution for the NE Yilgarn Craton.

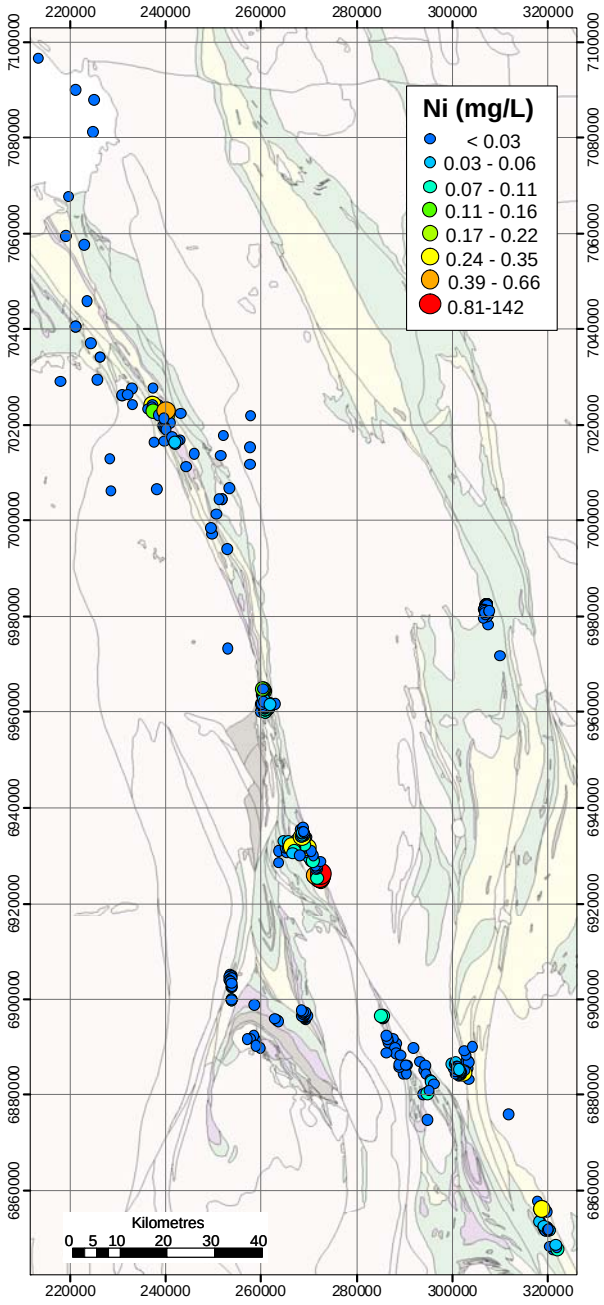

Figure 119: Groundwater Ni distribution for the NE Yilgarn Craton.

9.4 Use of indices

Derived indices and their linear combinations can be beneficial in defining anomalous samples, particularly for using pathfinder elements such as Co and PGEs that are not consistently distributed or detectable. The Ni index (Figure 121) depicts and ranks the mineralised regions. The Harmony site has the greatest values (and greatest ore reserves), with high scores for groundwaters at Camelot, Yakabindie and Honeymoon Well, and moderate scores at Waterloo and Weebo. The low Ni index scores for background areas support its use as an effective targeting tool. The Co index (Figure 122) gives similar results, though delineation was poorer, possibly due to detection limit issues.

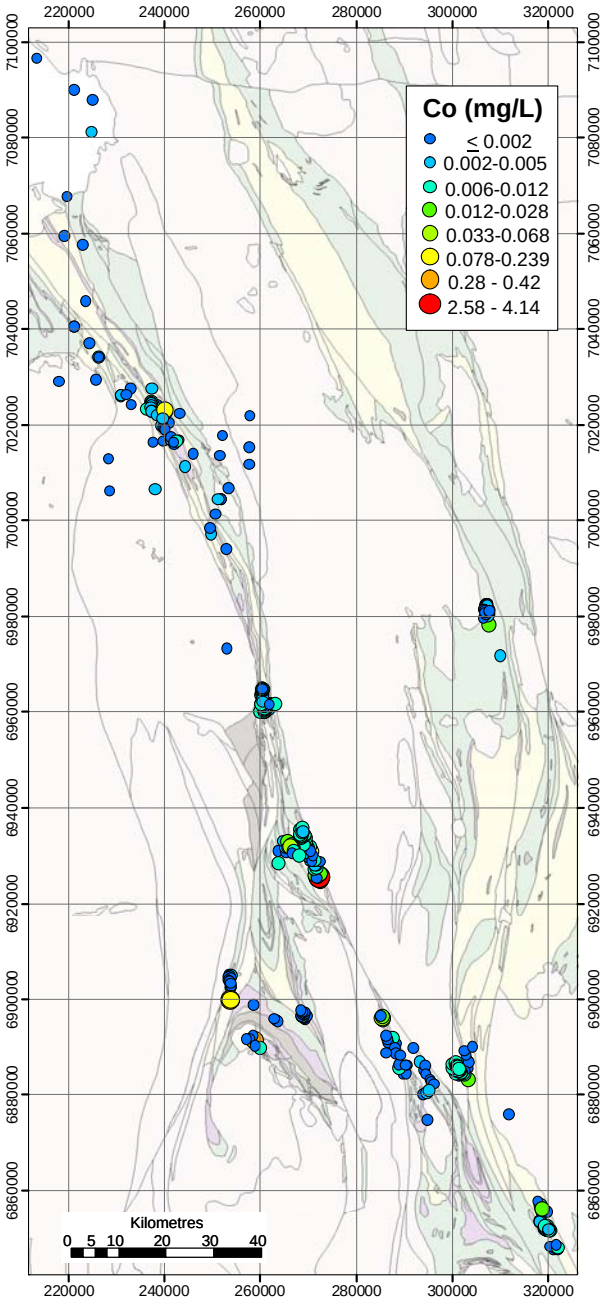

Figure 120: Groundwater Co distribution for the NE Yilgarn Craton.

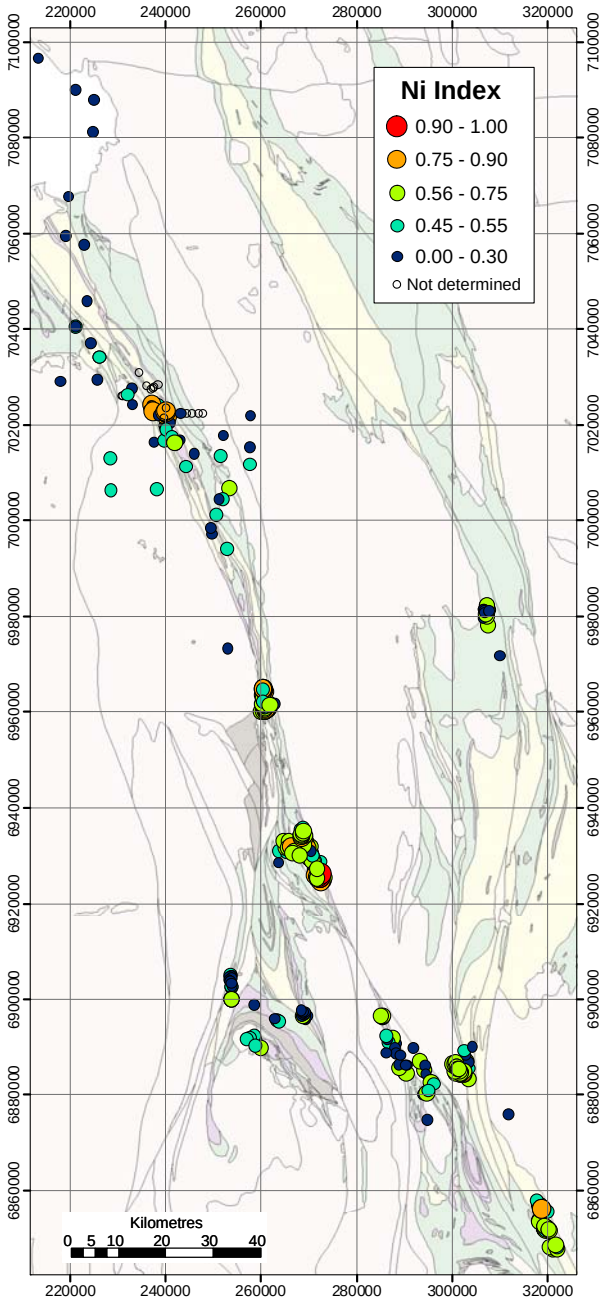

Figure 121: Groundwater Ni Index distribution for the NE Yilgarn Craton.

The Mineralisation index (Ni+Co+W+Pt; Figure 123) gives a better defined anomaly than any of the individual elements for some of the more moderate mineralised regions, such as Weebo and parts of Wildara associated with small NiS pods away from the main ore body. Using geochemical sulphide parameters (corresponding to the model presented for groundwater evolution around weathering sulphides; Section 3.3), two sulphide indices are used: the FeS index (pH-Eh+Fe+Mn; Figure 124) is controlled by common parameters associated with the oxidation of Fe-rich sulphides; and the AcidS index (Mo+Ba+Li+Al; Figure 125) relates to higher concentrations of metals due to the acid generation from sulphides. As expected for indices designed to indicate any sulphide, and postulated to give weaker signals for NiS (Section 3.3), these indices do not correlate well with Ni grade, and show a number of strong anomalies not apparently related to NiS, including various groundwaters at Wildara, and the Jaguar base metal VMS deposit to the SE.

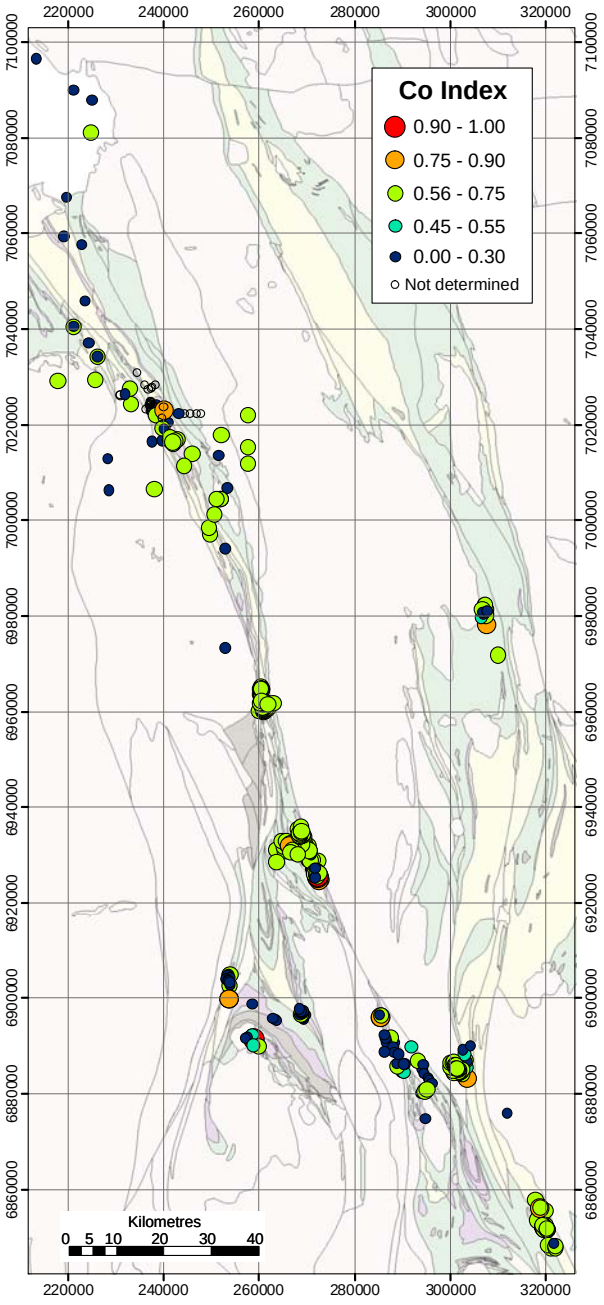

Figure 122: Groundwater Co Index distribution for the NE Yilgarn Craton.

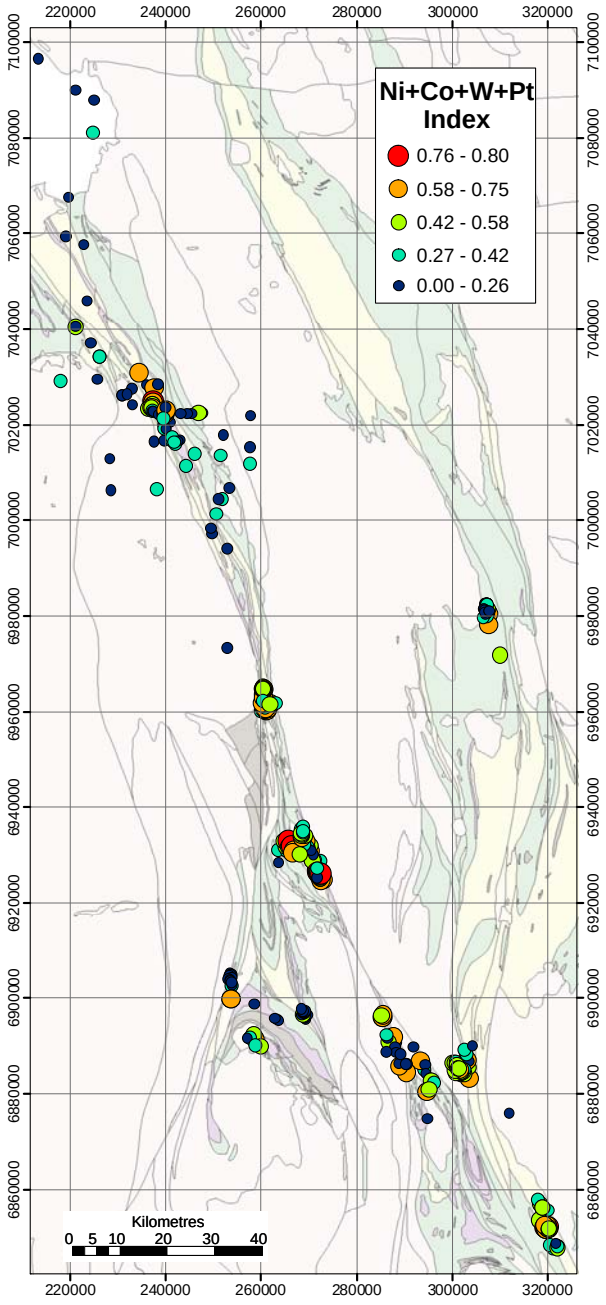

Figure 123: Groundwater Mineralisation Index (Ni+Co+W+Pt) distribution for the NE Yilgarn Craton.

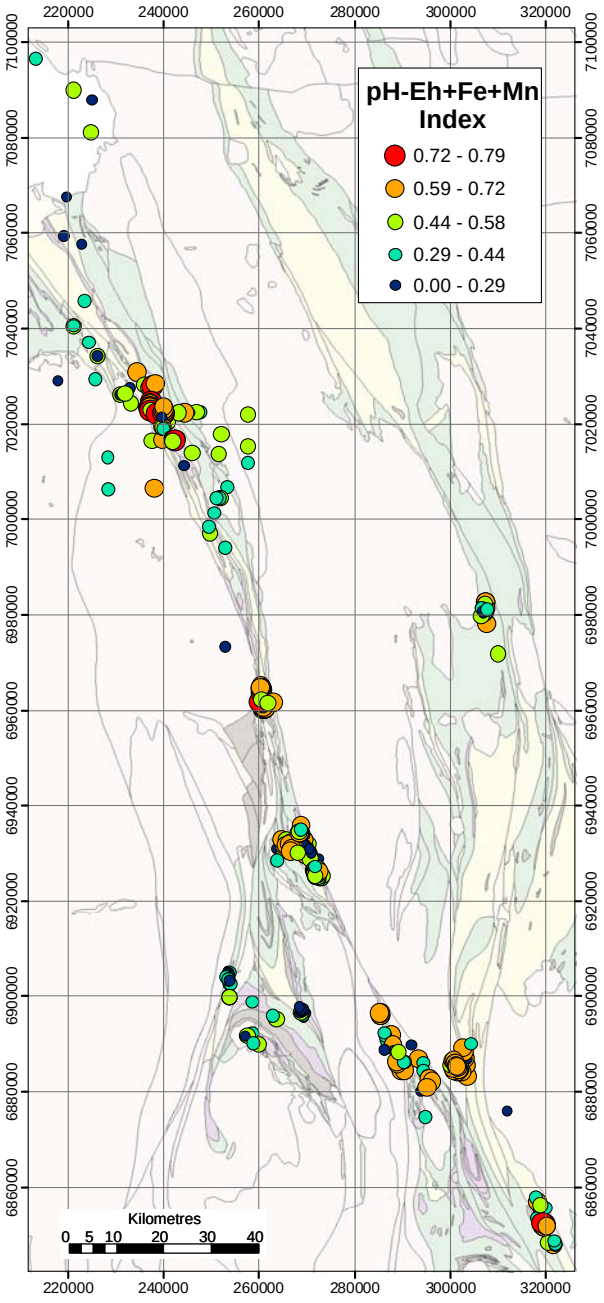

Figure 124: FeS groundwater index (pH-Eh+Fe+Mn) distribution for the NE Yilgarn Craton.

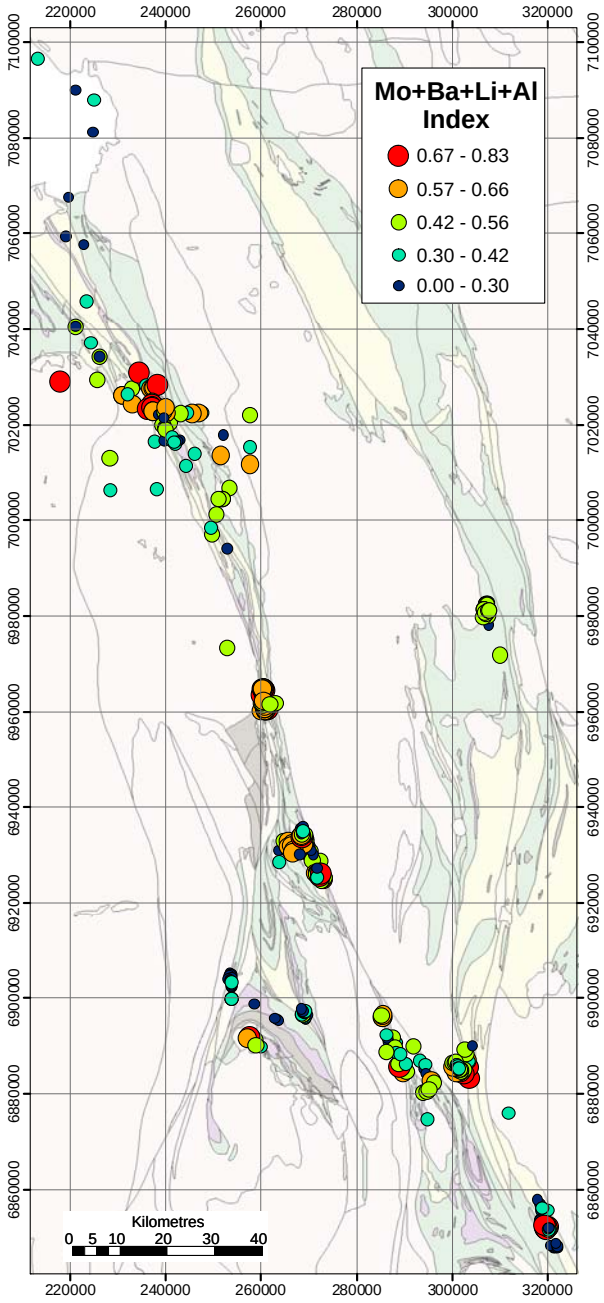

Figure 125: AcidS groundwater index (Mo+Ba+Li+Al) distribution for the NE Yilgarn Craton.

To emphasize mineralised vs. barren sulphides, these two sulphide parameters are subtracted from the Mineralisation index (Figure 126 and Figure 127), giving more specific anomalies related to NiS mineralisation. The only exception is the Jaguar deposit, which still has high index scores, because it is anomalous for some of the NiS pathfinders, particularly Pt and W (Figure 129). The Mineralisation-Cr index (Ni+Co+W+Pt-Cr; Figure 128) is designed to remove lithological effects. However, it is not as effective as the above combined mineralisation indices, producing more false positives and failing to detect the mineralisation around the Honeymoon Well area (Figure 128).

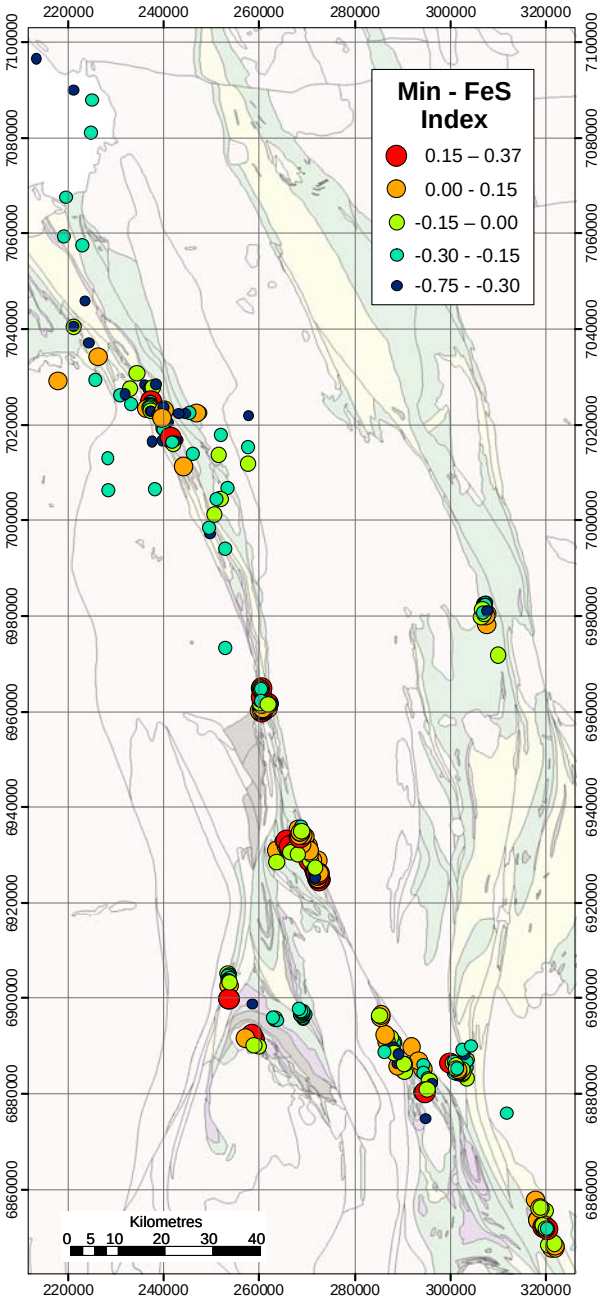

Figure 126: Groundwater Min - FeS Index (Ni+Co+W+Pt)-(pH-Eh+Fe+Mn) distribution for the NE Yilgarn Craton.

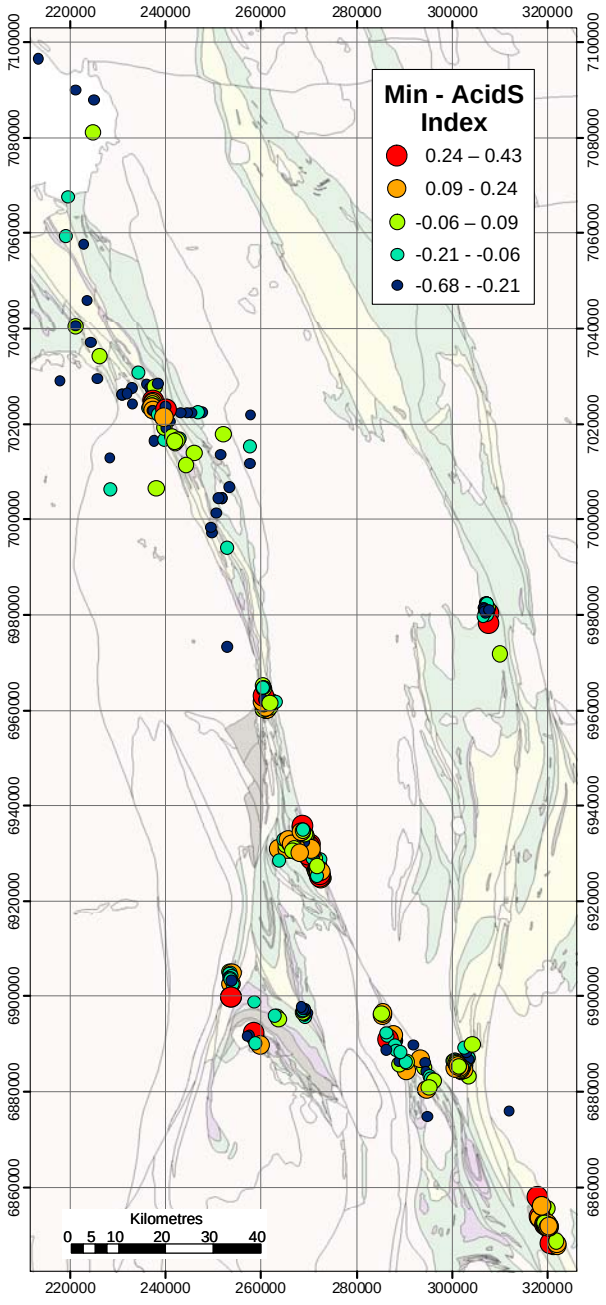

Figure 127: Groundwater Min - AcidS Index (Ni+Co+W+Pt)-(Mo+Ba+Li+Al) distribution for the NE Yilgarn Craton.

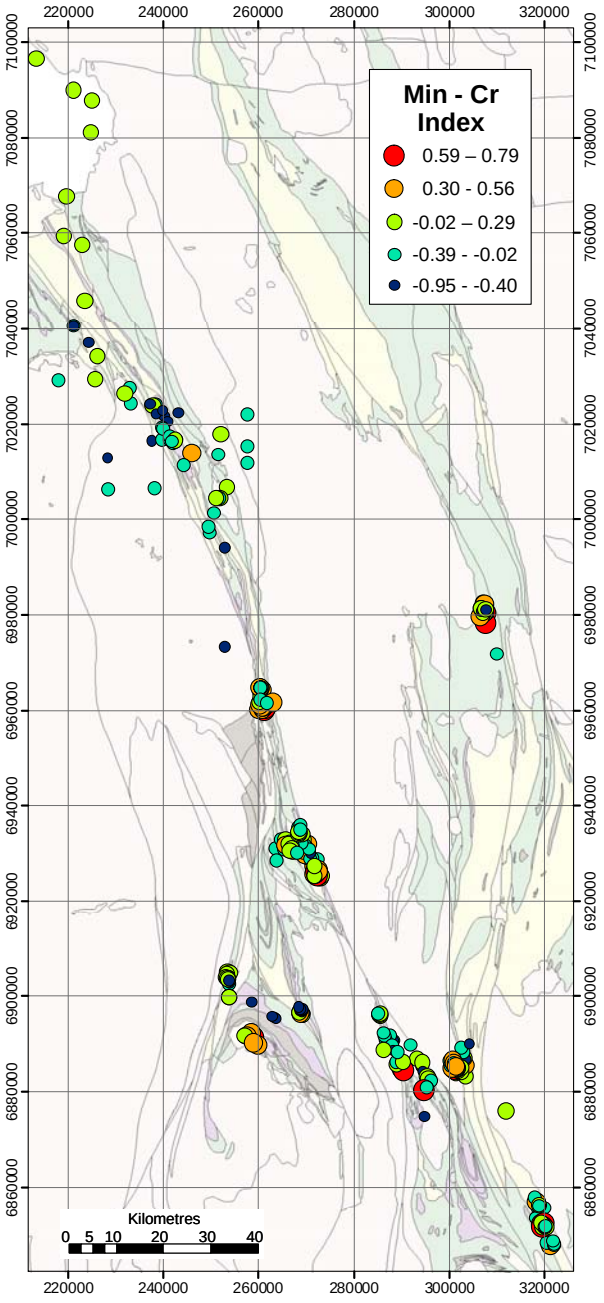

Figure 128: Groundwater Min - Cr Index (Ni+Co+W+Pt)-Cr distribution for the NE Yilgarn Craton.

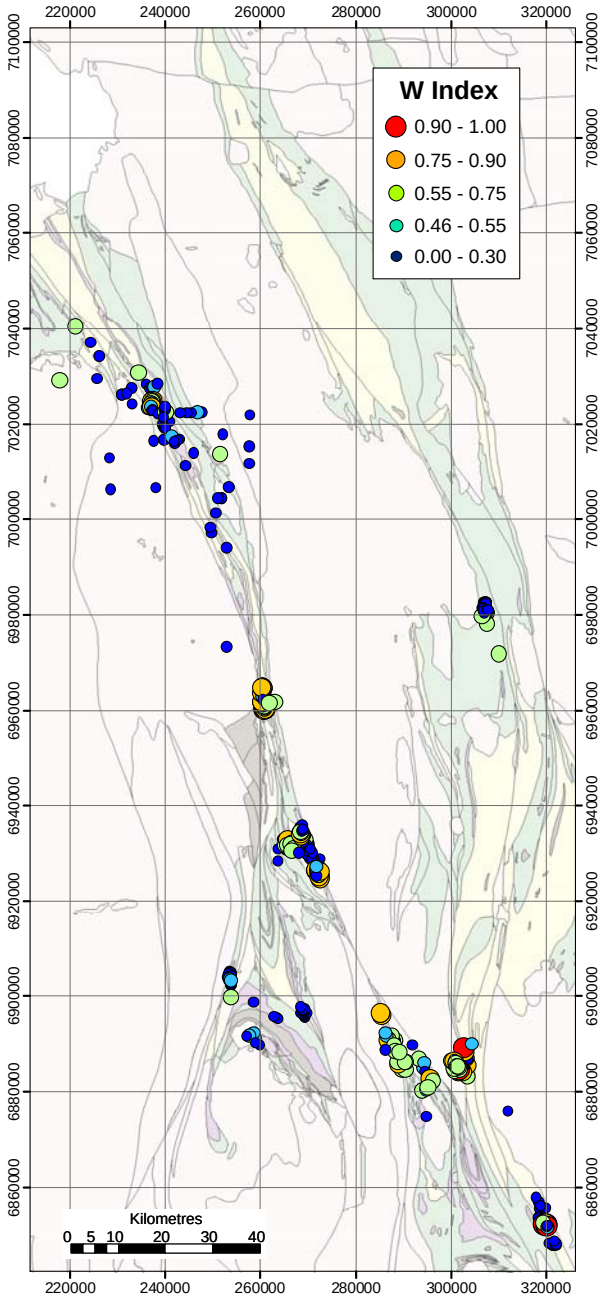

Figure 129: Groundwater W Index distribution for the NE Yilgarn Craton.

Tungsten is a good pathfinder element in the NE Yilgarn, with major mineralised regions delineated by the W index (Figure 129). The reason for the association of W with NiS is unclear, and should be investigated further. Dissolved W is a good groundwater pathfinder in the NE Yilgarn because the waters are neutral and oxyanions (*e.g.*, WO_4^{2-}) are not being bound to various minerals such as Fe oxides. The use of W as a vector is not applicable in saline and acidic conditions, such as the Kalgoorlie area (Gray, 2001). Other common oxyanions such as As and Sb (Figure 130) were not as useful as pathfinder elements for NiS; more commonly giving higher values around Au mineralisation (*e.g.*, directly east of Waterloo, at Mt Joel in the central east of the map, and NW of Honeymoon Well). Most other water samples were near or below detection limits for these metalloids.

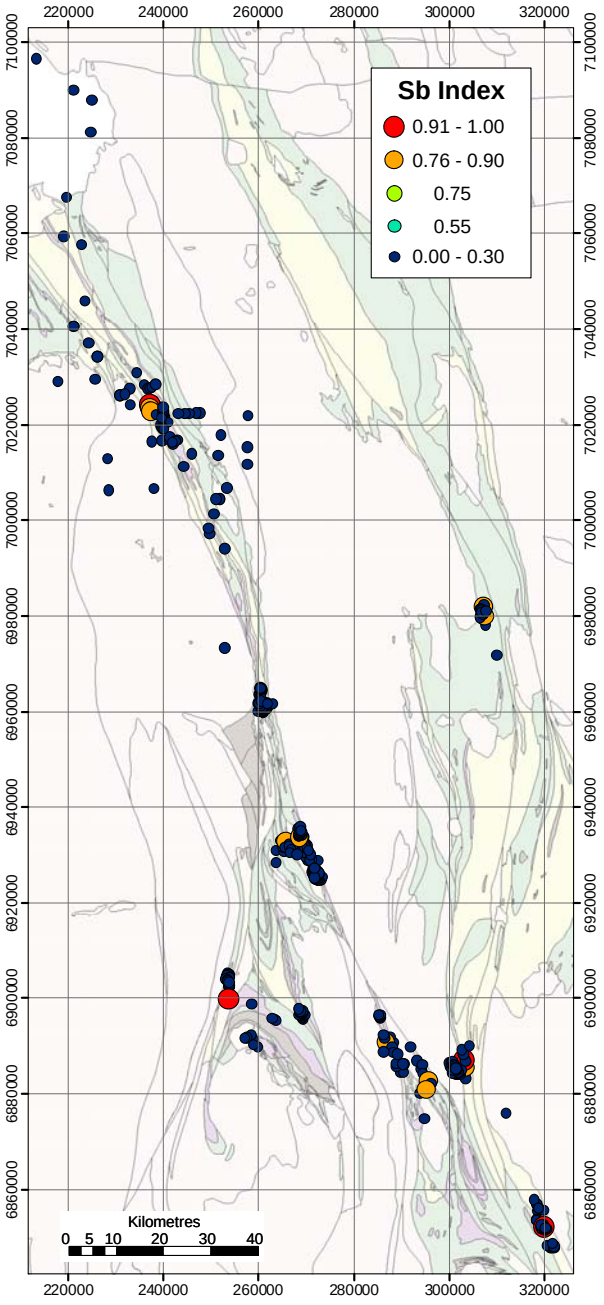

Figure 130: Groundwater Sb Index distribution for the NE Yilgarn Craton.

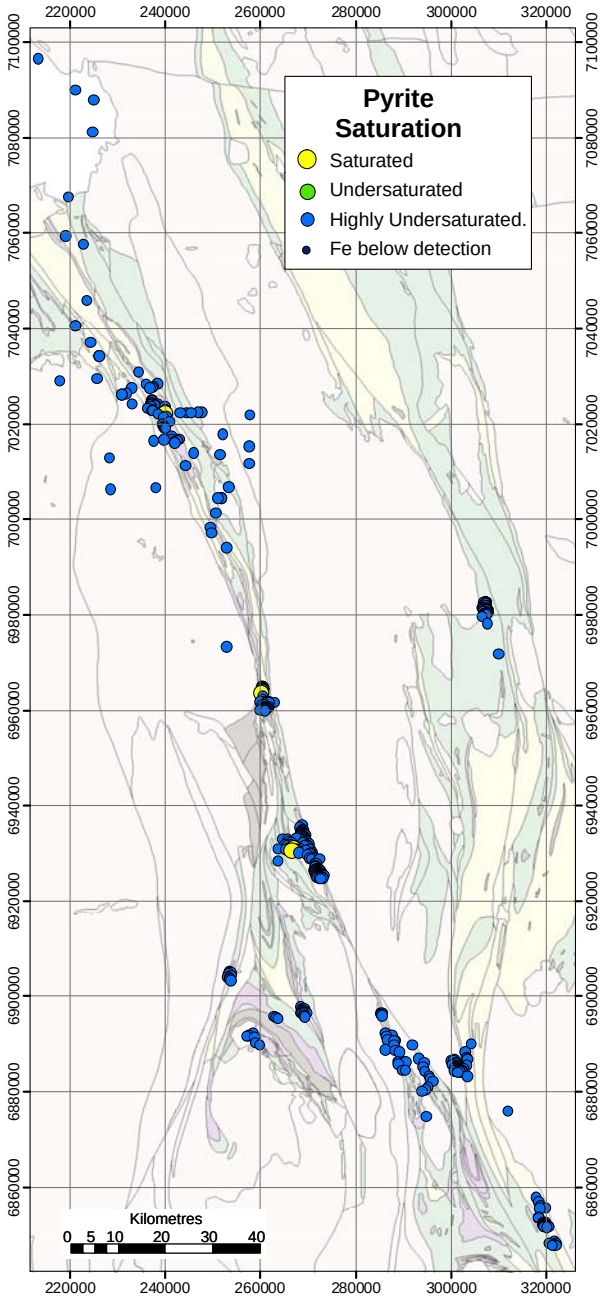

Figure 131: Distribution of groundwater SI of pyrite for the NE Yilgarn Craton.

9.5 Use of mineral saturation indices

Derived saturation indices (SI) allow further understanding of the groundwater chemistry than the bulk geochemistry alone. Groundwater data from all of the sites investigated were put into PHREEQE and the saturation of many mineral species was determined based on thermodynamics, activities and key water parameters such as pH and Eh (Section 2.2). The results aimed to improve understanding of the groundwater signature associated with the weathering of sulphides and other related minerals. With minor exceptions, SI values did not prove useful vectors towards mineralisation, and only selected data is presented.

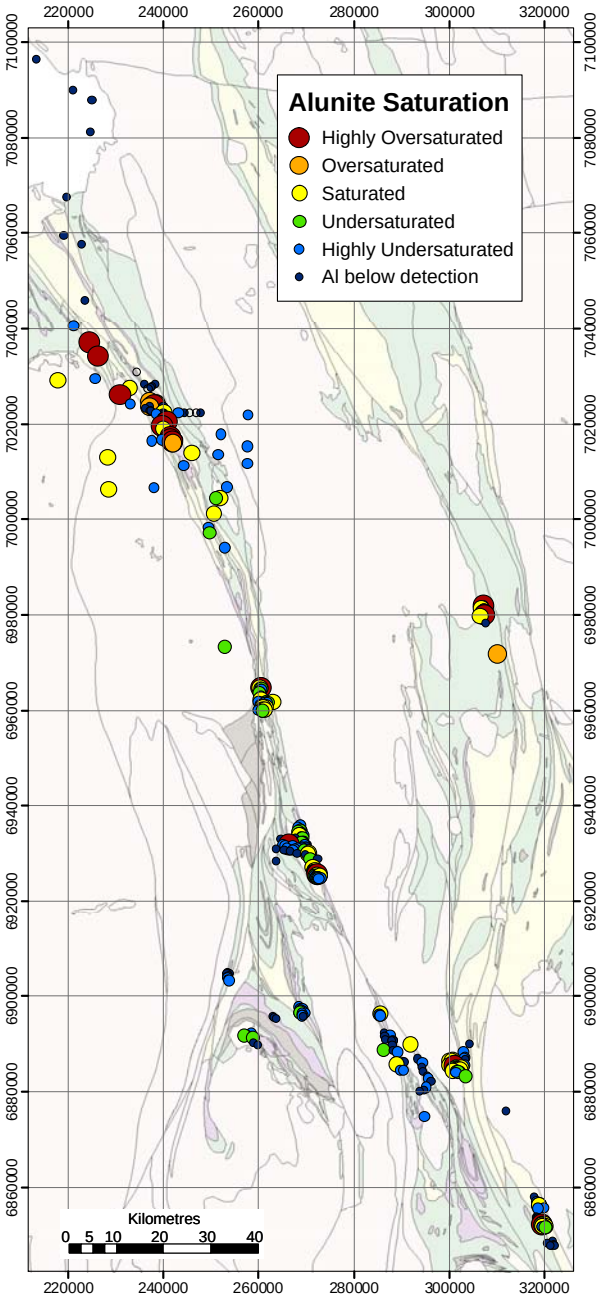

Figure 132: Distribution of groundwater SI of alunite for the NE Yilgarn Craton.

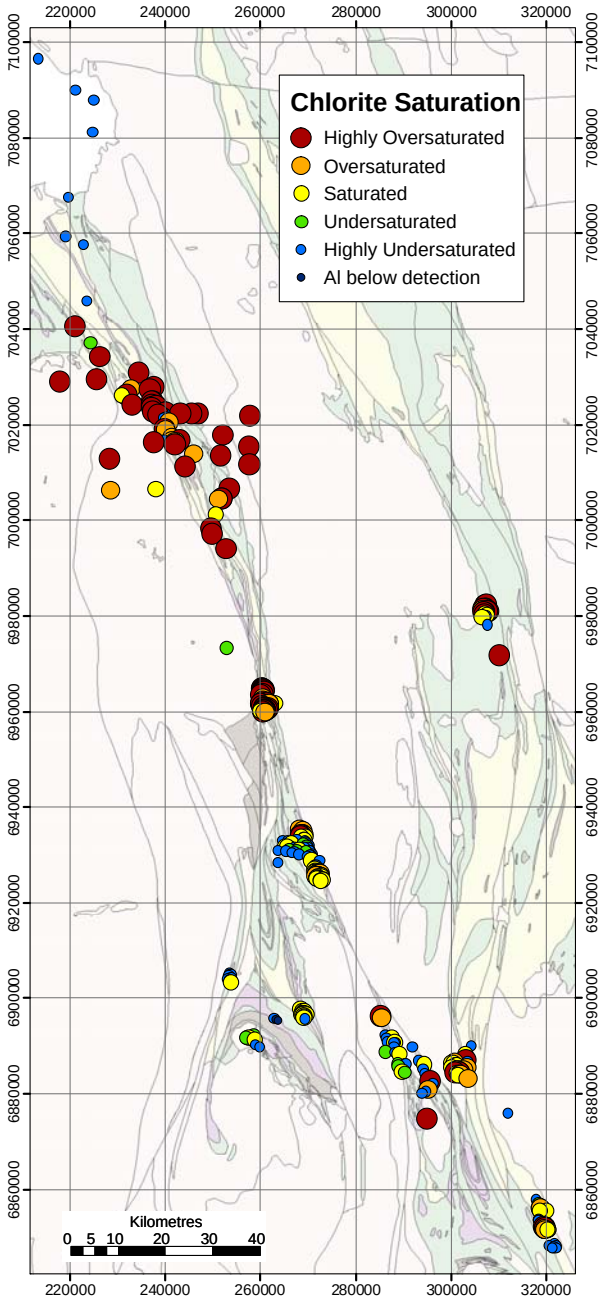

Figure 133: Distribution of groundwater SI of chlorite for the NE Yilgarn Craton.

Almost all groundwaters are undersaturated with respect to pyrite (Figure 131) and other sulphides, reflecting sampling at or above the weathering front. Alunite oversaturation (Figure 132) may reflect anomalous Al concentration due to sulphide oxidation and acid attack on wall rocks. In some cases, chlorite SI (Figure 133) may reflect primary control, although this is not the case at Honeymoon Well where more saline groundwaters have higher Mg concentration and are therefore oversaturated with respect to chlorite. Use of SI values for Ni minerals (*e*.g., $NiSiO_4$; Figure 134) does not appear to add value for direct hydrogeochemical exploration for NiS.

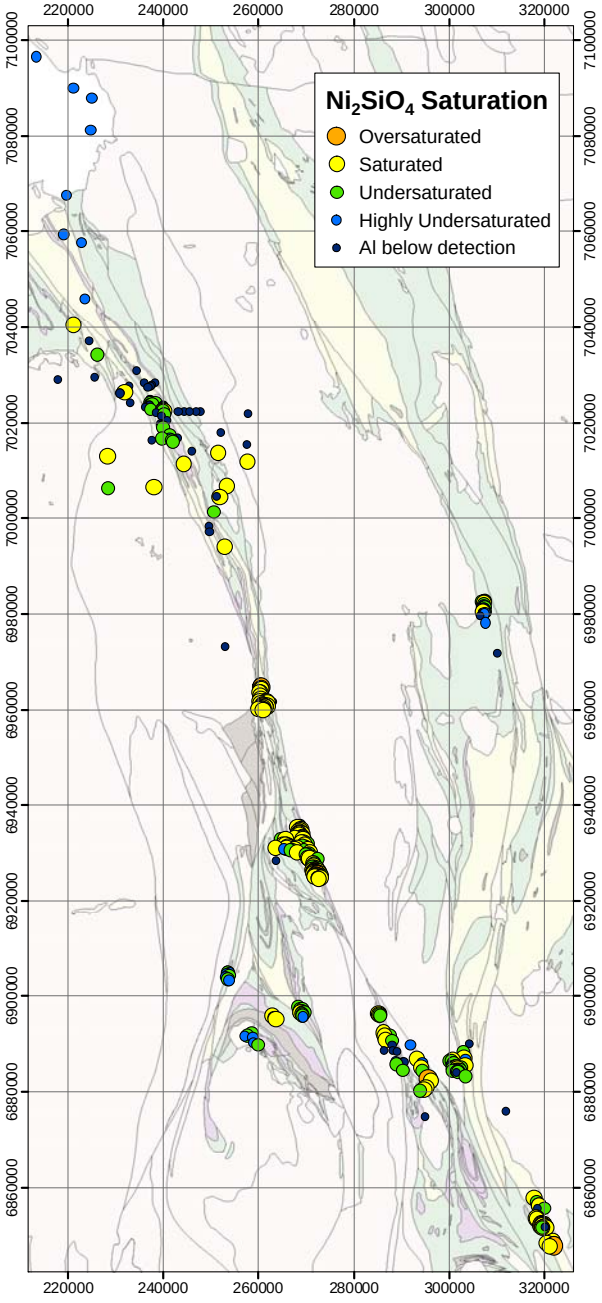

Figure 134: Distribution of groundwater SI of $NiSiO_4$ for the NE Yilgarn Craton

The results of the large scale investigation suggest significant potential for hydrogeochemistry to be a successful tool for broad scale exploration of NiS in the NE Yilgarn Craton, in addition to the deposit scale. Low salinities enable low analytical detection limits, providing a solid foundation for reliable data generation. The individual elements Ni, Co and W are the best vectors, whereas index combinations improve exploration utility in the NE Yilgarn and analogous environments.

10. METHOD DEVELOPMENT

10.1 Introduction

As part of this project, various sampling and analytical protocols were tested on the NE Yilgarn groundwaters. Filtration sizes of 0.1 and 0.45 µm were compared for selected major and trace elements, while anion and cation exchange resins were also tested and compared to the exchange capacity of activated C for unfiltered samples, with the goals of improving detection limits and developing a robust technique for industry groundwater exploration. Eleven samples were tested for the filtration comparison, while 28 samples were used for the assessment of the exchange resins and activated carbon. Previously, more than 200 samples have been collected using the activated carbon in the NE Yilgarn Craton for PGE analysis. Studies on carbon sachets and "black ooze" have continued on from other project work and though discussed here, are not contained within this project.

10.2 Blanks and duplicates

All samples analysed had blanks and duplicates incorporated into the procedures, both with the Ion Chromatography and alkalinity work at CSIRO laboratories and all ICP-MS/OES analysis at Ultratrace laboratories. Any positive blank values (very rare) were taken from the final numbers, and duplicates that were not reproducible were investigated and samples reanalysed if necessary. Generally, the data were reproducible (Figure 135). All data are available in Appendix 1.

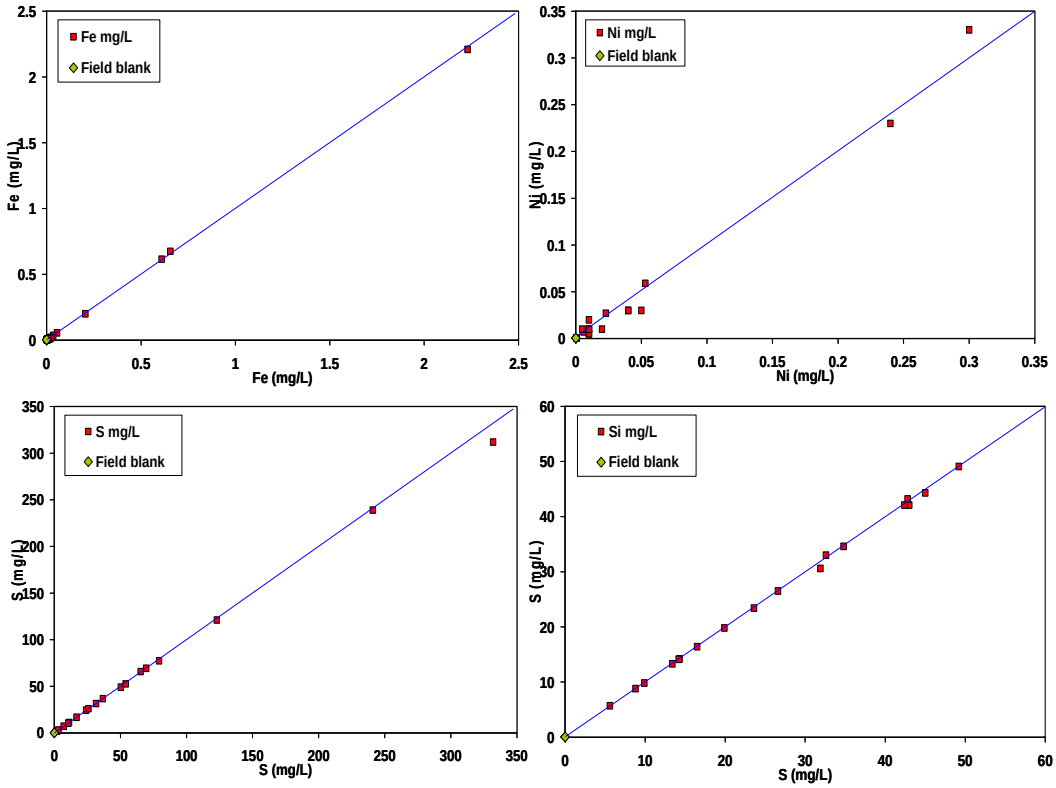

Figure 135: Duplicate results from the Wildara region for Fe, Ni, S, and Si by ICP-MS/OES.

10.3 Filtration comparison

A comparison between 0.1 µm and 0.45 µm filtration was conducted on samples from the Honeymoon Well region. Commonly 0.45 µm filtration is considered the standard method, primarily because this was the minimum pore size filter papers available during the time standards were introduced. Smaller diameter filtration paper is now more readily available. Clay minerals are commonly much smaller

than 0.45 µm and theoretically could pass through the filter and adsorb metal in solution prior to analytical determination or release elements on acidification. The most affected elements are Al, Fe, Ti, Mn, and trace elements that are associated with sparingly soluble oxyhydroxides and clay minerals (Kennedy and Zellwegger, 1974). Early studies determined significant quantities of Al, Fe and organic compounds are in the 0.5 - 0.1 µm size fraction in various waters (Armstrong, 1958; Kennedy and Zellwegger, 1974). These compounds could potentially pass through the 0.45 µm filter, but not the 0.1 µm filter, resulting in higher concentrations of metals, particularly Al, Fe and Mn in the 0.45 µm filtered solution (Kennedy and Zellwegger, 1974). These compounds could decrease metal contents in the finer filtered samples, even though the results would be more representative of the actual soluble metal content. Issues could arise in relating results between the different filtration sizes if standard filtration was not used in a hydrogeochemical exploration program.

This study found no significant difference between the 0.45 and 0.1 µm filter size for major anions (Cl, SO_4) and cations (Na, Mg, K, Ca) (Figure 136). Student's t-test also show no significant differences (Table 2) and the slopes of the best fit lines are very close to 1 (Table 2).

Table 2: Statistics for comparison of filtering methods for major ions at Honeymoon Well.

Element	Line of best fit	R^2	Student's t-test (2-tailed)
Cl	y=1.005x	0.997	P≤0.88
SO_4	y=1.006x	0.997	P≤0.90
Na	y=1.001x	0.997	P≤0.56
K	y=0.997x	0.997	P≤0.93
Ca	y=0.991x	0.996	P≤0.29
Mg	y=0.983x	0.996	P≤0.63

The increased salinity of some of the Honeymoon Well samples required large dilutions and minor element analyses for numerous samples had to be excluded due to the results being below detection limits. The results for U, Mo, Si and S show no difference between treatments (Figure 137 and Figure 138), similarly to the major anions and cations. The limited results for V, W and Cu and to a lesser extent Ni and Zn (Figure 137 and Figure 138) also indicate the there is no significant advantage to using the finer, more expensive filter. But, Al and Fe show variable sample concentrations. Iron is not consistently higher or lower i.e. there is no consistent difference between treatments (Figure 137 and Figure 138). There is no clear relationship between Fe and Al, i.e. if Fe is higher than expected, Al may not be higher for the same sample and filtration type (Figure 139). Aluminium concentrations are a little higher in the 0.1 µm filtration, which does not support the idea that small clays (aluminosilicate minerals) are getting through the 0.45 µm filter and being caught by the 0.1 µm filter. In comparison, the near-perfect correlation between filter sizes for Si relates to much higher dissolved Si and indicates the Si concentration is not influenced by the comparatively small concentrations of Al and Fe silicates that may pass through the filter membranes. The lack of significant difference between filter sizes for the trace elements suggests they are not influenced by Al and Fe i.e. Al and Fe do not dilute or concentrate the dissolved trace metals (Figure 137 and Figure 138).

The use of either tested filter size may well be acceptable for groundwater exploration in the NE Yilgarn, but further study of Fe and Al from the two filter sizes is required to fully assess the implications for groundwater studies in the other areas of the Yilgarn. At this stage the Fe and Al "dissolved" concentrations should be interpreted carefully in such neutral/fresh groundwaters.

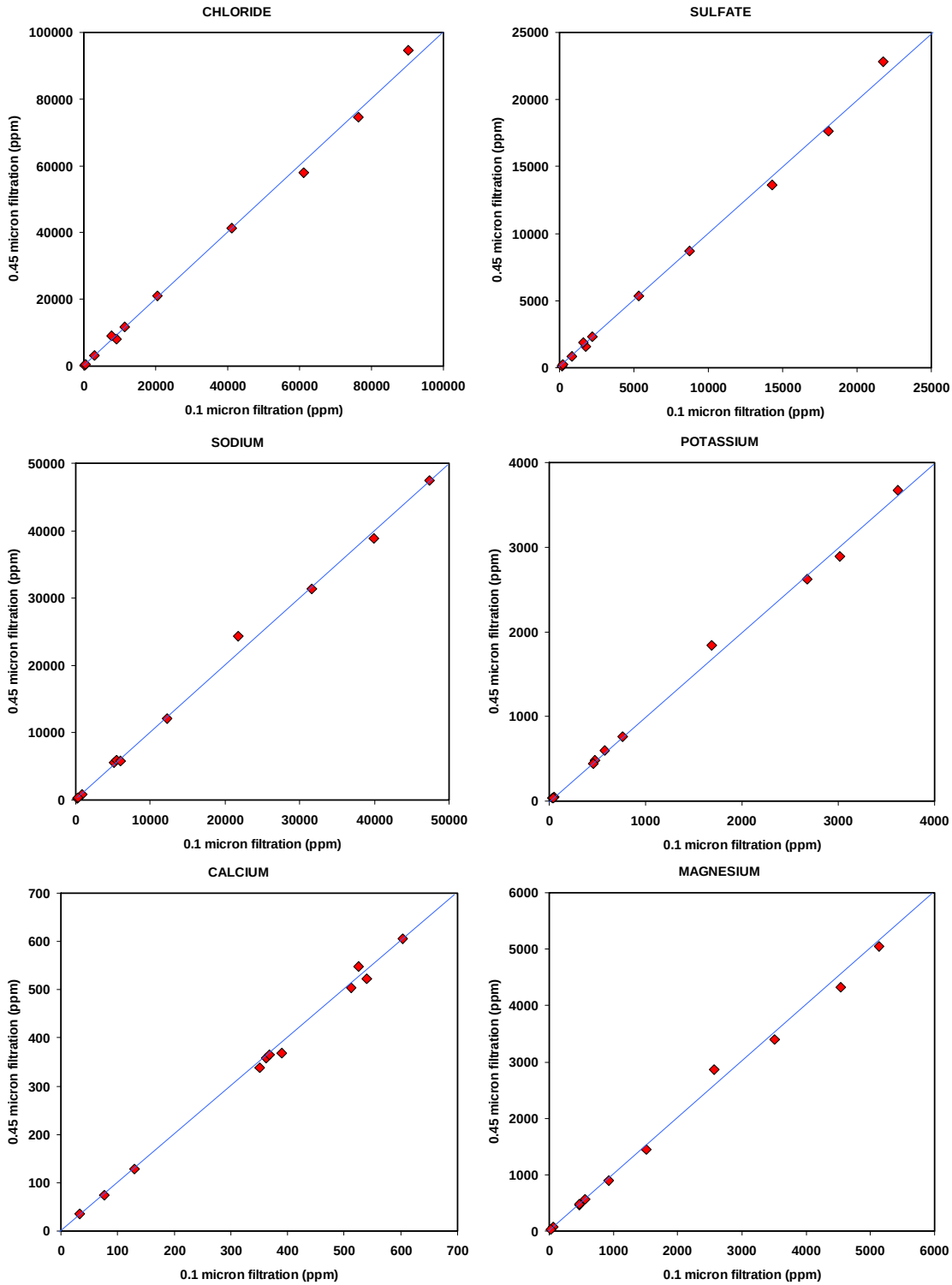

Figure 136: Major anions and cations compared from the 0.1 and 0.45 µm filtration treatment methods. The blue line represents the perfect correlation and with no differences between filtration. Error bars represent analytical detection limit.

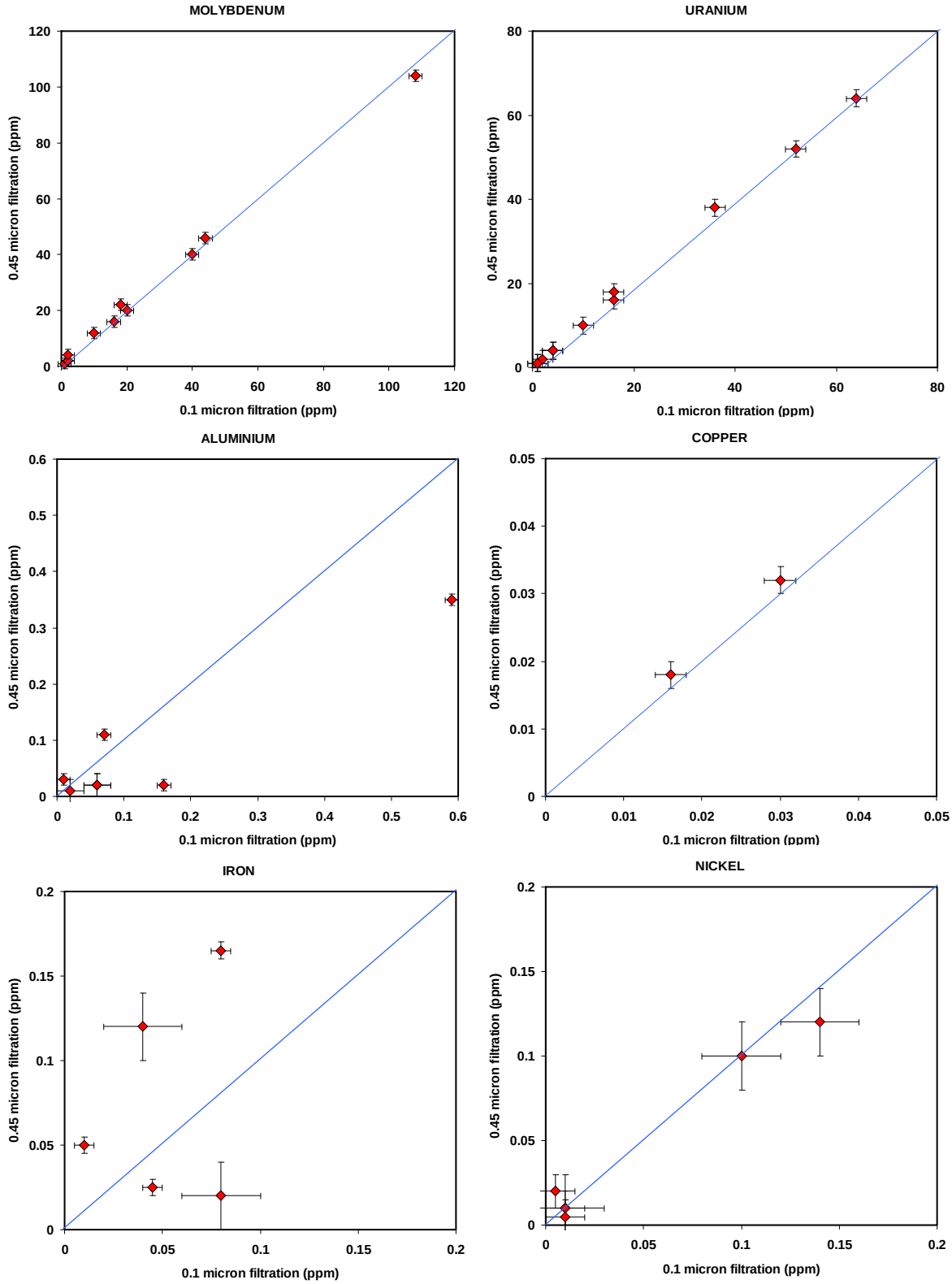

Figure 137: Mo, U, Al, Cu, Fe and Ni compared from the 0.1 and 0.45 µm filtration treatment methods. The blue line represents the perfect correlation with no differences between filtration. Error bars represent analytical detection limit. Results were excluded where the concentrations were at or below the detection limit.

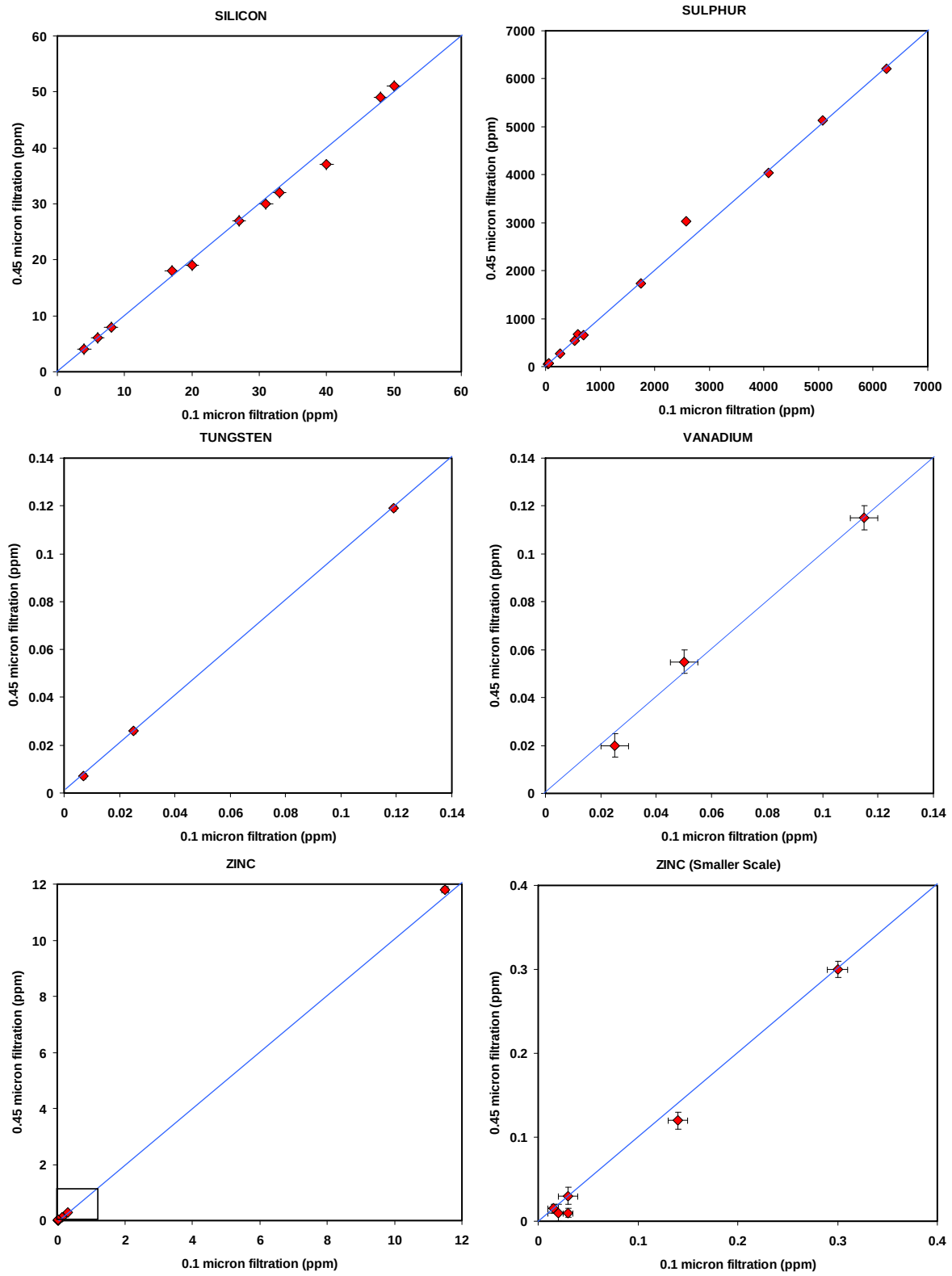

Figure 138: S, Si, W, V and Zn compared from the 0.1 and 0.45 µm filtration treatment methods. The blue line represents the perfect correlation with no differences between filtration. Error bars are applied based on the detection limit of the analysis. Results were excluded where the concentrations were at or below the detection limit. The cluster of Zn concentrations is shown again (bottom left) with a smaller scale to show the true distribution of results.

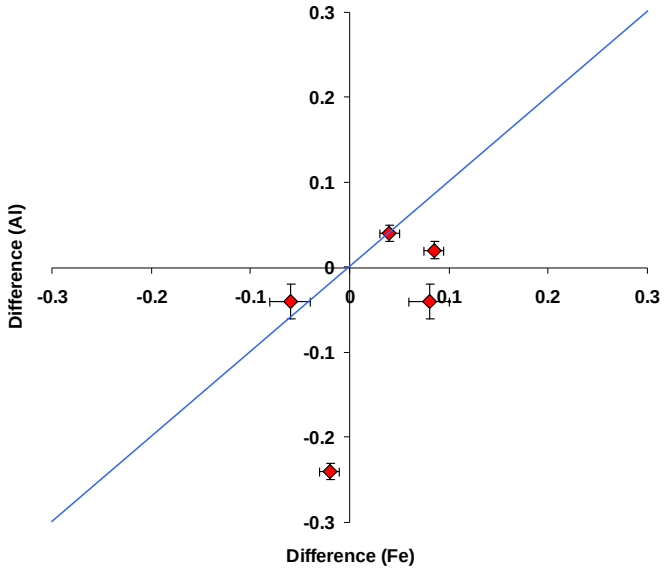

Figure 139: The difference for Al and Fe from the line of perfect correlation. The blue line represents where the difference between the two filtration treatments for Fe is the same as for Al. Error bars represent analytical detection limit.

10.4 Carbon sachets

Carbon sachets have previously been routinely used for Au analysis, and this is being extended to Ag, Pd, Pt, U, W and other metals. The use of C extracted W, Pt and Pd has been a useful vector to Ni mineralisation (Figure 140, Figure 141 and Figure 142). The PGEs in the NE Yilgarn are in very low concentrations (commonly < 1 ng/L) making the use of these elements as a pathfinder to mineralisation difficult. Results show that higher concentrations of Pt are found around the mineralisation, as well as any detectable Pd (Figure 141 and Figure 142). The activated carbon is the only technique employed in this study that can obtain low ng/L levels of detection and is particularly useful for Au and PGEs. Improving the detection of PGEs in groundwater may significantly enhance exploration success using hydrogeochemistry for NiS.

The carbon sampling is unfiltered, easy to use, collects anions and cations, and may be more applicable to exploration industry hydrogeochemical sampling.

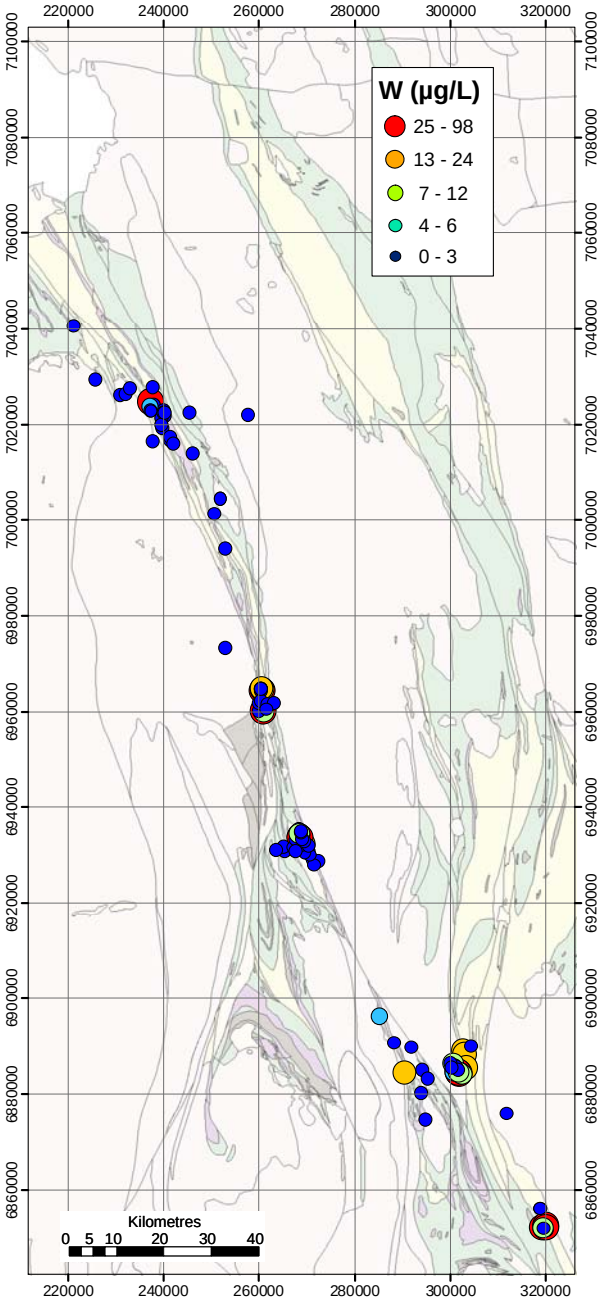

Figure 140: W adsorbed to activated C in groundwater of the NE Yilgarn.

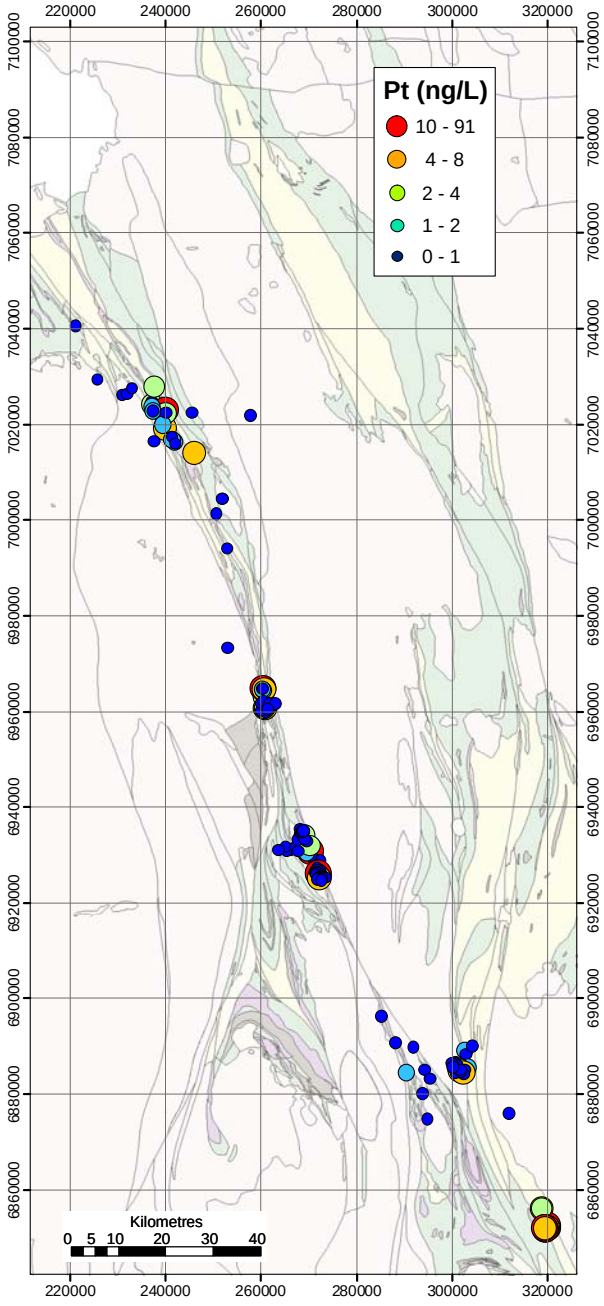

Figure 141: Pt adsorbed to activated C in groundwater of the NE Yilgarn.

C vs ICPMS

Tungsten has been a useful pathfinder element and is detectable in both direct measurement and with the activated carbon sachet. The activated carbon is a more field practical method than filtering and acidifying samples for direct measurement. Comparing the results from the two techniques indicates some correlation (R^2=0.81), but the direct ICPMS measurement detects approximately 7 times more W than the W extracted by activated C (Figure 143).

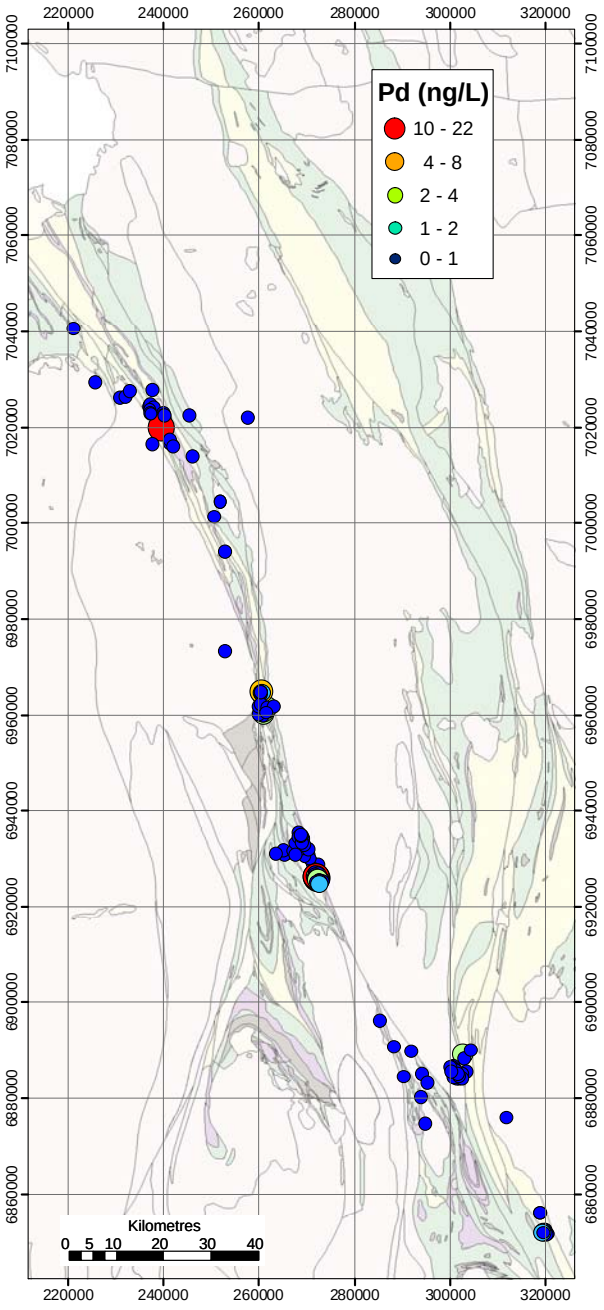

Figure 142: Pd adsorbed to activated C in groundwater of the NE Yilgarn

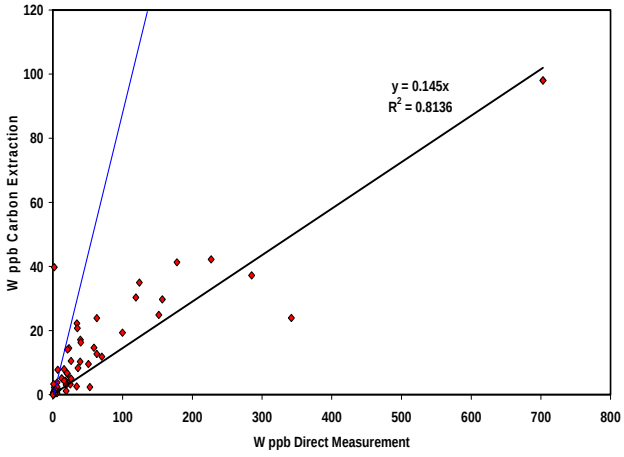

Figure 143: Tungsten measured by ICPMS directly and extracted by activated C.

10.5 Exchange Resins

Two forms of exchange resins were tested at Honeymoon Well for their potential as an easy field sampling technique. The anion exchange resin extracted metals were commonly below detection. Two exceptions were U and W. Silver was below detection for all samples except HW 21. This anomaly was also found using the carbon sachets and the cation exchange resin at this site, but was not detected directly using ICPMS. The water at this site was unremarkable in other key water parameters such as Eh, pH and TDS. The cation exchange resin extracted metals were also commonly below detection, although Cr, Fe, Ni, Pb and U were detected in numerous samples. The use of exchange resins for PGE detection was not improved compared to other techniques.

Evaluation of direct ICP-MS/OES measurement of acidified, filtered water with the cation exchange resin extracted metals showed poor correlation of Cr, Fe and Pb (Figure 144). The cation exchange resin (3% of total) removed less Ni than the carbon sachet (14% of total), and is probably not adding value for Ni exploration compared to the activated carbon. The fractions have an approximate linear relationship to the total concentrations (direct measurement). The metals extracted from the anion exchange resin were often below detection, with the exception of U and W, whose preferential sorption is due to these two elements forming mobile oxyanions (e.g. $UO_2(CO_3)_2^{2-}$ and WO_4^{2-}) in the neutral waters of the NE Yilgarn. Uranium was extracted and measured for both exchange resins and via direct measurement. Although direct determination is considered the best technique, there is some agreement between the techniques. Uranium concentration agreement between the direct measure and the anion exchange extractable U was very good (Figure 144). High U values by direct measurement were also high in the cations exchange resin extracted U (Figure 144). The resins did not improve the detection of PGE and were not superior to the activated carbon (4% of total W for anion exchange resin compared to 13% of total W for carbon). The results were similar to Ni and have a linear positive relationship for carbon, but are not related for the anion exchange resin (Figure 144). Preliminary results indicate there is some potential for exchange resins to be beneficial in hydrogeochemical sampling, but it is probably more effective to use direct measurement of filtered and acidified samples. The resins did not improve the detection of PGEs which is a major limiting factor in using hydrogeochemistry and PGEs as an exploration method.

Exchange resins replicates were good, with the exception of one anion exchange result for U. Many samples were below detection, so a thorough assessment was not possible. Other tests were conducted to assess the preferential sorption of metals to the resins and carbon. Sachets of all three resins (anion, cation and carbon) were placed in the same water sample. Comparing the results from the competing exchange sites to the single method sample indicates that most metals were adsorbed more in the single solutions. Again the limitations of detection did not provide a lot of useable data (Appendix 4 and 5), but the anion exchange resin out competed the cation exchange resin for Ag, whereas the carbon removed far more Ag in the limited sample set (Figure 145).

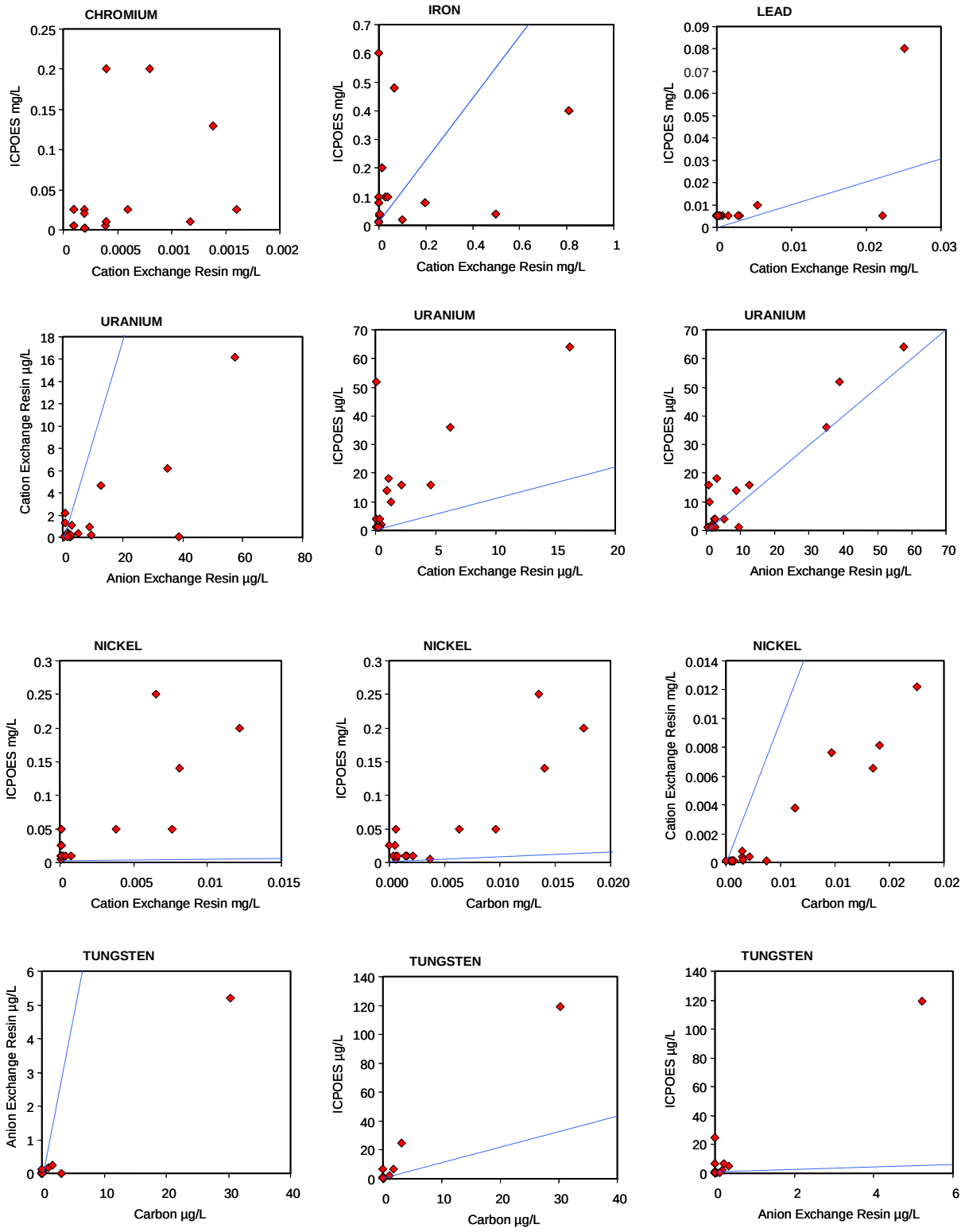

Figure 144: Scatter plots comparing concentrations of Cr, Fe, Pb, U, Ni and W determined by direct ICP-MS/OES, cation exchange resin, anion exchange resin and carbon.

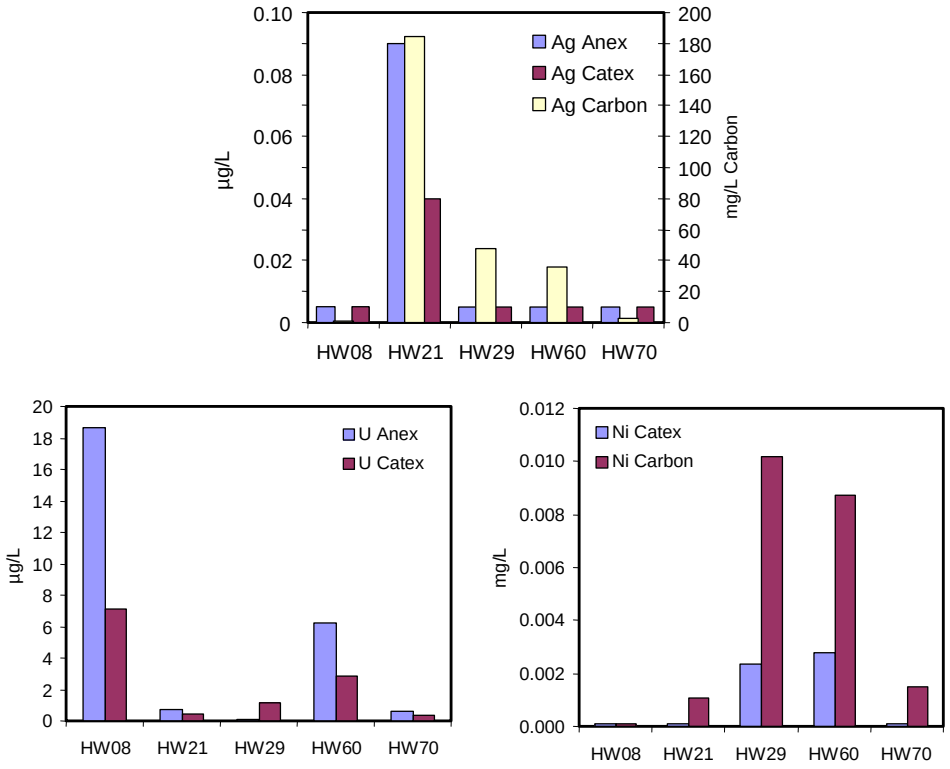

Figure 145: Comparison of adsorption capability for selected elements and exchange methods. The carbon adsorbs far more silver than the other two techniques and is plotted on a separate axis.

The cation exchange resin adsorbed significantly less Ni and Pb when in competition with the activated carbon and anion exchange resin (Figure 146), as did the anion exchange resin for U (Figure 147). Carbon results were also lower when competing against cation exchange, but did not seem to be influenced for the anion exchange of W (Figure 148). A major advantage of the carbon is that it enables collection of data on both negative and positive charged ions. Again, the limited sample set, and many numbers below detection only allow qualitative assessment.

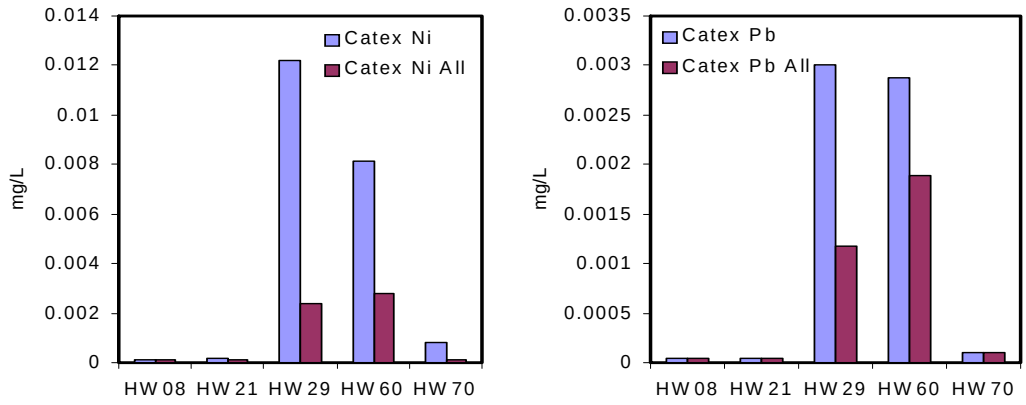

Figure 146: Comparison of competing adsorption with cation exchange resins. The *All* column represents the same water sample that was exposed to all three methods simultaneously, and the subsequent measure of the cation resin bound metals when competing with the other techniques.

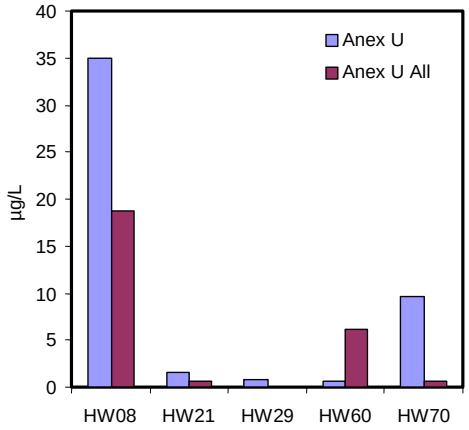

Figure 147: Comparison of competing adsorption for U with anion exchange resins. The *All* column represents the same water sample that was exposed to all three methods simultaneously, and the subsequent measure of the anion resin bound U when competing with the other techniques.

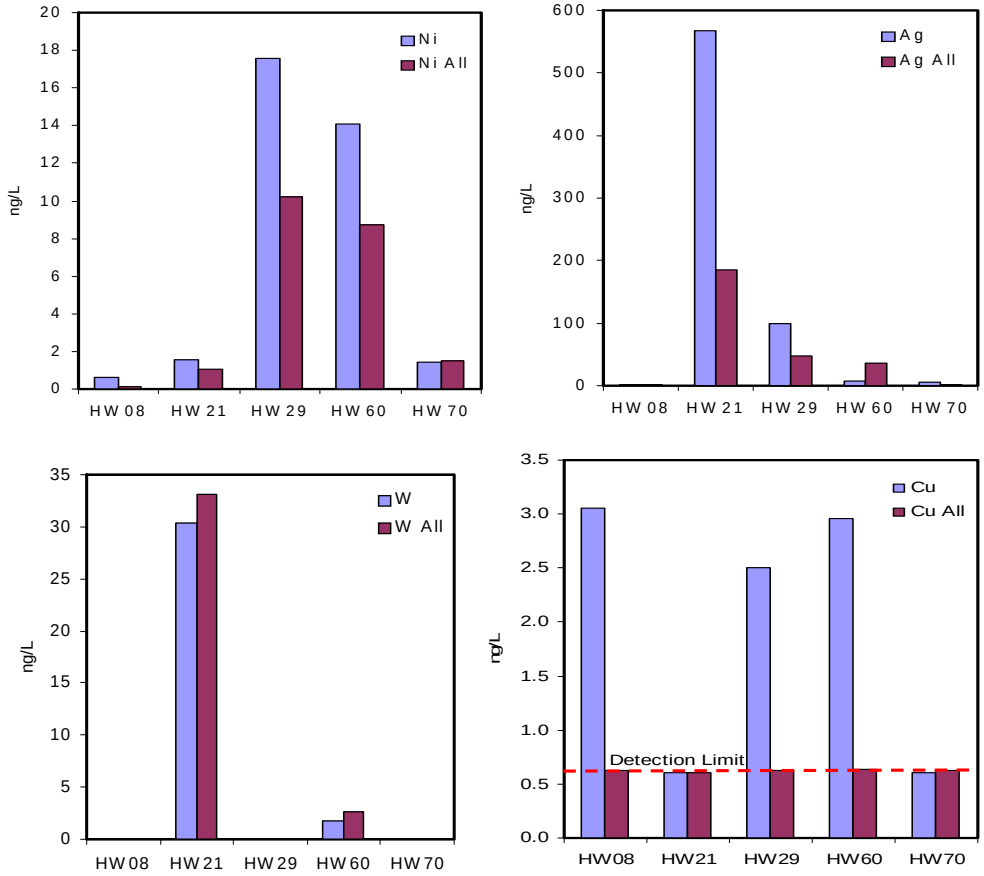

Figure 148: Comparison of competing adsorption for metals with carbon. The *All* column represents the same water sample that was exposed to all three methods simultaneously, and the subsequent measure of the carbon bound metals when competing with the other techniques.

10.6 Black ooze

A common occurrence when sampling groundwaters from within sulphides is a fine, low density, reduced black material, referred to as "Black Ooze". The material has a strong sulphur smell and rapidly clogs filter media. When exposed to air it rapidly oxidizes to a reddish brown colour. Close examination reveals many fine rocks fragments representative of the sample area, Fe-silicates, pyrite and traces of other S-bearing minerals. A complete characterization of this material has not been conducted as it is outside the scope of this project, but it is important to note that the material is not contamination such as biomatter from surface inflow, and is a common occurrence when sampling deep or highly reduced waters in the NE Yilgarn.

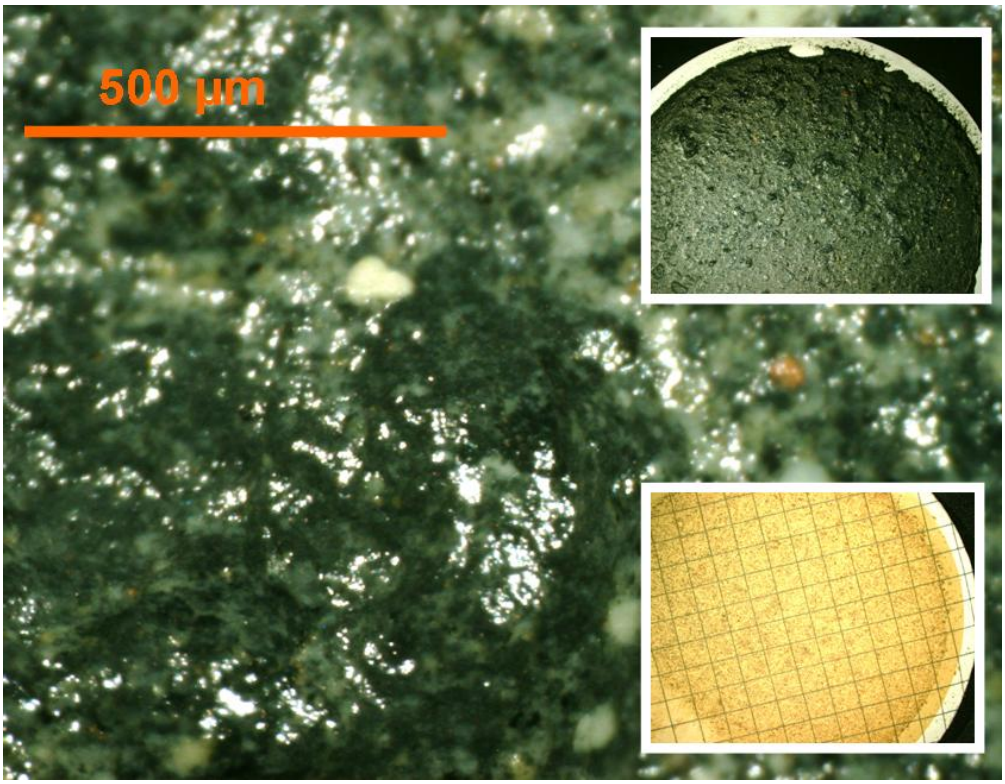

Figure 149: Black ooze filtrate from a water sample taken from a hole intersecting sulphides. Top inset is the initial filter paper with the lower inset showing the rapid oxidation of the material over 72 hours.

10.7 Sampling recommendations

The use of 0.45 µm filtration is recommended for field filtration of water samples as it is more cost effective and quicker than the 0.1 µm filtration. A sample that is filtered and acidified is important for the measurement of most elements. Carbon sachets are the preferred method for low level detection of Au and PGEs, proving better than the exchange resins tested (except for W using the anion exchange resin), and having the benefit of collecting both anionic and cationic species. Field measurement of Eh and pH is critical. Electrical conductivity and alkalinity are also beneficial measurements, and these can be measured in the laboratory. Alkalinity (sealed, no air space, unfiltered) and anion (filtered, not acidified) samples are recommended to be collected, but given the mineral saturation indices results were of little value, these samples are not as critical as the others.

Sample spacing is ideally 100-300 m for targeting mineralised sulphides, and 1-2 km for targeting sulphides, but optimization of sample spacing is continuing to be improved. Typically, samples are not available in well spaced locations, so opportunistic sampling of any available sites is recommended, and was the technique used in this study.

11. DISCUSSION AND CONCLUSIONS

The results of the study suggest significant potential for hydrogeochemistry for both regional (km spacing) to deposit (10 - 100's m spacing) scale exploration for NiS in the NE Yilgarn and analogous environments, with additional potential for use for drill holes representing near misses in under-explored, brownfield regions. The geochemical halo around NiS deposits has some false negatives *i.e*. samples that should be anomalous, but are not, but few false positives, so most high concentrations of metals associated with the NiS hydrogeochemical signature are indicative of sulphides and mineralisation. Sample spacing for mineralised exploration targeting is estimated to be a few hundred metres, although the signature of the sulphides and ultramafics is greater than this, potentially on the 1-2 km scale. Future data will improve this assessment of required sample spacing.

Chromium is the best indicator element for ultramafic rocks, whereas Ni, Co, Pt and W are the best individual pathfinders for NiS mineralisation. Using the Box-Cox transformation and the derived indices enhances the targeting capabilities with multielement data. The better performing indices for mineralisation targeting are the Miner-FeS and Miner-AcidS indices, which use the mineralisation signature (Ni+Co+W+Pt) and take away the groundwater signatures of Fe-rich sulphides (pH-Eh+Fe+Mn) or of metal released by acid producing sulphides (Mo+Ba+Li+Al). The larger and more mineralised deposits had the largest hydrogeochemical signatures. The best anomalies are observed for massive sulphides, with some disseminated deposits only delineated by using the combined Miner-FeS or Miner-AcidS indices.

The use of mineral saturation indices was in most instances not beneficial as a direct exploration method for NiS, as nearly all samples were under saturated with respect to most ore minerals. One notable exception is use of such analysis for minerals associated with U mineralisation. Although U exploration is not part of this study, preliminary results would indicate that hydrogeochemistry would be an effective tool for U exploration in the NE Yilgarn.

Filtering to 0.1 µm or 0.45 µm size gave similar results for groundwaters in the NE Yilgarn, which is important given the lower cost and faster filtering at 0.45 µm. Results indicate that the Fe and Al "dissolved" concentrations should be interpreted carefully in such neutral/fresh groundwater, although these seem to have little influence on the dilution or concentration of metals of interest in solution.

The two exchange resins tested did not enhance analytical or exploration success. In contrast, carbon sachets are routinely used for Au analysis, and can be successfully used to achieve lower detection for Ag, Pd and Pt, and as a qualitative method for U, W and other metals. The carbon sampling is unfiltered and easy to use, and is superior to the other exchange resins in that it adsorbs both negative and positive charged ions. Thus, carbon sampling is applicable for hydrogeochemical sampling in exploration. In particular, activated carbon extracted W, Pt and Pd are useful vectors to NiS mineralisation. However Pt and Pd are present in very low concentrations (commonly < 1 ng/L), and improving detection for PGE will enhance the exploration success for NiS using hydrogeochemistry.

ACKNOWLEDGEMENTS

The authors would like to thank BHP Billiton and LionOre for site-based assistance and support. Mark Pirlo and Andrew Hackett provided field and laboratory technical support, Ian Robertson contributed programming information in the preparation of the indexing algorithms, and Charles Butt and Michelle Carey gave helpful advice during preparation of the report. Financial support was supplied by the Co-operative Research Centre for Landscape Environment and Mineral Exploration (CRCLEME) and the four industry sponsors Anglo American, BHP Billiton, Inco and LionOre.

REFERENCES

Armstrong, F.A.J. 1958. Inorganic suspended matter in seawater. *Journal of Marine Research*, 17: 23-24.

Barnes, S.J., Hill, R.E.T. and Gole, M.J., 1988a. The Perseverance ultramafic complex, Western Australia: product of a komatiite lava river. Journal of Petrology, 29: 305-331.

Barnes, S.J., Gole, M.J. and Hill, R.E.T., 1988b. The Agnew nickel deposit, Western Australia. II. Sulphide geochemistry, with emphasis on the platinum group elements. Economic Geology, 83: 524-536.

Billington, L.G., 1984. Geological review of the Agnew nickel deposit, Western Australia. II. Sulphide deposits in mafic and unltramafic rocks. D.L. Buchanan and M.J. Jones (Eds.), London. The Institution of Mining and Metallurgy, pp 43 –54.

Box, G.E.P. and Cox, D.R. 1964. An analysis of transformations. *Journal of the Royal Statistical Society, Series B*, 26: 211-243.

Brand, N.W. 1997. Chemical and mineralogical characteristics of weathered komatiitic rocks, Yilgarn Craton, Western Australia: discrimination of nickel sulphide bearing and barren komatiites. Ph.D. Thesis, University of Western Australia. 373 pp. (unpublished).

Butt, C.R.M., Nickel, E.H. and Brand, N.W., 2006. The weathering of nickel sulfide deposits and implications for geochemical exploration. In: S.J. Barnes (Editor), Nickel Deposits of the Yilgarn Craton. Society of Economic Geologists Special Publication 13, Chapter 5 (in press).

Commander, D.P. (compiler), 1989. Hydrogeological map of Western Australia, 1:2,500,000. Geological Survey of Western Australia.

Drever, J.I., 1982. The Geochemistry of Natural Waters. Prentice-Hall, Inc., Englewood Cliffs, N.J. U.S.A. 388 p.

Gray, D.J. Unpublished data.

Gray, D.J., 2001. Hydrogeochemistry in the Yilgarn Craton. *Geochemistry: Exploration, Environment, Analysis*, 1: 253-264.

Gray, D.J., 2003. Naturally occurring Cr^{6+} in shallow groundwaters of the Yilgarn Craton, Western Australia. *Geochemistry: Exploration, Environment, Analysis*, 3: 359-368.

Gray, D.J., Phillips, Z. and Longman, G.D., 1999. Hydrogeochemical dispersion of nickel and other elements at Harmony, Western Australia. CSIRO Division of Exploration and Mining Restricted Report 647R. 34 pp.

Gole, M. and Woodhouse, M. 2000. Disseminated and massive nickel sulphide deposits, Honeymoon Well komatiite complex, Western Australia. Journal of the Virtual Explorer, 1.

Kennedy, V.C., Zellweger, G.W. and Jones, B.F. 1974. Filter pore-size effects on the analysis of Al, Fe, Mn, and Ti in water. *Water Resources Research*, 10(4): 785-790.

Mann, A.W., 1983. Hydrogeochemistry and weathering on the Yilgarn Block, Western Australia - ferrolysis and heavy metals in continental brines. Geochimica Cosmochimica Acta, 47: 181-190.

Marston, R.J., Groves, D.I., Hudson, D.R. and Ross, J.R., 1981. Nickel sulphide deposits in Western Australia: a review. Economic Geology, 76: 1330 –1363.

Martin, J.E. and Allchurch, P.D., 1975. Perserverance nickel deposit. In "Economic Geology of Australia and Papua New Guinea, I. Metals. C.L. Knight (Ed.), Melbourne. Australasian Institute of Mining and Metallurgy, pp 149 –155.

Noble, R.R.P. Unpublished. Distribution of arsenic in regolith above buried mineralisation: implications for exploration and environmental management. Ph.D. Thesis, Curtin University of Technology, Perth.

Parkhurst, D.L., Thorstenson, D.C. and Plummer, L.N., 1980. PHREEQE, a computer program for geochemical calculations. U.S. Geological Survey Water Resources Investigations 80-96, 210p.

Appendices: List of files supplied on the CD.

Digital version of the entire report (Adobe pdf document)

1) Raw and final geochemical water sampling data (excel spreadsheet)
2) Transformed data for indices (excel spreadsheet)
3) Results from saturation indices
4) Carbon sachet results
5) Exchange resin results
6) Exchange resin regeneration method